Protein and Lantibiotic Sequencing by Gas Phase Dissociation Involving Vibrational Excitation and Ion Electron Reactions

by

Anastasia Kalli

A dissertation submitted in partial fulfillment
of the requirements for the degree of
Doctor of Philosophy
(Chemistry)
in The University of Michigan
2009

Doctoral Committee:

Assistant Professor Kristina I. Hakansson, Chair
Professor David M. Lubman
Professor E. Neil G. Marsh
Professor David H. Sherman
Associate Professor Nils G. Walter

To My Dear Family

Acknowledgments

The journey of this dissertation comes to an end and I would like to take the opportunity to express my sincere gratitude to all those who helped and supported me during these years.

First and foremost, I would like to thank my advisor, Dr. Kristina Håkansson, for her guidance, and continuous support. Her insight, assistance and vast knowledge enabled me to perform the tasks required for the completion of this thesis. What I have learned from her is invaluable and I will always carry this knowledge to my future work. I sincerely thank Kristina for her encouragement and inspiration. I feel fortunate that I had the opportunity to work with her and I am grateful to her for everything she has taught me.

I would also like to thank my committee members for providing valuable suggestions and advice on my research proposal, data meeting and on my thesis; Prof. David Lubman, Prof. David Sherman, Prof. Neil Marsh and Prof. Nils Walter. None of the work presented in this dissertation would have been possible without their feedback.

I also want to acknowledge Prof. Mark Meyerhoff for his advice and support throughout my PhD studies. It was a great pleasure working with him as one of his teaching assistants.

During my thesis work I always had the encouragement of my dear former and present colleagues in the Hakansson group; Gabriella, Hangtian, Haichuan, Bo, Hyun Ju,

Jason, Katie, Wen, Ashley, Chris, and Noah. I truly enjoyed working with you and thank you for making my every day life more enjoyable. I want to especially thank Julie, Hye Kyong, Jingjie and Jiong for their continuous help and support. Thank you all for your friendship and kindness.

My thesis has been funded by an Eli Lilly Analytical Chemistry award to Kristina and the University of Michigan. I would like to thank the Department of Chemistry at the University of Michigan for providing me with financial support through a teaching assistantship. I am very grateful to the Rackham School of Graduate Studies for financially supporting me through the One Term Dissertation Fellowship.

The completion of this thesis would not have been accomplished without the help of my friends, here in Ann Arbor, Greece and Cyprus, who have encouraged me along this journey. Harris is especially acknowledged. I am truly indebted to Alexandros for his patience and support. He undoubtedly helped me to overcome the difficulties and challenges I have encountered during my studies and life. Last but not least, I am thankful to my family, especially my parents, my sisters and my two nieces, for their boundless love and support. This dissertation is dedicated to them.

Anastasia Kalli

December 18, 2008

Ann Arbor, MI

Table of Contents

List of Tables

Tables

List of Figures

Figures

List of Schemes

Schemes

List of Appendices

Appendix

List of Abbreviations

Abbreviations

AI-ECD	Activated ion electron capture dissociation
BSA	Bovine serum albumin
CID	Collision induced dissociation
ESI	Electrospray ionization
ECD	Electron capture dissociation
EDD	Electron detachment dissociation
EID	Electron induced dissociation
ETD	Electron transfer dissociation
FT-ICR	Fourier transform ion cyclotron resonance
Glu C	Endoproteinase Glu C
IRMPD	Infrared multiphoton dissociation
Lys C	Endoproteinase Lys C
Lys N	Metalloendopeptidase Lys N
m/z	Mass-to-charge ratio
MALDI	Matrix assisted laser desorption/ionization
MS	Mass spectrometry
MS/MS	Tandem mass spectrometry
PTMs	Post-translational modifications
ppm	parts per million
S/N	Signal-to-noise ratio
SORI	Sustained off-resonance irradiation
T	Tesla, a unit of magnetic field
Q	Quadrupole (mass filter)

Abstract

Protein and Lantibiotic Sequencing by Gas-Phase Dissociation Involving Vibrational Excitation and Ion-Electron Reactions

by

Anastasia Kalli

Chair: Kristina I. Håkansson

In proteomics, protein identification and characterization are largely performed by tandem mass spectrometry (MS/MS), in which sequence specific product ions are generated from precursor peptide or protein ions. Such MS/MS data can reveal the protein identity either by database search, or via *de novo* sequencing. However, successful and confident protein identification, either by database searching or by *de novo* sequencing, relies heavily on the extent and quality of the obtained sequence information generated by MS/MS. In addition, the higher the extent of fragmentation, the higher the probability of localizing post-translational modifications (PTMs).

Electron based reactions, electron capture dissociation (ECD) and electron detachment dissociation (EDD), have shown great promise for PTM analysis, and for improved peptide sequence coverage. In this thesis, ion electron reactions, ECD, EDD, and electron induced dissociation (EID), are explored for peptide sequencing, and for PTM analysis.

Disulfide bond formation is a PTM present in extracellular proteins. We demonstrate that EDD and infrared multiphoton dissociation (IRMPD) of peptide anions containing disulfide linkages result in preferential cleavage of S-S and C-S bonds and, therefore, both techniques can be used for probing disulfide bonds in peptide anions.

Factors such as precursor ion charge state and m/z value, peptide mass, and protease selection that may influence the dissociation outcome in ECD were investigated, aiming to improve peptide sequence coverage. We show that doubly protonated peptides do not fragment efficiently in ECD, and that precursor ion m/z value is the main factor determining a successful ECD outcome. Highly charged precursor ions at m/z < ~960 fragment efficiently in ECD and yield high peptide sequence coverage.

The utility of EID for dissociation of singly deprotonated species was also explored. We show that EID results in extensive fragmentation, providing structural information for peptide anions. For modified peptides, EID results in retention of sulfation and phosphorylation allowing localization of the modification site.

Vibrational excitation, collision induced dissociation and IRMPD, were explored for structural characterization of native and oxidized lantibiotics. These experiments provided insights into the fragmentation behavior of native and oxidized lantibiotics, allowing prediction of their fragmentation pathways.

Chapter 1

Introduction

1.1 Mass Spectrometry and Proteomics

The term "proteome" was first introduced in the mid-1990s by Wilkins and Williams[1] to define the entire protein complement expressed by a cell, tissue, or organism. Proteomics aims to identify proteins expressed in a cell or tissue as well as to define their post-translational modifications (PTMs), their expression levels, their functions, and their interactions with other molecules for obtaining a comprehensive understanding of biological systems at the protein level.[2-4] Since its inception, proteomics has emerged as an exciting new research area and it continues to rapidly expand.

For an analytical method to be suitable for proteomic analysis, it needs to fulfill several requirements because proteomes are highly diverse with high and unknown complexity.[5-8] The technique to be used must provide high sensitivity so proteins with low abundance can be detected, identified, and characterized. It is also important that this technique can deal with complex protein mixtures and that it can detect and identify

post-translational modifications. High sample throughput and wide dynamic range are also required, given that hundreds to thousands of proteins need to be analyzed.

Mass spectrometry (MS) has been established as the preferred method for proteomic analysis because it fulfils most of these demands.[9-14] High sensitivity, wide dynamic range, high mass accuracy, and high sample throughput can be achieved by modern mass spectrometers.[3, 11, 13, 14] For example, mass spectra and tandem mass spectra have been obtained in the low femtomole region[15, 16] whereas intact peptides have been detected at low attomole[17, 18] and even zeptomole[19] levels. Mass accuracies as low as 1-5 ppm can be achieved on a routine basis by Fourier transform ion cyclotron resonance (FT-ICR) and Fourier transform orbitrap mass spectrometers.[20-28] Moreover, MS has the ability to analyze complex protein mixtures and is highly suitable for identification of PTMs.[3, 12, 13, 29-32]

It should also be pointed out that the establishment of mass spectrometry as the preferred proteomics method would not have been possible without the development of electrospray ionization (ESI)[33, 34] and matrix-assisted laser desorption/ionization (MALDI),[35, 36] which made biomacromolecules amenable to mass spectrometric analysis. These ionization techniques softly ionize large nonvolatile biomolecules, such as peptides, proteins, oligonucleotides, lipids, and carbohydrates, and transfer them into the gas phase without significant fragmentation.

Another important factor that shifted the trend towards mass spectrometry for proteome analysis was the rapid growth in genomic databases. Genomic sequences are an important resource for identifying proteins by the correlation of mass spectrometric data of proteolytic peptides with genomic sequence databases.[5, 37, 38] Amino acid

sequences, peptide mass fingerprints (Section 1.2), and peptide tandem mass spectrometric data (Section 1.2) can be translated into DNA sequences and then compared with genomic sequence databases.[6]

Identifying protein populations isolated from cells or tissues is the first step in a proteomic experiment and the ability to do so in a systematic and unambiguous manner comprises a core component of proteomics research. Protein identification is most commonly achieved by the determination of peptide sequences. Methods for protein identification are discussed in section 1.2.

1.2 Protein Identification by Mass Spectrometry

Almost all protein identification is based on the analysis of peptides generated by proteolytic digestion of the protein of interest (bottom-up approach). This approach offers several advantages compared to the analysis of intact proteins (top-down approach). For example, gas-phase fragmentation of peptides is more efficient compared to proteins, and mass spectrometers are more sensitive to the detection of smaller molecules. Moreover, peptides can be more easily eluted from gels compared to elution of intact proteins.[39]

Peptide mass mapping or mass fingerprinting is one approach for protein identification.[40-45] The principle of this method is that, after cleavage with a specific proteolytic enzyme, every protein results in a unique set of peptide masses. In this approach, the mass spectrum of proteolytically derived peptides is acquired and a mass list with the experimental peptide masses is generated. This mass list constitutes a mass fingerprint unique for a specific protein. The resulting mass list is then compared to the theoretically expected peptide masses available in protein sequence databases. DNA

sequence databases can also be used. In the latter case, the DNA sequences are translated into protein sequences prior to *in silico* digestion. This approach is best suited for genetically well-characterized species for which the entire genome is known, or for which extensive protein or cDNA sequence databases are available.[29] For unambiguous protein identification with this approach, high mass accuracy is required[12, 46-48] because increased mass accuracy decreases the number of isobaric peptides for any given mass in a sequence database.[29] Also, matching a large number of peptides to cover a larger percentage of a protein sequence is essential to ensure correct assignments, paticularly as genomic and protein databases are continuing to grow rapidly.[46, 49]

The major limitation of peptide mass fingerprinting is that, for a protein to be identified, its sequence needs to exist in a database.[29] Another limitation of this approach is erroneous assignments due to errors in sequence databases, and due to the presence of PTMs or non-specific modifications occurring during sample extraction, separation, and preparation. Errors also arise from non-specific cleavage of the protein. Moreover, the presence of multiple proteins in the sample complicates mass spectral interpretation, since it is not apparent which peptides originate from the same protein. [2, 29, 50]

A second approach for protein identification is the "peptide sequence tag" which utilizes tandem mass spectrometry (MS/MS)[51] data to match product ions against predicted fragmentation spectra from proteins in a database.[52-54] In MS/MS (Section 1.5), peptide ions of interest are dissociated in the vacuum of the mass spectrometer and the resulting product ions are used for determination of the primary structure. The fragmentation data can also be searched against nucleotide databases.[3] The latter approach is undertaken by converting the short amino acid sequence information,

obtained from MS/MS, into a degenerate nucleotide sequence pattern that can be used to find matches within nucleotide databases.[55] Tandem mass spectra are usually generated by collision induced dissociation (CID,[56, 57] discussed in Section 1.4). The "peptide sequence tag" method makes use of the fact that the majority of tandem mass spectra contain a sufficient amount of product ions to allow specification of a unique amino acid sequence in a protein, and therefore allow identification of the protein. Although it is possible that a single peptide will correctly identify a protein, in closely related proteins sequence tags may be duplicated. Therefore, matching of multiple peptide sequences increases the confidence of identification and the probability of a correct assignment.[46]

With the peptide sequence tag method, proteins can be identified from complex protein mixtures, given that at least one CID spectrum is generated per protein. Therefore, it is not necessary to separate proteins to homogeneity prior to analysis, as is the case in the peptide mass fingerprinting approach.[58] Furthermore, sequence information obtained from a peptide in the peptide sequence tag approach is generally more specific and discriminative for protein identification compared to relying solely on the intact peptide masses that are used in the peptide mass fingerprinting approach.[3, 59] For these reasons, the peptide sequence tag approach is becoming the accepted method for protein identification over the peptide mass fingerprinting approach.[46]

Regardless of the database, protein or genome database, used for protein identification, both the peptide mass fingerprinting and the peptide sequence tag approaches require that the protein to be identified is included in the database. In cases where a protein is not included in a database, *de novo* sequencing is required for protein identification and characterization. *De novo* sequencing is also essential in cases in

which a significant number of peptides diverge from the predicted ones due to errors in databases, discrepancies between genomic sequences, or due to the presence of PTMs.[46] Furthermore, *de novo* sequencing can distinguish between proteins having a single amino acid change, i.e. isoforms, and reveals sites of modifications. An additional advantage of *de novo* sequencing is that false positive identifications arising from database searches due to limited fragmentation or side chain fragmentation can be eliminated.[60]

It should be noted that *de novo* sequencing by mass spectrometry remains a challenge because it not only requires complete protein sequence but also complete peptide sequence coverage. Complete protein sequence coverage refers to the detection of all generated proteolytic peptides after digestion of a protein of interest whereas complete peptide sequence coverage refers to the generation and detection of all possible sequence-specific product ions following fragmentation of proteolytic peptides. In practice, whether a large or small fraction of peptides generated from any protein is detected depends on the amount of protein present in the sample, and the efficiency of protein extraction and digestion, and peptide extraction.[46] Achieving 100% protein sequence coverage is still impractical on a routine basis,[39] particularly when hundreds to thousands of proteins need to be analyzed. One approach to optimize protein sequence coverage and be able to achieve complete or near complete protein sequence coverage is to use three or more different proteases, e.g., trypsin, chymotrypsin, Lys C, or Glu C for digestion so that overlapping peptides are generated.[60, 61] Product ion spectra of the peptides provide information about the primary structure of the protein. Cleavage between each pair of amino acids is essential for complete peptide sequence coverage.

However, as mentioned above, this is a rather difficult task and no such fragmentation technique currently exists that can routinely provide complete peptide sequence coverage.

The development of fragmentation techniques complementary to CID,[56, 57] which is by far the most widely used technique for ion activation, shows promise for improved peptide sequence coverage. Such dissociation techniques are discussed in Section 1.4. Sequencing by the means of Edman degradation and genomic sequencing to reveal peptide and protein primary structure is discussed below.

1.3 Primary Structure Determination

1.3.1. Edman Degradation

Protein sequencing by Edman degradation is the classical method of protein sequencing to determine protein identity.[62, 63] Edman sequencing involves reaction of the N-terminal amino group of the peptide, or protein, of interest with phenylisothiocyanate to yield phenylthiocarbamoyl peptides. Under mild acidic conditions, the phenylthiocarbamoyl derivative is cleaved at the peptide bond immediately adjacent to the modified residue to yield 2-anilinothiazolin-5-one and the peptide chain shortened by one amino acid. Following hydrolysis of the thiazolinone derivative, the phenylthiocarbamoyl amino acid is formed, which by ring formation is converted to 3-phenyl-2-thiohydantoin. The 3-phenyl-2-thiohydantoin derivative is extracted and identified by reverse-phase HPLC by comparing its retention time with that of a series of standards.[64] In several approaches, HPLC has been replaced by mass spectrometry. In such protocols, the peptide sequence is identified by measuring the mass of the cleaved 3-phenyl-2-thiohydantoin amino acid,[65] or the mass of the remaining underivatized peptide.[66]

Chait et al. combined a modified Edman degradation with mass spectrometric analysis for obtaining peptide sequence information.[67] Their approach, termed ladder sequencing, involves generation of a peptide ladder, each "step" of which differs by one amino acid, and readout of the sequence from a MALDI mass spectrum. In this approach, the Edman degradation is performed with an excess of phenylisothiocyanate in the presence of phenylisocyanate as terminating agent. The phenylcarbomoyl peptide is stable in acidic solution whereas the phenylthiocarbamoyl peptide is degraded. Therefore, in each cycle a small amount of peptide is blocked N-terminally and protected from further Edman degradation. A number of degradation cycles is performed and, at the end, the MALDI mass spectrum of the whole mixture is recorded. The mass differences of adjacent peaks correspond to particular amino acid residues and the order of their occurrence defines the peptide sequence. In this method, no intermediate isolation or analysis of released amino acid derivatives are required in each cycle.[67]

Edman degradation has several limitations. For example, proteins or peptides containing a modified N-terminus, such as acetyl-, formyl-, or pyroglutamyl- N-termini, cannot react with phenylisothiocyanate and, therefore, cannot be sequenced by Edman degradation.[37, 68] This drawback is significant, given that 80% of cellular proteins are blocked at their N-termini.[69] Methods for deblocking the N-terminus have been developed but they are not always efficient and they considerably increase the analysis time.[70] One method developed to overcome the N-terminal blockage problem is protein internal sequence analysis based on chemical or enzymatic digestion of gel separated proteins blotted to various membranes.[71-73] Following separation and purification of the resulting peptides, internal sequences are obtained by Edman degradation. This approach

allows generation of amino acid sequences from internal peptides even if the protein was blocked to traditional Edman sequencing, and it also provides significantly higher sequence coverage compared to N-terminal sequencing alone. In fact, this approach is required for proteins containing more than 50 residues because Edman degradation is not suitable for larger proteins due to the fact that each cycle is not 100% efficient. Because of this limited yield there will be a mixed population of molecules in the analyte after a large number of cycles, rather than a pure sample and, thus, single rounds of Edman degradation result in multiple peaks.[2]

Another limitation of Edman sequencing arises from the presence of unusual or modified amino acids, containing, e.g., phosphorylation and glycosylation sites or disulfide bonds, which cannot be identified, or which require elaborate analytical procedures for their identification.[37, 74-76] Given the high number of known post-translational modifications (~300), this limitation of Edman degradation poses a significant problem for the identification and characterization of modified peptides.[77]

Other drawbacks of Edman degradation are the limited applicability in cases when the peptide or protein of interest is available only at low concentrations, or when a mixture of peptides with similar chemico-physical properties are being analyzed so that they cannot be separated easily.[47, 78] Sequence data generated by Edman degradation can only be interpreted if the polypeptide is purified to near homogeneity before analysis.[74, 78] Furthermore, Edman degradation suffers from a relatively low sample throughput, making this approach unsuitable in cases where hundreds to thousands of proteins need to be analyzed.[2, 6, 79-82] Because of these limitations, Edman degradation is not the preferred method for protein sequencing in proteomics approaches. Also, as discussed above,

because mass spectrometry provides high sensitivity, high mass accuracy, and high sample throughout it has reduced the utility of Edman degradation.

1.3.2 Genomic Sequencing

Large scale genomic sequencing has simplified and facilitated the determination of peptide and protein primary structure in many organisms, because open reading frames (ORFs) in the nucleotide sequence serve as templates for the construction of the corresponding proteins. Expressed sequence tags can also be used to reveal potential proteins. However, use of DNA sequence information for predicting protein sequences has significant limitations. For example, the existence of an ORF in genomic data does not necessarily imply the existence of a functional gene.[3] In addition, the genome sequences of many organisms are still unknown,[83] and even for those that are known they frequently do not reflect the complete primary structure of the expressed proteins due to post-translational modifications, such as phosphorylation, sulfation, methylation, acetylation, glycosylation, and disulfide bonding, which cannot be predicted by the gene sequences.[7, 12, 83, 84] It is also well known that, in both eukaryotes and prokaryotes, the same gene can result in the expression of many protein variants because of single nucleotide polymorphism, gene splicing, alternative splicing of pre-mRNA, RNA editing, and proteolytic cleavage of the protein.[5, 7, 39, 84] A single spliced mRNA is usually chosen as template for each gene, and the many other mRNAs which result in protein isoforms are omitted, resulting in loss of the natural diversity of proteins.[7] For example, the human genome is estimated to contain about 23,000 genes whereas the total number of unique protein components encoded by this genome is on the order of several million due to extensive PTMs and alternative mRNAs splicing.[85]

Furthermore, proteomes are highly dynamic with protein expression changing in response to external factors, and during development whereas the genome is less dynamic over its lifetime. Therefore, genome sequences cannot be used for predicting changes in the proteome of a cell, tissue or organism.[2, 8]

1.4 Fourier Transform Ion Cyclotron Resonance Mass Spectrometry

Fourier transform ion cyclotron resonance (FT-ICR) mass spectrometry, introduced in 1974 by Comisarow and Marshall, [86, 87] is a technique that effectively converts the mass to charge ratio of an analyte to an experimentally measurable ion cyclotron orbital frequency.[88]

The main components of an FT-ICR instrument are the ionization source (usually ESI), the analyzer cell, the superconducting magnet, the ultra high vacuum system, and the data acquisition system. The analyzer cell is located in a strong, homogeneous, magnetic field. As the magnetic field strength increases, the performance of the FT-ICR instrument improves, including increased mass resolving power, mass accuracy, dynamic range and signal-to-noise ratio.[89, 90] The analyzer cell can adopt different geometries.[91, 92] A common geometry is the cylindrical cell (Figure 1.1). The analyzer cell consists of six electrodes; one front and one back trapping electrode, two opposite excitation electrodes, and two opposite detection electrodes. Ions are stored, mass analyzed and detected in the ICR cell.

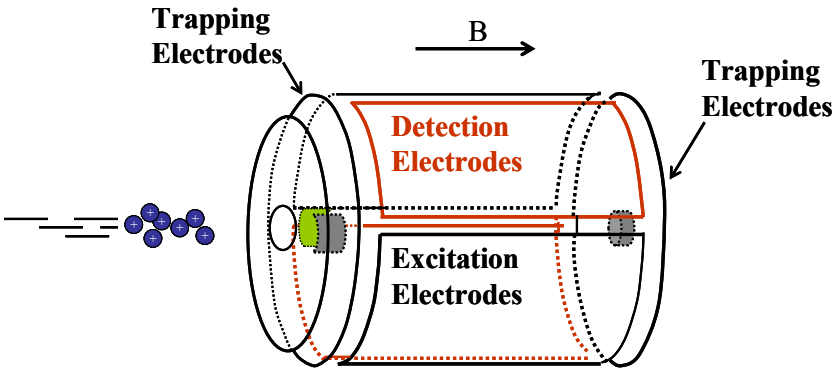

Figure 1.1. Schematic diagram of a cylindrical analyzer cell. The detection, excitation and trapping electrodes are indicated. In this representation, ions are entering from the left. The direction of the magnetic field (B) is also indicated.

The ultra high vacuum environment, provided by cryogenic or turbomolecular pumps, of the analyzer cell is required to achieve high resolution. Low pressure (10^{-9} to 10^{-10} Torr) is required only when ions are detected so that collisions happen infrequently.[93] Another advantage of the ultra high vacuum environment is that ions can be stored for extended periods of time, ranging from milliseconds to hours.[94, 95] This extensive ion trapping time is a distinct feature of FT-ICR instruments and it allows investigation of slow ion-molecule reactions and slow conformational changes in gas-phase biomolecules.

The ion motion in the ICR cell is governed by both electric and magnetic fields. The electric field arises from the voltages that are applied to the electrodes of the analyzer cell. However, the basic ion cyclotron motion is governed solely by the magnetic field (B). An ion moving in the presence of a magnetic field will experience a Lorentz force (F) given by equation 1:

$$\mathbf{F} = q\mathbf{v} \times \mathbf{B} \qquad (1)$$

where q is ion charge and v ion velocity. As a consequence of the Lorentz force, the ions travel in a circular orbit that is perpendicular to the magnetic field. Cyclotron motion is characterized by the frequency with which the ions repeat their orbit, called the cyclotron frequency (f_c). The cyclotron frequency, given by equation (2), is characterized by only three parameters; the strength of the magnetic field (B), which is constant, the charge of the ion (q), and the mass of the ion (m).

$$f_c = qB/2\pi m \quad (2)$$

The mass to charge ratio (m/q) of an ion is determined by measuring its cyclotron frequency. One important feature of equation (2) is that it is independent of ion kinetic energy and, therefore, ion kinetic energy has no influence on the accurate determination of the m/q ratio of ions. Furthermore, because the cyclotron frequency (f_c) can be measured very accurately, high mass accuracy can be achieved with FT-ICR MS instruments.

When ions are moving parallel to the magnetic field, the Lorentz force traps them radially in the magnetic field but does not prevent them from leaving the cell in the axial direction. In order to trap the ions in the cell, an electric potential is applied to the two end trapping plates, resulting in axial oscillation of the ions between the two plates and allowing trapping of the ions.

After ions are formed and trapped in the analyzer cell they have a small kinetic energy and random cyclotron phase. In order for the ions to be detected they need to be excited coherently to larger detectable cyclotron radii and come close to the detection electrodes. Excitation of ions is achieved by applying a spatially uniform electric field, via the excitation electrodes, which oscillates at the ion cyclotron frequencies of ions of

interest. Ions orbiting at these particular frequencies absorb energy and are coherently excited to higher kinetic energies so their cyclotron radii increase. All ions of the same mass to charge (m/q) ratio are excited coherently and undergo cyclotron motion as a packet. This coherently orbiting packet of ions moves alternately toward and away from the cell walls, generating an image current which is detected by the two opposite detection electrodes. The image current is amplified and digitized to yield a time domain signal. The time domain signal contains the frequencies of all ions in the cell and is converted to the frequency domain by Fourier transformation. By applying equation 2, frequencies are converted to m/z values. Figure 1.2 (lower left panel) shows the time domain signal obtained after excitation and detection of the ions.

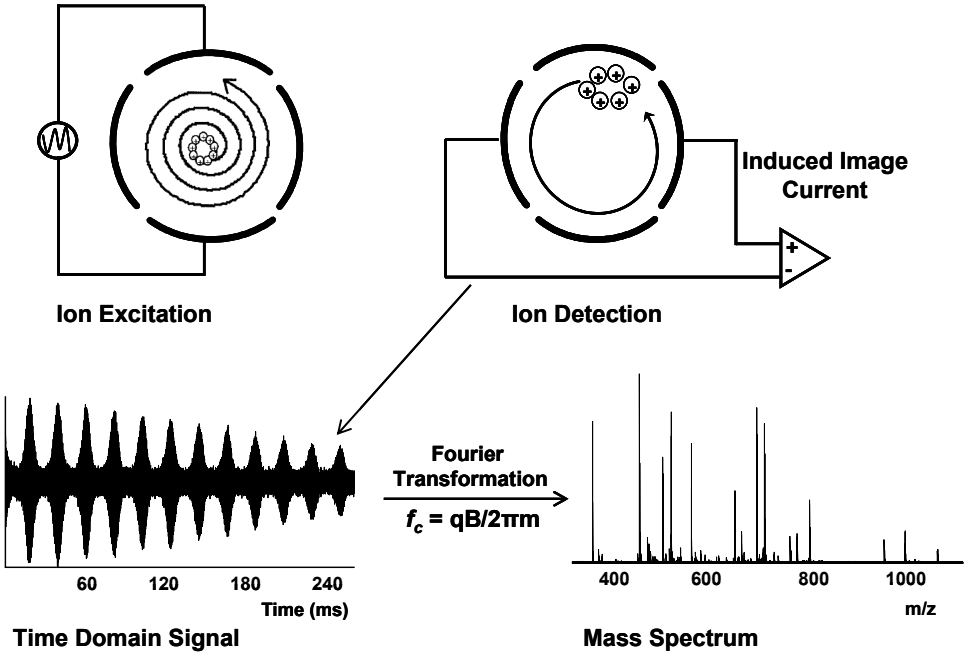

Figure 1.2. Excitation and detection events in an ICR cell, and generation of the time domain signal. A spatially uniform electric field oscillating at the ion cyclotron frequency is applied via the excitation plates. Ions in resonance with the applied frequencies will be excited coherently to a larger ion cyclotron radius. The coherently orbiting ion packets induce an image current in a pair of detection electrodes. The image current is amplified and digitized to yield the time domain signal which is converted to a frequency spectrum via Fourier transformation. The m/z spectrum is obtained from the frequency spectrum by applying equation 2.

The experiments presented in this thesis were collected with a 7T- ESI-quadrupole-FT-ICR mass spectrometer (Figure 3). ESI is the most common ionization technique for coupling to FT-ICR mass spectrometers.[96, 97] The popularity of this configuration is mainly because ESI generates multiply charged ions, which are detected at lower m/z ratios compared to singly charged ions, and FT-ICR MS performance degrades with increasing m/z.[90] For example, resolving power degrades with increasing m/z.[93] Furthermore, for electron capture dissociation (ECD, Section 1.5) and electron detachment dissociation (EDD, Section 1.5), multiply charged ions are required.

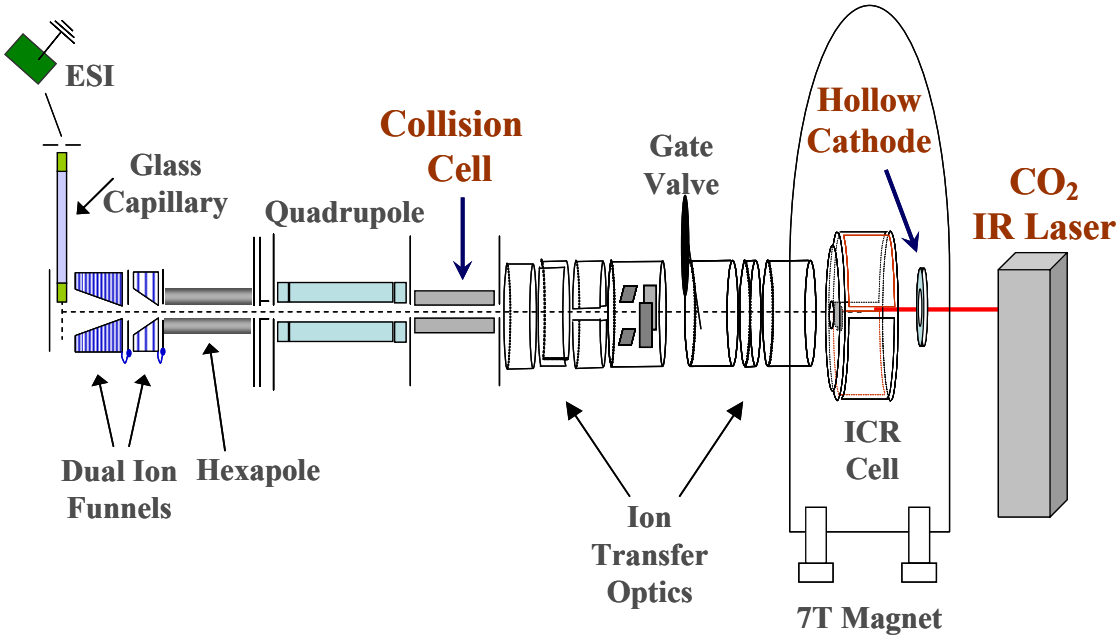

Figure 1.3. Schematic diagram of the 7 T-Q-FT-ICR mass spectrometer used in this work. The instrument is equipped with an ESI source, dual ion funnels, a quadrupole mass filter, a hexapole collision cell for CID experiments, a cylindrical infinity analyzer cell,[98] a hollow cathode for ion-electron reactions, and a 10.6 μm CO_2 laser for infrared multiphoton dissociation experiments.

The dual ion funnels[99-102] in the front of the instrument provide improved ion transmission and increased sensitivity. A quadrupole mass filter (Q), located between the ion source and the ICR cell, allows mass selective external ion accumulation prior to the

introduction of ions into the cell. This configuration improves the sensitivity and the dynamic range of the instrument.[103] A hexapole collision cell, located after the quadrupole, serves to externally accumulate ions, or to fragment these via collisions with a neutral gas (CID, Section 1.5), usually argon. Ions are transferred to the ICR analyzer cell with high voltage ion transfer optics that allow ions to overcome the magnetic mirror effect. An indirectly heated hollow dispenser cathode,[104] located at the rear of the ICR cell, provides electrons for ion-electron reactions. A 10.6 μm CO_2 IR laser beam provides photons for infrared multiphoton dissociation (IRMPD, Section 1.5) experiments.

FT-ICR mass spectrometry combines high mass accuracy, high mass resolving power, and high mass resolution and is considered one of the most powerful techniques in proteomics research.[105] As mentioned above, high mass accuracy can be obtained because frequency, which is the measured physical property in an FT-ICR MS experiment, can be determined very accurately. Mass accuracy down to 1 ppm can be obtained for large biomolecules.[28, 106] Even sub-ppm mass measurement accuracy for protein identification has been reported by Smith and co-workers using FT-ICR MS in an approach called accurate mass tag.[105, 107] High mass accuracy is essential when proteins are to be identified via a data base search because the accuracy of mass measurement has a significant effect on successful and unambiguous protein identification.[108]

Mass resolving power refers to a single spectral peak and is defined as $m/\Delta m$, where m represents the ionic mass and Δm is the mass spectral peak width at half maximum peak height. Resolution refers to the ability to separate two species with closely spaced mass values. For resolution, m represents the mass of the lighter species

to be resolved and $\Delta m = m_2 - m_1$ in which m_2 and m_1 are the masses of the two closely spaced species to be resolved. The resolving power is directly proportional to the duration of the time domain signal.[109] In the ultrahigh vacuum environment of the mass analyzer, the detection signal can last for several seconds and resolving power exceeding 10^6 can be achieved for large biomolecules. Unit mass resolution has been achieved for a 112 kDa protein.[110] Moreover, the isotopic resolution provided by FT-ICR MS allows direct determination of the charge state of ions from the spacing of the isotopic peaks.[111] Baseline resolution of two peptides differing by only 0.00045 Da at ~ 904 Da monoisotopic mass has been demonstrated in a 9.4 T FT-ICR mass spectrometer.[112]

1.5 Tandem Mass Spectrometry

In tandem mass spectrometry,[51] precursor ions are mass selected from a mixture and subjected to gas-phase fragmentation. The resulting product ions provide structural information for the precursor ions. Various dissociation techniques are available in FT-ICR MS, including sustained off-resonance irradiation collision induced dissociation (SORI-CID),[113] blackbody infrared radiative dissociation (BIRD),[114, 115] infrared multiphoton dissociation (IRMPD),[116, 117] surface induced dissociation (SID),[118-123] electron capture dissociation (ECD),[124, 125] and electron detachment dissociation (EDD).[126, 127] The fragmentation techniques used in the work presented here include CID, IRMPD, ECD, EDD, and EID. These techniques are summarized in Table 1.1 and discussed in detail below.

Table. 1.1. Summary of fragmentation techniques used in this dissertation.

MS/MS techniques	Vibrational activation		Ion-electron reactions		
	CID	IRMPD	ECD	EDD	EID
Fragmentation energy source	Slow heating by collisions between reactant ions and neutral gas molecules	Absorption of multiple resonant infrared photons	Low energy electron (< 1 eV) capture by positively charged ions	Electron detachment from negatively charged ions after irradiation with high energy electrons (> 10 eV)	Excitation of singly charged cations or anions after irradiation with high energy electrons (> 10 eV)
Precursor ion charge states	$\leq 1^-$ or $\geq 1^+$		$\geq 2^+$	$\leq 2^-$	$= 1^+$ or $= 1^-$
Peptide Fragmentation Features	Positively charged Ions: Cleavage at amide bonds (C-N) and labile bonds of post-translational modifications Negatively charged Ions: Cleavages at amide (C-N), amine (N-C_α) and C_α-C bonds		Cleavages at amine (N-C_α) bonds and retention of post-translational modifications	Cleavages at C_α-C bonds and retention of post-translational modifications	Cleavages at amide (C-N), amine (N-C_α) and C_α-C bonds

1.5.1 Dissociation via Vibrational Excitation

CID[56, 57] and IRMPD[116, 117] can be categorized as vibrational excitation or slow heating based dissociation techniques in which the product ions are formed via the lowest energy pathways.[128] Both CID and IRMPD result in cleavage of peptide backbone amide (C-N) bonds, producing *b*- and *y*- type product ions (Figure 1.4).[129]

In CID, precursor ions are activated by collisions with a neutral target gas, such as argon or helium. These collisions between the precursor ions and the neutral target gas are accompanied by a conversion of the ion translational energy into internal energy. The internal energy is rapidly redistributed within the ion and, once it exceeds the threshold dissociation energy, fragmentation occurs. CID is the most widely used MS/MS fragmentation technique.

In IRMPD, precursor ions are excited and subsequently fragmented by the absorption of multiple photons. The absorption occurs by IR active groups present in the ion, followed by rapid redistribution of energy over all vibrational degrees of freedom. The outcome is an internal energy distribution similar to CID. For photodissociation to occur, precursor ions must be able to absorb energy in the form of photons, producing excited states above the threshold of dissociation.[130, 131]

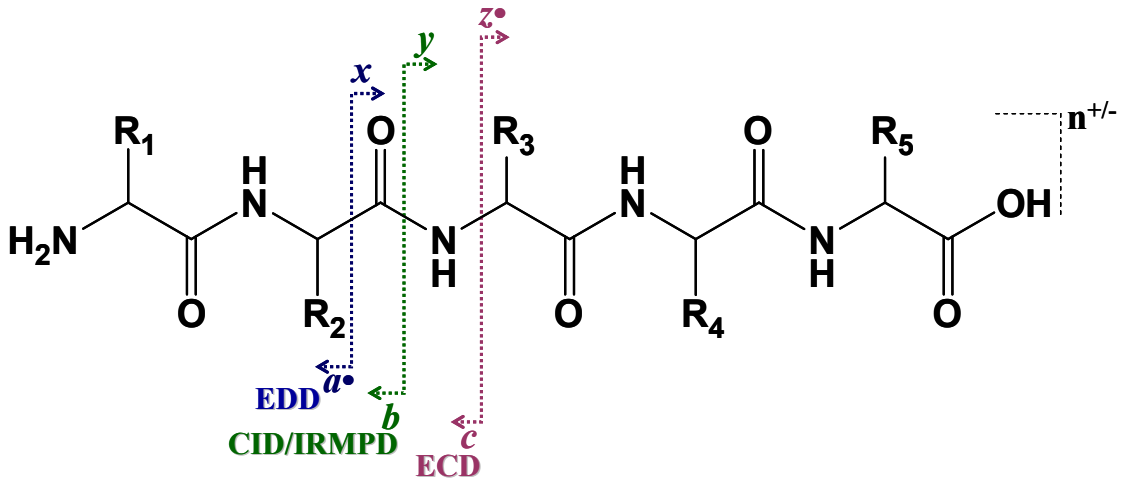

Figure 1.4. Peptide fragmentation and product ion nomenclature[129] following vibrational excitation (CID and IRMPD) and electron based dissociation techniques (ECD and EDD). CID and IRMPD result in cleavage of backbone amide bonds (C-N), yielding *b*- and *y*-type product ions. ECD induces cleavage of amine bonds (N-C_α), resulting in formation of *c*- and *z*-type product ions, and EDD results in cleavage of C_α-C bonds, yielding *a*- and *x*-type product ions.

The accepted fragmentation mechanism for peptide CID and IRMPD is the mobile proton model.[132-136] According to this mechanism, fragmentation of protonated peptides requires the involvement of a proton at the cleavage sites. Protons are initially located at basic sites, such as basic side chains or the amino terminus, and are typically internally solvated by amide carbonyl oxygens or amide nitrogens. Following activation, the proton is "mobilized" from the basic sites to the solvation sites to initiate backbone fragmentation. The energy required for proton "mobilization" from the basic side chains

or the amino terminus depends on the amino acid composition, with arginine-containing peptides requiring the greatest energy because Arg can strongly sequester the protons due to its high basicity.[132]

1.5.2 Dissociation via Electron Based Reactions

ECD,[125] introduced in 1998, and EDD,[126] introduced in 2001, are dissociation techniques involving gas phase ion-electron reactions and they are relatively new compared to CID and IRMPD. The fragmentation patterns observed in these two activation techniques are different from those observed in slow heating techniques and, therefore, electron based reactions are complementary to traditional MS/MS techniques.

In ECD, multiply charged precursor ions are irradiated with low energy (<1 eV) electrons, resulting in electron capture and formation of a radical species, $[M + nH]^{(n+1)+\bullet}$, called the charged reduced species (n = number of protons). This charged reduced species can undergo fragmentation to produce *c*- and *z*-type fragments as a result of amine, N-Cα, bond cleavage (Scheme 1.1 and Figure 1.4). The N-terminal *c*-type product ions are usually detected as even electron species, whereas the *z*-type product ions are detected as radical species.[125]

$$[M + nH]^{n+} + e^-_{<1\ eV} \longrightarrow [M + nH]^{(n-1)+\bullet} \longrightarrow \text{N-C}\alpha \text{ cleavage}$$

Scheme 1.1. Fragmentation pathway in ECD.

There are two major accepted mechanisms for ECD. According to the first mechanism (Scheme 1.2), electron attachment occurs at one of the protonation sites, usually a lysine ε-ammonium group, an arginine guanidinium group, a histidine imidazolium ring, or an N-terminal ammonium group.[137-144] Following electron capture at these protonation sites, a radical intermediate is formed that dissociates via hydrogen

atom migration. The hydrogen atom is captured by the carbonyl group of a sterically proximate amide bond, forming an aminoketyl intermediate that dissociates by cleavage of the adjacent N-Cα bond. This intermediate dissociates to form N-terminal *c*-type product ions and C-terminal *z*-type product ions.

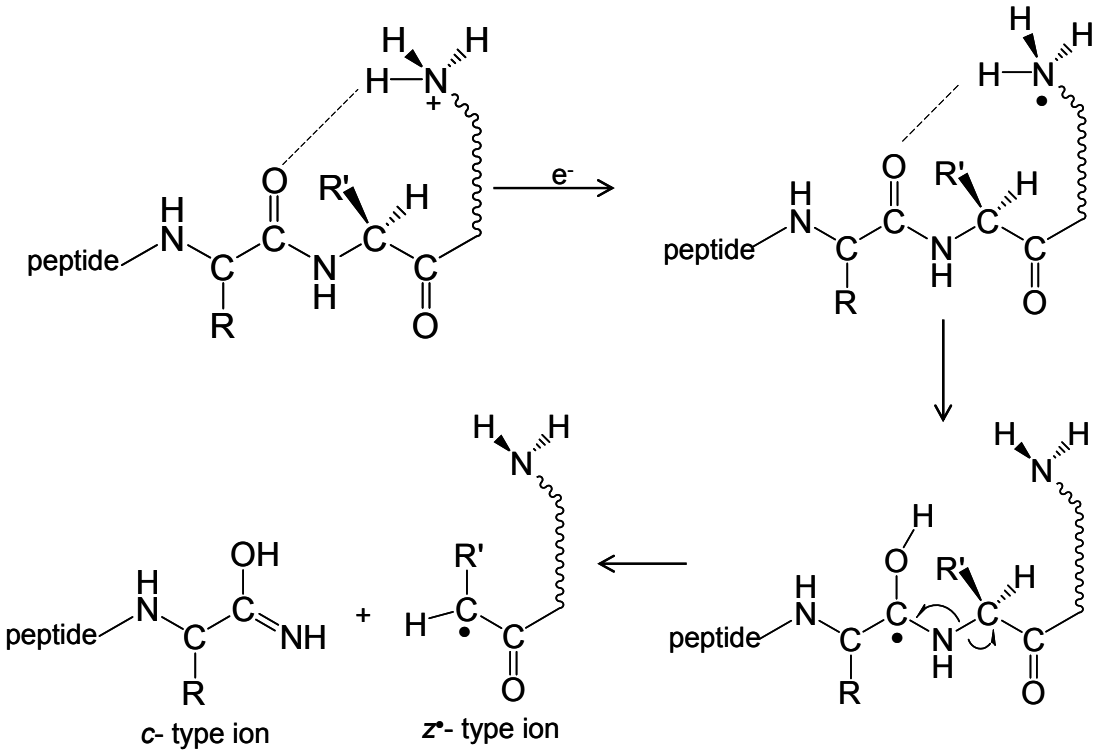

Scheme 1.2. ECD fragmentation mechanism. Scheme adapted from references [145] and [146].

The second mechanism (Scheme 1.3)[145-148] suggests electron capture in a π* orbital delocalized over an amide group to yield an electronically excited state of the charged reduced radical species. These amide superbases can exothermically abstract a proton from a close proximity proton donating group to form fragile aminoketyl radicals that generate backbone dissociation.

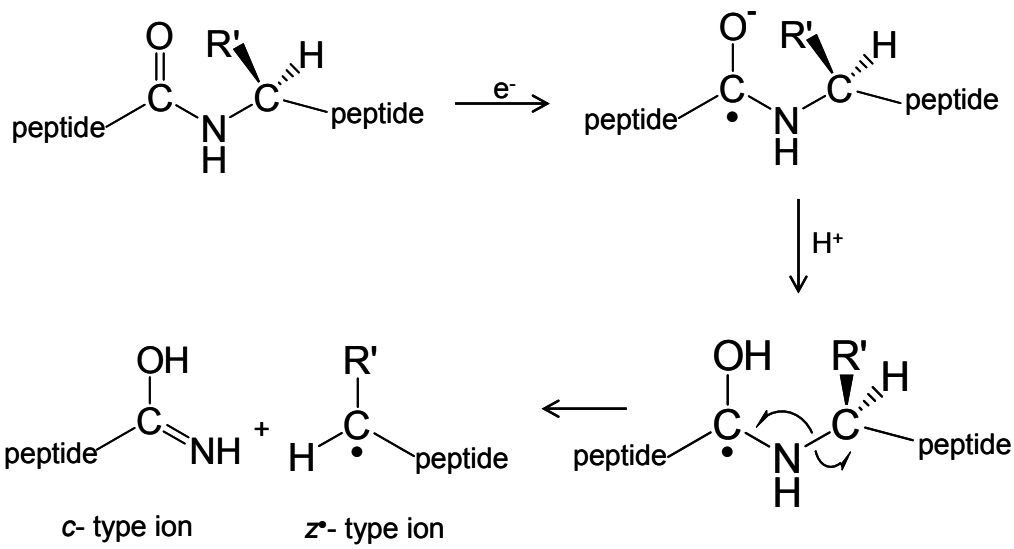

Scheme 1.3. ECD fragmentation mechanism. Scheme adapted from reference [146].

One main advantage of ECD compared to slow heating, such as CID or IRMPD, is the retention of labile PTMs. ECD has been successfully applied for the characterization and localization of phosphorylation,[149-153] glycosylation,[151, 154-157] and sulfation.[156, 158, 159] In contrast, following vibrational excitation of modified peptides, cleavage of the modification is observed. Furthermore, disulfide bonds, which show limited fragmentation in low energy CID, are preferentially cleaved in ECD.[160] Another advantage of ECD is that the cleavage sites show less sequence dependence and ECD therefore results in more extensive fragmentation,[125, 137, 144, 161-164] thus higher peptide sequence coverage can be obtained compared to CID. ECD is applicable to positively charged ions but requires at least two charges because one of the charges is neutralized upon electron capture. One disadvantage of ECD is its low fragmentation efficiency, that is, the percentage of precursor ions converted to product ions. [165-167]

EDD is applicable to negatively charged ions. In EDD, precursor ions are irradiated with higher energy electrons (> 10 eV), resulting in electron detachment and

formation of a charged reduced species, $[M - nH]^{(n-1)-\bullet\,(*)}$. This charged reduced species undergoes fragmentation mainly at the Cα-C bond to produce *a*- and *x*- type product ions (Scheme 1.4, Figure 1.4). The *x*-type product ions are mainly observed as even electron species, whereas *a*-type product ions are detected as odd electron species.[126, 127]

$$[M - nH]^{n-} + e^-_{>10\,eV} \longrightarrow [M - nH]^{(n-1)-\bullet\,(*)} + 2e- \longrightarrow C\alpha\text{-}C \text{ cleavage}$$

Scheme 1.4. Fragmentation pathway in EDD.

The proposed mechanism of EDD (Scheme 1.5)[127, 168] suggests that cleavage occurs near the deprotonation sites, which correspond to locations of acidic hydrogens. Following the hydrogens of carboxylic groups located at the side chains of aspartic and glutamic acid, and at the C-terminus, the next most acidic hydrogens are those located at amide nitrogens. Therefore, deprotonation can occur at backbone amide nitrogens. Following electron detachment from a deprotonation site, the radical site may be located at a backbone amide nitrogen. Bond cleavage N-terminal to such a radical site is expected, based on computational work,[127] to result in formation of N-terminal *a*• product ions and C-terminal even electron *x*-type product ions, in agreement with experimental data.

Similar to ECD, EDD has been shown to result in retention of labile PTMs, such as sulfation[126] and phosphorylation.[127, 152] EDD has also been applied to the characterization of oligonucleotides,[169, 170] and oligosaccharides.[171-173] One major drawback of EDD is that it exhibits even lower fragmentation efficiency than ECD.

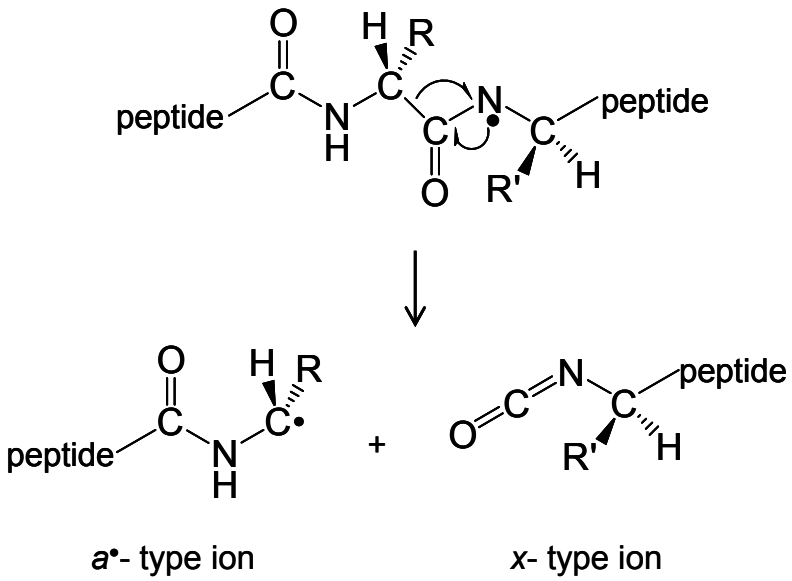

Scheme 1.5. EDD fragmentation mechanism. Scheme adapted from references [127] and [145].

Similar to ECD and EDD, electron induced dissociation (EID)[174, 175] is an electron based activation method. In EID, singly protonated, or deprotonated, species are irradiated with higher energy electrons (> 10 eV), resulting in fragmentation (Scheme 1.6).

$$[M \pm nH]^{\pm} + e^-_{>10\ eV} \longrightarrow [M \pm nH]^{\pm (*)} + e^- \longrightarrow \text{Fragments}$$

Scheme 1.6. Fragmentation pathway in EID of singly protonated, or deprotonated, precursor ions.

EID was initially applied to the fragmentation of small organic molecules in positive ion mode,[175-177] and it was later extended to sodium cationized precursor ions from the cyclic peptide gramicidin S.[178] Fragmentation patterns in EID were analogous to those observed in CID. The technique was initially termed electron impact excitation of ions from organics (EIEIO)[176, 177] and it was later termed EID.[174, 175]

For singly charged carbohydrates cations, EID was shown to result in full sequence coverage, similar to ECD of doubly charged precursor ions.[174] Recently, EID has been applied to singly protonated precursor ions of aromatic amino acids, cystine, and small peptides and it was demonstrated that it yielded different and complementary fragmentation compared to that observed in CID. [179]

Negative ion mode EID has been performed on singly charged precursor ions from phosphate-containing metabolites and it has been shown that it results in complementary fragmentation compared to CID.[180] EID of singly charged anions from sulfated glycosaminoglycans has also been investigated.[181]

1.6. Structural Characterization of Lantibiotics

As discussed above, tandem mass spectrometry is a valuable method for obtaining sequence information about a variety of biomolecules such as proteins, peptides oligonucleotides, and oligosaccharides. Lantibiotics are a unique class of antimicrobial peptides produced by Gram positive bacteria.[182-184] These molecules are highly modified and include thioether cross-linked amino acids, lanthionine and 3-methyllanthionine, and the unusual amino acids 2,3-didehydroalanine (Dha), (*Z*)-2-3,-didehydrobutyrine (Dhb), and β-hydroxy-aspartate.[185-187] Lantibiotics have recently drawn significant attention because they hold great promise for the development of novel antimicrobial agents for biomedical and food applications.[182, 183, 186, 188] Structural elucidation of lantibiotics has been hampered by the presence of unusual amino acids and thioether bridges, as these modifications block routine Edman sequencing. NMR spectroscopy has been proven to constitute an alternative method for obtaining structural information when significant quantities of pure samples are available.[189] Tandem mass spectrometry in positive ion

mode has been applied for structural elucidation of lantibiotics, however rather limited fragmentation was observed. For example, SORI-CID of nisin resulted in fragmentation mainly at the N- or C-terminus of the molecule, and in dissociation of the two thioether bridges located at the N-terminus.[190-192] Fragmentation of nisin A and Z, mersacidin and lacticin 481 has been examined in ECD.[193, 194] ECD of nisin resulted in extensive fragmentation, whereas mersacidin showed moderate fragmentation and lacticin 481 resulted in very limited fragmentation.

1.7. Dissertation Overview

The research work in this dissertation focuses mainly on the utilization of electron based dissociation techniques, EDD, ECD and EID, for peptide sequencing. The utility of EDD to probe disulfide bonds is also illustrated. The bottom-up approach, in which proteins are digested with a proteolytic enzyme and the resulting peptides are subjected to fragmentation to provide structural information, was used throughout this thesis. This choice was mainly made because most proteomics approaches, such as peptide mass fingerprinting, peptide sequence tag approach, and *de novo* sequencing, rely on the bottom-up approach. Finally, the utility of CID and IRMPD was examined and evaluated for structural characterization of highly modified antimicrobial peptides, i.e., lantibiotics.

Chapter 2 explores the application of EDD and negative ion mode IRMPD for the characterization of disulfide bonded peptides. Disulfide bonds are a post-translational modification present in many extracellular proteins and an important component of protein primary structure. The determination of the presence and connectivity of disulfide bonds is of great interest due to their importance for the stabilization of native structures of proteins. In addition, the determination of disulfide bridges is a significant

feature for complete characterization of protein primary structure. Our results demonstrate that EDD and IRMPD of peptide anions containing disulfide linkages result in preferential cleavage of S-S and C-S bonds. We furthermore show that, in EDD, the presence of tryptophan can compete with disulfide bond cleavage. These experiments also provide some insights into the EDD mechanism. This work has been published in the *International Journal of Mass Spectrometry* (2007, volume 263, page 71).

Chapters 3 and 4 focus on examining how precursor ion charge state, m/z ratio, and protease selection influence the ECD outcome. The aim of this work was to examine how peptide sequence coverage can be improved in ECD. Increasing peptide sequence coverage is essential in proteomics research because it facilitates *de novo* sequencing and improves protein identification via database searches. Moreover, improved peptide sequence coverage increases the probability of detecting PTMs. For instance, if product ions containing the modified amino acids are not observed, localization of modification sites is unfeasible.

In Chapter 3, we show that doubly protonated peptides, which are the kind of peptides that most bottom-up approaches rely on, do not fragment efficiently and therefore result in low ECD peptide sequence coverage. Their triply protonated counterparts provided high ECD peptide sequence coverage, reaching complete peptide sequence coverage in several cases. We also show that tryptic peptides exhibit higher ECD sequence coverage compared to chymotryptic and Glu-C digest peptides. This work has been published in the *Journal of Proteome Research* (2008, volume 7, page 2834).

In Chapter 4, ECD of longer triply protonated species is investigated and precursor ions at higher charge states (+4, +5, and +6) are examined. Our results reveal that the major factor affecting ECD outcome is the precursor ion m/z ratio. Triply protonated precursor ions detected at m/z > 960 showed limited fragmentation, in sharp contrast to triply protonated species at low m/z, which showed extensive ECD peptide sequence coverage. The majority of precursor ions at high charge states (+4, +5, and +6) were detected at low m/z values and exhibited good to high ECD peptide sequence coverage. The average percent ECD peptide sequence coverage obtained was almost identical for Lys C, Lys N and Glu C derived peptides.

Chapter 5 investigates the applicability of EID for the dissociation and characterization of singly deprotonated peptides and compares EID fragmentation patterns with those observed in negative ion mode CID of the same species. Obtaining informative spectra from singly protonated species is particularly useful for MALDI generated peptides, because MALDI produces predominantly singly charged ions. However, dissociation of singly charged species is more challenging, compared to that of multiply charged precursor ions because singly charged ions do not dissociate as efficiently as their multiply charged counterparts. Our results show that, in EID of singly deprotonated peptides, formation of *b*-, *y*-, *a*-, *x*-, *c*- and *z*-type product ions is observed. More extensive fragmentation was obtained in EID compared to that obtained in CID and, therefore, EID provides additional structural information. For modified peptides, EID resulted in retention of sulfation and phosphorylation, allowing localization of the modification site.

Chapter 6 focuses on gas-phase dissociation of lantibiotics upon vibrational excitation for obtaining structural information. Negative ion mode CID and IRMPD of native and oxidized lantibiotics is examined. In addition, we examine positive ion mode CID and IRMPD of oxidized lantibiotics. We show that negative ion mode IRMPD reveals information about the number of thioether bridges in such molecules. Some sequence information can be obtained from CID and IRMPD of native and oxidized lantibiotics.

A summary of all results in this dissertation is given in Chapter 7. Finally, two appendices are included. The first appendix demonstrates use of ultra-high resolution FT-ICR mass spectrometry to determine the intrinsic deuterium kinetic isotope effect in glutamate mutase by an intramolecular competition experiment. This work was a collaborative project with Professor Neil Marsh and part of this work has been published in *Angewandte Chemie* (2007, volume 46, page 8455). The second appendix examines the ECD fragmentation behavior of tryptic peptides derivatized with a fixed charge group (tris (2,4,6-trimethoxyphenyl)phosphonium-acetyl group). Our results demonstrate that ECD of doubly charged derivatized tryptic peptides results in formation of solely *c*-type product ions, simplifying spectral interpretation. However, as the precursor m/z value of the derivatized peptides increases, the ECD sequence coverage decreases. For multiply charged precursor ions, the derivatized and underivatized species resulted in identical or almost identical ECD peptide sequence coverage.

1.8. References

1. Wilkins, M. R.; Pasquali, C.; Appel, R. D.; Ou, K.; Golaz, O.; Sanchez, J. C.; Yan, J. X.; Gooley, A. A.; Hughes, G.; HumpherySmith, I.; Williams, K. L.; Hochstrasser, D. F., From proteins to proteomes: Large scale protein identification by two-dimensional electrophoresis and amino acid analysis. *Bio-Technology* **1996,** 14, 61-65.
2. Twyman, R. M., *Principles of Proteomics*. BIOS Scientific Publishers: York, UK, 2004.
3. Pandey, A.; Mann, M., Proteomics to study genes and genomes. *Nature* **2000,** 405, 837-846.
4. Wilkins, M. R.; Sanchez, J. C.; Gooley, A. A.; Appel, R. D.; HumpherySmith, I.; Hochstrasser, D. F.; Williams, K. L., Progress with proteome projects: Why all proteins expressed by a genome should be identified and how to do it. *Biotechnol. Gene Eng. Rev., Vol 13* **1996,** 13, 19-50.
5. Domon, B.; Aebersold, R., Review - Mass spectrometry and protein analysis. *Science* **2006,** 312, 212-217.
6. Gevaert, K.; Vandekerckhove, J., Protein identification methods in proteomics. *Electrophoresis* **2000,** 21, 1145-1154.
7. Phizicky, E.; Bastiaens, P. I. H.; Zhu, H.; Snyder, M.; Fields, S., Protein analysis on a proteomic scale. *Nature* **2003,** 422, 208-215.
8. Cahill, D. J.; Nordhoff, E.; O'Brien, J.; Klose, J.; Eickhoff, H.; Lenhrach, H., Bridging genomics and proteomics. In *Proteomics From protein sequence to function*, Pennington, S. R., Ed. BIOS Scientific New York, 2001.
9. James, P., Mass Spectrometry and the proteome; p1-9. In *Proteome Research: Mass Spectrometry*, James, P., Ed. Springer: New York, 2001.
10. Guerrera, I. C.; Kleiner, O., Application of mass spectrometry in proteomics. *Biosci. Rep.* **2005,** 25, 71-93.
11. Aebersold, R.; Mann, M., Mass spectrometry-based proteomics. *Nature* **2003,** 422, 198-207.
12. Kuster, B.; Mann, M., Identifying proteins and post-translational modifications by mass spectrometry. *Curr. Opin. Struct. Biol.* **1998,** 8, 393-400.
13. Roepstorff, P., Mass spectrometry in protein studies from genome to function. *Curr. Opin. Biotechnol.* **1997,** 8, 6-13.
14. Smith, R. D., Trends in mass spectrometry instrumentation for proteomics. *Trends Biotechnol.* **2002,** 20, S3-S7.
15. Morris, H. R.; Paxton, T.; Dell, A.; Langhorne, J.; Berg, M.; Bordoli, R. S.; Hoyes, J.; Bateman, R. H., High sensitivity collisionally-activated decomposition tandem mass spectrometry on a novel quadrupole/orthogonal-acceleration time-of-flight mass spectrometer. *Rapid Commun. Mass Spectrom.* **1996,** 10, 889-896.
16. Hakansson, K.; Emmett, M. R.; Hendrickson, C. L.; Marshall, A. G., High-sensitivity electron capture dissociation tandem FTICR mass spectrometry of microelectrosprayed peptides. *Anal. Chem.* **2001,** 73, 3605-3610.
17. Valaskovic, G. A.; Kelleher, N. L.; McLafferty, F. W., Attomole protein characterization by capillary electrophoresis mass spectrometry. *Science* **1996,** 273, 1199-1202.

18. Valaskovic, G. A.; Kelleher, N. L.; Little, D. P.; Aaserud, D. J.; McLafferty, F. W., Attomole-Sensitivity Electrospray Source for Large-Molecule Mass-Spectrometry. *Anal. Chem.* **1995,** 67, 3802-3805.
19. Andren, P. E.; Emmett, M. R.; Caprioli, R. M., Micro-Electrospray - Zeptomole-Attomole Per Microliter Sensitivity for Peptides. *J. Am. Soc. Mass Spectrom.* **1994,** 5, 867-869.
20. Bristow, A. W. T., Accurate mass measurement for the determination of elemental formula - A tutorial. *Mass Spectrom. Rev.* **2006,** 25, 99-111.
21. Scherl, A.; Shaffer, S. A.; Taylor, G. K.; Hernandez, P.; Appel, R. D.; Binz, P. A.; Goodlett, D. R., On the benefits of acquiring peptide fragment ions at high measured mass accuracy. *J. Am. Soc. Mass Spectrom.* **2008,** 19, 891-901.
22. Wu, S.; Kaiser, N. K.; Meng, D.; Anderson, G. A.; Zhang, K.; Bruce, J. E., Increased protein identification capabilities through novel tandem MS calibration strategies. *J. Proteome Res.* **2005,** 4, 1434-1441.
23. Zhang, L. K.; Rempel, D.; Pramanik, B. N.; Gross, M. L., Accurate mass measurements by Fourier transform mass spectrometry. *Mass Spectrom. Rev.* **2005,** 24, 286-309.
24. Makarov, A.; Denisov, E.; Lange, O.; Horning, S., Dynamic range of mass accuracy in LTQ orbitrap hybrid mass spectrometer. *J. Am. Soc. Mass Spectrom.* **2006,** 17, 1758-1758.
25. Olsen, J. V.; de Godoy, L. M. F.; Li, G. Q.; Macek, B.; Mortensen, P.; Pesch, R.; Makarov, A.; Lange, O.; Horning, S.; Mann, M., Parts per million mass accuracy on an orbitrap mass spectrometer via lock mass injection into a C-trap. *Mol. Cell. Proteomics* **2005,** 4, 2010-2021.
26. Olsen, J. V.; Mann, M., Improved peptide identification in proteomics by two consecutive stages of mass spectrometric fragmentation. *Proc. Natl. Acad. Sci. USA* **2004,** 101, 13417-13422.
27. Palmblad, M.; Wetterhall, M.; Markides, K.; Hakansson, P.; Bergquist, J., Analysis of enzymatically digested proteins and protein mixtures using a 9.4 Tesla Fourier transform ion cyclotron mass spectrometer. *Rapid Commun. Mass Spectrom.* **2000,** 14, 1029-1034.
28. Bruce, J. E.; Anderson, G. A.; Wen, J.; Harkewicz, R.; Smith, R. D., High mass-measurement accuracy and 100% sequence coverage of enzymatically digested bovine serum albumin from an ESI-FTICR mass spectrum. *Anal. Chem.* **1999,** 71, 2595-2599.
29. Aebersold, R.; Goodlett, D. R., Mass spectrometry in proteomics. *Chem. Rev.* **2001,** 101, 269-295.
30. Mann, M.; Jensen, O. N., Proteomic analysis of post-translational modifications. *Nat. Biotechnol.* **2003,** 21, 255-261.
31. Meng, F. Y.; Forbes, A. J.; Miller, L. M.; Kelleher, N. L., Detection and localization of protein modifications by high resolution tandem mass spectrometry. *Mass Spectrom. Rev.* **2005,** 24, 126-134.
32. Fenselau, C.; Vestling, M. M.; Cotter, R. J., Mass spectrometric analysis of proteins. *Curr. Opin. Biotechnol.* **1993,** 4, 14-19.

33. Fenn, J. B.; Mann, M.; Meng, C. K.; Wong, S. F.; Whitehouse, C. M., Electrospray Ionization for Mass-Spectrometry of Large Biomolecules. *Science* **1989,** 246, 64-71.
34. Fenn, J. B.; Mann, M.; Meng, C. K.; Wong, S. F.; Whitehouse, C. M., Electrospray Ionization-Principles and Practice. *Mass Spectrom. Rev.* **1990,** 9, 37-70.
35. Hillenkamp, F.; Karas, M.; Beavis, R. C.; Chait, B. T., Matrix-Assisted Laser Desorption Ionization Mass-Spectrometry of Biopolymers. *Anal. Chem.* **1991,** 63, A1193-A1202.
36. Tanaka, K.; Waki, H.; Ido, Y.; Akita, S.; Yoshida, Y.; Yoshida, T.; Matsuo, T., Protein and polymer analyses up to m/z 100 000 by laser ionization time-of-flight mass spectrometry. *Rapid Commun. Mass Spectrom.* **1988,** 2, 151-153.
37. Fenselau, C., Beyond Gene Sequencing - Analysis of Protein-Structure with Mass-Spectrometry. *Annu. Rev. Biophys. Biophys. Chem.* **1991,** 20, 205-220.
38. Patterson, S. D.; Aebersold, R. H., Proteomics: the first decade and beyond. *Nat. Genet.* **2003,** 33, 311-323.
39. Rappsilber, J.; Mann, M., What does it mean to identify a protein in proteomics? *Trends Biochem. Sci.* **2002,** 27, 74-78.
40. Henzel, W. J.; Billeci, T. M.; Stults, J. T.; Wong, S. C.; Grimley, C.; Watanabe, C., Identifying Proteins from 2-Dimensional Gels by Molecular Mass Searching of Peptide-Fragments in Protein-Sequence Databases. *Proc. Natl. Acad. Sci. USA* **1993,** 90, 5011-5015.
41. James, P.; Quadroni, M.; Carafoli, E.; Gonnet, G., Protein Identification by Mass Profile Fingerprinting. *Biochem. Biophys. Res. Commun.* **1993,** 195, 58-64.
42. Pappin, D. J. C.; Hojrup, P.; Bleasby, A. J., Rapid Identification of Proteins by Peptide-Mass Finger Printing *Curr. Biol.* **1993,** 3, 327-332.
43. Yates, J. R.; Speicher, S.; Griffin, P. R.; Hunkapiller, T., Peptide Mass Maps - a Highly Informative Approach to Protein Identification. *Anal. Biochem.* **1993,** 214, 397-408.
44. Morris, H. R.; Panico, M.; Taylor, G. W., Fab-Mapping of Recombinant-DNA Protein Products. *Biochem. Biophys. Res. Commun.* **1983,** 117, 299-305.
45. Mann, M.; Hojrup, P.; Roepstorff, P., Use of Mass-Spectrometric Molecular-Weight Information to Identify Proteins in Sequence Databases. *Biol. Mass Spectrom.* **1993,** 22, 338-345.
46. Baldwin, M. A., Protein identification by mass spectrometry - Issues to be considered. *Mol. Cell. Proteomics* **2004,** 3, 1-9.
47. Jensen, O. N.; Podtelejnikov, A. V.; Mann, M., Identification of the components of simple protein mixtures by high accuracy peptide mass mapping and database searching. *Anal. Chem.* **1997,** 69, 4741-4750.
48. Fenyo, D.; Qin, J.; Chait, B. T., Protein identification using mass spectrometric information. *Electrophoresis* **1998,** 19, 998-1005.
49. Dainese, P.; James, P., Protein Identification by Peptide-Mass Fingerprinting. In *Proteome Research: Mass Specrtrometry*, James, P., Ed. Springer: New York, 2001.
50. Patterson, S. D.; Aebersold, R.; Goodlett, D. R., Mass spectrometry-based methods for protein identification and phosphorylation site analysis. In

Proteomics From protein to function, Pennington, S. R.; Dunn, M. J., Eds. BIOS Scientific Publishers: New York, 2001.
51. McLafferty, F. W., *Tandem Mass Spectrometry*. Wiley: New York, 1983.
52. Wilm, M.; Mann, M., Analytical properties of the nanoelectrospray ion source. *Anal. Chem.* **1996,** 68, 1-8.
53. Eng, J. K.; McCormack, A. L.; Yates, J. R., An Approach to Correlate Tandem Mass-Spectral Data of Peptides with Amino-Acid-Sequences in a Protein Database. *J. Am. Soc. Mass Spectrom.* **1994,** 5, 976-989.
54. Mann, M.; Wilm, M., Error Tolerant Identification of Peptides in Sequence Databases by Peptide Sequence Tags. *Anal. Chem.* **1994,** 66, 4390-4399.
55. Mann, M., A shortcut to interesting human genes: Peptide sequence tags, expressed-sequence tags and computers. *Trends Bioechem. Sci.* **1996,** 21, 494-495.
56. Hayes, R. N.; Gross, M. L., Collision-Induced Dissociation. *Methods Enzymol.* **1990,** 193, 237-263.
57. McLuckey, S. A., Principles of Collisional Activation in Analytical Mass-Spectrometry. *J. Am. Soc. Mass Spectrom.* **1992,** 3, 599-614.
58. Link, A. J.; Eng, J.; Schieltz, D. M.; Carmack, E.; Mize, G. J.; Morris, D. R.; Garvik, B. M.; Yates, J. R., Direct analysis of protein complexes using mass spectrometry. *Nat. Biotechnol.* **1999,** 17, 676-682.
59. Mann, M.; Hendrickson, R. C.; Pandey, A., Analysis of proteins and proteomes by mass spectrometry. *Annu. Rev. Biochem.* **2001,** 70, 437-473.
60. Reinders, J.; Lewandrowski, U.; Moebius, J.; Wagner, Y.; Sickmann, A., Challenges in mass spectrometry-based proteomics. *Proteomics* **2004,** 4, 3686-3703.
61. Branca, R. M. M.; Bodo, G.; Bagyinka, C.; Prokai, L., De novo sequencing of a 21-kDa cytochrome c(4) from Thiocapsa roseopersicina by nanoelectrospray ionization ion-trap and Fourier-transform icon-cyclotron resonance mass spectrometry. *J. Mass. Spectrom.* **2007,** 42, 1569-1582.
62. Edman, P., Method for Determination of the Amino Acid Sequence in Peptides. *Acta Chem. Scand.* **1950,** 4, 283-293.
63. Edman, P.; Begg, G., A Protein Sequenator. *Eur. J. Biochem.* **1967,** 1, 80-91.
64. Metzger, J. W., Ladder Sequencing of Peptides and Proteins - a Combination of Edman Degradation and Mass-Spectrometry. *Angew. Chem. Int. Ed.* **1994,** 33, 723-725.
65. Aebersold, R.; Bures, E. J.; Namchuk, M.; Goghari, M. H.; Shushan, B.; Covey, T. C., Design, Synthesis, and Characterization of a Protein Sequencing Reagent Yielding Amino-Acid Derivatives with Enhanced Detectability by Mass-Spectrometry. *Protein Sci.* **1992,** 1, 494-503.
66. Katakuse, I.; Matsuo, T.; Matsuda, H.; Shimonishi, Y.; Hong, Y. M.; Izumi, Y., Sequence Determination of a Peptide with 55 Amino-Acid-Residues by Edman Degradation and Field Desorption Mass-Spectrometry. *Biomed. Mass Spectrom.* **1982,** 9, 64-68.
67. Chait, B. T.; Wang, R.; Beavis, R. C.; Kent, S. B. H., Protein Ladder Sequencing. *Science* **1993,** 262, 89-92.

68. Johnson, R. S.; Biemann, K., The Primary Structure of Thioredoxin from Chromatium Vinosum Determined by High-Performance Tandem Mass-Spectrometry. *Biochemistry* **1987,** 26, 1209-1214.
69. Brown, J. L.; Roberts, W. K., Evidence That Approximately 80 Per Cent of Soluble-Proteins from Ehrlich Ascites-Cells Are N-Alpha-Acetylated. *J. Biol. Chem.* **1976,** 251, 1009-1014.
70. Nokihara, K., Procedures leading to primary structure determination of proteins in complex mixtures by gel electrophoresis and modern micro-scale analyses. *Anal. Chim. Acta* **1998,** 372, 21-32.
71. Aebersold, R. H.; Teplow, D. B.; Hood, L. E.; Kent, S. B. H., Electroblotting onto Activated Glass - High-Efficiency Preparation of Proteins from Analytical Sodium Dodecyl Sulfate-Polyacrylamide Gels for Direct Sequence-Analysis. *J. Biol. Chem.* **1986,** 261, 4229-4238.
72. Vandekerckhove, J.; Bauw, G.; Puype, M.; Vandamme, J.; Vanmontagu, M., Protein-Blotting on Polybrene-Coated Glass-Fiber Sheets - a Basis for Acid-Hydrolysis and Gas-Phase Sequencing of Picomole Quantities of Protein Previously Separated on Sodium Dodecyl-Sulfate Polyacrylamide-Gel. *Eur. J. Biochem.* **1985,** 152, 9-19.
73. Aebersold, R. H.; Leavitt, J.; Saavedra, R. A.; Hood, L. E.; Kent, S. B. H., Internal Amino-Acid Sequence-Analysis of Proteins Separated by One-Dimensional or Two-Dimensional Gel-Electrophoresis after Insitu Protease Digestion on Nitrocellulose. *Proc. Natl. Acad. Sci. USA* **1987,** 84, 6970-6974.
74. Aebersol, R., Mass spectrometry of proteins and peptides in biotechnology. *Curr. Opin. Biotechnol.* **1993,** 4, 412-419.
75. Meyer, H. E.; Hoffmannposorske, E.; Donelladeana, A.; Korte, H., Sequence-Analysis of Phosphotyrosine-Containing Peptides. *Methods Enzymol.* **1991,** 201, 206-224.
76. Meyer, H. E.; Hoffmannposorske, E.; Korte, H.; Heilmeyer, L. M. G., Sequence-Analysis of Phosphoserine-Containing Peptides - Modification for Picomolar Sensitivity. *Febs Lett.* **1986,** 204, 61-66.
77. Khidekel, N.; Hsieh-Wilson, L. C., A 'molecular switchboard' - covalent modifications to proteins and their impact on transcription. *Org. Biomol. Chem.* **2004,** 2, 1-7.
78. Biemann, K.; Papayannopoulos, I. A., Amino-Acid Sequencing of Proteins. *Acc. Chem. Res.* **1994,** 27, 370-378.
79. Gooley, A. A.; Ou, K.; Russell, J.; Wilkins, M. R.; Sanchez, J. C.; Hochstrasser, D. F.; Williams, K. L., A role for Edman degradation in proteome studies. *Electrophoresis* **1997,** 18, 1068-1072.
80. Palzkill, T., *Proteomics*. Kluwer Academic Publishers: Norwell, 2002.
81. Totty, N. F.; Waterfield, M. D.; Hsuan, J. J., Accelerated High-Sensitivity Microsequencing of Proteins and Peptides Using a Miniature Reaction Cartridge. *Protein Sci.* **1992,** 1, 1215-1224.
82. Wilkins, M. R.; Gooley, A. A., Protein Identification in Proteomics Project. In *Proteome Research: New Frontiers in Functional Genomics*, Wilkins, M. R. W., K L.; Appel, R.D.; Hochstrasser, D.F., Ed. Springer: New York, 1997.

83. Standing, K. G., Peptide and protein de novo sequencing by mass spectrometry. *Curr. Opin. Struct. Biol.* **2003,** 13, 595-601.
84. Creighton, T. E., *Proteins Structures and Molecular Properties*. W.H. Freeman and Company: New York, 1993.
85. Speicher, D. W., Overview of proteome analysis. In *Proteome Analysis Interpreting the Genome*, Speicher, D. W., Ed. Elsevier: Oxford, UK, 2004.
86. Comisarow, M. B.; Marshall, A. G., Frequency-Sweep Fourier-Transform Ion-Cyclotron Resonance Spectroscopy. *Chem. Phys. Lett.* **1974,** 26, 489-490.
87. Comisarow, M. B.; Marshall, A. G., Fourier-Transform Ion-Cyclotron Resonance Spectroscopy. *Chem. Phys. Lett.* **1974,** 25, 282-283.
88. Marshall, A. G.; Grosshans, P. B., Fourier-Transform Ion-Cyclotron Resonance Mass-Spectrometry - the Teenage Years. *Anal. Chem.* **1991,** 63, A215-A229.
89. Marshall, A. G.; Guan, S. H., Advantages of high magnetic field for Fourier transform ion cyclotron resonance mass spectrometry. *Rapid Commun. Mass Spectrom.* **1996,** 10, 1819-1823.
90. Marshall, A. G.; Hendrickson, C. L.; Jackson, G. S., Fourier transform ion cyclotron resonance mass spectrometry: A primer. *Mass Spectrom. Rev.* **1998,** 17, 1-35.
91. Marshall, A. G.; Hendrickson, C. L., Fourier transform ion cyclotron resonance detection: principles and experimental configurations. *Int. J. Mass Spectrom.* **2002,** 215, 59-75.
92. Guan, S. H.; Marshall, A. G., Ion Traps for Fourier-Transform Ion-Cyclotron Resonance Mass-Spectrometry - Principles and Design of Geometric and Electric Configurations. *Int. J. Mass Spectrom. Ion Processes* **1995,** 146, 261-296.
93. Amster, I. J., Fourier transform mass spectrometry. *J. Mass Spectrom.* **1996,** 31, 1325-1337.
94. Heeren, R. M. A.; Kleinnijenhuis, A. J.; McDonnell, L. A.; Mize, T. H., A mini-review of mass spectrometry using high-performance FTICR-MS methods. *Anal. Bioanal. Chem.* **2004,** 378, 1048-1058.
95. Freitas, M. A.; Hendrickson, C. L.; Emmett, M. R.; Marshall, A. G., High-field Fourier transform ion cyclotron resonance mass spectrometry for simultaneous trapping and gas-phase hydrogen/deuterium exchange of peptide ions. *J. Am. Soc. Mass Spectrom.* **1998,** 9, 1012-1019.
96. Hendrickson, C. L.; Emmett, M. R., Electrospray ionization Fourier transform ion cyclotron resonance mass spectrometry. *Annu. Rev. Phys. Chem.* **1999,** 50, 517-536.
97. Barrow, M. P.; Burkitt, W. I.; Derrick, P. J., Principles of Fourier transform ion cyclotron resonance mass spectrometry and its application in structural biology. *Analyst* **2005,** 130, 18-28.
98. Caravatti, P.; Allemann, M., The Infinity Cell - a New Trapped-Ion Cell with Radiofrequency Covered Trapping Electrodes for Fourier-Transform Ion-Cyclotron Resonance Mass-Spectrometry. *Org. Mass Spectrom.* **1991,** 26, 514-518.
99. Julian, R. R.; Mabbett, S. R.; Jarrold, M. F., Ion funnels for the masses: Experiments and simulations with a simplified ion funnel. *J. Am. Soc. Mass Spectrom.* **2005,** 16, 1708-1712.

100. Shaffer, S. A.; Tolmachev, A.; Prior, D. C.; Anderson, G. A.; Udseth, H. R.; Smith, R. D., Characterization of an improved electrodynamic ion funnel interface for electrospray ionization mass spectrometry. *Anal. Chem.* **1999,** 71, 2957-2964.
101. Shaffer, S. A.; Prior, D. C.; Anderson, G. A.; Udseth, H. R.; Smith, R. D., An ion funnel interface for improved ion focusing and sensitivity using electrospray ionization mass spectrometry. *Anal. Chem.* **1998,** 70, 4111-4119.
102. Shaffer, S. A.; Tang, K. Q.; Anderson, G. A.; Prior, D. C.; Udseth, H. R.; Smith, R. D., A novel ion funnel for focusing ions at elevated pressure using electrospray ionization mass spectrometry. *Rapid Commun. Mass Spectom.* **1997,** 11, 1813-1817.
103. Belov, M. E.; Nikolaev, E. N.; Anderson, G. A.; Auberry, K. J.; Harkewicz, R.; Smith, R. D., Electrospray ionization-Fourier transform ion cyclotron mass spectrometry using ion preselection and external accumulation for ultrahigh sensitivity. *J. Am. Soc. Mass Spectrom.* **2001,** 12, 38-48.
104. Tsybin, Y. O.; Witt, M.; Baykut, G.; Kjeldsen, F.; Hakansson, P., Combined infrared multiphoton dissociation and electron capture dissociation with a hollow electron beam in Fourier transform ion cyclotron resonance mass spectrometry. *Rapid Commun. Mass Spectrom.* **2003,** 17, 1759-1768.
105. Bogdanov, B.; Smith, R. D., Proteomics by FTICR mass spectrometry: Top down and bottom up. *Mass Spectrom. Rev.* **2005,** 24, 168-200.
106. Green, M. K.; Vestling, M. M.; Johnston, M. V.; Larsen, B. S., Distinguishing small molecular mass differences of proteins by mass spectrometry. *Anal. Biochem.* **1998,** 260, 204-211.
107. Conrads, T. P.; Anderson, G. A.; Veenstra, T. D.; Pasa-Tolic, L.; Smith, R. D., Utility of accurate mass tags for proteome-wide protein identification. *Anal. Chem.* **2000,** 72, 3349-3354.
108. Yates, J. R., Database searching using mass spectrometry data. *Electrophoresis* **1998,** 19, 893-900.
109. Marshall, A. G.; Comisarow, M. B.; Parisod, G., Theory of Fourier-Transform Ion-Cyclotron Resonance Mass Spectroscopy-Iii .1. Relaxation and Spectral-Line Shape in Fourier-Transform Ion Resonance Spectroscopy. *J. Chem. Phys.* **1979,** 71, 4434-4444.
110. Kelleher, N. L.; Senko, M. W.; Siegel, M. M.; McLafferty, F. W., Unit resolution mass spectra of 112 kDa molecules with 3 Da accuracy. *J. Am. Soc. Mass Spectrom.* **1997,** 8, 380-383.
111. Henry, K. D.; McLafferty, F. W., Electrospray Ionization with Fourier-Transform Mass-Spectrometry - Charge State Assignment from Resolved Isotopic Peaks. *Org. Mass Spectrom.* **1990,** 25, 490-492.
112. He, F.; Hendrickson, C. L.; Marshall, A. G., Baseline mass resolution of peptide isobars: A record for molecular mass resolution. *Anal. Chem.* **2001,** 73, 647-650.
113. Gauthier, J. W.; Trautman, T. R.; Jacobson, D. B., Sustained Off-Resonance Irradiation for Collision-Activated Dissociation Involving Fourier-Transform Mass-Spectrometry - Collision-Activated Dissociation Technique That Emulates Infrared Multiphoton Dissociation. *Anal. Chim. Acta* **1991,** 246, 211-225.
114. Dunbar, R. C.; McMahon, T. B., Activation of unimolecular reactions by ambient blackbody radiation. *Science* **1998,** 279, 194-197.

115. Price, W. D.; Schnier, P. D.; Williams, E. R., Tandem mass spectrometry of large biomolecule ions by blackbody infrared radiative dissociation. *Anal. Chem.* **1996,** 68, 859-866.
116. Little, D. P.; Speir, J. P.; Senko, M. W.; Oconnor, P. B.; McLafferty, F. W., Infrared Multiphoton Dissociation of Large Multiply-Charged Ions for Biomolecule Sequencing. *Anal. Chem.* **1994,** 66, 2809-2815.
117. Woodin, R. L.; Bomse, D. S.; Beauchamp, J. L., Multi-Photon Dissociation of Molecules with Low-Power Continuous Wave Infrared-Laser Radiation. *J. Am. Chem. Soc.* **1978,** 100, 3248-3250.
118. Laskin, J.; Denisov, E. V.; Shukla, A. K.; Barlow, S. E.; Futrell, J. H., Surface-induced dissociation in a Fourier transform ion cyclotron resonance mass spectrometer: Instrument design and evaluation. *Anal. Chem.* **2002,** 74, 3255-3261.
119. Laskin, J.; Denisov, E.; Futrell, J., Comparative study of collision-induced and surface-induced dissociation. 2. Fragmentation of small alanine-containing peptides in FT-ICR MS. *J. Phys. Chem. B* **2001,** 105, 1895-1900.
120. Dongre, A. R.; Somogyi, A.; Wysocki, V. H., Surface-induced dissociation: An effective tool to probe structure, energetics and fragmentation mechanisms of protonated peptides. *J. Mass Spectrom.* **1996,** 31, 339-350.
121. Chorush, R. A.; Little, D. P.; Beu, S. C.; Wood, T. D.; McLafferty, F. W., Surface-Induced Dissociation of Multiply Protonated Proteins. *Anal. Chem.* **1995,** 67, 1042-1046.
122. Ijames, C. F.; Wilkins, C. L., Surface-Induced Dissociation by Fourier-Transform Mass-Spectrometry. *Anal. Chem.* **1990,** 62, 1295-1299.
123. Mabud, M. D. A.; Dekrey, M. J.; Cooks, R. G., Surface-Induced Dissociation of Molecular-Ions. *Int. J. Mass Spectrom. Ion Processes* **1985,** 67, 285-294.
124. Zubarev, R. A., Electron-capture dissociation tandem mass spectrometry. *Curr. Opin. Biotechnol.* **2004,** 15, 12-16.
125. Zubarev, R. A.; Kelleher, N. L.; McLafferty, F. W., Electron capture dissociation of multiply charged protein cations. A nonergodic process. *J. Am. Chem. Soc.* **1998,** 120, 3265-3266.
126. Budnik, B. A.; Haselmann, K. F.; Zubarev, R. A., Electron detachment dissociation of peptide di-anions: an electron-hole recombination phenomenon. *Chem. Phys. Lett.* **2001,** 342, 299-302.
127. Kjeldsen, F.; Silivra, O. A.; Ivonin, I. A.; Haselmann, K. F.; Gorshkov, M.; Zubarev, R. A., C-alpha-C backbone fragmentation dominates in electron detachment dissociation of gas-phase polypeptide polyanions. *Chem. Eur. J.* **2005,** 11, 1803-1812.
128. McLuckey, S. A.; Goeringer, D. E., Slow heating methods in tandem mass spectrometry. *J. Mass Spectrom.* **1997,** 32, 461-474.
129. Roepstorff, P.; Fohlman, J., Proposal for a Common Nomenclature for Sequence Ions in Mass-Spectra of Peptides. *Biomed. Mass Spectrom.* **1984,** 11, 601-601.
130. Sleno, L.; Volmer, D. A., Ion activation methods for tandem mass spectrometry. *J. Mass Spectrom.* **2004,** 39, 1091-1112.
131. Laskin, J.; Futrell, J. H., Activation of large ions in FT-ICR mass spectrometry. *Mass Spectrom. Rev.* **2005,** 24, 135-167.

132. Dongre, A. R.; Jones, J. L.; Somogyi, A.; Wysocki, V. H., Influence of peptide composition, gas-phase basicity, and chemical modification on fragmentation efficiency: Evidence for the mobile proton model. *J. Am. Chem. Soc.* **1996,** 118, 8365-8374.
133. Paizs, P.; Suhai, S., Fragmentation pathways of protonated peptides. *Mass Spectrom. Rev.* **2005,** 24, 508-548.
134. Wysocki, V. H.; Tsaprailis, G.; Smith, L. L.; Breci, L. A., Special feature: Commentary - Mobile and localized protons: a framework for understanding peptide dissociation. *J. Mass Spectrom.* **2000,** 35, 1399-1406.
135. Biemann, K.; Martin, S. A., Mass-Spectrometric Determination of the Amino-Acid-Sequence of Peptides and Proteins. *Mass Spectrom. Rev.* **1987,** 6, 1-75.
136. Tsaprailis, G.; Nair, H.; Somogyi, A.; Wysocki, V. H.; Zhong, W. Q.; Futrell, J. H.; Summerfield, S. G.; Gaskell, S. J., Influence of secondary structure on the fragmentation of protonated peptides. *J. Am. Chem. Soc.* **1999,** 121, 5142-5154.
137. Kruger, N. A.; Zubarev, R. A.; Carpenter, B. K.; Kelleher, N. L.; Horn, D. M.; McLafferty, F. W., Electron capture versus energetic dissociation of protein ions. *Int. J. Mass Spectrom.* **1999,** 183, 1-5.
138. Zubarev, R. A., Reactions of polypeptide ions with electrons in the gas phase. *Mass Spectrom. Rev.* **2003,** 22, 57-77.
139. Zubarev, R. A.; Haselmann, K. F.; Budnik, B.; Kjeldsen, F.; Jensen, F., Towards an understanding of the mechanism of electron-capture dissociation: a historical perspective and modern ideas. *Eur. J. Mass Spectrom.* **2002,** 8, 337-349.
140. Syrstad, E. A.; Turecek, F., Hydrogen atom adducts to the amide bond. Generation and energetics of the amino(hydroxy)methyl radical in the gas phase. *J. Phys. Chem. A* **2001,** 105, 11144-11155.
141. Turecek, F., N-C-alpha bond dissociation energies and kinetics in amide and peptide radicals. Is the dissociation a non-ergodic process? *J. Am. Chem. Soc.* **2003,** 125, 5954-5963.
142. Turecek, F.; Syrstad, E. A., Mechanism and energetics of intramolecular hydrogen transfer in amide and peptide radicals and cation-radicals. *J. Am. Chem. Soc.* **2003,** 125, 3353-3369.
143. Turecek, F.; Syrstad, E. A.; Seymour, J. L.; Chen, X. H.; Yao, C. X., Peptide cation-radicals. A computational study of the competition between peptide N-C alpha, bond cleavage and loss of the side chain in the GlyPhe-NH2+2H (+center dot) cation-radical. *J. Mass Spectrom.* **2003,** 38, 1093-1104.
144. Zubarev, R. A.; Horn, D. M.; Fridriksson, E. K.; Kelleher, N. L.; Kruger, N. A.; Lewis, M. A.; Carpenter, B. K.; McLafferty, F. W., Electron capture dissociation for structural characterization of multiply charged protein cations. *Anal. Chem.* **2000,** 72, 563-573.
145. Anusiewicz, W.; Berdys-Kochanska, J.; Simons, J., Electron attachment step in electron capture dissociation (ECD) and electron transfer dissociation (ETD). *J. Phys. Chem. A* **2005,** 109, 5801-5813.
146. Chen, X. H.; Turecek, F., The arginine anomaly: Arginine radicals are poor hydrogen atom donors in electron transfer induced dissociations. *J. Am. Chem. Soc.* **2006,** 128, 12520-12530.

147. Sobczyk, M.; Anusiewicz, W.; Berdys-Kochanska, J.; Sawicka, A.; Skurski, P.; Simons, J., Coulomb-assisted dissociative electron attachment: Application to a model peptide. *J. Phys. Chem. A* **2005,** 109, 250-258.
148. Syrstad, E. A.; Turecek, F., Toward a general mechanism of electron capture dissociation. *J. Am. Soc. Mass Spectrom.* **2005,** 16, 208-224.
149. Chalmers, M. J.; Hakansson, K.; Johnson, R.; Smith, R.; Shen, J. W.; Emmett, M. R.; Marshall, A. G., Protein kinase A phosphorylation characterized by tandem Fourier transform ion cyclotron resonance mass spectrometry. *Proteomics* **2004,** 4, 970-981.
150. Coon, J. J.; Ueberheide, B.; Syka, J. E. P.; Dryhurst, D. D.; Ausio, J.; Shabanowitz, J.; Hunt, D. F., Protein identification using sequential ion/ion reactions and tandem mass spectrometry. *Proc. Natl. Acad. Sci. U.S.A* **2005,** 102, 9463-9468.
151. Kjeldsen, F.; Haselmann, K. F.; Budnik, B. A.; Sorensen, E. S.; Zubarev, R. A., Complete characterization of posttranslational modification sites in the bovine milk protein PP3 by tandem mass spectrometry with electron capture dissociation as the last stage. *Anal. Chem.* **2003,** 75, 2355-2361.
152. Kweon, H. K.; Hakansson, K., Metal oxide-based enrichment combined with gas-phase ion-electron reactions for improved mass spectrometric characterization of protein phosphorylation. *J. Proteome. Res.* **2008,** 7, 749-755.
153. Stensballe, A.; Jensen, O. N.; Olsen, J. V.; Haselmann, K. F.; Zubarev, R. A., Electron capture dissociation of singly and multiply phosphorylated peptides. *Rapid Commun. Mass Spectrom.* **2000,** 14, 1793-1800.
154. Adamson, J. T.; Hakansson, K., Infrared multiphoton dissociation and electron capture dissociation of high-mannose type glycopeptides. *J. Proteome Res.* **2006,** 5, 493-501.
155. Hakansson, K.; Cooper, H. J.; Emmett, M. R.; Costello, C. E.; Marshall, A. G.; Nilsson, C. L., Electron capture dissociation and infrared multiphoton dissociation MS/MS of an N-glycosylated tryptic peptide to yield complementary sequence information. *Anal. Chem.* **2001,** 73, 4530-4536.
156. Haselmann, K. F.; Budnik, B. A.; Olsen, J. V.; Nielsen, M. L.; Reis, C. A.; Clausen, H.; Johnsen, A. H.; Zubarev, R. A., Advantages of external accumulation for electron capture dissociation in Fourier transform mass spectrometry. *Anal. Chem.* **2001,** 73, 2998-3005.
157. Mirgorodskaya, E.; Roepstorff, P.; Zubarev, R. A., Localization of O-glycosylation sites in peptides by electron capture dissociation in a fourier transform mass spectrometer. *Anal. Chem.* **1999,** 71, 4431-4436.
158. Kelleher, R. L.; Zubarev, R. A.; Bush, K.; Furie, B.; Furie, B. C.; McLafferty, F. W.; Walsh, C. T., Localization of labile posttranslational modifications by electron capture dissociation: The case of gamma-carboxyglutamic acid. *Anal. Chem.* **1999,** 71, 4250-4253.
159. Liu, H.; Hakansson, K., Electron capture dissociation of tyrosine O-sulfated peptides complexed with divalent metal cations. *Anal. Chem.* **2006,** 78, 7570-7576.
160. Zubarev, R. A.; Kruger, N. A.; Fridriksson, E. K.; Lewis, M. A.; Horn, D. M.; Carpenter, B. K.; McLafferty, F. W., Electron capture dissociation of gaseous

multiply-charged proteins is favored at disulfide bonds and other sites of high hydrogen atom affinity. *J. Am. Chem. Soc.* **1999,** 121, 2857-2862.
161. Axelsson, J.; Palmblad, M.; Hakansson, K.; Hakansson, P., Electron capture dissociation of substance P using a commercially available Fourier transform ion cyclotron resonance mass spectrometer. *Rapid Commun. Mass Spectrom.* **1999,** 13, 474-477.
162. Cooper, H. J.; Hakansson, K.; Marshall, A. G., The role of electron capture dissociation in biomolecular analysis. *Mass Spectrom. Rev.* **2005,** 24, 201-222.
163. Kruger, N. A.; Zubarev, R. A.; Horn, D. M.; McLafferty, F. W., Electron capture dissociation of multiply charged peptide cations. *Int. J. Mass Spectrom.* **1999,** 187, 787-793.
164. Zubarev, R., Protein primary structure using orthogonal fragmentation techniques in Fourier transform mass spectrometry. *Expert Rev. Proteomics* **2006,** 3, 251-261.
165. Gorshkov, M. V.; Masselon, C. D.; Nikolaev, E. N.; Udseth, H. R.; Pasa-Tolic, L.; Smith, R. D., Considerations for electron capture dissociation efficiency in FTICR mass spectrometry. *Int. J. Mass Spectrom.* **2004,** 234, 131-136.
166. McFarland, M. A.; Chalmers, M. J.; Quinn, J. P.; Hendrickson, C. L.; Marshall, A. G., Evaluation and optimization of electron capture dissociation efficiency in Fourier transform ion cyclotron resonance mass spectrometry. *J. Am. Soc. Mass Spectrom.* **2005,** 16, 1060-1066.
167. Mormann, M.; Peter-Katalinic, J., Improvement of electron capture efficiency by resonant excitation. *Rapid Commun. Mass Spectrom.* **2003,** 17, 2208-2214.
168. Anusiewicz, I.; Jasionowski, M.; Skurski, P.; Simons, J., Backbone and side-chain cleavages in electron detachment dissociation (EDD). *J. Phys. Chem. A* **2005,** 109, 11332-11337.
169. Yang, J.; Mo, J. J.; Adamson, J. T.; Hakansson, K., Characterization of oligodeoxynucleotides by electron detachment dissociation Fourier transform ion cyclotron resonance mass spectrometry. *Anal. Chem.* **2005,** 77, 1876-1882.
170. Mo, J.; Hakansson, K., Characterization of nucleic acid higher order structure by high-resolution tandem mass spectrometry. *Anal. Bioanal. Chem.* **2006**.
171. McFarland, M. A.; Marshall, A. G.; Hendrickson, C. L.; Nilsson, C. L.; Fredman, P.; Mansson, J. E., Structural characterization of the GM1 ganglioside by infrared multiphoton dissociation/electron capture dissociation, and electron detachment dissociation electrospray ionization FT-ICR MS/MS. *J. Am. Soc. Mass Spectrom.* **2005,** 16, 752-762.
172. Adamson, J. T.; Hakansson, K., Electron detachment dissociation of neutral and sialylated oligosaccharides. *J. Am. Soc. Mass Spectrom.* **2007,** 18, 2162-2172.
173. Wolff, J. J.; Amster, I. J.; Chi, L. L.; Linhardt, R. J., Electron detachment dissociation of glycosaminoglycan tetrasaccharides. *J. Am. Soc. Mass Spectrom.* **2007,** 18, 234-244.
174. Budnik, B. A.; Haselmann, K. F.; Elkin, Y. N.; Gorbach, V. I.; Zubarev, R. A., Applications of electron-ion dissociation reactions for analysis of polycationic chitooligosaccharides in Fourier transform mass spectrometry. *Anal. Chem.* **2003,** 75, 5994-6001.

175. Gord, J. R.; Horning, S. R.; Wood, J. M.; Cooks, R. G.; Freiser, B. S., Energy Deposition During Electron-Induced Dissociation. *J. Am. Soc. Mass Spectrom.* **1993,** 4, 145-151.
176. Cody, R. B.; Freiser, B. S., Electron-Impact Excitation of Ions from Organics - Alternative to Collision-Induced Dissociation. *Anal. Chem.* **1979,** 51, 547-551.
177. Cody, R. B.; Freiser, B. S., Electron-Impact Excitation of Ions in Fourier-Transform Mass-Spectrometry. *Anal. Chem.* **1987,** 59, 1054-1056.
178. Wang, B. H.; McLafferty, F. W., Electron-Impact Excitation of Ions from Larger Organic-Molecules. *Org. Mass Spectrom.* **1990,** 25, 554-556.
179. Lioe, H.; O'Hair, R. A. J., Comparison of collision-induced dissociation and electron-induced dissociation of singly protonated aromatic amino acids, cystine and related simple peptides using a hybrid linear ion trap-FT-ICR mass spectrometer. *Anal. Bioanal. Chem.* **2007,** 389, 1429-1437.
180. Yoo, H. J.; Liu, H. C.; Hakansson, K., Infrared multiphoton dissociation and electron-induced dissociation as alternative MS/MS strategies for metabolite identification. *Anal. Chem.* **2007,** 79, 7858-7866.
181. Wolff, J. J.; Laremore, T. N.; Aslam, H.; Linhardt, R. J.; Amster, I. J., Electron-Induced Dissociation of Glycosaminoglycan Tetrasaccharides. *J. Am. Soc. Mass Spectrom.* **2008,** 19, 1449-1458.
182. Nagao, J. I.; Asaduzzaman, S. M.; Aso, Y.; Okuda, K.; Nakayama, J.; Sonomoto, K., Lantibiotics: Insight and foresight for new paradigm. *J. Biosci. Bioeng.* **2006,** 102, 139-149.
183. Patton, G. C.; van der Donk, W. A., New developments in lantibiotic biosynthesis and mode of action. *Curr. Opin. Microbiol.* **2005,** 8, 543-551.
184. Willey, J. M.; van der Donk, W. A., Lantibiotics: Peptides of diverse structure and function. *Annu. Rev. Microbiol.* **2007,** 61, 477-501.
185. Jack, R. W.; Sahl, H. G., Unique Peptide Modifications Involved in the Biosynthesis of Lantibiotics. *Trends Biotechnol.* **1995,** 13, 269-278.
186. Sahl, H.-G.; Bierbaum, G., Lantibiotics: Biosynthesis and biological activities of uniquely modified peptides from gram-positive bacteria. *Annu. Rev. Microbiol.* **1998**, 41-79.
187. Xie, L. L.; van der Donk, W. A., Post-translational modifications during lantibiotic biosynthesis. *Curr. Opin. Chem. Biol.* **2004,** 8, 498-507.
188. van Kraaij, C.; Breukink, E.; Rollema, H. S.; Bongers, R. S.; Kosters, H. A.; de Kruijff, B.; Kuipers, O. P., Engineering a disulfide bond and free thiols in the lantibiotic nisin Z. *Eur. J. Biochem.* **2000,** 267, 901-909.
189. Chatterjee, C.; Paul, M.; Xie, L. L.; van der Donk, W. A., Biosynthesis and mode of action of lantibiotics. *Chem. Rev.* **2005,** 105, 633-683.
190. Lavanant, H.; Derrick, P. J.; Heck, A. J. R.; Mellon, F. A., Analysis of nisin A and some of its variants using Fourier transform ion cyclotron resonance mass spectrometry. *Anal. Biochem.* **1998,** 255, 74-89.
191. Lavanant, H.; Heck, A.; Derrick, P. J.; Mellon, F. A.; Parr, A.; Dodd, H. M.; Giffard, C. J.; Horn, N.; Gasson, M. J., Characterisation of genetically modified nisin molecules by Fourier transform ion cyclotron resonance mass spectrometry. *Eur. Mass Spectrom.* **1998,** 4, 405-416.

192. Molina, H.; Horn, D. M.; Tang, N.; Mathivanan, S.; Pandey, A., Global proteomic profiling of phosphopeptides using electron transfer dissociation tandem mass spectrometry. *Proc. Natl. Acad. Sci. USA* **2007,** 104, 2199-2204.
193. Kleinnijenhuis, A. J.; Duursma, M. C.; Breukink, E.; Heeren, R. M. A.; Heck, A. J. R., Localization of intramolecular monosulfide bridges in lantibiotics determined with electron capture induced dissociation. *Anal. Chem.* **2003,** 75, 3219-3225.
194. Kleinnijenhuis, A. J.; Heck, A. J. R.; Duursma, M. C.; Heeren, R. M. A., Does double electron capture lead to the formation of biradicals? An ECD-SORI-CID study on lacticin 481. *J. Am. Soc. Mass Spectrom.* **2005,** 16, 1595-1601.

Chapter 2

Preferential Cleavage of S-S and C-S Bonds in Electron Detachment Dissociation and Infrared Multiphoton Dissociation of Disulfide-Linked Peptide Anions

2.1. Introduction

Tandem mass spectrometry (MS/MS)[1] is widely used for peptide sequencing and protein characterization. [2-7] Several dissociation techniques, including collision activated dissociation (CID). [8, 9] infrared multiphoton dissociation (IRMPD),[10, 11] surface induced dissociation (SID), [12-14] UV photodissociation, [15, 16] electron capture dissociation (ECD), [17] electron detachment dissociation (EDD), [18] and electron transfer dissociation (ETD), [19] have been employed for peptide ion fragmentation. Each technique has unique advantages and disadvantages and the mode of fragmentation needs to be carefully chosen to suit a particular application. For a protein to be completely characterized, identification and localization of post-translational modifications (PTMs) such as phosphorylation, glycosylation, acetylation, methylation, sulfation, and disulfide bond formation, is essential. That is because such modifications can determine protein function and activity as well as interactions with other molecules.[20, 21] Disulfide bond

formation is a PTM occurring in extracellular proteins. Determination of the presence and connectivity of disulfide bonds is of great interest due to their importance for the stabilization of the native structures of proteins.[21-24] Thus, knowledge considering disulfide bridging is a significant component for a complete understanding of the chemical structure and folding of a protein.[24, 25]

Traditionally, determination of disulfide linkages by mass spectrometry is performed by comparing spectra of proteolytic peptides obtained with and without reduction and alkylation of the disulfide bonds. MS/MS is an alternative approach, offering the advantage of decreased analysis time. However, low energy CID of cations, which is by far the most widely used fragmentation strategy, yields little cleavage of disulfide bonds. Thus, alternative dissociation methods are needed. Disulfide bonds can cleave in high energy CID[26] and in matrix-assisted laser desorption/ionization post-source decay (MALDI-PSD)[27], which also involves high energy deposition. In addition, McLafferty and co-workers demonstrated that ECD, which involves gas-phase cation radical chemistry, preferentially cleaves disulfide bonds[28]. Zubarev and co-workers have noted similarities between ECD and MALDI in-source decay (ISD) in terms of peptide backbone cleavage and retention of PTMs and proposed that ISD is mediated by hydrogen radicals.[29] Another similarity is indeed the facile cleavage of disulfide bonds that has been reported in MALDI ISD.[30, 31] Furthermore, Fung et al. recently demonstrated that photodissociation at 157 nm provides cleavage of both intra and intermolecular disulfide bonds in peptides and proteins.[32] That process was proposed to occur via electronic excitation and radical intermediates. Finally, ETD, which involves

electron transfer from small anions and in many ways is analogous to ECD, also provides disulfide bond cleavage in peptide cations.[33]

Chrisman and McLuckey have demonstrated that CID of peptide anions containing disulfide bridges results in preferential cleavage of S-S and C-S bonds [34]. This strategy was recently extended by Zhang and Kaltashov.[35] In addition, Standing and co-workers showed that the singly charged anion of insulin decays into its constituent A and B chains, involving cleavage of two intermolecular disulfide bonds, following MALDI.[36] Although not nearly as extensively used as positive ion mode for protein analysis, negative ion mode can provide complementary information and is particularly valuable for acidic proteins,[37] constituting ~50% of the protein pool, and for characterization of acidic PTMs, such as phosphorylation,[38] and sulfation.[39] For example Bigwarfe and Wood reported negative ion mode detection of a number of tryptic peptides that were not observed in positive mode.[40] They also highlighted the importance of employing both positive and negative ion mode for the improvement of protein sequence coverage and identification. In addition, Cassady and co-workers have shown that positive and negative ion PSD provide complementary information on peptide primary structure.[41] Fragmentation pathways of deprotonated peptides are not as well understood as those of protonated peptides. However, Bowie and co-workers have employed a combination of experiments and theory to investigate CID dissociation pathways of singly deprotonated peptide ions.[42] That approach was recently applied to peptides containing an intramolecular disulfide bridge.[43] [43]

EDD is a rather recently introduced technique for dissociation of negative ions via a radical ion intermediate.[18] This technique has been shown to be analogous to ECD in that

more random peptide backbone cleavage can be obtained compared to CID[44] and that PTMs[18, 45, 46] as well as higher order structure[47] can be retained. In EDD precursor ions are irradiated with >10 eV electrons, resulting in electron detachment and subsequent fragmentation. A major fragmentation pathway in EDD of peptides is cleavage of backbone C_α-C bonds, forming *x*- and *a*•-type product ions.[18, 45] Cleavage of N-C_α bonds, producing *c* and *z*• ions, is also observed as well as *y*-type product ions.[18, 44] The details of the EDD fragmentation process are still a matter of investigation, however, Zubarev and co-workers proposed that cleavage occurs near the location of negative charges.[45] Thus, EDD backbone cleavage should occur near acidic residues. Following the C-terminus and the side chains of aspartic and glutamic acid, the next most acidic sites in peptides are backbone amide nitrogens [45, 48] and a unidirectional mechanism in which the radical sites are located on amide nitrogens has been proposed for the formation of *x* and *a*• ions.[45]

Here, we employ EDD and IRMPD in an electrospray ionization quadrupole-Fourier transform ion cyclotron resonance (ESI-Q-FTICR) mass spectrometer to characterize disulfide-bonded peptide anions. One goal of these experiments was to address further similarities, or differences, between ECD and EDD with disulfide bond cleavage constituting the behavior under investigation. IRMPD is preferred over CID in the cell of an FT-ICR instrument because there is no need for the introduction of collision gas, which deteriorates instrument performance and adds analysis time.[49, 50] Because IRMPD and CID are similar activation methods (both are based on slow heating of ions), we expected to observe disulfide bond cleavage in negative mode IRMPD. However, to our knowledge, such experiments have not previously been reported.

2.2. Experimental Procedures

2.2.1. Sample Preparation

Chicken egg white lysozyme and insulin from bovine pancreas were purchased from Sigma (St. Louis, MO). 3.1 nanomoles of lysozyme were digested with trypsin (Princeton Separations, Aldelphia, NJ) at a 1:20 enzyme to protein ratio for 10 hours at 37 $^{\circ}$C. Insulin (1.8 nanomoles) was digested with Glu-C (Roche, Indianapolis, IN) at 1:20 or 1:40 enzyme to protein ratios for nine hours at 25 ^{0}C. The reactions were quenched with 0.1% formic acid (Acros Organics, Morris Plains, NJ). For lysozyme, the digested samples were desalted with C18 Ziptips (Millipore, Billerica, MA). For peptide pairs containing one intermolecular disulfide bond, improved recovery was obtained from the remaining solution after desalting, therefore that solution was used. The solution was diluted with 300 μL electrospray solvent containing 40% 2-propanol and 10 mM ammonium bicarbonate (Fisher Scientific, Fair Lawn, NJ). For peptide pairs containing one intermolecular and one intramolecular disulfide bond, the desalted solution was used after dilution with 600 μL spraying solvent, containing 40% 2-propanol and 10 mM ammonium bicarbonate or 20 mM tripropylamine. For insulin, no desalting was performed following digestion. The digested samples were diluted to a final concentration of 1.8 μM in 1 mL spraying solvent containing 40% 2-propanol and 5 mM ammonium acetate (Fisher).

The peptides p-Glu-Gln-D-Trp-Phe-D-Trp-D-Trp-Met-NH_2, H-Trp-His-Trp-Leu-Gln-Leu-OH, H-Gly-Asn-Leu-Trp-Ala-Tyr-Gly-His-Phe-Met-NH_2, and p-Glu-Val-Asn-Phe-Ser-Pro-Gly-Trp-Gly-Tyr-NH_2 were obtained from Sigma and the peptide H-Asp-Tyr-Met-Gly-Trp-Met-Asp-Phe-NH_2 was obtained from Advanced Chemtech

(Louisville, KY) and used without further purification. The first two peptides were electrosprayed at 10 μM, and the three latter ones were electrosprayed at 5 μM from a spraying solvent containing 50% 2-propanol and 10 mM ammonium acetate.

2.2.2. Mass Spectrometry

All experiments were performed with an actively shielded 7 Tesla Q-FT-ICR mass spectrometer (Apex-Q, Bruker Daltonics, Billerica MA), which has been previously described.[47] The proteolytic mixtures were electrosprayed in negative ion mode at a flow rate of 80 μL/h, and the peptides were electrosprayed at a flow rate of 70 μL/h. Ions were accumulated in the first hexapole for 0.1 s, transferred through the mass selective quadrupole (10 m/z isolation window) and mass selectively accumulated in the second hexapole for 1 to 5 s for IRMPD experiments and 1 to 6 s for EDD experiments. All spectra were acquired with XMASS (version 6.1, Bruker Daltonics) using 256k or 512k data points and summed over 16 to 64 scans. Data processing was performed with the MIDAS analysis software.[51] [52] EDD spectra were internally calibrated using the calculated masses of the precursor ion and the charge reduced species. IRMPD spectra were externally calibrated (see below), except for the peptide C6&C127 (Scheme 1a) for which internal calibration was performed using the calculated masses of the precursor and the $[M - H]^-$ ions. Oxidized insulin chain A (Sigma) was used as the external calibrant for the peptides C30&C115 (Scheme 1b), C62&C68-C74&C96 (Scheme 1c), C7A&C7B-C6A&C11A (Scheme 1f) and for the intact molecule of insulin (Scheme 1d). The pp60C-SRC carboxy-terminal phosphoregulatory peptide (Advanced Chemtech) was used as the external calibrant for the peptide C20A&C19B (Scheme 1e). Specifically, the b_6 (m/z = 676.2617) and y_{11} (m/z = 1443.5049) product ions from oxidized insulin chain

A were used for the peptide C30&C115, the $[M - 2H]^{2-}$ (m/z = 1263.9491) and b_8 (m/z = 898.2928) ions were used for the peptide C62&C68-C74&C96, the b_8 and y_{13} (m/z = 1629.6054) ions were used for the peptide C7A&C7B-C6A&C11A, and the b_{10} (m/z = 1084.3933) and y_{13} ions were used for insulin For the peptide C20A&C19B, the b_8 (m/z = 933.3961) and y_5 (m/z = 527.2471) product ions from pp60C-SRC carboxy-terminal phosphoregulatory peptide were used for calibration. Only peak assignments with a mass accuracy better than 15 ppm were accepted.

IRMPD experiments were performed with a vertically mounted 25 W, 10.6 μm, CO_2 laser (Synrad, Mukilteo, WA). Photon irradiation was performed for 0.05 to 0.08 s at 40 to 45% laser power, except in one case, peptide C6&C127 (see below), for which the photon irradiation was performed at 30% laser power. EDD experiments were performed with an indirectly heated hollow dispenser cathode at a bias voltage of – (18-19.2) V and an irradiation time of 0.4 to 1 s. A lens electrode located in front of the hollow cathode was kept at (19-20) V.

2.3. Results and Discussion

Lysozyme contains four disulfide bridges between cysteine 6 and cysteine 127, cysteine 30 and cysteine 115, cysteine 64 and cysteine 80, and between cysteine 76 and cysteine 94.[53] Following proteolytic digestion with trypsin, three disulfide bond-containing species were detected with negative ion mode electrospray ionization. Two of these consisted of two peptide chains connected via an intermolecular disulfide bond; the peptide GCR disulfide-linked to the peptide CELAAAMK, here abbreviated as C6&C127 (Scheme 2.1.a), and the peptide CK disulfide-linked to GYSLGNWVCAAK, here abbreviated as C30&C115 (Scheme 2.1.b). We will refer to the sequences GCR and

CK as R_1 and to the sequences CELAAAMK and GYSLGNWVCAAK as R_2 (Schemes 2.1.a and b). The third species contains an additional intramolecular disulfide bond in one of the peptides; WWCNDGR (R_1) disulfide-linked to NLCNIPCSALLSSDITASVNCAK (R_2,) with an intramolecular disulfide bond between C3 and C21 of the R_2 peptide chain (Scheme 2.1.c). This species will be referred to as C62&C68-C74&C96.

Insulin contains two polypeptide chains linked together with two intermolecular disulfide bridges between cysteine 7 of chain A and cysteine 7 of chain B and between cysteine 20 of chain A and cysteine 19 of chain B. In addition to these intermolecular disulfide bridges, insulin contains one intramolecular disulfide bond formed between cysteine 6 and cysteine 11 of chain A (Scheme 2.1.d) [54, 55]. Proteolytic digestion of insulin with Glu-C resulted in detection of two disulfide bond-containing species in negative ion mode. The first species contained one intermolecular disulfide bond: the peptide NYCN of chain A, disulfide-linked with the peptide ALYLVCGE of chain B, here referred to as C20A&C19B (Scheme 2.1.e). The second species contained one intermolecular disulfide bond and one intramolecular disulfide bond: the peptide GIVEQCCASVCSLYQLE of chain A disulfide-linked to the peptide FVNQHLCGSHLVE of chain B, here referred to as C7A&C7B-C6A&C11A (Scheme 2.1.f).

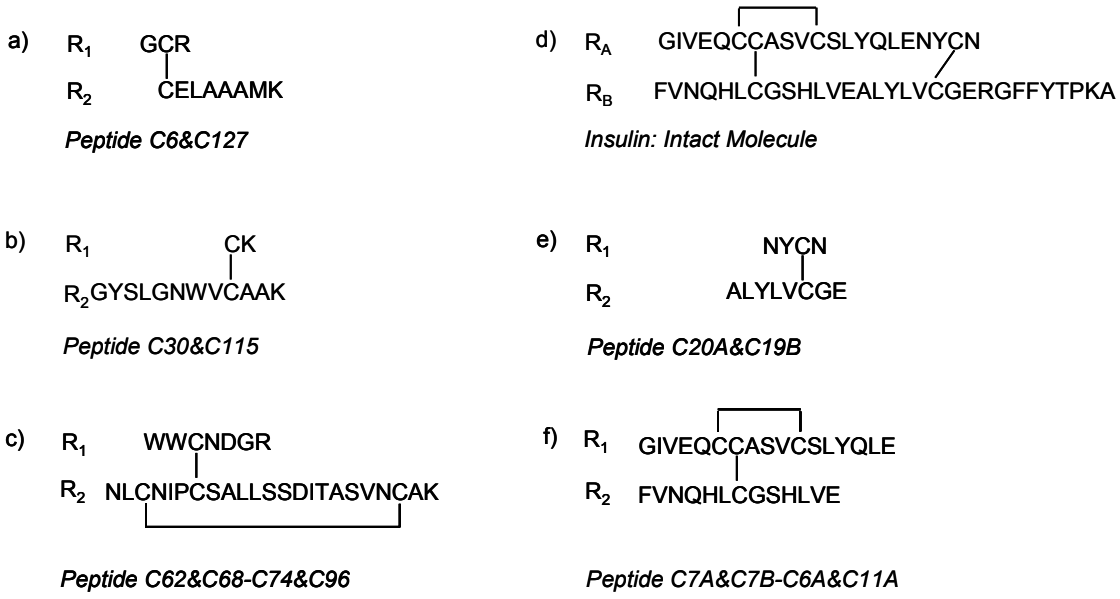

Scheme 2.1. Structures of disulfide-bonded peptide pairs characterized by negative ion mode IRMPD and EDD.

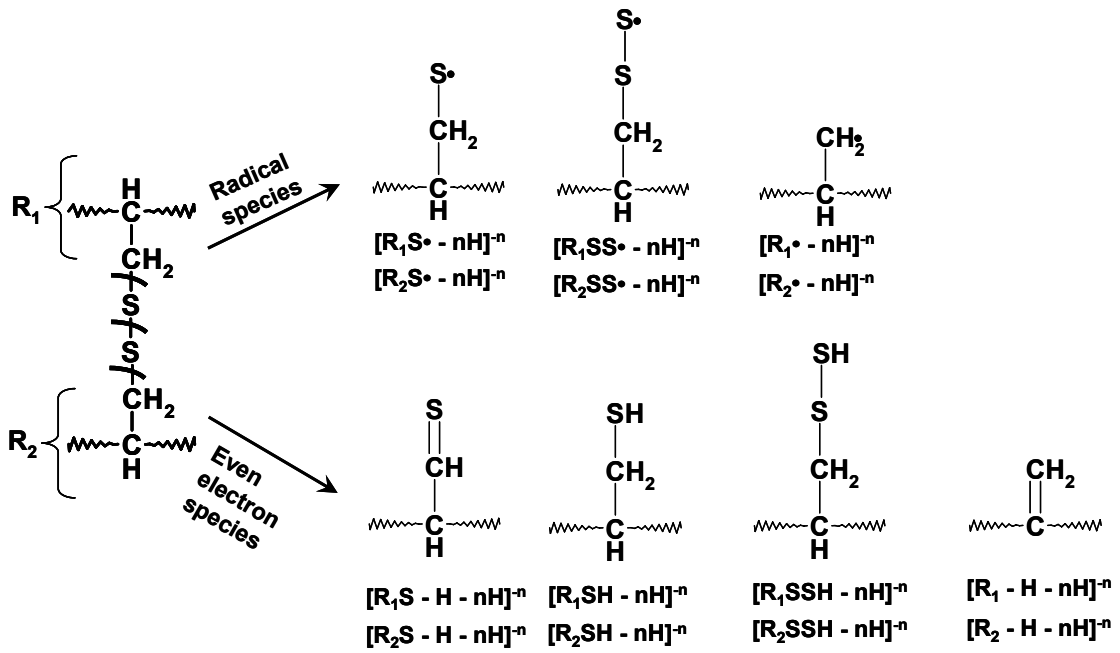

Scheme 2.2 Structures and nomenclature used for the product ions observed in IRMPD and EDD.

2.3.1 EDD and IRMPD of Peptide Pairs Containing one Intermolecular Disulfide Bond

C6&C127. Figure 2.1.A shows the EDD tandem mass spectrum of the doubly deprotonated ($[M - 2H]^{2-}$) ions of the peptide pair C6&C127 (Scheme 2.1a). The dominant product ions correspond to cleavage of either the intermolecular S-S bond or its neighboring C-S bonds, resulting in product ions containing none, one, or two sulfur atoms, respectively (see Scheme 2.2 for the product ion nomenclature). No product ions corresponding to peptide backbone cleavage are observed although neutral loss of CO_2 is seen, which constitutes a ubiquitous fragmentation channel in EDD.[18, 44] This behavior can be rationalized within the previously proposed mechanism for EDD peptide fragmentation, depicting cleavage close to sites of deprotonation,[45] because the R_2 peptide chain contains a glutamic acid residue next to the disulfide bond. The previously proposed cleavage mechanism also involves radical migration to the complementary fragment, consistent with the observation of primarily even-electron fragments containing the R_2 peptide chain. The only exception is the larger product $[R_2SSH - H]^-$, which also appears in its radical form $[R_2SS\bullet - H]^-$, see inset. However, that product could be a result of electron detachment from a deprotonated R_1 C-terminus, also located in close proximity to the disulfide bond. Nevertheless, detection of this radical product ion implies that the disulfide cleavage mechanism in EDD is different from the one in negative ion mode CID, which also results in prominent S-S and C-S bond cleavage.[34] We have previously noted that doubly charged product ions are observed in EDD of doubly charged precursor ions[47] and, furthermore, Zubarev and co-workers have demonstrated that extensive fragmentation of *singly* charged precursors occurs from ~10 eV electron irradiation.[56] In both cases, several observed product ions are of the same

type as those observed in CID/IRMPD and are believed to be a consequence of concomitant precursor ion vibrational excitation. Thus, one can envision that the observed disulfide cleavage in EDD originates from such a process but, because we observe radical product ions, we believe the cleavage mechanism is different than that in CID/IRMPD.

To further explore whether EDD cleaves disulfide bonds in a manner different from vibrational excitation, we compared the EDD data to IRMPD of the same species. The corresponding spectrum for the peptide pair C6&C127 is shown in Fig. 2.1.B. As for EDD and previous CID, S-S and C-S bond cleavage dominate although no radical ions are observed from IRMPD, as expected. The inset in Fig. 1b reveals that the dominant product ion is a mixture of two species, $[R_2SH - 2H]^-$ and $[R_2S - 2H]^-$ (see Scheme 2.2 for nomenclature), where the former is somewhat more dominant. This mixture was also observed in EDD although the latter species was less abundant compared to IRMPD (Fig. 2.1.A inset). CO_2 loss is not observed in IRMPD, further corroborating a cleavage mechanism different from that in EDD. In ECD of disulfide-bonded peptide cations a mixture of odd-electron RS• and even-electron RSH products is also observed [28]. Cleavage of S-S bonds is highly favored over the backbone amine bond cleavage typically observed in ECD. One difference between ECD and EDD of disulfide-bonded peptides is the lack of backbone product ions in EDD, which could be a result of the low EDD fragmentation efficiency.[49] An alternative explanation is that electron detachment from disulfide bonds is favored over the previously proposed detachment from deprotonated acidic residues and deprotonated backbone amide hydrogens.[18, 45] Indeed, disulfide bonds are easily oxidized to form radical cations.[57] The vertical ionization

energy (IE) has been measured to be 8.46-9.1 eV,[58] i.e., significantly lower than the electron energy used here (18-19.2 eV). This possibility will be further discussed below.

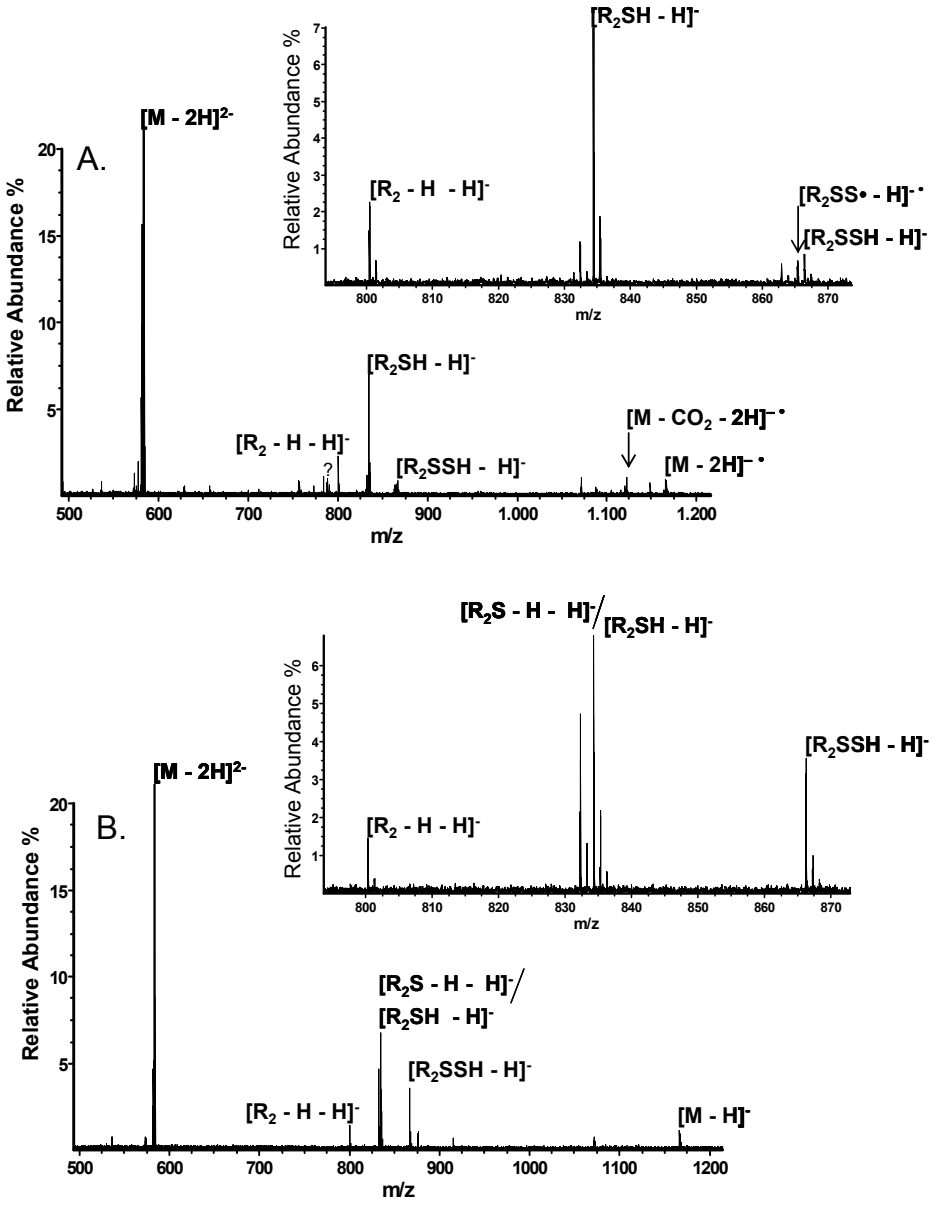

Figure 2.1. EDD (A) and IRMPD (B) of the doubly deprotonated ions of the peptide pair C6&C127. One radical and two even-electron products are detected in EDD whereas solely even-electron species are observed in IRMPD. In some cases (e.g., insets), mixtures of product ions in which hydrogen atoms were transferred between the two chains, R_1 and R_2, are observed (see Scheme 2.2 for product ion structures and nomenclature). $^{?}$ = unidentified product ion.

C30&C115 and C20A&C19B. Further information on the EDD behavior of disulfide-linked peptide pairs is gained from Fig. 2.2.A, which shows EDD of the peptides C30&C115 (Scheme 2.1.b). Here, radical product ions dominate (see inset), consistent with the hypothesis above, that electron detachment occurs from the proximal C-terminus of the R_1 peptide chain, leaving the radical site on the R_2 chain. As for the peptide C6&C127 (Fig. 2.1.A), CO_2 loss is observed but to a lower extent than disulfide bond cleavage. IRMPD of C30&C115 (Fig. 2.2.B) was very similar to IRMPD of C6&C127 in that disulfide bond cleavage to form even-electron product ions dominates. However, only $[R_2 - 2H]^-$ and $[R_2S - 2H]^-$ ions are observed in this case. A third example is given in Fig. 2.3.A, which shows EDD of the peptide C20A&C19B (Scheme 2.1.e). Again, S-S and C-S bond cleavages as well as CO_2 loss constitute the only observable fragmentation pathways. However, for this peptide pair, products containing both the R_1 and R_2 peptide chains are detected. The R_1 C-terminus is closer to the disulfide bond than the R_2 C-terminus. Consistently, the R_1-containing product ion is primarily an even-electron species whereas the R_2-containing products are predominantly radical species. IRMPD of C20A&C19B (Fig. 2.3.B) also provided product ions containing both the R_1 and R_2 peptide chains. In addition, neutral losses of water and ammonia are seen as well as a neutral loss of 129 Da. The latter product most likely corresponds to loss of the R_2 C-terminal glutamic acid residue through a rearrangement reaction in which one of the carboxyl oxygens is retained, i.e. formation of a $[b + H_2O]$ ion, as previously reported for protonated peptides.[59]

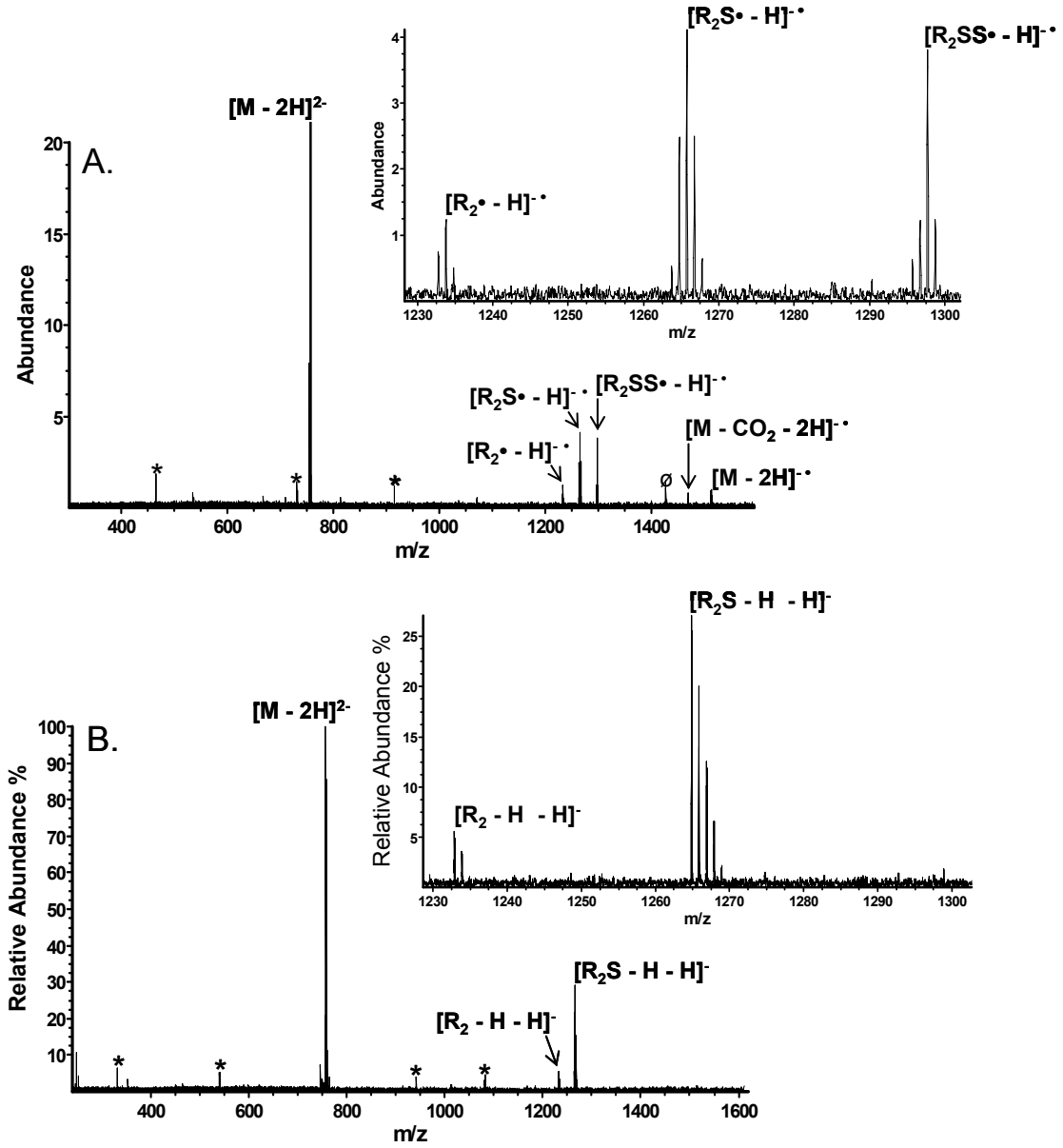

Figure 2.2. EDD (A) and IRMPD (B) of the peptide pair C30&C115. As for C6&C127 (Fig. 2.1.A), EDD resulted in cleavage of both S-S and C-S bonds. However, here, radical product ions are mainly observed whereas IRMPD again resulted in formation of even-electron species, supporting a cleavage mechanism different from that in EDD. The R_2 chain containing two sulfur atoms was not observed in IRMPD whereas this product ion was present as an odd electron species following EDD. * = noise peaks, $^{\varnothing}$ = peak from imperfect isolation.

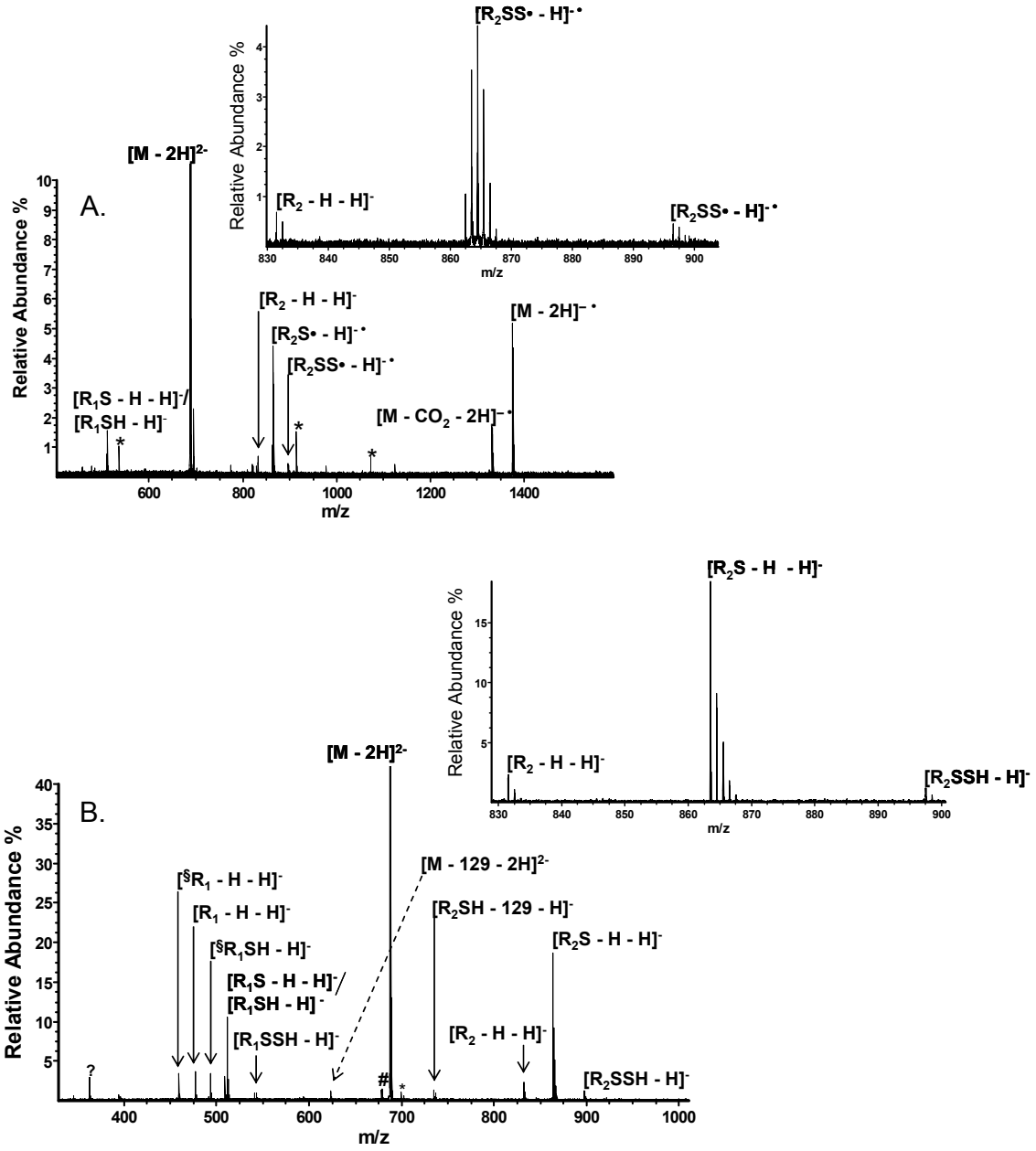

Figure 2.3. EDD (A) and IRMPD (B) of the peptide pair C20A&C19B. In EDD, the charge reduced species dominates the spectrum, however, product ions corresponding to cleavage of S-S and C-S bonds in both peptide chains are also observed, similar to IRMPD. The product ion corresponding to chain R_1 is a mixture of two species. * = noise peaks, # = ammonia loss, § = water loss.

2.3.2. EDD and IRMPD of Peptide Pairs Containing one Intermolecular and one Intramolecular Disulfide Bond

C7A&C7B-C6A&C11A. The EDD mass spectrum of the $[M - 3H]^{3-}$ ions of the peptide pair C7A&C7B-C6A&C11A is shown in Figure 2.4.A. Compared to the peptides discussed above, this peptide pair contains an additional intramolecular disulfide bond in the R_1 chain (see Scheme 2.1.f). The EDD spectrum is dominated by the charge-reduced radical species, $[M - 3H]^{2-\bullet}$. Charge reduction as a dominant process has previously been observed in EDD of nucleic acid anions and it has been proposed to be due to retention of hydrogen bonding, which prevents product ions from separating,[47, 60] similar to the behavior found in ECD.[61] Here, cleavage of the intramolecular disulfide bond would result in product ion pairs that are covalently linked, rendering it even more difficult to produce separated (and hence detectable) product ions. However, cleavage of the intermolecular disulfide bond should result in detectable product ions, which are observed although their relative abundance is lower than for peptide pairs lacking an intramolecular disulfide (Figs. 2.1.-2.3.). Interestingly, only product ions corresponding to S-S cleavage are observed whereas products corresponding to C-S bond cleavages are absent. However, the former products were more abundant for all peptide pairs discussed above (Figs. 2.1.-2.3.) so the absence of C-S cleavages could simply be a signal-to-noise (S/N) issue. Consistent with competition between intra- and intermolecular disulfide bond cleavage, the product ion corresponding to neutral CO_2 loss (whose detection is independent of disulfide cleavage) displays a higher relative abundance as compared to the peptides lacking an intramolecular disulfide.

The cleavages observed in EDD of the peptide pair C7A&C7B-C6A&C11A (Fig. 2.4.A) cannot be readily explained within the previously proposed EDD mechanism[45]

because there are no acidic sites close to the intermolecular disulfide bond. The glutamic acid at the fourth position in the R_1 peptide chain could possibly explain the cleavage of the intramolecular disulfide bond. However, it does not appear to be involved in cleavage of the intermolecular disulfide because the corresponding product ion containing the R_2 peptide chain is predominantly an even-electron species (see inset) whereas the product containing the R_1 peptide chain is observed both as a predominantly even-electron species (doubly charged) and as a predominantly radical species (singly charged). As mentioned above (and further discussed below), an alternative explanation could be direct electron detachment from the disulfide bond. IRMPD of the same species resulted in richer fragmentation than EDD (see Fig. 2.4.B) in which both S-S (to form both $[RSH - nH]^{n-}$ and $[RS - nH]^{n-}$ ions (n = 1,2), as above), C-S, and one backbone bond are cleaved. In addition, cleavage of the intramolecular disulfide bond is observed, as evidenced by the detection of the product ions, $[R_1 - 3H - 2H]^{2-}$, $[R_1 - S - 3H - 2H]^{2-}$, $[R_1 - 2S - 3H - 2H]^{2-}$. The former product ion corresponds to cleavage of the intramolecular S-S bond, while the two latter correspond to cleavage of the neighboring C-S bonds. One backbone product ion corresponding to a $[b_{12} + H_2O]$ ion of chain R_2 is observed. As discussed above, such product ions can be formed from elimination of the C-terminal glutamic acid residue in a rearrangement reaction.[59]

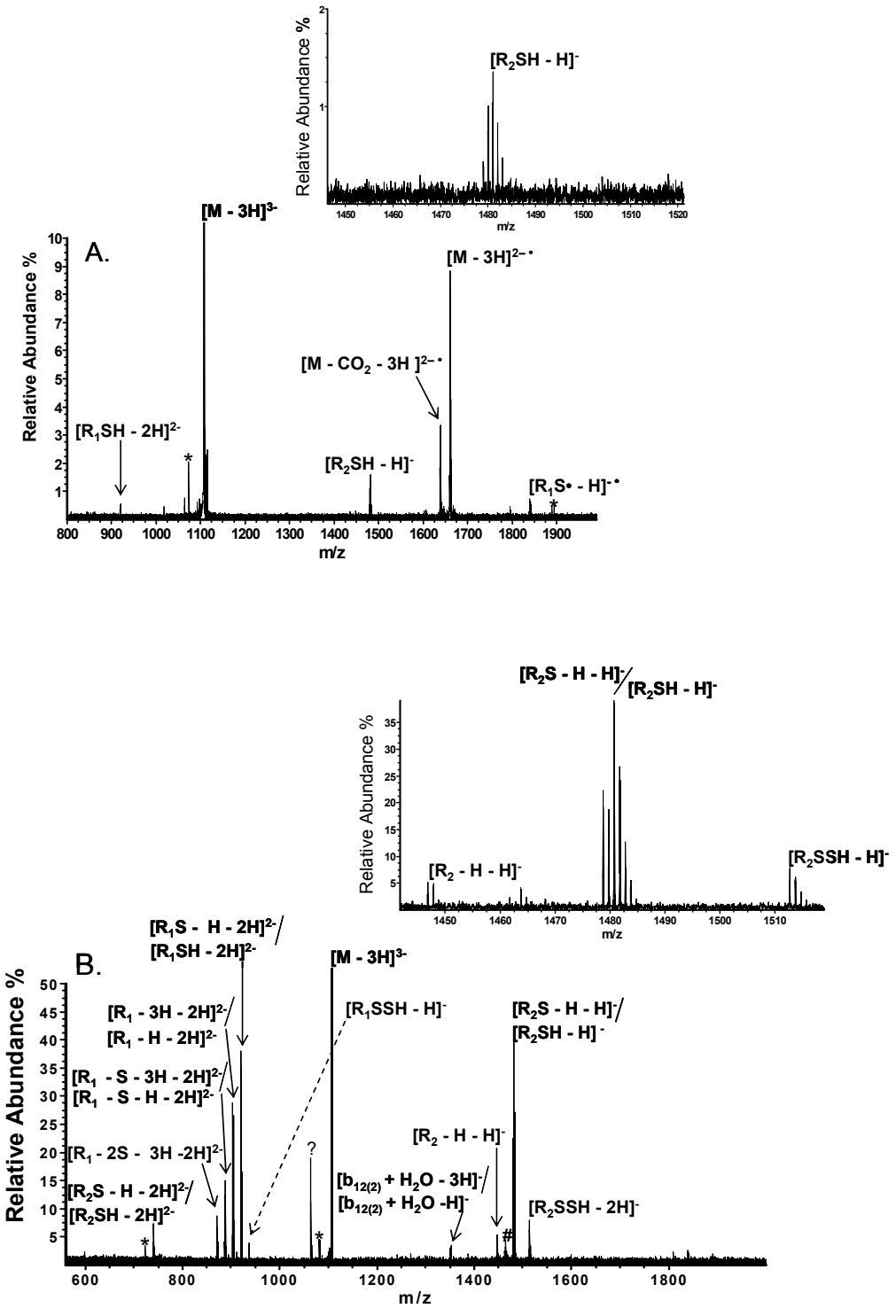

Figure 2.4. EDD (A) and IRMPD (B) of the peptide pair C7A&C7B-C6A&C11A. No product ions corresponding to cleavage of C-S bonds are observed in EDD whereas both C-S and S-S bond cleavage is seen in IRMPD. The product ions $[R_1 - 3H - 2H]^{2-}$, $[R_1 - S - 3H - 2H]^{2-}$ and $[R_1 - 2S - 3H - 2H]^{2-}$ result from intramolecular bond cleavage in the R_1 peptide chain. * = noise peaks, # = ammonia loss

C62&C68-C74&C96. A second example of EDD of a peptide pair containing both an intermolecular and an intramolecular disulfide bond, C62&C68-C74&C96 (see Scheme 2.1.c), is shown in Figure 2.5.A. For this species, very limited fragmentation is observed. Neither S-S, nor C-S bond cleavage is seen although charge reduction to form $[M - 3H]^{2-\bullet}$ as well as CO_2 loss are observed. Because the two latter product ions were significantly more abundant than products corresponding to S-S bond cleavage for the C7A&C7B-C6A&C11A peptide pair discussed above (Fig. 2.4.A), the absence of such products for the current peptide could be due to limited dynamic range (i.e., S/N ratio). An alternative explanation for the low fragmentation efficiency of both C7A&C7B-C6A&C11A and C62&C68-C74&C96 could be that a different charge state (3^-) was fragmented as compared to the peptides with solely an intermolecular disulfide bond (2^-). These charge states were chosen for fragmentation because they constituted the most abundant species following electrospray ionization. The charge state effect in EDD has not been well established although one can envision that an increased precursor ion charge may lower the fragmentation efficiency due to increased Coulomb repulsion, which can reduce the electron interaction cross-section. However, in EDD of oligonucleotides, higher charge states (4^- and 3^-) were found to dissociate more efficiently than doubly deprotonated ions. This behavior was attributed to a higher degree of gas-phase unfolding for the more highly charged ions (thereby preventing product ion pairs from remaining bound).[62] For the peptides characterized here, gas-phase conformational flexibility is limited due to the presence of the intramolecular disulfide bond. Quadruply deprotonated ions were not observed, however, EDD of

doubly deprotonated precursor ions resulted in a slightly decreased fragmentation efficiency (Figure 2.6).

In addition to the $[M - 3H]^{2-\bullet}$ and CO_2 loss product ions mentioned above, EDD of C62&C68-C74&C96 resulted in a product corresponding to neutral loss of 129. This species cannot result from elimination of a C-terminal glutamic acid residue because this peptide pair was produced by trypsin rather than Glu-C digestion. Possible assignments (within the 15 ppm criterion) are $c_{22(2)}^{2-\bullet}$ or $z_{22(2)}^{2-\bullet}$ from backbone cleavage within the R_2 peptide chain without S-S or C-S bond cleavage. However, because the latter cleavages dominated in all EDD spectra shown above and we did not previously observe any EDD product ions that resulted from backbone cleavage, we also considered alternative assignments. One possibility is neutral loss of C_9H_7N (129.058 amu), which corresponds to a tryptophan side chain. Loss of 129 was observed in CID of fast atom bombardment-generated deprotonated tryptophan and has been proposed to result from charge migration (producing a deprotonated N-terminus) followed by formation of an indole anion and hydride transfer.[63] In ECD, neutral loss of 131.074 has been attributed to an even-electron fragment from the Trp side chain, originating from proton solvation onto Trp.[64] Consistent with the proposed EDD mechanism,[45] loss of 129 in EDD could involve amide deprotonation, similar to CID. Alternatively, deprotonation of the Trp side chain, followed by electron detachment from Trp may explain this behavior. However, it is also interesting to note that tryptophan has the lowest vertical ionization energy of all amino acids (7.07-11.61 eV), depending on conformation.[65] This IE can be lower than the ionization energy for the disulfide bond (8.46-9.1 eV).[58] thus suggesting that direct electron detachment from Trp can compete with detachment from disulfide bonds, as

discussed in more detail below. On the other hand, loss of 129 was not observed in EDD of the peptide pair C30&C115 (Fig. 2a), which also contains a tryptophan residue. However, the C62&C68-C74&C96 peptide pair discussed here contains two Trp residues, which may strengthen this effect.

The IRMPD mass spectrum of the peptide pair C62&C68-C74&C96 is shown in figure 2.5.B. This spectrum is less informative than the corresponding spectrum for the peptide pair C7A&C7B-C6A&C11A (Fig. 2.4.B), which contained a mixture of S-S, C-S, and peptide backbone cleavages. However, it is more informative than the EDD spectrum for the same species (Fig. 2.5.A) in that both S-S and C-S bond cleavage is observed although the former dominates.

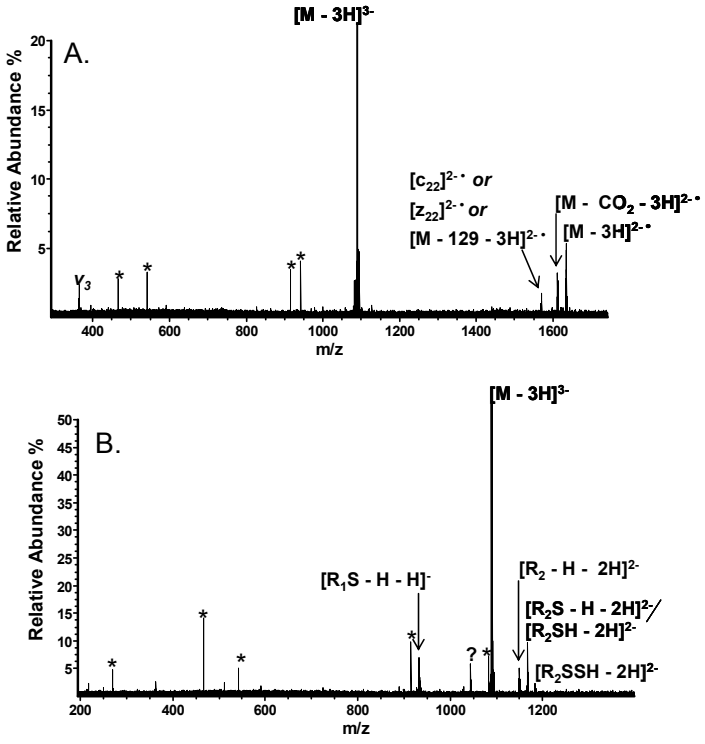

Figure 2.5. EDD (A) and IRMPD (B) of the triply deprotonated ions of the peptide pair C62&C68-C74&C96. No product ions corresponding to S-S or C-S bond cleavage are observed in EDD although charge reduction, CO_2 loss, and neutral loss of 129 Da are detected. The latter product ion presumably corresponds to loss of the tryptophan side chain. * = noise peaks, ? = unidentified product ion.

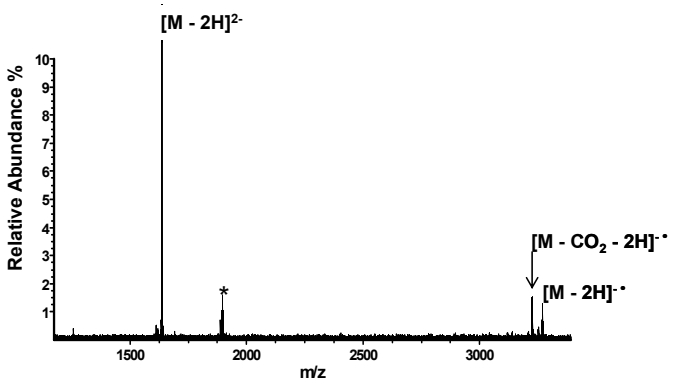

Figure 2.6. EDD of the doubly deprotonated ions of the peptide pair C62&C68 C74&C96. Very limited fragmentation is observed. * = noise peak

2.3.3. The Role of Tryptophan in EDD

To further characterize the influence of tryptophan on the EDD behavior, we subjected a range of different Trp-containing peptides to electron irradiation. EDD of the doubly deprotonated peptide pEVNFSPGWGT-NH_2 (peptide 1) is shown in Fig. 2.7.A. Here, selective cleavage on the N-terminal side of tryptophan is observed in the form of an abundant c_7 ion. In addition, neutral loss of 129 from the charge-reduced species is detected, as was observed for the peptide pair C62&C68-C74&C96 discussed above. The peptide H-GNLWATGHFM-NH_2 (peptide 2) displayed only limited fragmentation in EDD. However, an abundant product ion corresponding to loss of 129 Da and a z_6• fragment ion corresponding to cleavage next to the tryptophan residue were observed (Fig. 2.7.B). By contrast, EDD of the peptide H-DYMGWMDF-NH_2 (peptide 3) did not result in loss of 129 (Fig. 2.8). Here, the charge-reduced $[M - 2H]^{-\bullet}$ species was the most prominent product ion followed by CO_2 loss. All these peptides contain one tryptophan residue, as does the peptide pair C30&C115. However, the latter peptide as well as peptide 3 did not display 129 loss. Those two peptides are different from the other two (peptides 1 and 2) in that two acidic sites are present (the two C-termina for C30&C115

and the two aspartic acid residues for peptide 3). Thus, amide or tryptophan side chain deprotonation is unlikely. However, peptides 1 and 2 only contain one acidic site (the C-terminus) and amide or tryptophan deprotonation is therefore much more likely for the doubly deprotonated precursors, consistent with the mechanism for tryptophan side chain loss proposed above.

Figure 2.7.C. shows the EDD mass spectrum from the doubly deprotonated peptide H-WHWLQL-OH, which contains two Trp residues. Here, neutral loss of 129 constitutes the dominant product ion. Similarly, even more pronounced loss of 129 is detected in EDD of pEQWFWWM-NH_2, which contains three tryptophans (Fig. 2.7.D). The latter spectrum also displays pronounced backbone cleavage although backbone product ions are less abundant than the product corresponding to neutral loss of 129. The two latter EDD spectra corroborate our claim that the presence of two Trp residues in C62&C68-C74&C96 can enhance the fragmentation pathway resulting in loss of 129 and thereby suppress disulfide cleavage.

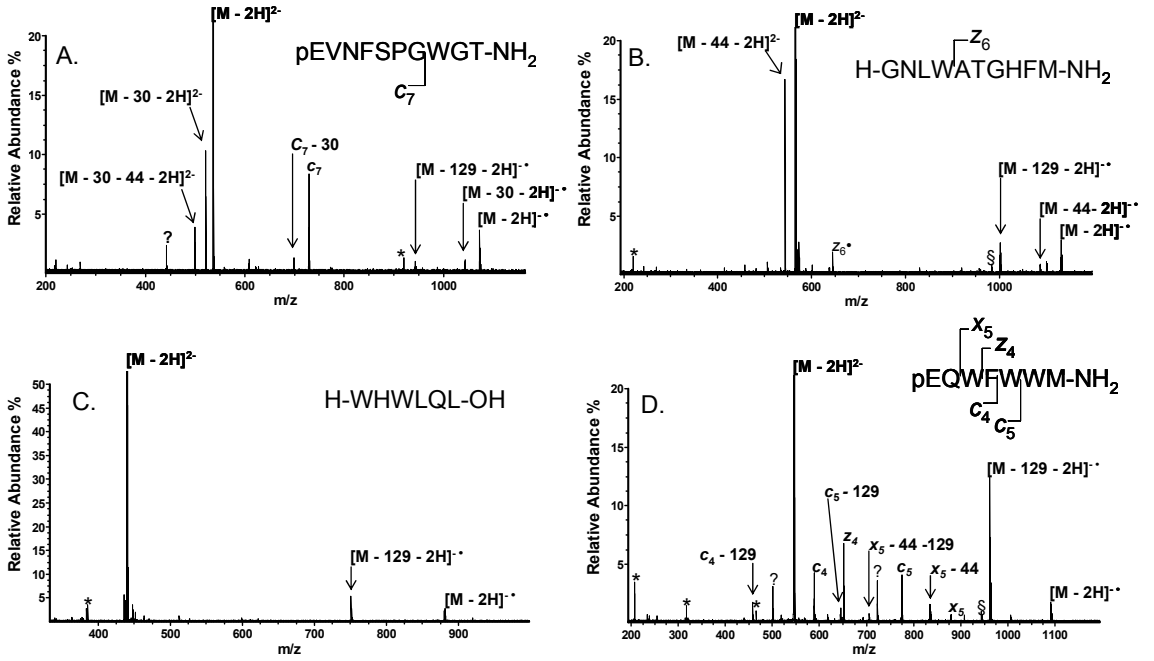

Figure 2.7. EDD of tryptophan-containing peptides. Neutral loss of 129 (tryptophan side chain) is observed in all cases with an abundance correlating with the number of Trp residues. Peptide backbone cleavage next to tryptophan is also prevalent. In A), neutral loss of 30 Da (HCHO, 30.0106 Da) corresponds to cleavage of a serine side chain while neutral loss of 44 Da (MeCHO, 44.0262 Da) corresponds to threonine side chain cleavage. In B), neutral loss of the threonine side chain is observed (44 Da, MeCHO) from the charged reduced species The neutral loss of MeCHO from the precursor ion was present prior to electron irradiation..In D), neutral loss of 44 Da (•$CONH_2$, 44.0136 Da) is observed from the x_5 product ion and attributed to the loss of the amidated C-terminus. Tryptophans in D) are D-Trp. * = noise peaks, $^{?}$ = unidentified product ion, § = water loss.

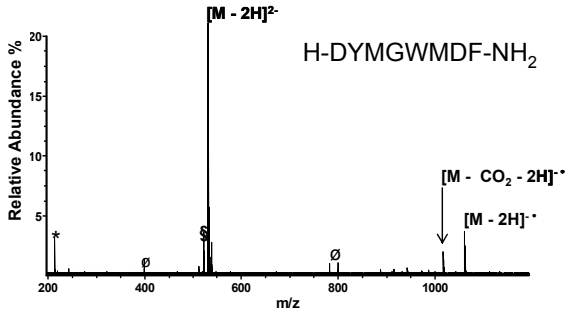

Figure 2.8. EDD of the doubly deprotonated peptide H-DYMGWMDF-NH_2. Only formation of the charge-reduced species and CO_2 loss was observed. An x_7 product ion was also observed but with low abundance (not labeled). No cleavages corresponding to the loss of the tryptophan side chain is detected. * = noise peak, §= water loss, $^{∅}$ =. peak from imperfect isolation.

2.3.4. EDD and IRMPD of Intact Insulin Molecule

EDD of quadruply deprotonated insulin (Fig. 2.9.A) resulted in formation of a charge reduced species and a product ion corresponding to loss of CO_2 from the charge reduced species. No product ions corresponding to cleavage of S-S or C-S bonds were observed. However, two disulfide bridges need to be cleaved in order to detect such products. Nevertheless, such behavior was observed in ECD of insulin cations.[28] Similarly, IRMPD of insulin anions (Fig. 2.9.B) resulted in cleavage of both the intermolecular disulfide bonds to produce separated A and B chains. In addition, backbone cleavages of chain B were observed. These results are similar to those obtained from negative ion mode CID of insulin.[34] In particular, one *c*-type product ion corresponding to cleavage N-terminal to cysteine was detected although this product can also be assigned as an internal fragment corresponding to the sequence LVEALYLVCGERGFFYTP of chain B minus water.

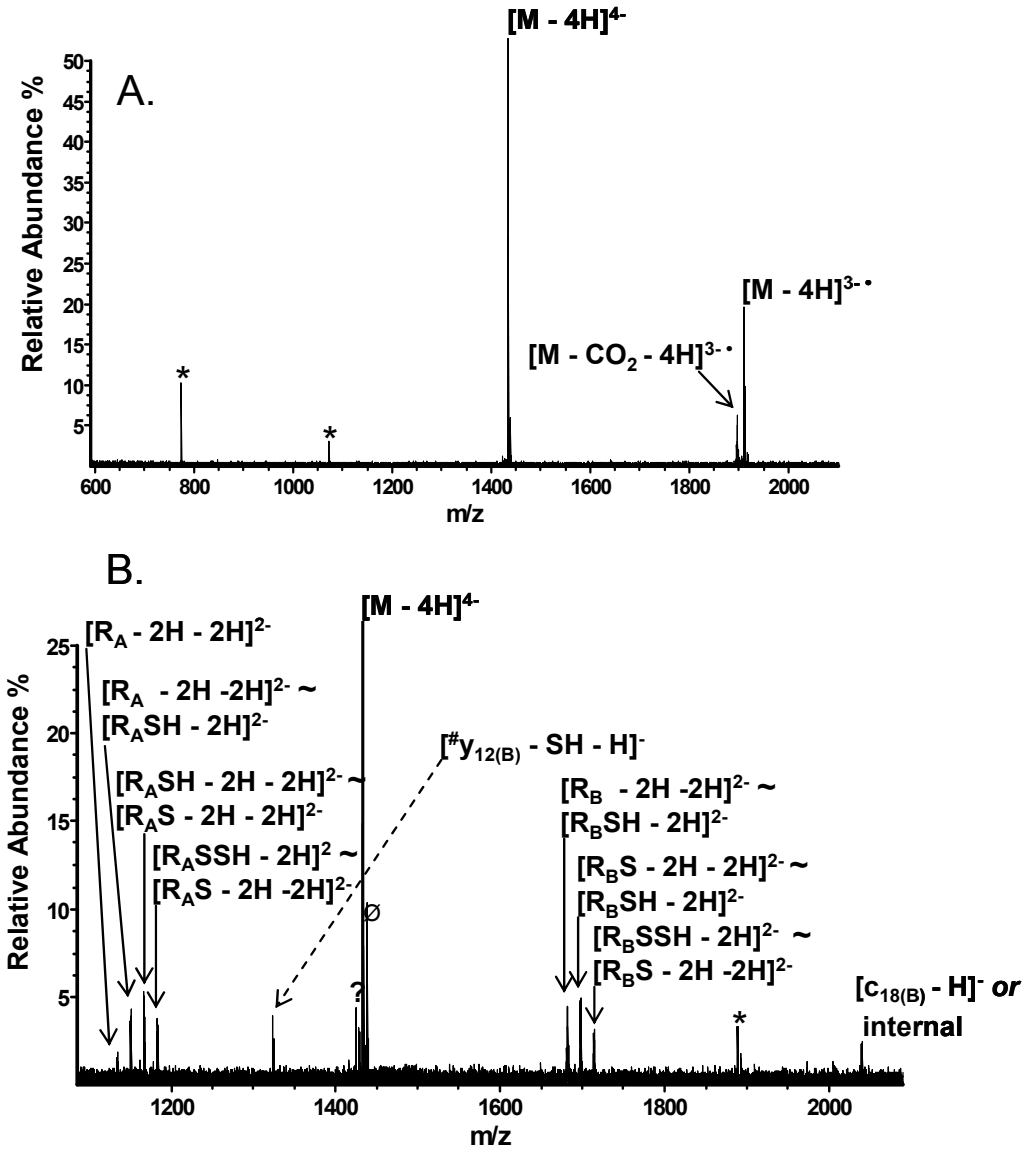

Figure 2.9. EDD (A) and IRMPD (B) of the quadruply deprotonated intact molecule of insulin. Only charge reduction and CO_2 loss are observed in EDD. IRMPD results in preferential cleavage of S-S and C-S bonds. In addition, two backbone product ions from chain B are seen. The two cysteine residues in product ions following S-S bond cleavage have different structures in which $[R_B - 2H - 2H]^{2-} \sim [R_BSH - 2H]^{2-}$ indicate that one cysteine exhibited loss of sulfur whereas the second one did not (see Scheme 2.2 for structures and nomenclature of product ions). * = noise peak, $^{?}$ = unidentified product ions, $^{\varnothing}$ = peak from imperfect isolation, $^{\#}$ = ammonia loss.

2.4. Conclusions

Electron detachment dissociation of multiply charged disulfide-bonded peptide anions results in preferential cleavage of C-S and S-S bonds in many cases. However, in the case of insulin for which multiple disulfide linkages are present, EDD did not provide any detectable disulfide bond cleavage. In addition, the presence of tryptophan in a polypeptide chain can alter the preferred fragmentation pathway in EDD and yield abundant product ions corresponding to the loss of its side chain. This behavior correlates with the vertical ionization energies of a disulfide bond and tryptophan, respectively. By contrast, the IRMPD fragmentation behavior was more consistent, showing strongly favored cleavage of both S-S and C-S bonds in all peptides investigated, even in cases where multiple disulfide linkages were present. Thus, the mechanism of disulfide bond cleavage appears to be different in IRMPD compared to EDD, further corroborated by the formation of mainly odd-electron species in EDD and exclusively even-electron species in IRMPD. Nevertheless, both these fragmentation techniques can be useful for probing disulfide bonding in peptide anions.

2.5. References

1. McLafferty, F. W., *Tandem Mass Spectrometry*. Wiley: New York, 1983.
2. Hunt, D. F.; Yates, J. R.; Shabanowitz, J.; Winston, S.; Hauer, C. R., Protein Sequencing by Tandem Mass-Spectrometry. *Proc. Natl. Acad. Sci. U.S.A* **1986,** 83, 6233-6237.
3. Biemann, K.; Papayannopoulos, I. A., Amino-Acid Sequencing of Proteins. *Acc. Chem. Res.* **1994,** 27, 370-378.
4. Gross, M. L., Tandem Mass-Spectrometric Strategies for Determining Structure of Biologically Interesting Molecules. *Acc. Chem. Res.* **1994,** 27, 361-369.
5. Siuzdak, G., The Emergence of Mass-Spectrometry in Biochemical-Research. *Proc. Natl. Acad. Sci. U.S.A* **1994,** 91, 11290-11297.
6. Yates, J. R., Mass spectrometry and the age of the proteome. *J. Mass Spectrom.* **1998,** 33, 1-19.
7. Mann, M.; Hendrickson, R. C.; Pandey, A., Analysis of proteins and proteomes by mass spectrometry. *Annu. Rev. Biochem.* **2001,** 70, 437-473.
8. Hayes, R. N.; Gross, M. L., Collision-Induced Dissociation. *Methods Enzymol.* **1990,** 193, 237-263.
9. McLuckey, S. A., Principles of Collisional Activation in Analytical Mass-Spectrometry. *J. Am. Soc. Mass Spectrom.* **1992,** 3, 599-614.
10. Woodin, R. L.; Bomse, D. S.; Beauchamp, J. L., Multi-Photon Dissociation of Molecules with Low-Power Continuous Wave Infrared-Laser Radiation. *J. Am. Chem. Soc.* **1978,** 100, 3248-3250.
11. Little, D. P.; Speir, J. P.; Senko, M. W.; Oconnor, P. B.; McLafferty, F. W., Infrared Multiphoton Dissociation of Large Multiply-Charged Ions for Biomolecule Sequencing. *Anal. Chem.* **1994,** 66, 2809-2815.
12. Cole, R. B.; Lemeillour, S.; Tabet, J. C., Surface-Induced Dissociation of Protonated Peptides - Implications of Initial Kinetic-Energy Spread. *Anal. Chem.* **1992,** 64, 365-371.
13. Mabud, M. D. A.; Dekrey, M. J.; Cooks, R. G., Surface-Induced Dissociation of Molecular-Ions. *Int. J. Mass Spectrom. Ion Processes* **1985,** 67, 285-294.
14. McCormack, A. L.; Jones, J. L.; Wysocki, V. H., Surface-Induced Dissociation of Multiply Protonated Peptides. *J. Am. Soc. Mass Spectrom.* **1992,** 3, 859-862.
15. Williams, E. R.; Furlong, J. J. P.; McLafferty, F. W., Efficiency of Collisionally-Activated Dissociation and 193-Nm Photodissociation of Peptide Ions in Fourier-Transform Mass-Spectrometry. *J. Am. Soc. Mass Spectrom.* **1990,** 1, 288-294.
16. Thompson, M. S.; Cui, W. D.; Reilly, J. P., Fragmentation of singly charged peptide ions by photodissociation at lambda=157 nm. *Angew. Chem. Int. Ed.* **2004,** 43, 4791-4794.
17. Zubarev, R. A.; Kelleher, N. L.; McLafferty, F. W., Electron capture dissociation of multiply charged protein cations. A nonergodic process. *J. Am. Chem. Soc.* **1998,** 120, 3265-3266.
18. Budnik, B. A.; Haselmann, K. F.; Zubarev, R. A., Electron detachment dissociation of peptide di-anions: an electron-hole recombination phenomenon. *Chem. Phys. Lett.* **2001,** 342, 299-302.

19. Syka, J. E. P.; Coon, J. J.; Schroeder, M. J.; Shabanowitz, J.; Hunt, D. F., Peptide and protein sequence analysis by electron transfer dissociation mass spectrometry. *Proc. Natl. Acad. Sci. U.S.A* **2004,** 101, 9528-9533.
20. Seo, J.; Lee, K. J., Post-translational modifications and their biological functions: Proteomic analysis and systematic approaches. *Journal of Biochemistry and Molecular Biology* **2004,** 37, 35-44.
21. Creighton, T. E., *Proteins Structures and Molecular Properties*. W.H. Freeman and Company: New York, 1993.
22. Fersht, A., *Structure and Mechanism in Protein Science*. W.H. Freeman and Company: New York, 1999.
23. Pace, C. N.; Grimsley, G. R.; Thomson, J. A.; Barnett, B. J., Conformational Stability and Activity of Ribonuclease-T1 with Zero, One, and 2 Intact Disulfide Bonds. *J. Biol. Chem.* **1988,** 263, 11820-11825.
24. Wedemeyer, W. J.; Welker, E.; Narayan, M.; Scheraga, H. A., Disulfide bonds and protein folding. *Biochemistry* **2000,** 39, 4207-4216.
25. Gorman, J. J.; Wallis, T. P.; Pitt, J. J., Protein disulfide bond determination by mass spectrometry. *Mass Spectrom. Rev.* **2002,** 21, 183-216.
26. Bean, M. F.; Carr, S. A., Characterization of Disulfide Bond Position in Proteins and Sequence-Analysis of Cystine-Bridged Peptides by Tandem Mass-Spectrometry. *Anal. Biochem.* **1992,** 201, 216-226.
27. Jones, M. D.; Patterson, S. D.; Lu, H. S., Determination of disulfide bonds in highly bridged disulfide-linked peptides by matrix-assisted laser desorption/ionization mass spectrometry with postsource decay. *Anal. Chem.* **1998,** 70, 136-143.
28. Zubarev, R. A.; Kruger, N. A.; Fridriksson, E. K.; Lewis, M. A.; Horn, D. M.; Carpenter, B. K.; McLafferty, F. W., Electron capture dissociation of gaseous multiply-charged proteins is favored at disulfide bonds and other sites of high hydrogen atom affinity. *J. Am. Chem. Soc.* **1999,** 121, 2857-2862.
29. Kocher, T.; Engstrom, A.; Zubarev, R. A., Fragmentation of peptides in MALDI in-source decay mediated by hydrogen radicals. *Anal. Chem.* **2005,** 77, 172-177.
30. Patterson, S. D.; Katta, V., Prompt Fragmentation of Disulflde-Linked Peptides During Matrix-Assisted Laser-Desorption Ionization Mass-Spectrometry. *Anal. Chem.* **1994,** 66, 3727-3732.
31. Gorman, J. J.; Ferguson, B. L.; Nguyen, T. B., Use of 2,6-dihydroxyacetophenone for analysis of fragile peptides, disulphide bonding and small proteins by matrix-assisted laser desorption ionization. *Rapid Commun. Mass Spectrom.* **1996,** 10, 529-536.
32. Fung, Y. M. E.; Kjeldsen, F.; Silivra, O. A.; Chan, T. W. D.; Zubarev, R. A., Facile disulfide bond cleavage in gaseous peptide and protein cations by ultraviolet photodissociation at 157 nm. *Angew. Chem. Int. Ed.* **2005,** 44, 6399-6403.
33. Chrisman, P. A.; Pitteri, S. J.; Hogan, J. M.; McLuckey, S. A., SO2- electron transfer ion/ion reactions with disulfide linked polypeptide ions. *J. Am. Soc. Mass Spectrom.* **2005,** 16, 1020-1030.

34. Chrisman, P. A.; McLuckey, S. A., Dissociations of disulfide-linked gaseous polypeptide/protein anions: Ion chemistry with implications for protein identification and characterization. *J. Proteome Res.* **2002,** 1, 549-557.
35. Zhang, M.; Kaltashov, I. A., Mapping of protein disulfide bonds using negative ion fragmentation with a brodband precursorselection. *Anal. Chem.* **2006,** 78, 4820-4829.
36. Zhou, J.; Ens, W.; Poppeschriemer, N.; Standing, K. G.; Westmore, J. B., Cleavage of Interchain Disulfide Bonds Following Matrix-Assisted Laser-Desorption. *Int. J. Mass Spectrom. Ion Processes* **1993,** 126, 115-122.
37. Ewing, N. P.; Cassady, C. J., Dissociation of multiply charged negative ions for hirudin (54-65), fibrinopeptide B, and insulin A (oxidized). *J. Am. Soc. Mass Spectrom.* **2001,** 12, 105-116.
38. Janek, K.; Wenschuh, H.; Bienert, M.; Krause, E., Phosphopeptide analysis by positive and negative ion matrix-assisted laser desorption/ionization mass spectrometry. *Rapid Commun. Mass Spectrom.* **2001,** 15, 1593-1599.
39. Yagami, T.; Kitagawa, K.; Futaki, S., Liquid Secondary-Ion Mass-Spectrometry of Peptides Containing Multiple Tyrosine-O-Sulfates. *Rapid Commun. Mass Spectrom.* **1995,** 9, 1335-1341.
40. Bigwarfe, P. M.; Wood, T. D., Effect of ionization mode in the analysis of proteolytic protein digests. *Int. J. Mass Spectrom.* **2004,** 234, 185-202.
41. Jai-nhuknan, J.; Cassady, C. J., Negative ion postsource decay time-of-flight mass spectrometry of peptides containing acidic amino acid residues. *Anal. Chem.* **1998,** 70, 5122-5128.
42. Bowie, J. H.; Brinkworth, C. S.; Dua, S., Collision-induced fragmentations of the (M-H)(-) parent anions of underivatized peptides: An aid to structure determination and some unusual negative ion cleavages. *Mass Spectrom. Rev.* **2002,** 21, 87-107.
43. Bilusich, D.; Maselli, V. M.; Brinkworth, C. S.; Samguina, T.; Lebedev, A. T.; Bowie, J. H., Direct identification of intramolecular disulfide links in peptides using negative ion electrospray mass spectra of underivatised peptides. A joint experimental and theoretical study. *Rapid Commun. Mass Spectrom.* **2005,** 19, 3063-3074.
44. Haselmann, K. F.; Budnik, B. A.; Kjeldsen, F.; Nielsen, M. L.; Olsen, J. V.; Zubarev, R. A., Electronic excitation gives informative fragmentation of polypeptide cations and anions. *Eur. J. Mass Spectrom.* **2002,** 8, 117-121.
45. Kjeldsen, F.; Silivra, O. A.; Ivonin, I. A.; Haselmann, K. F.; Gorshkov, M.; Zubarev, R. A., C-alpha-C backbone fragmentation dominates in electron detachment dissociation of gas-phase polypeptide polyanions. *Chem. Eur. J.* **2005,** 11, 1803-1812.
46. Kweon, H. K.; Hakansson, K. In *characterization of phospopeptides by electron detachment dissociation in FT-ICR Mass Spectrometry*, 53rd ASMS, Proceedings of the 53rd ASMS Conference on Mass Spectrometry and Allied Topics, San Antonio, TX,, June 5-9, 2005; Proceedings of the 53rd ASMS Conference on Mass Spectrometry and Allied Topics, San Antonio, TX,, June 5-9, 2005.

47. Yang, J.; Mo, J. J.; Adamson, J. T.; Hakansson, K., Characterization of oligodeoxynucleotides by electron detachment dissociation Fourier transform ion cyclotron resonance mass spectrometry. *Anal. Chem.* **2005,** 77, 1876-1882.
48. Bilusich, D.; Brinkworth, C. S.; Bowie, J. H., Negative ion mass spectra of Cys-containing peptides. The characteristic Cys gamma backbone cleavage: a joint experimental and theoretical study. *Rapid Commun. Mass Spectrom.* **2004,** 18, 544-552.
49. McFarland, M. A.; Marshall, A. G.; Hendrickson, C. L.; Nilsson, C. L.; Fredman, P.; Mansson, J. E., Structural characterization of the GM1 ganglioside by infrared multiphoton dissociation/electron capture dissociation, and electron detachment dissociation electrospray ionization FT-ICR MS/MS. *J. Am. Soc. Mass Spectrom.* **2005,** 16, 752-762.
50. Hakansson, K.; Cooper, H. J.; Hudgins, R. R.; Nilsson, C. L., High resolution tandem mass spectrometry for structural biochemistry. *Curr. Org. Chem.* **2003,** 7, 1503-1525.
51. Senko, M. W.; Canterbury, J. D.; Guan, S. H.; Marshall, A. G., A high-performance modular data system for Fourier transform ion cyclotron resonance mass spectrometry. *Rapid Communications in Mass Spectrometry* **1996,** 10, 1839-1844.
52. Senko, M. W.; Canterbury, J. D.; Guan, S. H.; Marshall, A. G., A high-performance modular data system for Fourier transform ion cyclotron resonance mass spectrometry. *Rapid Commun. Mass Spectrom.* **1996,** 10, 1839-1844.
53. Jolles, P., Lysozymes - a Chapter of Molecular Biology. *Angew. Chem. Int. Ed.* **1969,** 8, 227-239.
54. Smith, L. F., Species Variation in Amino Acid Sequence of Insulin. *Am. J. Med.* **1966,** 40, 662-666.
55. Ryle, A. P.; Sanger, F.; Smith, L. F.; Kitai, R., Disulphide Bonds of Insulin. *Biochem. J.* **1955,** 60, 541-556.
56. Budnik, B. A.; Haselmann, K. F.; Elkin, Y. N.; Gorbach, V. I.; Zubarev, R. A., Applications of electron-ion dissociation reactions for analysis of polycationic chitooligosaccharides in Fourier transform mass spectrometry. *Anal. Chem.* **2003,** 75, 5994-6001.
57. Leeck, D. T.; Kenttamaa, H. I., Heat of Formation of the Radical-Cation of Dimethyl Disulfide. *Org. Mass Spectrom.* **1994,** 29, 106-107.
58. Butler, J. J.; Baer, T.; Evans, S. A., Energetics and Structures of Organosulfur Ions - Ch3ssch3+, Ch3ss+, C2h5s+, and Ch2sh+. *J. Am. Chem. Soc.* **1983,** 105, 3451-3455.
59. Thorne, G. C.; Gaskell, S. J., Elucidation of some fragmentations of small peptides using sequential mass spectrometry on a hybrid instrument. *Rapid Commun. Mass Spectrom.* **1989,** 3, 217-221.
60. Mo, J.; Hakansson, K., Characterization of nucleic acid higher order structure by high-resolution tandem mass spectrometry. *Anal. Bioanal. Chem.* **2006**.
61. Horn, D. M.; Ge, Y.; McLafferty, F. W., Activated ion electron capture dissociation for mass spectral sequencing of larger (42 kDa) proteins. *Anal. Chem.* **2000,** 72, 4778-4784.

62. Yang, J.; Hakansson, K. In *Fragmentation pathways of oligodeoxy and oligoribonucleotides in electron deatachment dissociation*, 53rd ASMS, Proceedings of the 53rd ASMS Conference on Mass Spectrometry and Allied Topics, San Antonio, TX,, June 5-9, 2005;
63. Waugh, R. J.; Bowie, J. H.; Hayes, R. N., Collision-Induced Dissociations of Deprotonated Peptides - Dipeptides Containing Phenylalanine, Tyrosine, Histidine and Tryptophan. *Int. J. Mass Spectrom. Ion Processes* **1991,** 107, 333-347.
64. Haselmann, K. F.; Budnik, B. A.; Kjeldsen, F.; Polfer, N. C.; Zubarev, R. A., Can the (M center dot-X) region in electron capture dissociation provide reliable information on amino acid composition of polypeptides? *Eur. J. Mass Spectrom.* **2002,** 8, 461-469.
65. Dehareng, D.; Dive, G., Vertical ionization energies of alpha-L-amino acids as a function of their conformation: an ab initio study. *Int. J. Mol. Sci.* **2004,** 5, 301-332.

Chapter 3

Comparison of the Electron Capture Dissociation Fragmentation Behavior of Doubly and Triply protonated Peptides from Trypsin, Glu C and Chymotrypsin Digestion

3.1. Introduction

Mass spectrometry has become the method of choice for protein identification, characterization and quantification due to its high accuracy and sensitivity that allow analysis of low abundance proteins and also its ability to analyze complex protein samples from cells, tissues and organisms.[1-4] Bottom-up[5-10] and top-down[11-13] approaches are both used in mass spectrometric protein analysis, with the former being the most widely applied. In the bottom-up approach, proteins are digested with a sequence-specific protease and the derived proteolytic peptides are analyzed by tandem mass spectrometry to provide sequence information for protein identification.

In tandem mass spectrometry, individual peptides are first selected and then fragmented by, e.g., collisions with an inert gas. Preferably, a single fragmentation technique should result in the formation of a sufficient number of product ions to unambiguously identify a peptide and subsequently the corresponding protein in a

database search, either based on MS/MS data from a single peptide or from multiple peptides from the same protein. However, in cases where genome data are not available to generate a protein database, or when peptides are posttranslationally modified, *de novo* sequencing may be required. *De novo* sequencing by mass spectrometry remains a challenge because it requires cleavage between each pair of amino acid residues and detection of all generated products.

Collision activated dissociation (CID),[14, 15] which induces cleavage of peptide backbone amide bonds to generate N-terminal *b* and C-terminal *y*-type ions, is by far the most widely used technique for obtaining peptide sequence information by MS/MS. However, in some cases, CID results only in uninformative neutral losses or selective cleavage at specific residues, thereby preventing formation of a sufficient number of product ions for peptide identification.[16, 17] Electron capture dissociation (ECD)[18, 19] and electron transfer dissociation (ETD),[20] which result in extensive cleavage of peptide backbone N-C_α bonds to form N-terminal *c* and C-terminal *z*-type product ions, are complementary to CID and constitute promising methods for *de novo sequencing* of peptides and proteins. In ECD, precursor ions are irradiated with low energy (<1 eV) electrons, resulting in electron capture by multiply charged cations and subsequent fragmentation. Because ECD provides more random backbone bond cleavages and does not show high specificity with respect to the identity of the neighboring amino acids, more extensive sequence coverage can be obtained compared to "slow heating" techniques such as CID.[19, 21-24] Another advantage of ECD and ETD compared to CID is the retention of labile posttranslational modifications,[25, 26] such as phosphorylation,[20, 27-29] glycosylation[30-35] and sulfation.[33, 36, 37]

It has been suggested that ECD and ETD proceed via a similar or identical cleavage mechanism. Furthermore, it has been demonstrated that doubly protonated precursor ions exhibit limited fragmentation in conventional (i.e., no ion activation or heating) ETD.[38-40] However, elevated bath gas temperatures for precursor ion activation[39] or supplementary collisional activation of the charge reduced species[40] increase the sequence coverage obtained for tryptic doubly protonated precursor ions in ETD. For model peptides, ETD of triply protonated peptides resulted in more extensive sequence coverage compared to doubly protonated peptides.[38] In ECD, limited fragmentation of doubly protonated peptides has not been reported. McLuckey and coworkers suggested that the lower reaction exothermicities, the possibly lower energy partitioning into product ions, and the higher product ion cooling rates associated with electron transfer experiments could explain why ETD might show more dependence on parent ion charge than ECD.[38] However, no direct comparison between doubly and triply protonated peptides has been performed in ECD. Previous experiments examining the relationship between peptide sequence coverage and precursor ion charge state were performed exclusively on model peptides and focused on a variety of charge states. For example, Williams and coworkers[41] have characterized ECD of the $[M + 2H]^{2+}$ to $[M + 5H]^{5+}$ precursor ions of a synthetic peptide. The $[M + 3H]^{3+}$ and the $[M + 4H]^{4+}$ precursor ions resulted in almost identical fragmentation behavior and a wider range of product ions was observed for these charge states compared to the doubly protonated precursor ions. However, the $[M + 5H]^{5+}$ precursor ion showed less fragmentation compared to the triply and quadruply protonated species. Zubarev and coworkers[42] suggested that, for model peptides, the frequencies of N-C_α bond cleavages in ECD are less dependent on the precursor ion

charge state, the total number of basic sites, and the nature of the terminal group compared to amide bond cleavage in CID.

Even though these experiments provided some insights into the effect of precursor ion charge state on peptide sequence coverage, they were performed on model peptides and, therefore, they do not necessarily represent the ECD fragmentation behavior of proteolytically derived peptides. Since proteolytic peptides are the kind of peptides encountered in bottom-up proteomics, examining their ECD fragmentation behavior is of particular interest. Furthermore, most bottom-up proteomics approaches and nearly all mass spectrometric *de novo* sequencing approaches rely on tryptic doubly protonated peptides. To which extent tryptic doubly protonated peptides provide the highest possible sequence coverage in ECD remains to be answered. Increasing the number of observed product ions in ECD would be an essential step to improve *de novo* sequencing. For these reasons we were interested in investigating and comparing the ECD fragmentation behavior of proteolytically derived peptides. Therefore, we examined the ECD fragmentation behavior of 64 doubly and 64 triply protonated proteolytic peptides (i.e., 128 total peptide ions), containing up to four missed cleavages (10-23 residues long), from trypsin, Glu C and chymotrypsin digestion. By these experiments we were aiming to address whether triply protonated peptides result in greater degree of sequence coverage compared to doubly protonated peptides, as is the case in ETD, and also to seek the optimum enzyme (in terms of maximum MS/MS peptide sequence coverage obtained), if any, for ECD. Only peptides that appeared in both the 2+ and 3+ charge states were chosen for analysis, i.e., the amino acid sequences of doubly and triply protonated peptides were the same. This choice was made to ensure that observed

differences in fragmentation behavior were due to differences in charge state (and/or structural differences associated with charge state) rather than due to differences in the amino acid context of individual peptides. Budnik et al have suggested that "ECD cleavage frequencies are determined primarily by the local sequence"[42] and Savitski et.al. have also reported sequence preferences in ECD.[43] Finally, we compare our results for tryptic doubly protonated peptides with those previously reported for ETD.[40]

3.2. Experimental Procedures

3.2.1. Sample Preparation

To obtain proteolytic peptides containing none or several missed cleavages, digestion conditions, time, and enzyme to protein ratio were varied. Trypsin (Promega, Madison, WI) and chymotrypsin (Sigma, St. Louis, MO) digestions were performed in 50 mM ammonium bicarbonate (Fisher Scientific, Fair Lawn, NJ) at 37 ^{0}C and 30 ^{0}C, respectively, unless otherwise noted and Glu C (Roche, Indianapolis, IN) digestions were performed in 25 mM ammonium bicarbonate at 26-27 ^{0}C.

Apomyoglobin from horse skeletal muscle (0.47 nmol, Sigma) was digested with trypsin, Glu C, or chymotrypsin at an enzyme to protein ratio of 1:50. Chymotrypsin digestion was performed in 100 mM Tris-HCl (Promega) and 10mM calcium chloride (Fisher). Digestion time was 90 min or seven hours for trypsin, 75 min or eight hours for Glu C and 12 hours for chymotrypsin. Bovine brain calmodulin (0.60 nmol, Sigma) digestion was performed at 1:50 enzyme to protein ratio for trypsin and chymotrypsin. Trypsin digestion was performed for three or eight hours, and chymotrypsin digestion was performed for eight hours. For Glu C digestion, a ratio of 1:30 enzyme to protein was used and the digestion time was five or nine hours. Bovine heart cytochrome *c* (0.21

nmol, Sigma) was digested with trypsin at an enzyme to protein ratio of 1:30 for 12 hours. For chymotrypsin digestion, cytochrome *c* was first heat denatured in a water bath for 10 min at 98 ^{0}C and then placed in an ice bath for ~five minutes. Chymotrypsin was then added at a 1:50 enzyme to protein ratio and digestion proceeded for five hours. Ubiquitin from bovine red blood cells (0.34 nmol, Sigma) was digested with trypsin at a 1:50 enzyme to protein ratio for three hours. BSA (0.45 nmol, Sigma) was reduced with 10 mM dithiothreitol (DTT, Sigma, St. Louis, MO) in 50 mM ammonium bicarbonate for 45 min at 56 ^{0}C and then carboxyamidomethylated with 50 mM iodoacetamide (Sigma, St. Louis, MO) in 50 mM ammonium bicarbonate in darkness for one hour. Following reduction and alkylation, BSA was digested with trypsin at an enzyme to protein ratio of 1:50 for four hours, or at a ratio of 1:100 for 45 minutes. Glu C digestions were performed at an enzyme to protein ratio of 1:50 for 10 hours, or at a ratio of 1:100 for three hours and chymotrypsin digestion were performed at 1:50 enzyme to protein ratio for seven or 10 hours, or at 1:100 enzyme to protein ratio for one or three hours. All reactions were quenched with 0.2-0.5 % formic acid (Acros Organics, Morris Plains, NJ). The digested samples were desalted with C_{18} Ziptips (Millipore, Billerica, MA) and diluted into 600-740 μL electrospray solvent containing 50% acetonitrile (Fisher) and 0.1% formic acid.

3.2.2. Mass Spectrometry

All experiments were performed with an actively shielded 7T quadrupole Fourier transform ion cyclotron resonance (Q-FT-ICR) mass spectrometer (Apex-Q, Bruker Daltonics, Billerica, MA), which has been previously described.[44] Proteolytic mixtures were electrosprayed in positive ion mode at a flow rate of 70 μL/hour. Ions were

accumulated in the first hexapole for 0.1 s, transferred through the mass selective quadrupole (1-6 m/z isolation window), mass selectively accumulated in the second hexapole for 0.1 to 5 s, transferred through high-voltage ion optics, and captured in the ICR cell[45] by dynamic trapping. This accumulation sequence was looped 2-5 times to maximize precursor ion signal. The accumulation time in the second hexapole and the number of loops of the accumulation sequence were varied to ensure that the total signal of ions entering the ICR cell for the ECD experiments was very similar (9×10^6 to 1×10^7 absolute abundance (single scan) in XMASS software) for all peptides examined. Further precursor ion isolation was achieved by correlated harmonic excitation fields[46] inside the ICR cell.

Peptides that were detected as both doubly and triply protonated species were selected for ECD experiments. ECD was performed with an indirectly heated hollow dispenser cathode at a bias voltage of 0.01-0.50 V and an irradiation time of 30-80 ms. A lens electrode located in front of the hollow cathode was kept at 1.0 V. All spectra were acquired with XMASS (version 6.1, Bruker Daltonics) using 256 or 512 K data points and summed over 64 scans. Data processing was performed with the MIDAS analysis software.[47] Internal frequency-to-mass calibration was performed by Microsoft Excel using a two term calibration equation. The calculated masses of the precursor ions and the charge-reduced species were used for calibration. In some cases the precursor ion and abundant *c'* or *z*• product ions were used for calibration. In these cases, calibration was repeated with the precursor ion and one additional product ion to ensure correct assignments. Product ion spectra were interpreted using the MS Product function (http://prospector.ucsf.edu/prospector/4.0.8/html/msprod.htm) in Protein Prospector.

Only peak assignments with a mass accuracy better than 15 ppm were accepted (most assignments were within 10 ppm, however, the relatively high error tolerance is due to low signal-to-noise ratios of some fragment ions, and the use of in-cell isolation).

3.2.3. Mascot Search

ECD data obtained for doubly or triply protonated peptides from the investigated proteins were combined and a Mascot MS/MS search was performed (http://www.matrixscience.com/cgi/search_form.pl?FORMVER=2&SEARCH=MIS). The tandem mass spectra were searched against the SwissProt data base and the taxonomy used was Mamalia (mammals). Searches were performed for both trypsin and chymotrypsin digests allowing up to 4 missed cleavages. No Glu C search was performed because Mascot does not currently support that enzyme. The peptide mass tolerance was set to 15 ppm and the MS/MS mass tolerance was set to 0.02 Da. The instrument setting was "FTMS-ECD".

3.3. Results and Discussion

A total of 128 doubly and triply protonated peptides from trypsin, chymotrypsin and Glu C digestion of apomyoglobin, calmodulin, cytochrome *c*, ubiquitin, and BSA were characterized by ECD. Trypsin cleaves at the C-terminal side of lysine and arginine, while chymotrypsin cleaves at the C-terminal side of tyrosine, phenylalanine, tryptophan, leucine, and methionine and Glu C provides cleavage at the C-terminal side of glutamic acid. Peptides resulting from these enzymatic digestions vary in length from 10-23 amino acid residues and they contain none or up to four missed cleavages. 48 of these peptides were tryptic peptides, 40 were chymotryptic peptides and another 40 peptides were derived from Glu C digestion.

The percent peptide sequence coverage was defined as: number of observed backbone N-Cα cleavages/number of N-Cα backbone bonds) × 100. When calculating the number of N-Cα backbone bonds in peptides we do include Pro linkages, unless otherwise indicated, even though ECD cleavage at the N-terminal side of Pro is generally not observed. Because of hydrogen rearrangements, N-terminal product ions are assigned here as c' (or $c\bullet$) and C-terminal product ions as $z\bullet$ (or z'), according to the nomenclature proposed by Zubarev and co-workers in which "′" denotes a hydrogen.[48] Formation of $c\bullet/z'$ versus $c'/z\bullet$ due to hydrogen rearrangement has been previously observed in ECD.[24] Hydrogen rearrangement to and from $z\bullet$ product ions has been extensively characterized in a large dataset of doubly protonated tryptic peptides and it has been shown to be as high as 47%.[49] Furthermore, hydrogen abstraction from c'-type fragments to form $c\bullet$-type product ions, has been examined in synthetic peptides and it was found that extensive hydrogen rearrangement and H/D scrambling occurs in ECD.[50] Recently, it was demonstrated that the rate and direction of hydrogen atom transfer between N-terminal and C-terminal product ions can be used to distinguish N- from C-terminal product ions in ECD.[51]

3.3.1. Triply Protonated Peptides Showing the Same or Less ECD Fragmentation Compared to Doubly Protonated Peptides

A total of nine triply protonated peptides (Table 3.1, peptides 1 to 9) showed the same number of N-Cα backbone cleavages, resulting in the same amount of peptide sequence coverage as their doubly protonated counterparts. Three of these peptides are derived from Glu C digestion, two are chymotryptic peptides and four are tryptic peptides. Peptides 10, 11, 13. and 14 in Table 3.1 showed one more backbone cleavage when the doubly protonated peptides were fragmenting in ECD compared to the

corresponding triply protonated species. Doubly protonated peptide 12 in Table 3.1 showed two more ECD fragments compared to the corresponding triply protonated peptide. The triply protonated peptides which resulted in less ECD fragmentation compared to their doubly protonated counterparts represent 7.8% of all peptides examined and they are short length peptides showing an average of 12 amino acid residues. These peptides are mainly chymotryptic (4.6% out of 7.8%). Only one tryptic and one Glu C digest peptide showed increased fragmentation when the doubly protonated species were subjected to ECD. Our data, shown in Table 3.1, is in agreement with ETD experiments, in which it was shown that short length doubly protonated peptides fragment sufficiently in ETD.[39] For all the $[M + 3H]^{3+}$ peptides, more *c*-type product ions were detected compared to the $[M + 2H]^{2+}$ species. Thus, a main advantage of fragmenting $[M + 3H]^{3+}$ ions is the formation of complementary fragment pairs. Only one doubly protonated peptide, peptide 1 in Table 3.1, showed complementary product ions in contrast to triply protonated peptides, which all showed formation of complementary fragment pairs. The presence of complementary product ions is highly useful in spectral interpretation and for further verification of the peptide sequence, not only when searching databases but also when *de novo sequencing* is required. However, complementary product ions are less common in ECD of doubly protonated peptides than in CID because one of the charges is neutralized by electron capture.

Differences in fragmentation behavior of doubly and triply protonated peptides can also be attributed to differences in their gas phase structures/conformations. Structural dependence of the ECD fragmentation outcome as well as dependence on differences in sites of charge solvation have been previously reported in a number of experimental

configurations.[52-57] Structural effects may explain the behavior of the peptides which did not show improved fragmentation in their 3+ charge states compared to their 2+ charge states.

Table 3.1. ECD fragmentation summary of doubly and triply protonated peptides with triply protonated species showing the same or less fragmentation compared to their doubly protonated counterparts [a]

Peptide #	$[M + 2H]^{2+}$	Seq.Cov. (%)	$[M + 3H]^{3+}$	Seq.Cov. (%)
1 Apom.	LFTGHPETLEK	70%	LFTGHPETLEK	70%
2 BSA	HLVDEPQNLIK	90%	HLVDEPQNLIK	90%
3 Cyt *c*	TGPNLHGLFGR	60%	TGPNLHGLFGR	60%
4 Apom.	LFRNDIAAKYKE	91%	LFRNDIAAKYKE	91%
5 Apom.	VLIRLFTGHPETLE	77%	VLIRLFTGHPETLE	77%
6 BSA	KDLGEEHFKGL	90%	KDLGEEHFKGL	90%
7 BSA	SLHTLFGDELCK	82%	SLHTLFGDELCK	82%
8 BSA	DKLKHLVDEPQNL	83%	DKLKHLVDEPQNL	83%
9 BSA	DYLSLILNRLCVLHE	86%	DYLSLILNRLCVLHE	86%
10 BSA	VPKAFDEKLF	89%	VPKAFDEKLF	78%
11 BSA	SRRHPEYAVSVL	73%	SRRHPEYAVSVL	67%
12 BSA	SRRHPEYAVSVLL	83%	SRRHPEYAVSVLL	64%
13 BSA	YAVSVLLRLAKEYE	85%	YAVSVLLRLAKEYE	77%
14 Cyt *c*.	TGQAPGFSYTDANK	92%	TGQAPGFSYTDANK	85%

[a] These peptides have smaller size, showing an average length of 12 amino acid residues. Although no increase in sequence coverage was observed in ECD of the $[M + 3H]^{3+}$ ions, more complementary fragment pairs were detected compared to ECD of the corresponding $[M +2H]^{2+}$ ions. Also, a larger number of *c*-type ions is observed for the triply protonated species. Proteolytic peptides with Lys (K) at the C-terminus are derived from trypsin digestion, peptides with a C-terminal Glu (E) are derived from Glu C digestion and peptides with Leu (L) or Phe (F) at the C-terminus are chymotryptic peptides. Apom, Peptides are derived from apomyoglobin digestion; BSA, Peptides are from BSA digestion; Cyt *c*, Peptides are from cytochrome *c* digestion.

3.3.2. Triply Protonated Peptides Showing Greater Degree of Sequence Coverage Compared to their Doubly Protonated Counterparts

Table 3.2 displays peptides in which ECD of the $[M + 3H]^{3+}$ precursor ions resulted in more N-Cα backbone bond cleavages, compared to the $[M + 2H]^{2+}$ precursor ions, thus improving peptide sequence coverage. These peptides represent 33% of the examined peptides. Eleven of these peptides derived from Glu C digestion, five are tryptic peptides, and five are chymotryptic peptides. Similar to the peptides discussed above, with the exception of two peptides (peptides 20 and 21 in Table 3.2, which produced one complementary fragment pair each), complementary product ions are absent for doubly protonated peptides, whereas triply protonated peptides produced a high number of complementary fragment pairs. Notably, the increase in peptide sequence coverage is very similar for all three peptide types, i.e., chymotryptic, tryptic and Glu C digest peptides. Overall, ECD of triply protonated chymotryptic peptides resulted in a 19% increase in peptide sequence coverage versus 22% for Glu C digest peptides and 20% for tryptic peptides. An increased production of *z*- and *c*-type ions was seen for the majority (95 %) of peptides examined (see also discussion below).

Figure 3.1 shows ECD spectra of both the doubly and triply protonated form of a Glu- C digest peptide from apomyoglobin (peptide 34, Table 3.2.). ECD of the $[M + 2H]^{2+}$ precursor ions resulted in cleavages at 10 out of 17 backbone interresidue bonds, whereas ECD of the $[M + 3H]^{3+}$ precursors yielded cleavages at 15 out of 17 backbone bonds. ECD of the triply protonated peptide resulted in formation of 26 out of 34 possible *c*- and *z*-type product ions whereas only 10 *c*- and *z*-type ions were formed in ECD of the doubly protonated peptide. Both $z\bullet/(z')$ and $c'/(c\bullet)$ product ions were observed for the $[M + 2H]^{2+}$ precursor ions whereas only one product ion, $z_5\bullet$, showed

hydrogen rearrangement (hydrogen loss) for the triply protonated precursor ions. Hydrogen loss from z• ions has recently been studied in detail by Zubarev and co-workers.[49] Their work reported that H• loss occurs when serine, threonine or tryptophan are adjacent to the radical site formed following N-C_α backbone bond cleavage. Consistently, the observed (z_5• - H•) fragment has an N-terminal tryptophan residue.

As mentioned above the fragmentation outcome in ECD is believed to be influenced by the gas-phase conformation of precursor ions.[55, 56] The higher sequence coverage observed for triply protonated peptides is likely due to more unfolded gas-phase conformations (due to increased Coulomb repulsion). In addition, charge-reduced precursor ions resulting from electron capture by doubly protonated species are singly charged and, therefore, there is no Coulomb repulsion that can assist in product pair separation.[51] Consistently, we observed that charge reduced $[M + 2H]^{+\bullet}$ ions dominate ECD spectra of doubly protonated peptides. By contrast, abundant even electron $[M + 2H]^{2+}$ products were observed in ECD of triply protonated peptides. The corresponding hydrogen loss has been previously examined and it was suggested that more highly charged and more unfolded charge-reduced ions lose H• atoms to a larger extent,[53] consistent with our observations.

Another important factor for the higher amount of product ions observed for triply protonated peptides is the existence of two charges instead of one following electron capture. The increased availability of charge increases the probability of fragments being charged and thereby detectable.

Table 3.2. ECD fragmentation summary of doubly and triply protonated peptides with the latter yielding higher sequence coverage compared to the former [a]

Peptide #	$[M + 2H]^{2+}$	Seq.Cov. (%)	$[M + 3H]^{3+}$	Seq.Cov. (%)
15 Apom.	VLIRLFTGHPE	60%	VLIRLFTGHPE	70%
16 Calm.	MKDTDSEEEIR	80%	MKDTDSEEEIR	90%
17 BSA	IARRHPYFYAPE	55%	IARRHPYFYAPE	73%
18 Apom.	KFDKFKHLKTEAE	83%	KFDKFKHLKTEAE	88%
19 Calm.	KDTDSEEEIREAF	75%	KDTDSEEEIREAF	92%
20 Apom.	TGHPETLEKFDKF	67%	TGHPETLEKFDKF	83%
21 BSA	DDPHACYSTVFDK	67%	DDPHACYSTVFDK	83%
22 BSA	IKQNCDQFEKLGEY	62%	IKQNCDQFEKLGEY	92%
23 BSA	LLYYANKYNGVFQE	85%	LLYYANKYNGVFQE	92%
24 Cyt *c*.	AGIKKKGEREDLIAY	79%	AGIKKKGEREDLIAY	86%
25 Apom.	YLEFISDAIIHVLHSK	67%	YLEFISDAIIHVLHSK	87%
26 Ubiq.	TITLEVEPSDTIENVK	57%	TITLEVEPSDTIENVK	86%
27 BSA	KLFTFHADICTLPDTE	60%	KLFTFHADICTLPDTE	86%
28 BSA	SHAGCEKSLHTLFGDE	53%	SHAGCEKSLHTLFGDE	93%
29 BSA	EATLEECCAKDDPHACY	50%	EATLEECCAKDDPHACY	75%
30 Cyt *c*.	GITWGEETLMEYLENPK	50%	GITWGEETLMEYLENPK	75%
31 Calm.	AFRVFDKDGNGYISAAE	56%	AFRVFDKDGNGYISAAE	81%
32 Calm. I.	AFSLFDKDGDGTITTKE	75%	AFSLFDKDGDGTITTKE	94%
33 Calm. ..	FLTMMARKMKDTDSEEE	50%	FLTMMARKMKDTDSEEE	81%
34 Apom.	GLSDGEWQQVLNVWGKVE	59%	GLSDGEWQQVLNVWGKVE	88%
35 BSA	ACFAVEGPKLVVSTQTALA	83%	ACFAVEGPKLVVSTQTALA	88%

[a] For all peptides listed in this table, ECD of the $[M + 3H]^{3+}$ precursor ions resulted in the formation of significantly more *c*- and *z*- type product ions and also in higher sequence coverage. Only two doubly protonated species showed complementary product ions, whereas tripl protonated peptides yielded high numbers of complementary fragment pairs. Proteolytic peptides with Lys (K) or Arg (R) at the C-terminus are derived from trypsin digestion, peptides with a C-terminal Glu (E) are derived from Glu C digestion, and peptides with Phe (F) or Tyr (Y) at the C-terminus are chymotryptic peptides. Calm, Peptides are from Calmodulin digestion; Apom, Peptides are derived from apomyoglobin digestion; BSA, Peptides are from BSA digestion; Ubiq, Peptides are from ubiquitin digestion; Cyt *c*, Peptides are from cytochrome *c* digestion. Peptide 35 derived from Clu-C digestion and it contains the C-terminal of the protein.

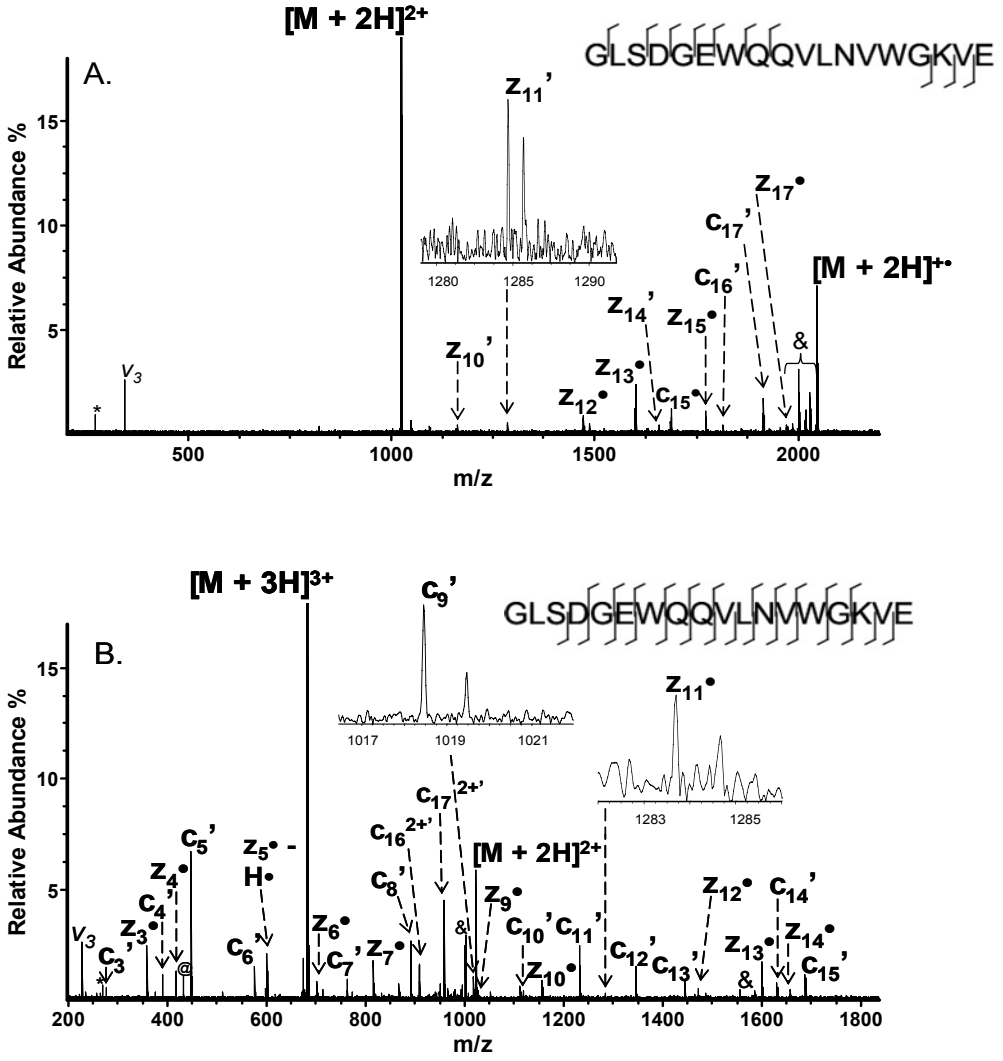

Figure 3.1. ECD of A) doubly and B) triply protonated peptide from apomyoglobin Glu C digestion. ECD of the doubly charged peptide resulted in formation of 10 out of 34 possible backbone product ions, whereas ECD of the triply charged ion yielded 26 product ions. No complementary fragment pairs were detected for the doubly protonated species. Two doubly charged product ions, c_{16}' and c_{17}', were observed in the ECD spectrum of the $[M + 3H]^{3+}$ precursor ion. All others product ions are singly charged. $^{(*)}$ electronic noise peaks, $^{\&}$ = neutral losses, v_3 = 3rd harmonic $^{@}$ = *y*-type product ion.

3.3.3. Doubly Protonated Peptides Showing Poor ECD Fragmentation

ECD of all triply protonated peptides listed in Table 3.3 resulted in a significant increase in sequence coverage compared to ECD of the corresponding doubly protonated species. These doubly protonated peptides showed less than 50% sequence coverage

from ECD and they represent 23% of all peptides examined. Eight of these peptides are chymotryptic peptides, three are Glu C digest peptides, and four are from trypsin digestion. All peptides listed in Table 3.3, independently of the proteolytic enzyme used, behaved similarly in ECD, showing significantly more fragmentation for triply protonated precursors compared to doubly protonated precursors. This behavior is similar to that of the peptides discussed in the previous section.

Peptides displayed in Table 3.3 are generally longer compared to the peptides shown in Tables 3.1 and 3.2. On average, peptides in Table 3.1 are 12 amino acid residues long versus an average of 15 amino acid residues for peptides shown in Table 3.2 and an average of 18 amino acid residues for peptides displayed in Table 3.3. In ETD, it has been observed that, for doubly protonated peptides, the extent of fragmentation decreases with increasing peptide size.[39, 40] For example, ETD of an eight residue, doubly protonated, tryptic peptide resulted in cleavages at every possible N-Cα backbone bond whereas ETD of a 22 residue peptide showed only three product ions under non-heated conditions.[39] Our results are similar to those reported from ETD: as the peptide length increases, doubly protonated species tend to show limited fragmentation in ECD. Peptide 50, the largest peptide examined here, showed only 14% sequence coverage from doubly protonated precursors. In contrast, the extent of fragmentation for triply protonated precursor examined here does not appear to be affected by the peptide size.

Table 3.3 ECD fragmentation summary of doubly and triply protonated peptides with the former showing poor sequence coverage [a]

Peptide #	$[M + 2H]^{2+}$	Seq.Cov. (%)	$[M + 3H]^{3+}$	Seq.Cov. (%)
36 $_{BSA}$	MPCTEDYLSLILNR	38%	MPCTEDYLSLILNR	85%
37 $_{BSA}$	VDKCCAADDKEACF	38%	VDKCCAADDKEACF	85%
38 $_{Calm}$	TNLGEKLTDEEVDEM	43%	TNLGEKLTDEEVDEM	93%
39 $_{Calm}$	SLFDKDGDGTITTKEL	47%	SLFDKDGDGTITTKEL	93%
40 $_{Calm}$	IREADIDGDQGVNYEEF	38%	IREADIDGDQGVNYEEF	88%
41 $_{Calm}$	MIREADIDGDGQVNYEE	25%	MIREADIDGDGQVNYEE	81%
42 $_{BSA}$	LKPDPNTLCDEFKADEK	31%	LKPDPNTLCDEFKADEK	81%
43 $_{Cyt\ c}$	GITWGEETLMEYLENPKK	47%	GITWGEETLMEYLENPKK	70%
44 $_{BSA}$	LLKHKPKATEEQLKTVME	41%	LLKHKPKATEEQLKTVME	88%
45 $_{BSA}$	NVWGKVEADIAGHGQEVL	41%	NVWGKVEADIAGHGQEVL	94%
46 $_{BSA}$	LQQCPFDEHVKLVNELTEF	22%	LQQCPFDEHVKLVNELTEF	67%
47 $_{BSA}$	TRKVPQVSTPTLVEVSRSL	22%	TRKVPQVSTPTLVEVSRSL	88%
48 $_{Calm}$	LRHVMTNLGEKLTDEEVDE	17%	LRHVMTNLGEKLTDEEVDE	67%
49 $_{Calm}$	EADIDGDGQVNYEEFVQMMTAK	29%	EADIDGDGQVNYEEFVQMMTAK	90%
50 $_{Apom.}$	HSKHPGDFGADAQGAMTKALELF	14%	HSKHPGDFGADAQGAMTKALELF	82%

[a] As the peptide size increases, $[M + 2H]^{2+}$ ions tend to show limited fragmentation. In sharp contrast, their triply protonated counterparts yielded a large number of both *c*- and *z*-type ions, resulting in peptide sequence coverages ranging from 67 to 93%. Proteolytic peptides with Lys (K) or Arg (R) at the C-terminus are derived from trypsin digestion, peptides with a C-terminal Glu (E) are Glu C derived peptides, and proteolytic peptides having a C-terminal Phe (F) or Leu (L) or Phe (F) are chymotryptic peptides. BSA, Peptides are from BSA digestion; Calm, Peptides are from Calmodulin digestion; Apom, Peptides are derived from apomyoglobin digestion; Cyt *c*, Peptides are from cytochrome *c* digestion; (^), indicates that these product ions cannot be distinguished based on their masses.

It is worth noting that the doubly protonated forms of some of the peptides in Table 3.3 exhibit extremely low fragmentation, which poses a problem for protein identification/peptide sequencing. For example, ECD of the $[M + 2H]^{2+}$ ions of both peptides 48 and 50 resulted in only three backbone fragments, rendering peptide sequencing unfeasible. In sharp contrast, ECD of the corresponding triply protonated species showed cleavage at 12 of 16 backbone bonds for peptide 48 and 18 of 21 backbone bonds for peptide 50, thereby increasing the sequence coverage by 50 and 68%, respectively.

Figure 3.2 displays ECD spectra of the doubly and triply protonated precursors of a peptide from a BSA tryptic digest. Only five out of 24 possible backbone cleavages are observed in the ECD spectrum of the doubly protonated species, as opposed to 19 backbone fragments in the spectrum of the triply protonated species. ECD of the $[M + 3H]^{3+}$ ions resulted in cleavages at 11 out of 12 N-Cα backbone bonds (counting the N-terminal side of Pro, which is generally not observed in ECD). Also, all but three complementary fragment pairs are detected for the triply protonated precursors. Unsurprisingly, no complementary fragment pairs were observed in ECD of the doubly protonated precursors.

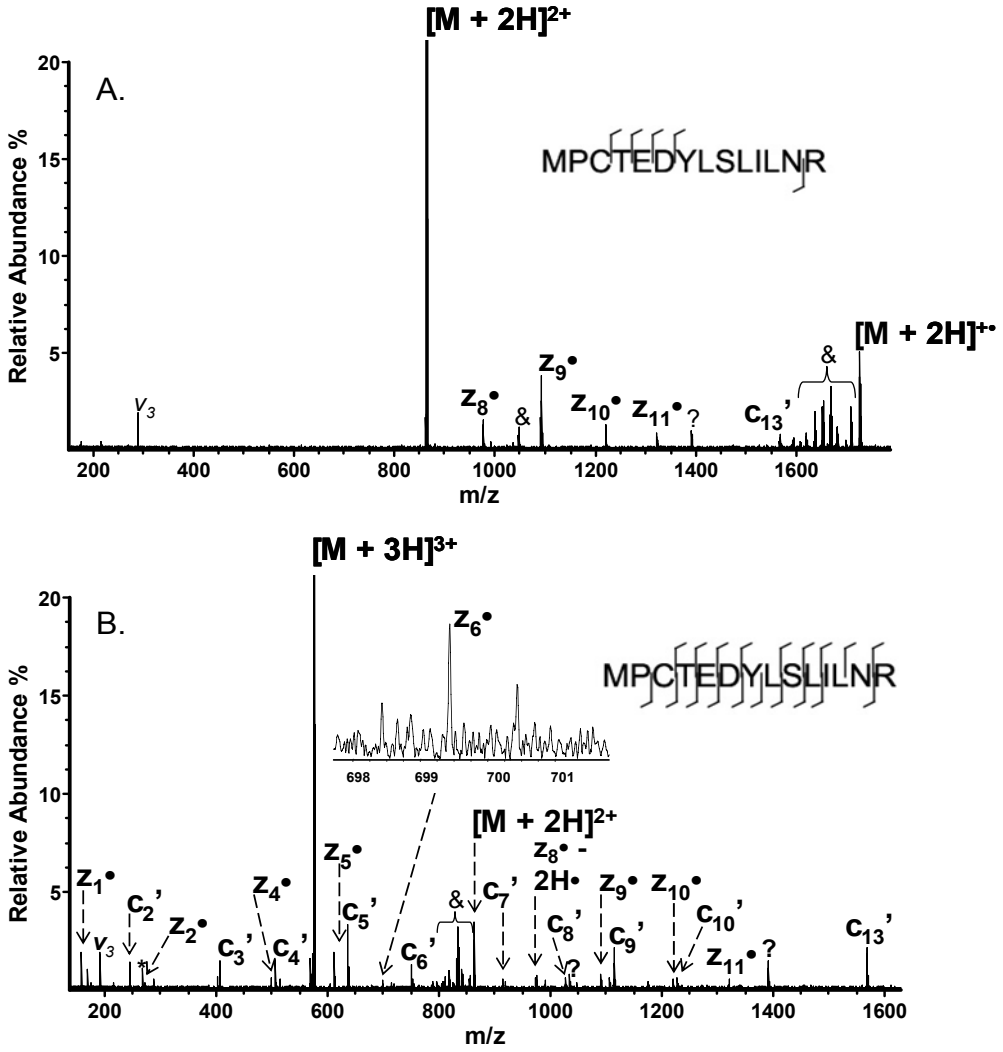

Figure 3.2. ECD of A) doubly and B) triply protonated peptide from BSA trypsin digest. For the doubly charged precursor ion, five out of 12 possible N-Cα backbone bond cleavages were observed whereas ECD of the triply protonated precursor showed cleavages at 11 backbone interresidue bonds. * = electronic noise peaks, & =, neutral losses, v_3 = 3rd harmonic, ? = unidentified product ions.

3.3.4. Triply Protonated Peptides Showing Cleavages at Every Possible N-Cα Backbone Bond

ECD of all $[M + 3H]^{3+}$ peptides in Table 3.4 showed dissociation at all possible nonproline N-C_α bonds, as opposed to ECD of the corresponding doubly protonated species, which showed varying, lower degrees of sequence coverage. These peptides represent 22% of all peptides characterized and they are mainly tryptic peptides (17% out

of 22%). These peptides further demonstrate that ECD of triply protonated precursors produce more product ions compared to the corresponding doubly protonated species, thereby increasing the sequence information that can be obtained.

In analogy to the doubly protonated peptides in Tables 3.1, 3.2 and 3.3, with the exception of peptides 51, 55, and 62 (Table 3.4), doubly protonated peptides in Table 3.4 showed no complementary fragment pairs. For four of these 14 doubly protonated peptides, the sequence coverage was high (87%-93%), however, it was still lower compared to the complete sequence coverage achieved when their triply protonated counterparts were fragmented by ECD.

ECD of triply protonated peptides 52, 53, 54, 56, 58 and 59 in Table 3.4, resulted not only in full sequence coverage but also in formation of almost all possible *c* and *z*-type product ions.

ECD of triply protonated peptide 51 (Table 3.4) resulted in formation of six *b*-type ions, in addition to the formation of *c*- and *z*-type ions, whereas ECD of the corresponding doubly protonated species showed only one *b*-type ion. ECD of triply protonated peptide H-ADQLTEEQIAFK-OH (data not shown) resulted in formation of 11 *b* ions but, similar to peptide 51, only one *b* ion was observed in ECD of the $[M + 2H]^{2+}$ precursor ions. Formation of *b* ions in ECD has been previously discussed[58-60] and it has been proposed to be a consequence of charge location,[60] peptide ion conformation,[58] and low gas-phase basicity.[59, 60]

Table 3.4. ECD fragmentation summary of doubly and triply-protonated peptides with triply protonated peptides showing dissociation at every possible N-Cα backbone bond [a]

Peptide #	$[M + 2H]^{2+}$	Seq.Cov. (%)	$[M + 3H]^{3+}$	Seq.Cov. (%)
51 Apom.	HGTVVLTALGGILK	92%	HGTVVLTALGGILK	100%
52 BSA	SQKFPKAEFVEVTKL	64%	SQKFPKAEFVEVTKL	93%
53 BSA	KVPQVSTPTLVEVSR	64%	KVPQVSTPTLVEVSR	85%
54 Calm.	VFDKDGNGYISAAELR	60%	VFDKDGNGYISAAELR	100%
55 Apom.	HPGDFGADAQGAMTK	71%	HPGDFGADAQGAMTK	93%
56 Apom.	VEADIAGHGQEVLIR	79%	VEADIAGHGQEVLIR	100%
57 Cyt *c*.	KTGQAPGFSYTDANK	79%	KTGQAPGFSYTDANK	93%
58 BSA	RPCFSALTPDETYVPK	47%	RPCFSALTPDETYVPK	80%
59 BSA	RHPYFYAPELLYYANK	53%	RHPYFYAPELLYYANK	87%
60 BSA	NFVAFVDKCCAADDKE	87%	NFVAFVDKCCAADDKE	100%
61 Calm.	EAFSLFDKDGDGTITTK	88%	EAFSLFDKDGDGTITTTK	100%
62 Apom.	GLSDGEWQQVLNVWGK	93%	GLSDGEWQQVLNVWGK	100%
63 Apom.	LKPLAQSHATKHKIPIKYLE	47%	LKPLAQSHATKHKIPIKYLE	84%
64 Apom.	TALGGILKKKGHHEAELKPL	47%	TALGGILKKKGHHEAELKPL	95%

[a] These peptides are mainly tryptic peptides. Cleavages N-terminal to proline are generally not observed in ECD. Similar to other triply protonated peptides (Tables 3.1-3.3), a large number of complementary fragment pairs was observed compared to doubly protonated peptides, which resulted in less ECD product ions with only one peptide showing complementary fragment pairs. Proteolytic peptides with Lys (K) or Arg (R) at the C-terminus are derived from trypsin digestion, peptides with a C-terminal Glu (E) are Glu C derived peptides, and proteolytic peptides having a C-terminal Leu (L) are chymotryptic peptides. Apom, Peptides are derived from apomyoglobin digestion; BSA, Peptides are from BSA digestion; Calm, Peptides are from calmodulin digestion; Cyt *c,* Peptides are from cytochrome *c* digestion.

Figure 3.3 displays one example, from a BSA tryptic peptide, of ECD in which triply protonated precursor ions generated every possible *c*- and *z*-type ion, with the exception of z_1. By contrast, only one *z* and six *c*-type product ions are observed for the doubly protonated precursors. In general, ECD of doubly protonated tryptic peptides results in dominant formation of C-terminal *z*-type ions due to the presence of a basic amino acid at the C-terminus.[61] However, peptide 59 contains a missed trypsin cleavage site and therefore has an arginine residue at the N-terminus in addition to a C-terminal lysine. Preferred neutralization of lysine over arginine in ECD has been proposed to be either due to differences in gas-phase basicity,[62] or due to differences in their hydrogen donating properties.[55] Independently of mechanism, charge retention at arginine results in detection of N-terminal product ions (*c*-type ions). The same behavior, i.e., detection of *c*- rather than *z*-type product ions, was observed for peptide 58 (Table 3.4), which also contains an N-terminal arginine. Peptide 55 (Table 3.4), which contains a lysine at the C-terminus and a histidine at the N-terminus, and peptide 57 (Table 3.4), which contains lysine at both ends, produced both *c*- and *z*-type ions.

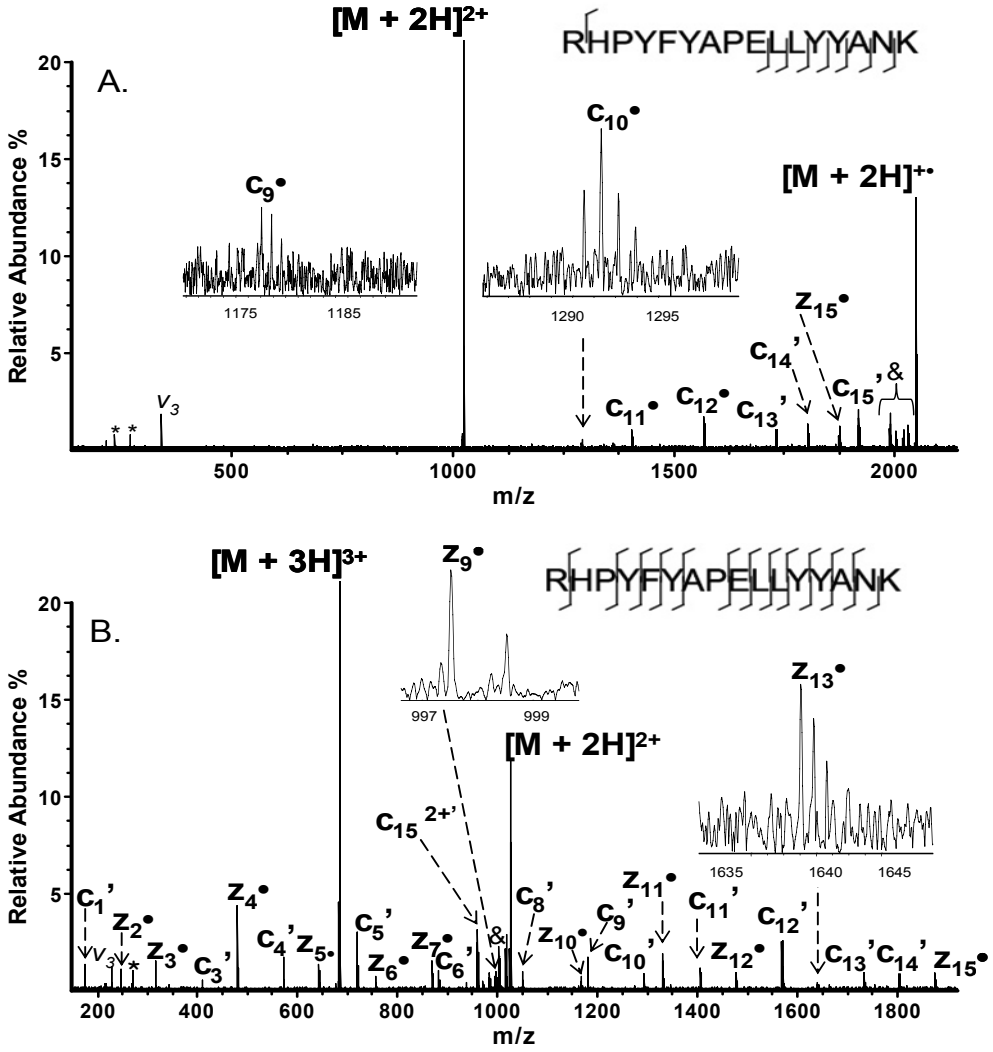

Figure 3.3. ECD of A) doubly and B) triply protonated precursor ions of a tryptic peptide from BSA. ECD of the triply charged precursor ions resulted in cleavages at all possible N-Cα backbone bonds and almost all of the possible complementary fragment pairs were detected. One more product ion, c_9•, is present in the ECD spectrum of the $[M + 2H]^{2+}$ but at low abundance (shown in the inset). One product ion, c_{15}', was detected as a doubly charged ion for the $[M + 3H]^{3+}$ precursor ion whereas all others fragments were singly charged. * = electronic noise peaks, & = neutral losses, v_3 = 3rd harmonic.

3.3.5. Evaluation and Comparison of the Three Proteolytic Enzymes Examined and Comparison between ECD of Doubly and Triply Protonated Peptides

In order to directly compare the three proteolytic enzymes used in this work, we recalculated the sequence coverages, excluding cleavages N-terminal to proline. This precaution was necessary because tryptic, chymotryptic and Glu C digest peptides do not

contain the same number of Pro residues. More specifically, the tryptic peptides examined, contained 5.4% Pro, versus 3.6% for chymotryptic peptides and 2.5% for Glu C digest peptides. The average length of proteolytic peptides from the three enzymes is comparable: tryptic peptides were on average 14.9 amino acids long, whereas chymotryptic peptides were on average 15.3 amino acids long and Glu C digest peptides had an average length of 15.7 amino acid residues. A detailed graph showing the peptide length produced by each proteolytic enzyme examined is shown in Figure 3.4.

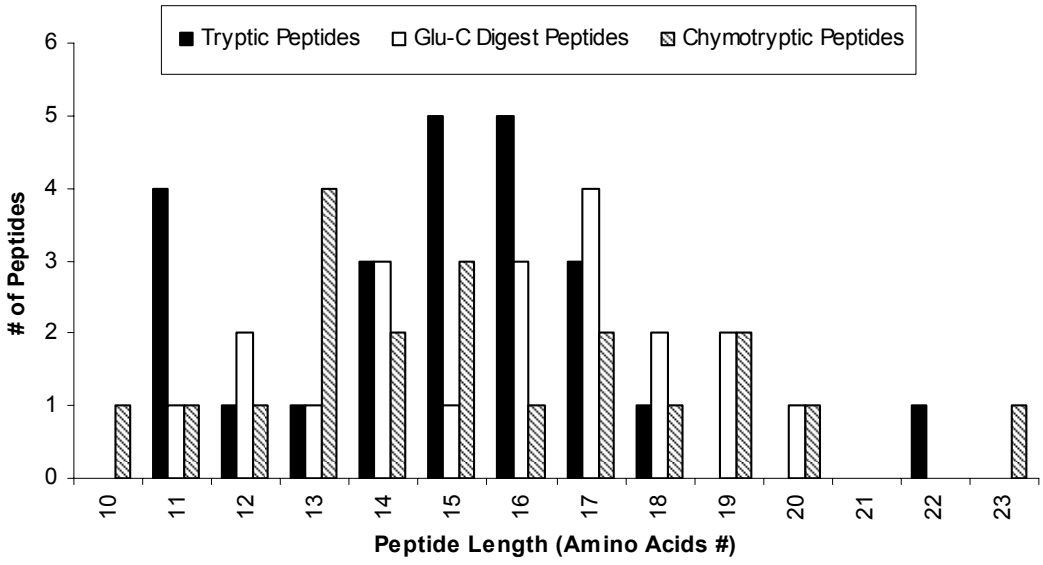

Figure 3.4. Number of peptides as a function of peptide length for the different proteolytic enzymes examined.

Table 3.5 displays the total number of observed N-Cα backbone bond cleavages, the total number of observed *c*- and *z*-type product ions, and the number of detected complementary fragment pairs for all doubly and triply protonated proteolytic peptides. For both doubly and triply protonated species, tryptic peptides exhibit a higher degree of sequence coverage, and generated a higher number of complementary fragment pairs.

Due to the presence of a basic residue at the C-terminus (as discussed above), a larger number of *z*-type product ions was observed for tryptic peptides compared to chymotryptic and Glu C digest peptides. The number of *c*-type ions is comparable for all three enzymes examined. For doubly protonated precursor ions, chymotryptic peptides show the lowest degree of ECD fragmentation, whereas chymotryptic and Glu C digest peptides show similar sequence coverage for triply protonated precursors. Differences in fragmentation behavior can be attributed to different gas-phase structures/conformations and different charge solvation patterns, as discussed above. The higher degree of sequence coverage obtained for tryptic peptides can also be attributed to the fact that tryptic peptides examined here were shorter in length, as discussed above, compared to chymotryptic peptides and peptides derived from Glu C digestion.

Table 3.5 also illustrates that triply protonated precursors produce more ECD fragments and yield dramatically increased numbers of complementary fragment pairs (44%) compared to doubly protonated precursors. Complementary fragment pairs are rare in ECD spectra of doubly protonated precursor ions. Increasing the number of complementary fragment pairs is essential because it improves the confidence in protein identification by database searching. In addition, a significant increase (27%) in the peptide sequence coverage is observed for triply protonated precursors as compared to the corresponding doubly protonated species. This increase was particularly high (34%) for chymotryptic peptides.

Table 3.5. ECD summary for A) all doubly and B) all triply protonated peptides examined [a]

A. Doubly-protonated peptides	Tryptic peptides	Glu-C digest peptides	Chymotryptic peptides
# of total backbone N-C_α cleavages	214/314 68%	168/269 62%	149/275 54%
# of total product ions	222/628 (127 z• / z' 95 c' / c•) 35%	169/538 (63 z• / z' 106 c' / c•) 31%	150/550 (62 z• / z' 88 c' / c•) 27%
# of complementary fragment pairs	7/314 2.2%	1/269 0.37%	1/275 0.36%

B. Triply-protonated peptides	Tryptic peptides	Glu-C digest peptides	Chymotryptic peptides
# of total backbone N-C_α cleavages	290/314 92%	235/269 87%	242/275 88%
# of total product ions	485/628 (216 z• / z' 269 c' / c•) 77%	327/538 (113 z• / z' 214 c' / c•) 61%	342/550 (123 z• / z' 219 c' / c•) 62%
# of complementary fragment pairs	194/314 62%	92/269 34%	100/275 36%

[a] Total number of observed N-C_α bond cleavages, total number of *c*- and *z*-type product ions, and total number of complementary fragment pairs observed is listed for all peptides. Here, cleavages N-terminal to proline were excluded because the Pro composition was different for tryptic, chymotryptic and Glu C digest peptides. Triply protonated peptides produced more ECD fragments and generated a dramatically increased number of complementary product pairs. A significant increase (27%) in peptide sequence coverage was also observed. ECD of tryptic peptides provided higher sequence coverage than for chymotryptic and GluC digest peptides for both doubly and triply protonated precursors.

Figure 3.5 shows a direct comparison between doubly and triply protonated precursor ions as a function of observed sequence coverage. Doubly protonated precursor ions show a wide range of sequence coverages, ranging from 14 to 92%. By

contrast, triply protonated precursors show a sequence coverage ranging from 64 to 100% with only one triply protonated peptide showing a 60% sequence coverage. 75% of the triply protonated precursors showed a sequence coverage between 80 and 100%.

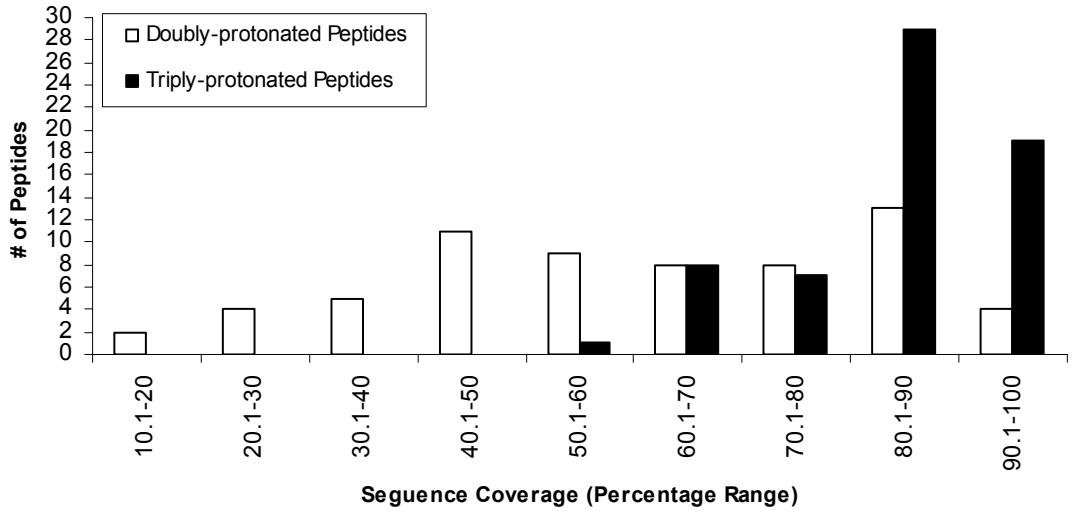

Figure 3.5. Percent peptide sequence coverage obtained in ECD for all doubly and triply protonated peptides examined. Higher sequence coverage is observed for triply protonated peptides.

Figure 3.6 shows the sequence coverage obtained for each proteolytic peptide as a function of precursor ion m/z ratio. Notably, full sequence coverage is mainly observed for tryptic triply protonated peptides. Only three doubly protonated peptides showed full sequence coverage, and two of these peptides are tryptic peptides. Furthermore, sequence coverage for doubly protonated peptides shows a strong dependence on precursor ion m/z ratio. The sequence coverage decreases with increasing precursor ion m/z ratio, in analogy with reported ETD fragmentation behavior of doubly protonated peptides.[39, 40] This decrease in sequence coverage is seen for all doubly protonated peptides examined, independent of which proteolytic enzyme was used for protein

digestion. For longer peptides, the advantage of fragmenting triply protonated precursors in ECD versus doubly protonated precursors becomes even more apparent than for shorter ones. For the peptide lengths of 10 to 23 amino acids examined here, triply protonated precursors do not show a strong dependence on precursor ion m/z ratio. However, it is possible that a maximum peptide length for which high sequence coverage is obtained exists for each charge state, as has been suggested for ETD.[39] This question could not be answered based on our current data set for triply protonated species.

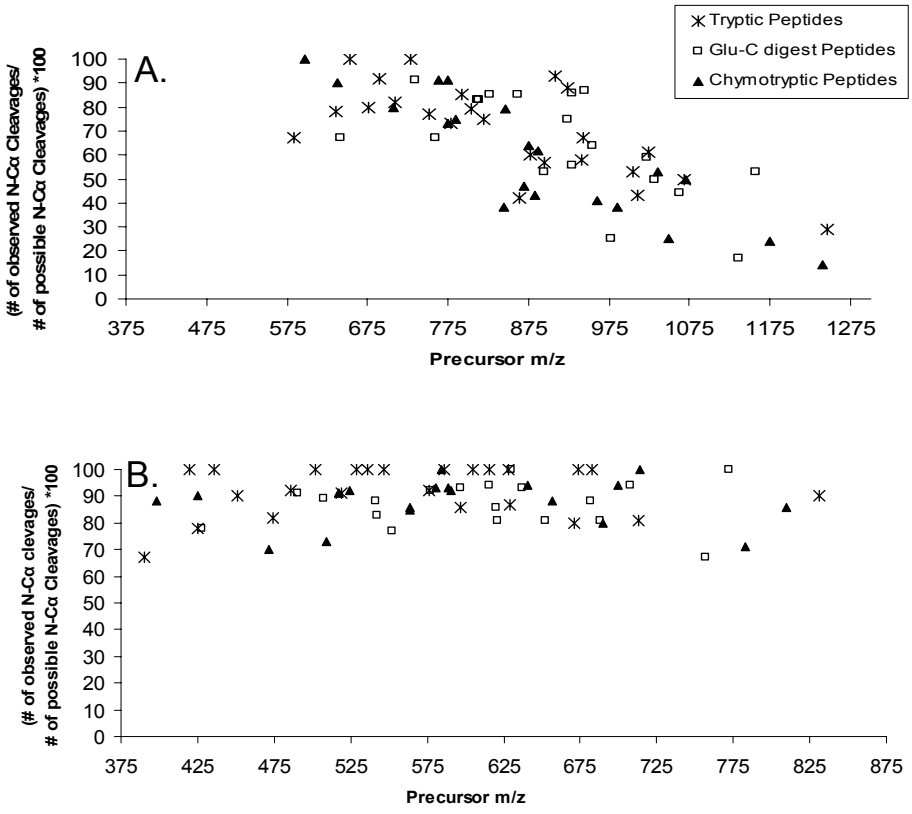

Figure 3.6. ECD sequence coverage as a function of precursor ions m/z ratio for A) doubly and B) triply protonated proteolytic peptides. For doubly protonated peptides, sequence coverage decreases with increasing peptide size.

We also calculated the occurrence of even-electron z′ and radical c•-type product ions (which are due to hydrogen transfer between z•/c′ ion pairs) based on the first peak in the isotopic distribution for each product ion (i.e., if a mixture of radical and even-electron products was observed, the isotopic cluster was assigned as a radical species). This occurrence was calculated as: number of observed z′ and c•-type product ions / total number of observed z•/z′ and c′/c• product ions. These data indicate that formation of z′ versus z• and c• versus c′ was more frequent in ECD spectra of doubly protonated precursors (12%) compared to ECD spectra of triply protonated precursors (5%). Such rearrangements may complicate spectral interpretation, particularly when analyzing unknowns and, thus, triply protonated precursor ions offer an additional advantage. We also noted that one and two hydrogen atom losses from *z*• product ions were prevalent when Thr residues were adjacent to the radical site, in agreement with previously reported results.[49]

Finally, we compared the Mascot MS/MS protein identification scores for ECD of doubly and triply protonated peptides from BSA and calmodulin. In all examined cases, significantly higher scores were obtained for the triply protonated species. Specifically, search against all BSA tryptic doubly protonated species resulted in a Mascot score of 220 versus 898 obtained for the triply protonated species. The same trend was observed for BSA chymotryptic peptides, for which the score for doubly protonated species was 216 versus 783 for the triply protonated species. For calmodulin tryptic peptides, we obtained a score of 134 for the doubly protonated species versus a score of 548 for the triply protonated species. The higher Mascot scores obtained for triply protonated species are a result of both the higher MS/MS peptide sequence coverage, the higher

number of complementary fragment pairs, as well as the lower degree of hydrogen atom rearrangement for triply protonated species compared to their doubly protonated counterparts. The Mascot search engine does not support hydrogen atom rearrangements. Similar results were recently reported by Kjeldsen et.al. who demonstrated that ETD of triply protonated proteolytic peptides, generated via charge enhancement with *m*-nitrobenzyl alcohol, yielded higher Mascot scores compared to the corresponding doubly protonated peptides.[63]

3.4. Conclusions

We believe the data presented above constitute the first systematic comparison of the ECD fragmentation behavior of doubly vs. triply protonated peptides resulting from different proteolytic enzymes. Our results demonstrate that ECD of triply protonated precursor ions significantly increases the number of *c*-and *z*-type product ions as compared to doubly protonated precursors. In addition, tryptic peptides were found to provide higher degree of sequence coverage compared to chymotryptic and Glu C digest peptides. Although it has been suggested that trypsin is not the optimum enzyme for ETD,[64] our results indicate that the presence of two basic sites, the N-terminus and the basic C-terminal residue, contributes to the observation of both C- and N-terminal product ions, thereby increasing the peptide sequence coverage.

When comparing the peptide sequence coverage obtained for doubly protonated tryptic peptides in ECD with that obtained in ETD, the results are very similar. ETD of doubly protonated tryptic peptides resulted in an average sequence coverage of 62.5%,[40] whereas we obtained an average of 64.1% for ECD of doubly protonated tryptic peptides. Some variation between these two values are likely due to differences in the length of the

examined peptides (as mentioned above, the extent of ECD and ETD fragmentation decreases with increasing precursor ion m/z ratio, which relates to peptide length). The tryptic peptides characterized by ETD ranged from seven to 16 amino acids in length, whereas the tryptic peptides examined in our experiments ranged from 11 to 18 amino acids with one peptide containing 22 amino acids.

In summary, we have shown that ECD of triply protonated precursor ions increases peptide sequence coverage by 26% compared to doubly protonated precursor ions. In addition, the number of complementary fragment pairs increases by 44%. The large number of complementary fragment pairs detected from triply protonated precursors, and the higher degree of sequence coverage achieved by fragmenting this charge state in ECD can improve protein identification via data base searching, and facilitate *de novo* protein sequencing. However, a remaining challenge is to routinely be able to achieve 100% sequence coverage for proteolytic peptides in ECD.

3.5. References

1. Aebersold, R.; Mann, M., Mass spectrometry-based proteomics. *Nature* **2003,** 422, 198-207.
2. Guerrera, I. C.; Kleiner, O., Application of mass spectrometry in proteomics. *Biosci. Rep.* **2005,** 25, 71-93.
3. Liu, T.; Belov, M. E.; Jaitly, N.; Qian, W. J.; Smith, R. D., Accurate mass measurements in proteomics. *Chem. Rev.* **2007,** 107, 3621-3653.
4. Zubarev, R.; Mann, M., On the proper use of mass accuracy in proteomics. *Mol. Cell. Proteomics* **2007,** 6, 377-381.
5. Aebersold, R.; Goodlett, D. R., Mass spectrometry in proteomics. *Chem. Rev.* **2001,** 101, 269-295.
6. Biemann, K.; Papayannopoulos, I. A., Amino-Acid Sequencing of Proteins. *Acc. Chem. Res.* **1994,** 27, 370-378.
7. Henzel, W. J.; Billeci, T. M.; Stults, J. T.; Wong, S. C.; Grimley, C.; Watanabe, C., Identifying Proteins from 2-Dimensional Gels by Molecular Mass Searching of Peptide-Fragments in Protein-Sequence Databases. *Proc. Natl. ACID. Sci. USA* **1993,** 90, 5011-5015.
8. Mann, M.; Wilm, M., Error Tolerant Identification of Peptides in Sequence Databases by Peptide Sequence Tags. *Anal. Chem.* **1994,** 66, 4390-4399.
9. Qin, J.; Fenyo, D.; Zhao, Y. M.; Hall, W. W.; Chao, D. M.; Wilson, C. J.; Young, R. A.; Chait, B. T., A strategy for rapid, high confidence protein identification. *Anal. Chem.* **1997,** 69, 3995-4001.
10. Yates, J. R., Mass spectrometry and the age of the proteome. *J. Mass Spectrom.* **1998,** 33, 1-19.
11. Ge, Y.; Lawhorn, B. G.; ElNaggar, M.; Strauss, E.; Park, J. H.; Begley, T. P.; McLafferty, F. W., Top down characterization of larger proteins (45 kDa) by electron capture dissociation mass spectrometry. *J. Am. Chem. Soc.* **2002,** 124, 672-678.
12. Han, X. M.; Jin, M.; Breuker, K.; McLafferty, F. W., Extending top-down mass spectrometry to proteins with masses greater than 200 kilodaltons. *Science* **2006,** 314, 109-112.
13. Kelleher, N. L.; Lin, H. Y.; Valaskovic, G. A.; Aaserud, D. J.; Fridriksson, E. K.; McLafferty, F. W., Top down versus bottom up protein characterization by tandem high-resolution mass spectrometry. *J. Am. Chem. Soc.* **1999,** 121, 806-812.
14. Hayes, R. N.; Gross, M. L., Collision-Induced Dissociation. *Methods Enzymol.* **1990,** 193, 237-263.
15. McLuckey, S. A., Principles of Collisional Activation in Analytical Mass-Spectrometry. *J. Am. Soc. Mass Spectrom.* **1992,** 3, 599-614.
16. Simpson, R. J.; Connolly, L. M.; Eddes, J. S.; Pereira, J. J.; Moritz, R. L.; Reid, G. E., Proteomic analysis of the human colon carcinoma cell line (LIM 1215): Development of a membrane protein database. *Electrophoresis* **2000,** 21, 1707-1732.

17. Zubarev, R., Protein primary structure using orthogonal fragmentation techniques in Fourier transform mass spectrometry. *Expert Rev. Proteomics* **2006,** 3, 251-261.
18. Zubarev, R. A., Electron-capture dissociation tandem mass spectrometry. *Curr. Opin. Biotechnol.* **2004,** 15, 12-16.
19. Zubarev, R. A.; Kelleher, N. L.; McLafferty, F. W., Electron capture dissociation of multiply charged protein cations. A nonergodic process. *J. Am. Chem. Soc.* **1998,** 120, 3265-3266.
20. Syka, J. E. P.; Coon, J. J.; Schroeder, M. J.; Shabanowitz, J.; Hunt, D. F., Peptide and protein sequence analysis by electron transfer dissociation mass spectrometry. *Proc. Natl. ACID. Sci. U.S.A* **2004,** 101, 9528-9533.
21. Axelsson, J.; Palmblad, M.; Hakansson, K.; Hakansson, P., Electron capture dissociation of substance P using a commercially available Fourier transform ion cyclotron resonance mass spectrometer. *Rapid Commun. Mass Spectrom.* **1999,** 13, 474-477.
22. Kruger, N. A.; Zubarev, R. A.; Carpenter, B. K.; Kelleher, N. L.; Horn, D. M.; McLafferty, F. W., Electron capture versus energetic dissociation of protein ions. *Int. J. Mass Spectrom.* **1999,** 183, 1-5.
23. Kruger, N. A.; Zubarev, R. A.; Horn, D. M.; McLafferty, F. W., Electron capture dissociation of multiply charged peptide cations. *Int. J. Mass Spectrom.* **1999,** 187, 787-793.
24. Zubarev, R. A.; Horn, D. M.; Fridriksson, E. K.; Kelleher, N. L.; Kruger, N. A.; Lewis, M. A.; Carpenter, B. K.; McLafferty, F. W., Electron capture dissociation for structural characterization of multiply charged protein cations. *Anal. Chem.* **2000,** 72, 563-573.
25. Cooper, H. J.; Hakansson, K.; Marshall, A. G., The role of electron capture dissociation in biomolecular analysis. *Mass Spectrom. Rev.* **2005,** 24, 201-222.
26. Mikesh, L. M.; Ueberheide, B.; Chi, A.; Coon, J. J.; Syka, J. E. P.; Shabanowitz, J.; Hunt, D. F., The utility of ETD mass spectrometry in proteomic analysis. *Biochim. Biophys. Acta* **2006,** 1764, 1811-1822.
27. Chalmers, M. J.; Hakansson, K.; Johnson, R.; Smith, R.; Shen, J. W.; Emmett, M. R.; Marshall, A. G., Protein kinase A phosphorylation characterized by tandem Fourier transform ion cyclotron resonance mass spectrometry. *Proteomics* **2004,** 4, 970-981.
28. Shi, S. D. H.; Hemling, M. E.; Carr, S. A.; Horn, D. M.; Lindh, I.; McLafferty, F. W., Phosphopeptide/phosphoprotein mapping by electron capture dissociation mass spectrometry. *Anal. Chem.* **2001,** 73, 19-22.
29. Stensballe, A.; Jensen, O. N.; Olsen, J. V.; Haselmann, K. F.; Zubarev, R. A., Electron capture dissociation of singly and multiply phosphorylated peptides. *Rapid Commun. Mass Spectrom.* **2000,** 14, 1793-1800.
30. Adamson, J. T.; Hakansson, K., Infrared multiphoton dissociation and electron capture dissociation of high-mannose type glycopeptides. *J. Protome Res.* **2006,** 5, 493-501.
31. Hakansson, K.; Chalmers, M. J.; Quinn, J. P.; McFarland, M. A.; Hendrickson, C. L.; Marshall, A. G., Combined electron capture and infrared multiphoton

dissociation for multistage MS/MS in a Fourier transform ion cyclotron resonance mass spectrometer. *Anal. Chem.* **2003,** 75, 3256-3262.

32. Hakansson, K.; Cooper, H. J.; Emmett, M. R.; Costello, C. E.; Marshall, A. G.; Nilsson, C. L., Electron capture dissociation and infrared multiphoton dissociation MS/MS of an N-glycosylated tryptic peptide to yield complementary sequence information. *Anal. Chem.* **2001,** 73, 4530-4536.
33. Haselmann, K. F.; Budnik, B. A.; Olsen, J. V.; Nielsen, M. L.; Reis, C. A.; Clausen, H.; Johnsen, A. H.; Zubarev, R. A., Advantages of external accumulation for electron capture dissociation in Fourier transform mass spectrometry. *Anal. Chem.* **2001,** 73, 2998-3005.
34. Hogan, J. M.; Pitteri, S. J.; Chrisman, P. A.; McLuckey, S. A., Complementary structural information from a tryptic N-linked glycopeptide via electron transfer ion/ion reactions and collision-induced dissociation. *J. Proteome Res.* **2005,** 4, 628-632.
35. Mirgorodskaya, E.; Roepstorff, P.; Zubarev, R. A., Localization of O-glycosylation sites in peptides by electron capture dissociation in a fourier transform mass spectrometer. *Anal. Chem.* **1999,** 71, 4431-4436.
36. Kelleher, R. L.; Zubarev, R. A.; Bush, K.; Furie, B.; Furie, B. C.; McLafferty, F. W.; Walsh, C. T., Localization of labile posttranslational modifications by electron capture dissociation: The case of gamma-carboxyglutamic acid. *Anal. Chem.* **1999,** 71, 4250-4253.
37. Liu, H.; Hakansson, K., Electron capture dissociation of tyrosine O-sulfated peptides complexed with divalent metal cations. *Anal. Chem.* **2006,** 78, 7570-7576.
38. Pitteri, S. J.; Chrisman, P. A.; Hogan, J. M.; McLuckey, S. A., Electron transfer ion/ion reactions in a three-dimensional quadrupole ion trap: Reactions of doubly and triply protonated peptides with SO2 center dot. *Anal. Chem.* **2005,** 77, 1831-1839.
39. Pitteri, S. J.; Chrisman, P. A.; McLuckey, S. A., Electron-transfer ion/ion reactions of doubly protonated peptides: Effect of elevated bath gas temperature. *Anal. Chem.* **2005,** 77, 5662-5669.
40. Swaney, D. L.; McAlister, G. C.; Wirtala, M.; Schwartz, J. C.; Syka, J. E. P.; Coon, J. J., Supplemental activation method for high-efficiency electron-transfer dissociation of doubly protonated peptide precursors. *Anal. Chem.* **2007,** 79, 477-485.
41. Iavarone, A. T.; Paech, K.; Williams, E. R., Effects of charge state and cationizing agent on the electron capture dissociation of a peptide. *Anal. Chem.* **2004,** 76, 2231-2238.
42. Budnik, B. A.; Nielsen, M. L.; Olsen, J. V.; Haselmann, K. F.; Horth, P.; Haehnel, W.; Zubarev, R. A., Can relative cleavage frequencies in peptides provide additional sequence information? *Int. J. Mass Spectrom.* **2002,** 219, 283-294.
43. Savitski, M. M.; Kjeldsen, F.; Nielsen, M. L.; Zubarev, R. A., Complementary sequence preferences of electron-capture dissociation and vibrational excitation in fragmentation of polypeptide polycations. *Angew. Chem. Int. Ed.* **2006,** 45, 5301-5303.

44. Yang, J.; Mo, J. J.; Adamson, J. T.; Hakansson, K., Characterization of oligodeoxynucleotides by electron detachment dissociation Fourier transform ion cyclotron resonance mass spectrometry. *Anal. Chem.* **2005,** 77, 1876-1882.
45. Caravatti, P.; Allemann, M., The Infinity Cell - a New Trapped-Ion Cell with Radiofrequency Covered Trapping Electrodes for Fourier-Transform Ion-Cyclotron Resonance Mass-Spectrometry. *Org. Mass Spectrom.* **1991,** 26, 514-518.
46. de Koning, L. J.; Nibbering, N. M. M.; van Orden, S. L.; Laukien, F. H., Mass selection of ions in a Fourier transform ion cyclotron resonance trap using correlated harmonic excitation fields (CHEF). *Int. J. Mass Spectrom.* **1997,** 165, 209-219.
47. Senko, M. W.; Canterbury, J. D.; Guan, S. H.; Marshall, A. G., A high-performance modular data system for Fourier transform ion cyclotron resonance mass spectrometry. *Rapid Commun. Mass Spectrom.* **1996,** 10, 1839-1844.
48. Kjeldsen, F.; Haselmann, K. F.; Budnik, B. A.; Jensen, F.; Zubarev, R. A., Dissociative capture of hot (3-13 eV) electrons by polypeptide polycations: an efficient process accompanied by secondary fragmentation. *Chem. Phys. Lett.* **2002,** 356, 201-206.
49. Savitski, M. M.; Kjeldsen, F.; Nielsen, M. L.; Zubarev, R. A., Hydrogen rearrangement to and from radical z fragments in electron capture dissociation of peptides. *J. Am. Soc. Mass Spectrom.* **2007,** 18, 113-120.
50. O'Connor, P. B.; Lin, C.; Cournoyer, J. J.; Pittman, J. L.; Belyayev, M.; Budnik, B. A., Long-lived electron capture dissociation product ions experience radical migration via hydrogen abstraction. *J. Am. Soc. Mass Spectrom.* **2006,** 17, 576-585.
51. Tsybin, Y. O.; He, H.; Emmett, M. R.; Hendrickson, C. L.; Marshall, A. G., Ion activation in electron capture dissociation to distinguish between N-terminal and C-terminal productions. *Anal. Chem.* **2007,** 79, 7596-7602.
52. Adams, C. M.; Kjeldsen, F.; Zubarev, R. A.; Budnik, B. A.; Haselmann, K. F., Electron capture dissociation distinguishes a single D-amino acid in a protein and probes the tertiary structure. *J. Am. Soc. Mass Spectrom.* **2004,** 15, 1087-1098.
53. Breuker, K.; Oh, H. B.; Cerda, B. A.; Horn, D. M.; McLafferty, F. W., Hydrogen atom loss in electron-capture dissociation: a Fourier transform-ion cyclotron resonance study with single isotopomeric ubiquitin ions. *Eur. J. Mass Spectrom.* **2002,** 8, 177-180.
54. Breuker, K.; Oh, H. B.; Horn, D. M.; Cerda, B. A.; McLafferty, F. W., Detailed unfolding and folding of gaseous ubiquitin ions characterized by electron capture dissociation. *J. Am. Chem. Soc.* **2002,** 124, 6407-6420.
55. Chen, X. H.; Turecek, F., The arginine anomaly: Arginine radicals are poor hydrogen atom donors in electron transfer induced dissociations. *J. Am. Chem. Soc.* **2006,** 128, 12520-12530.
56. Mihalca, R.; Kleinnijenhuis, A. J.; McDonnell, L. A.; Heck, A. J. R.; Heeren, R. M. A., Electron capture dissociation at low temperatures reveals selective dissociations. *J. Am. Soc. Mass Spectrom.* **2004,** 15, 1869-1873.
57. Oh, H.; Breuker, K.; Sze, S. K.; Ge, Y.; Carpenter, B. K.; McLafferty, F. W., Secondary and tertiary structures of gaseous protein ions characterized by electron

capture dissociation mass spectrometry and photofragment spectroscopy. *Proc. Natl. ACID. Sci. U.S.A* **2002,** 99, 15863-15868.
58. Cooper, H. J., Investigation of the presence of b ions in electron capture dissociation mass spectra. *J. Am. Soc. Mass Spectrom.* **2005,** 16, 1932-1940.
59. Haselmann, K. F.; Schmidt, M., Do b-ions occur from vibrational excitation upon H-desorption in electron capture dissociation? *Rapid Commun. Mass Spectrom.* **2007,** 21, 1003-1008.
60. Liu, H. C.; Hakansson, K., Abundant b-type ions produced in electron capture dissociation of peptides without basic amino acid residues. *J. Am. Soc Mass Spectrom.* **2007,** 18, 2007-2013.
61. Hakansson, K.; Emmett, M. R.; Hendrickson, C. L.; Marshall, A. G., High-sensitivity electron capture dissociation tandem FTICR mass spectrometry of microelectrosprayed peptides. *Anal. Chem.* **2001,** 73, 3605-3610.
62. Polfer, N. C.; Haselmann, K. F.; Langridge-Smith, P. R. R.; Barran, P. E., Structural investigation of naturally occurring peptides by electron capture dissociation and AMBER force field modelling. *Mol. Phys.* **2005,** 103, 1481-1489.
63. Kjeldsen, F.; Giessing, A. M. B.; Ingrell, C. R.; Jensen, O. N., Peptide sequencing and characterization of post-translational modifications by enhanced ion-charging and liquid chromatography electron-transfer dissociation tandem mass spectrometry. *Anal. Chem.* **2007,** 79, 9243-9252.
64. Wong, S. L. C.; Han, X.; Cociorva, D.; Xu, T.; Yates, J. R. In *Application of electron transfer dissociation (ETD) mass spectrometry in proteomics analysis*, Proceedings of the 55th ASMS Conference on Mass Spectrometry and Allied Topics, Indianapolis, IN, June 2007, DVD-ROM. .

Chapter 4

Electron Capture Dissociation of Highly Charged Proteolytic Peptides from Lys N, Lys C and Glu C Digestion

4.1. Introduction

Primary structure of peptides and proteins can be obtained from their gas-phase dissociation in tandem mass spectrometry (MS/MS). In such experiments, individual peptide ions are activated and fragmented to yield ladder-like product ion spectra which provide sequence information based on the characteristic mass differences between amino acids. MS/MS is a powerful method for obtaining primary structure information for peptides and proteins[1-14] and has been key to the success of proteomics research. Sequencing by MS/MS is preferred over other methods such as Edman degradation, due to its ability to identify unnatural or modified amino acid residues, including blocked amino termini, and also due to its ability to determine the sequence of peptides present in complex mixtures.[15-19] In proteomics, the utilized gas-phase dissociation technique should result in a sufficient number of sequence-informative product ions so that the peptide, or protein, can be successfully identified and characterized.

Collision induced dissociation (CID),[20, 21] which results in cleavage of peptide amide bonds to produce N-terminal *b*-type ions and C-terminal *y*-type ions, is the most commonly used technique to obtain structural information from peptide ions. However, in some cases CID produces internal product ions and neutral losses, or results in selective cleavage at specific residues.[22-25] In such cases the fragmentation data obtained by CID is not sufficient to identify the peptide, or protein, and an alternative fragmentation technique is needed. Electron capture dissociation (ECD)[26, 27] and electron transfer dissociation (ETD),[28, 29] which result in extensive cleavage of peptide backbone N-Cα bonds to produce N-terminal *c*-type and C-terminal *z*-type product ions are complementary to CID and constitute promising tools for peptide and protein sequencing. In ECD, multiply charged cations are irradiated with low energy (<1 eV) electrons, resulting in electron capture and subsequent fragmentation. In ETD, an electron is transferred from an anionic reagent to peptide, or protein, cations leading to fragmentation similar to ECD. In both techniques, a radical cation intermediate is generated via electron capture/transfer and, thus, one even-electron and one radical product ion is formed upon dissociation. The C-terminal *z*-type product ions generally contain the radical site and are therefore designated *z*•-type ions. However, hydrogen migration between complementary product ions is frequently observed in ECD,[30-33] resulting in complementary *c*• and *z*'-type ions (the prime specifically denotes a hydrogen as proposed by Zubarev).[34]

One main advantage of ECD and ETD, compared to CID, is the retention of labile post-translational modifications[28, 35] such as phosphorylation,[29, 36-41] glycosylation[41-47] and sulfation.[45, 48, 49] In addition, ECD and ETD show less sequence dependence and result in

more extensive fragmentation,[22, 27, 33, 50-53] thus higher peptide sequence coverage can be obtained compared to CID. However, both electron based reactions are not very effective for the dissociation of large size doubly protonated species.[30, 54-56]

McLuckey and co-workers demonstrated that, for model peptides, triply charged species produce more ETD product ions, compared to their doubly protonated counterparts, resulting in greater degree of sequence coverage.[54] The same group showed that, for doubly protonated tryptic peptides, ETD sequence coverage and percent ETD decrease with increasing peptide size:[55] for small size peptides (<7 amino acids) a high ETD sequence coverage was obtained, whereas medium size peptides (>8 amino acids) gave an average sequence coverage of 48%, and larger size peptides (>14 amino acids) yielded an average sequence coverage of only 23%. These authors suggested that, for a given charge state, there is a maximum peptide size for which high ETD sequence coverage can be obtained. To increase the ETD sequence coverage for medium and large size doubly protonated peptides, which were not fragmented efficiently in conventional ETD, the precursor ions were activated by use of elevated bath gas temperatures.[55] Coon and co-workers examined the ETD fragmentation behavior of 755 doubly protonated tryptic peptides and observed a decrease in product ion yield with increasing precursor mass-to-charge (m/z) value.[56] A supplemental collision activation method that targets the nondissociated electron transfer species was proposed (termed ETcaD), and shown to improve both the ETD efficiency and the peptide sequence coverage for doubly protonated species.[56]

In Chapter 3 we examined and characterized the ECD fragmentation behavior of doubly and triply protonated proteolytic peptides from trypsin, chymotrypsin and Glu C

digestion.[30] ECD of triply protonated peptides resulted in higher peptide sequence coverage and also in a higher number of complementary fragment pairs. Doubly protonated species showed a decrease in ECD sequence coverage with increasing precursor m/z value, in agreement with the reported ETD fragmentation behavior of doubly protonated peptides. By contrast, the ECD sequence coverage for medium size (10-23 amino acid residues) triply protonated peptides did not show a strong dependence on the precursor m/z value.[30] However, because a limited m/z range (391-832 as compared to 585-1245 for doubly protonated peptides) was investigated, it is possible that highly charged ions also may show a decrease in ECD sequence coverage as a function of precursor m/z value. Nevertheless, these ECD and ETD experiments suggest that highly charged precursor ions are more desired for both fragmentation techniques.

One approach to increase the charge state of peptide and protein ions utilizes the addition of m-nitrobenzyl alcohol into the electrospray solution, so called "supercharging".[57-59] It has been shown that addition of 0.1% m-nitrobenyl alcohol changes the predominant charge state from +2 to ≥+3 for bovine serum albumin tryptic peptides.[23] This strategy also increased the average charge state of phosphopeptides by 0.5 charge units. Triply protonated peptides, generated via supercharging, resulted in higher ETD efficiency and higher Mascot[60] identification scores compared to the corresponding doubly protonated species.[23] Nonenzymatic digestion of proteins by microwave D-cleavage, which leads to site specific cleavage at aspartic acid, is another approach to produce highly charged precursor ions.[22] Because of the relatively low occurrence of aspartic acid residues (~5%) in proteins, microwave D-cleavage produces large peptides that tend to be highly charged due to the presence of several basic amino

acids within their sequences. These highly charged peptide ions exhibit extensive fragmentation in ETD.

Multiply charged precursor ions can also be obtained by enzymatic digestion with proteases such as Lys C, Asp N, Glu C, and Arg C.[23, 38, 61] Similar to the microwave D-cleavage digestion, enzymatic digestion with Lys C, Asp N, Glu C, and Arg C generates longer peptides that tend to be multiply charged. Karger and co-workers examined the ETD and CID fragmentation behavior of large size peptides generated by Lys C digestion.[62] These authors demonstrated that doubly charged peptides show better fragmentation in CID whereas large precursor ions at higher charge states are more extensively fragmented in ETD or ETcaD. Coon and co-workers compared ETD and CID of small to medium size peptides varying from +2 to +5 charge state and reported that ETD outperformed CID for all charge states greater than two.[61] These experiments also revealed that the main factor for a successful ETD experiment is the ratio of residues/charge and that, regardless of the precursor ion charge state, ETD fragmentation decreases with increasing precursor m/z value.

Here, we explore the effect of protease selection in ECD of multiply charged (+3 to +6), medium size (1600 – 4800 Da) peptides generated by Lys C, Lys N and Glu C digestion. These experiments also aimed to characterize the extent of fragmentation, measured by the total number of $z\bullet/z'$ and $c'/c\bullet$ type ions, and the sequence coverage, measured by the total number of backbone amine bond cleavages, for highly charged proteolytic peptides. Lys C and Glu C are extensively applied in proteomics research whereas Lys N has not been extensively combined with gas-phase dissociation for peptide sequencing. Lys N is a metalloendopeptidase that catalyzes specific cleavage of

acyl-lysine bonds (-X-Lys) in peptides and proteins.[63] Recently, Lys N digestion was combined with ETcaD and the fragmentation behavior of doubly protonated species was examined.[64] It was shown that Lys N derived peptides containing a single lysine residue produce solely *c*-type product ions in ETD, thereby simplifying spectral interpretation, whereas peptides containing more than one basic residue produce both *c*- and *z*- type product ions.

Here, we explore the utility of Lys N digestion in combination with ECD for the characterization of multiply charged ions. We also examine ECD of doubly protonated peptides from Lys C and Lys N digestion, containing identical amino acid composition but differing in the location of the lysine residue, to address whether the charge location affects ECD fragmentation behavior. Furthermore, we examine whether factors such as precursor ion mass, charge, or m/z value influence ECD fragmentation of medium size peptides carrying multiple charges.

To address these questions, ECD of 152 proteolytic peptides generated from Lys C, Lys N and Glu C digestion was investigated. The proteolytic peptides selected for fragmentation were highly charged, +3 to +6, and contain 14-41 amino acid residues (1600 – 4800 Da).

4.2. Experimental Procedures

4.2.1. Sample Preparation

Digestion conditions, time and enzyme to protein ratio, were varied to optimize the abundance of the proteolytic peptides of interest and also to allow for none and several missed cleavages. Bovine serum albumin (BSA), lactoferrin from bovine colostrum, human apo-transferrin and carbonic anhydrase II from bovine erythrocytes were obtained

from Sigma (St Louis, MO). Lys C (Sigma, St Louis, MO) digestions were performed in 100 mM ammonium bicarbonate (pH = 8.4) (Fisher Scientific, Fair Lawn, NJ) at 37 ^{0}C. Lys N (Associates of Cape Cod Incorporated, East Falmouth, MA) digestions were performed in 50 mM ammonium bicarbonate (pH = 8.4 or 9.5) at 37 ^{0}C. Lys N is inhibited by dithiothreitol (DTT),[63] which must therefore be removed prior to adding the enzyme (DTT is used for disulfide reduction prior to digestion as described below). DTT was removed with microcon centrifugal filter devices (3,000 nominal molecular weight limit, Millipore Corporation, Bedford, MA). Glu C (Roche, Indianapolis, IN) digestions were performed in 50 mM ammonium bicarbonate at 25-26 ^{0}C.

Carbonic anhydrase II (0.34 nmol) was first denatured in 6 M urea (Sigma) for 45 min at 56 ^{0}C. The urea concentration was diluted to 1 M before adding the enzyme. Lys C was added at an enzyme to protein ratio of 1:100 and Lys N was added at an enzyme to protein ratio of 1:100 or 1:150. Digestions were performed for 5 hours. BSA (0.45 nmol) was reduced with 10 mM DTT (Sigma) in 50 mM ammonium bicarbonate (Fisher Scientific) for 45 min at 56 ^{0}C and then carboxymethylated with 50 mM iodoacetamide (Sigma) in 50 mM ammonium bicarbonate in darkness for 1 h. Following reduction and alkylation, BSA was digested with Glu C at an enzyme to protein ratio of 1:50, 1:75, or 1:100 for 3h, 5h or 9 hours. Lys C digestions were performed at 1:50 or 1:75 enzyme to protein ratio for 75 min or 6 hours. After DTT removal, Lys N was added at an enzyme to protein ratio of 1:50, 1:75, or 1:150 for 75 min or 6 hours.

Apo-transferrin (0.45 nmol) and lactoferrin (0.45 nmol) were denatured, reduced and alkylated. For denaturation and reduction, urea and DTT were added to a final concentration of 6 M and 10 mM, respectively, in the presence of 50 mM ammonium

bicarbonate. In the case of lactoferrin, 6.8 M urea was used. Mixtures were incubated for 45 min at 56 ^{0}C. Alkylation was performed as described above. Before addition of enzymes, urea was diluted to 1 M, or removed with microcon centrifugal filter devices (3,000 nominal molecular weight limit). Apo-transferrin was digested with Glu C at an enzyme to protein ratio of 1:50, 1:100, or 1:150 for 75 min, 5 h, 8 h, or 12 h. Lys C was added at an enzyme to protein ratio of 1:50, 1:75, 1:100, or 1:150 for 75 min, 6 hours, or 14 hours. For Lys N digestion, ratios of 1:50, 1:100, or 1:150 were used and the digestion proceeded for 75 min, 3 h, or 8 h. For lactoferrin digestion, Glu C was added at an enzyme to protein ratio of 1:30 or 1:100 for 14 h. Lys C digestion was performed at a ratio of 1:50 for 12 h and Lys N digestion was performed at ratios of 1:50, 1:100, or 1:150 and the digestion time was 5 h or 12 h. All reactions were quenched with 0.2-0.5 % formic acid (Acros Organics, Morris Plains, NJ). Digested samples were desalted with C_{18} Ziptips (Millipore, Billerica, MA) and diluted with 500-740 µl electrospray solvent containing 50% acetonitrile (Fisher) and 0.1 % formic acid.

4.2.2. Mass Spectrometry

All experiments were performed with an actively shielded 7T quadrupole-Fourier transform ion cyclotron resonance (Q-FT-ICR) mass spectrometer (Apex-Q, Bruker Daltonics, Billerica, MA), which has been previously described.[65] Proteolytic mixtures were electrosprayed in positive ion mode at a flow rate of 70 µL/hour. Ions were accumulated in the first hexapole for 0.1 s, transferred through the mass selective quadrupole (2-6 m/z isolation window), mass selectively accumulated in the second hexapole for 0.3 to 4 s, transferred through high-voltage ion optics, and captured in the ICR cell by dynamic trapping. This accumulation sequence was looped 2-4 times to maximize precursor ion signal. The accumulation time in the second hexapole and the

number of loops of the accumulation sequence were varied to ensure that the total signal of ions entering the ICR cell for the ECD experiments was very similar (9×10^6 to 1×10^7 absolute abundance (single scan) in XMASS software) for all peptides examined. Further precursor ion isolation was achieved by correlated harmonic excitation fields[66] inside the ICR cell.

Peptides that were detected at charge states from +3 to +6 (containing 14 to 41 amino acid residues, corresponding to 1645 - 4779 Da) were selected for ECD experiments. ECD was performed with an indirectly heated hollow dispenser cathode at a bias voltage of 0.01-0.30 V and an irradiation time of 30-60 ms. A lens electrode located in front of the hollow cathode was kept at 1.0 V. All spectra were acquired with XMASS (version 6.1, Bruker Daltonics) using 512 K data points and summed over 64 scans. Data processing was performed with the MIDAS analysis software.[67] Internal frequency-to-mass calibration was performed by Microsoft Excel using a two term calibration equation.[68] The calculated masses of the precursor ions and the charge-reduced species were used for calibration. In some cases, the precursor ion and abundant *c'* or *z*• product ions were used for calibration. In these cases, calibration was repeated with the precursor ion and one additional product ion to ensure correct assignments. Product ion spectra were interpreted with the aid of the MS Product function in Protein Prospector (http://prospector.ucsf.edu/prospector/4.0.8/html/msprod.htm). Only peak assignments with a mass accuracy better than 15 ppm were accepted (most assignments were within 10 ppm, however, the relatively high error tolerance is due to low signal-to-noise ratios of some product ions, and the use of in-cell isolation).

4.3. Results and Discussion

One hundred and fifty two peptides, ranging from 14 to 41 amino acid residues, from Lys C, Lys N, and Glu C digestion were fragmented by ECD. Fifty of these peptides were from Lys C digestion, 51 were from Lys N digestion, and 51 were derived from Glu C digestion (a detailed graph showing the number of peptides examined as a function of their length for the different proteolytic enzymes is shown in Figure 4.1). The percent sequence coverage was defined as follows: (number of observed backbone N-Cα cleavages/number of N-Cα backbone bonds) ×100. ECD cleavage at the N-terminal side of proline is generally not observed due to its cyclic structure (even though a backbone N-Cα bond is cleaved, the two fragments will be connected through the proline side chain). In order to be able to directly compare the ECD sequence coverage obtained from each proteolytic enzyme, the sequence coverage was calculated by excluding cleavages N-terminal to proline. This precaution was necessary because Lys N, Lys C and Glu C digest peptides do not contain the same number of Pro residues.

Hydrogen rearrangements are commonly observed in ECD.[30-33] Therefore, both radical and even-electron product ions must be considered. N-terminal product ions are assigned as $c'/c^{\bullet}$, and C-terminal product ions are assigned as $z^{\bullet}/z'$. Hydrogen atom loss from $z^{\bullet}$ type product ions to form $z^{\bullet}$ - H and $z^{\bullet}$ - 2H is also observed in ECD when serine, threonine or tryptophan are adjacent to the radical site formed following N-Cα backbone bond cleavage.[32] Therefore, when assigning *z* type product ions this hydrogen atom loss was also taken into account for those specific residues. Furthermore, some *c*'-type product ions, 1.4% of all *c*'-type fragments observed, showed addition of one hydrogen

atom to form *c*" ions. This hydrogen addition was observed for long *c*-type fragments containing 21-38 amino acid residues.

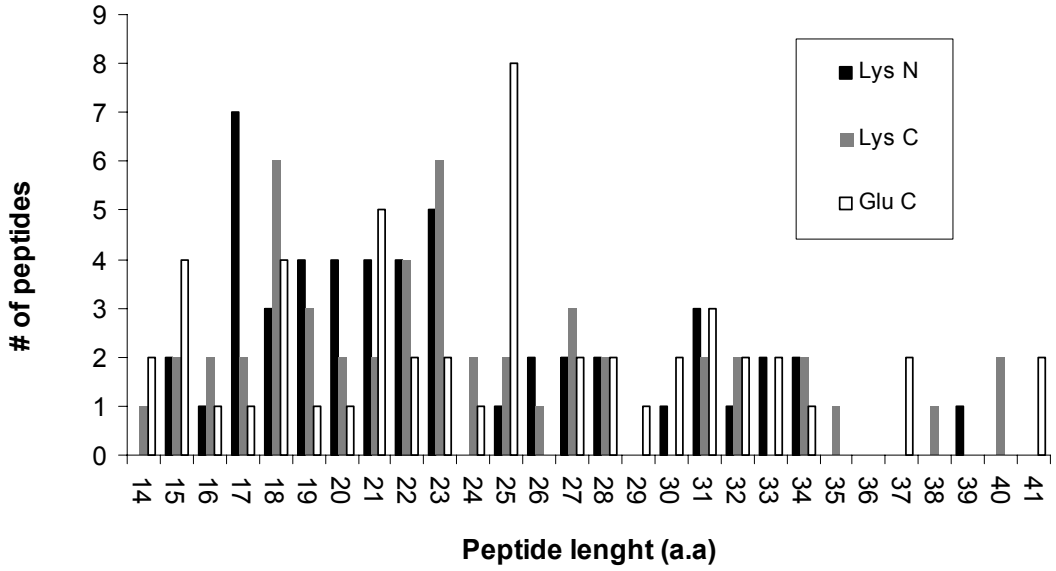

Figure 4.1. Number of peptides as a function of peptide length for all proteolytically derived peptides examined.

4.3.1. ECD of Triply Protonated Peptides

The ECD sequence coverage as a function of the precursor ion m/z value for triply protonated species is displayed in Figure 4.2. The triply protonated peptides examined contain 14 to 27 amino acid residues. Detailed fragmentation patterns, i.e., identities of all *c* and *z*-type product ions, for the triply protonated species are shown in Tables 4.1, 4.2 and 4.3. Similar trends were observed for all triply protonated peptides, independent of which proteolytic enzyme was used for digestion: a decrease in peptide sequence coverage was observed with increasing precursor ion m/z value. Triply protonated peptides at low m/z values (≤880) showed good ECD peptide sequence coverage, ranging from 43% to 100%. Most of these peptides, 31 out of 44, exhibited high ECD sequence coverage ranging from 80%-100% and only one peptide showed a sequence coverage as

low as 43%. Peptides at higher m/z values (>960) exhibited decreased ECD sequence coverage. Some of these peptides showed poor sequence coverage (29%-36%) and only one peptide at m/z 974, from Glu C digestion, showed good ECD sequence coverage (69%). These data suggest that peptides at high m/z values do not fragment efficiently in ECD, therefore, the m/z ratio of precursor ions should be taken into consideration when sequence information is to be derived from ECD. Alternatively, activated ion ECD (AI-ECD, in which ECD is combined with collisional or IR activation) can be employed to increase structural information, as has been demonstrated for proteins and for glycosylated and phosphorylated peptides.[43, 69, 70] As mentioned above, the trend of decreasing ECD sequence coverage with increasing precursor ion m/z value was also observed for doubly protonated peptides, in both ECD and ETD.[30, 55, 56]

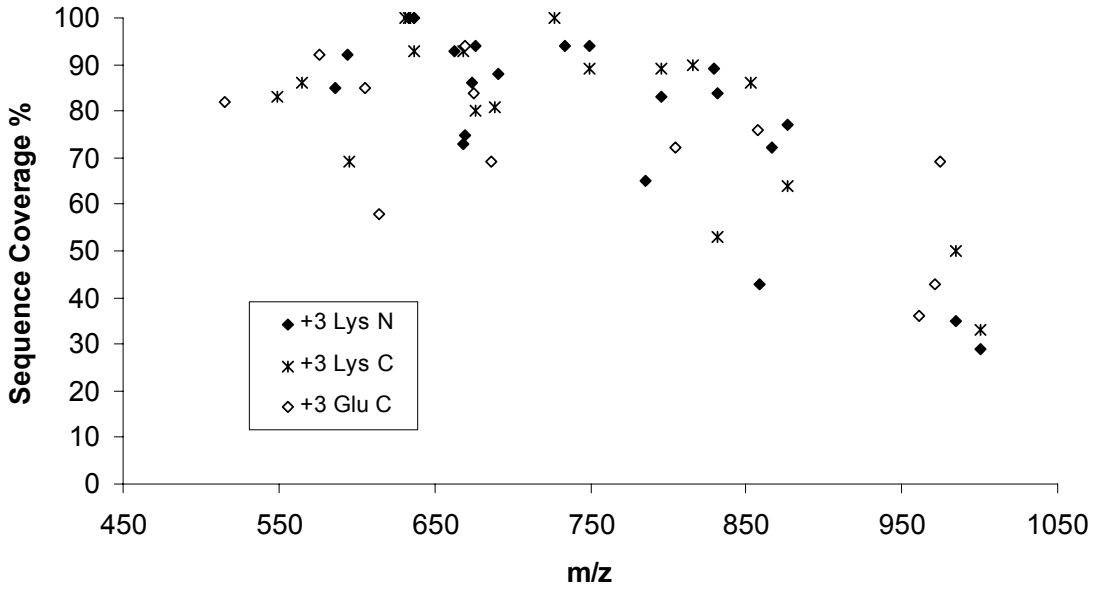

Figure 4.2. ECD sequence coverage as a function of m/z ratio for triply protonated proteolytic peptides from Lys C, Lys N and Glu C digestion. Independent of the proteolytic enzyme used for digestion, sequence coverage decreases with increasing precursor ion m/z ratio.

Table 4.1. ECD fragmentation summary of all triply protonated peptides from Lys C digestion

Charge	Peptide Sequence	Seq. Cov. %
+3	GACLLPKIETMREK	83%
+3	AEFVEVTKLVTDLTK	86%
+3	CSTSSLLEACTFRRP	69%
+3	LFTFHADICTLPDTEK*	93%
+3	EFQLFSSPHGKDLLFK	100%
+3	LGEYGFQNALIVRYTRK*	80%
+3	FPKAEFVEVTKLVTDLTK	81%
+3	DFPIANGERQSPVDIDTK*	93%
+3	VPQVSTPTLVEVSRSLGK*	100%
+3	ECCHGDLLECADDRADLAK*	89%
+3	SRSFQLFGSPPGQRDLLFK	100%
+3	INHCRFDEFFSEGCAPGSKK*	89%
+3	GLVLIAFSQYLQQCPFDEHVK*	53%
+3	YLYEIARRHPVFYAPELLYYANK*	50%
+3	SCHTAVGRTAGWNIPMGLLYNK	90%
+3	LGGRPTYEEYLGTEYVTAIANLK	86%
+3	EGYYGYTGAFRCLVEKGDVAFVK*	64%
+3	CCTESLVNRRPCFSALTPDETYVPK*	33%

* Peptides of the same composition but with a lysine residue at the N-terminus rather than the C-terminus were generated by Lys N digestion and also examined with ECD (see also Table 4.2).

Table 4.2. ECD fragmentation summary for all triply protonated Lys N derived peptides

Charge	Peptide Sequence	Seq. Cov. %
+3	KEDPQTFYYAVAVVK	85%
+3	KPDPNTLCDEFKADE	92%
+3	KLFTFHADICTLPDTE*	100%
+3	KLKPDPNTLCDEFKADE	86%
+3	KLGEYGFQNALIVRYTR*	94%
+3	KEDLIWELLNQAQEHFG	88%
+3	VPDKTVRWCAVSEHEAT	93%
+3	KDFPIANGERQSPVDIDT*	73%
+3	KVPQVSTPTLVEVSRSLG*	100%
+3	KVASLRETYGDMADCCE	75%
+3	KHLVDEPQNLIKQNCDQFE	65%
+3	KECCHGDLLECADDRADLA*	94%
+3	KSDNCEDTPEAGYFAVAVVK	94%
+3	KINHCRFDEFFSEGCAPGSK*	83%
+3	KGLVLIAFSQYLQQCPFDEHV*	84%
+3	KLKHLVDEPQNLIKQNCDQFE	72%
+3	KYNGVFQECCQAEDKGACLLP	89%
+3	KYLYEIARRHPVFYAPELLYYAN*	35%
+3	KEGYYGYTGAFRCLVEKGDVAFV*	77%
+3	KKSCHTAVGRTAGWNIPMGLLYN	43%
+3	KCCTESLVNRRPCFSALTPDETYVP*	29%

***** Peptides of the same composition but with a lysine residue at the C-terminus rather than the N-terminus were generated by Lys C digestion and also examined with ECD (see also Table 4.1).

Table 4.3. ECD fragmentation summary for all triply protonated species from Glu C digestion

Charge	Peptide Sequence	Seq. Cov. %
+3	KSHCIAEVEKDAIPE	92%
+3	AGRDPYKLRPVAAE	82%
+3	VPDKTVRWCAVSEHE	85%
+3	APRKNVRWCTISQPE	58%
+3	YVTAIANLKKCSTSPLLE	94%
+3	YVKAVGNLRKCSTSSLLE	84%
+3	CLAKLGGRPTYEEYLGTE	69%
+3	NLPPLTADFAEDKDVCKNYQE	72%
+3	YLGTEYVTAIANLKKCSTSPLLE	76%
+3	YGFQNALIVRYTRKVPQVSTPTLVE	36%
+3	SLVNRRPCFSALTPDETYVPKAFDE	43%
+3	GLSDGEWQQVLNVWGKVEADIAGHGQE	69%

The lower extent of ECD fragmentation observed for larger peptides could be attributed to the presence of gas-phase intramolecular non-covalent interactions: when the number of charges remains unchanged, non-covalent interactions are expected to increase with increasing peptide size. Non-covalent interactions lower ECD and ETD fragmentation efficiency because such interactions prevent complementary product ion pairs from separating following backbone bond cleavages.[33, 61, 70-72]

Table 4.4 summarizes the average ECD sequence coverage, the total number of product ions, and the number of complementary fragment pairs observed for triply protonated peptides. Lys N and Lys C peptides showed an almost identical ECD sequence coverage, whereas Glu C peptides exhibited lower ECD sequence coverage.

Furthermore, Glu C digest peptides showed the lowest extent of fragmentation compared to Lys N and Lys C digest peptides, in terms of total product ions, and complementary fragment pairs. The average peptide length of Glu C digest peptides was higher compared to the average peptide length of Lys N and Lys C digest peptides. Therefore, the lower ECD sequence coverage obtained for Glu C digest peptides can be due to the higher average peptide length of these peptides and accompanying increased non-covalent interactions as discussed above.

Table 4.4. ECD summary of triply protonated peptides [a]

$[M + 3H]^{3+}$	Lys N digest peptides	Lys C digest peptides	Glu C digest peptides
# of total backbone N-C_α cleavages	274/357 77%	237/303 78%	145/206 70%
# of total product ions	394/714 (138 z• / z' 256 c• / c') 55%	366/606 (180 z• / z' 186 c• / c') 60%	189/412 (75 z• / z' 114 c• / c') 46%
# of complementary fragment pairs	120/357 34%	125/303 41%	43/206 21%
Average Peptide Length	19.1	19.0	19.3

[a] Total number of observed N-Cα backbone bond cleavages, total number of *c*- and *z*-type product ions, and total number of complementary fragment pairs observed are listed for all Lys N, Lys C, and Glu C digest peptides. Glu C derived peptides have the highest average peptide length and showed the lowest extent of fragmentation. Lys C and Lys N derived peptides showed an almost identical ECD sequence coverage. Higher numbers of total product ions and complementary fragment pairs are observed for Lys C digest peptides.

Lys C digest peptides showed a higher total number of product ions, and a higher number of complementary fragment pairs as compared to Lys N and Glu C derived peptides. Furthermore, peptides from Lys C digestion produced an almost identical number of *z*- and *c*-type product ions. This behavior can be explained based on the

presence of a positive charge at both peptide termini for Lys C derived peptides (one at the N-terminal amine group and one at the C-terminal lysine residue), which could facilitate detection of both N- and C-terminal product ions. In contrast, Lys N digest peptides produced a significantly higher number of *c*-type fragment ions, compared to *z*-type product ions, due to the presence of a lysine residue at the peptide N-termini. Similar to Lys N digest peptides, Glu C digest peptides produced less *z*-type product ions compared to *c*-type product ions, in agreement with the absence of a basic residue at the C-terminus of Glu C derived peptides.

We note that the average ECD sequence coverage obtained here for longer triply protonated peptides generated by Lys N, Lys C, and Glu C digestion is lower compared to that obtained in our previous work (Chapter 3) for shorter triply protonated peptides derived from trypsin, chymotrypsin, and Glu C digestion.[30] The average peptide length for triply protonated species in our previous work was 15.3 amino acid residues whereas triply protonated species examined here have an average peptide length of 19.1 residues. As documented in Fig. 4.2, peptide sequence coverage decreases with increasing precursor ion m/z value, therefore it is not surprising that the longer peptides examined here showed less fragmentation compared to shorter peptides carrying the same number of charges.

4.3.2. ECD of Multiply Protonated Peptides with Four, Five, and Six Charges

Detailed fragmentation behavior of all examined multiply protonated peptides at charge states 4^+, 5^+, and 6^+ is shown in Tables 4.5-4.10. The quadruply protonated peptides contain 14-33 amino acid residues whereas $[M + 5H]^{5+}$ precursor ions consist of 18-40 amino acid residues. $[M + 6H]^{6+}$ precursor ions contain 29-41 amino acid residues with one peptide from Glu C digestion containing 21 amino acid residues.

Table 4.5. ECD fragmentation summary for all quadruply protonated species from Lys C digestion

Charge	**Peptide Sequence**	Seq. Cov. %
+4	LGEYGFQNALIVRYTRK	94%
+4	FPKAEFVEVTKLVTDLTK	69%
+4	SKEFQLFSSPHGKDLLFK	100%
+4	SRSFQLFGSPPGQRDLLFK	100%
+4	INHCRFDEFFSEGCAPGSKK*	83%
+4	GLVLIAFSQVLQQCPFDEHVK	63%
+4	YLYEIARRHPYFYAPELLYYANK*	100%
+4	ADRDQYELLCLDNTRKPVDEYK*	85%
+4	DLLFRDDTVCLAKLHDRNTYEK	90%
+4	SCHTAVGRTAGWNIPMGLLYNK	85%
+4	LGAPSITCVRRAFALECIRAIAEK	68%
+4	LGGRPTYEEYLGTEYVTAIANLKK	91%
+4	EGYYGYTGAFRCLVEKGDVAFVK	95%
+4	CCTESLVNRRPCFSALTPDETYVPK	95%
+4	SHCIAEVEKDAIPENLPPLTADFAEDK*	78%
+4	FRTLNFNAEGEPELLMLANWRPAQPLK	91%
+4	DAFLGSFLYEYSRRHPEYAVSVLLRLAK	62%
+4	SHCIAEVEKDAIPENLPPLTADFAEDKDVCK*	84%
+4	SCHTGLGRSAGWNIPIGLLYCDLPEPRKPLEK	52%

* Peptides with the same composition but with a lysine residue at the N-terminus rather than the C-terminus were generated by Lys N digestion and also examined with ECD (see also Table 4.6). ^ = Product ions that cannot be distinguished based on their mass.

Table 4.6. ECD fragmentation summary for all quadruply protonated species derived from Lys N digestion

Charge	Peptide Sequence	Seq. Cov. %
+4	VPDKTVRWCAVSEHEAT	93%
+4	KNLNREDFRLLCLDGTR	94%
+4	KLFTFHADICTLPDTEKQIK	100%
+4	KHLVDEPQNLIKQNCDQFE	88%
+4	KINHCRFDEFFSEGCAPGS	88%
+4	KHQTVPQNTGGKNPDPWA	86%
+4	KINHCRFDEFFSEGCAPGSK*	89%
+4	KLKHLVDEPQNLIKQNCDQFE	84%
+4	KHSSLDCVLRPTEGYLAVAVVK	90%
+4	KYLYEIARRHPVFYAPELLYYAN *	80%
+4	KPVEEYANCHLARAPNHAVVTR	100%
+4	KADRDQYELLCLDNTRKPVDEY *	85%
+4	KKSCHTAVGRTAGWNIPMGLLYN	95%
+4	KSHCIAEVEKDAIPENLPPLTADFAED*	61%
+4	KDFPIANGERQSPVDIDTKAVVQDPAL	91%
+4	KECHLAQVPSHAVVARSVDGKEDLIW	83%
+4	KSHCIAEVEKDAIPENLPPLTADFAEDKDVC *	89%
+4	KMYLGEYVTAIRNLREGTCPEAPTDECKPV	85%
+4	KPLALVYGEATSRRMVNNGHSFNVEYDDSQD	69%
+4	KKSCHTGLGRSAGWNIPIGLLYCDLPEPRKPLE	61%

* Peptides with the same amino acid composition but with a lysine residue at the C-terminus rather than the N-terminus were generated by Lys C digestion and also examined with ECD (see also Table 4.5). The peptide VPDTVRWCAVSEHEAT contains the N-terminus of the protein (apotransferrin).

Table 4.7. ECD fragmentation summary for all quadruply protonated Glu C derived peptides

Charge	Peptide Sequence	Seq. Cov. %
+4	VTKLVTDLTKVHKE	85%
+4	DFRLLCLDGTRKPVTE	86%
+4	VPDKTVRWCAVSEHE	92%
+4	VSRSLGKVGTRCCTKPE	80%
+4	LLKHKPKATEEQLKTVME	94%
+4	RALKAWSVARLSQKFPKAE	88%
+4	CCQAEDKGACLLPKIETMRE	83%
+4	YANCHLARAPNHAVVTRKDKE	89%
+4	RALKAWSVARLSQKFPKAEFVE	90%
+4	TKDLLFRDDTVCLAKLHDRNTYE	86%
+4	KYLGEEYVKAVGNLRKCSTSSLLE	87%
+4	YGFQNALIVRYTRKVPQVSTPTLVE	76%
+4	CADDRADLAKYICDNQDTISSKLKE	83%
+4	CFLSHKDDSPDLPKLKPDPNTLCDE	80%
+4	SLVNRRPCFSALTPDETYVPKAFDE	95%
+4	FAKTCVADESHAGCEKSLHTLFGDE	83%
+4	YKDCHLAQVPSHTVVARSMGGKEDLIWE	81%
+4	FISDAIIHVLHSKHPGDFGADAQGAMTKALE	86%

Table 4.8. ECD fragmentation summary for all $[M + 5H]^{5+}$ and all $[M + 6H]^{6+}$ precursor ions from Lys C digestion

Charge	**Peptide Sequence**	Seq. Cov. %
+5	SKEFQLFSSPHGKDLLFK	63%
+5	YLYEIARRHPYFYAPELLYYANK	90%
+5	INHCRFDEFFSEGCAPGSKKDSSLCK	88%
+5	HNGPEHWHKDFPIANGERQSPVDIDTK	78%
+5	DAFLGSFLYEYSRRHPEYAVSVLLRLAK*	88%
+5	MYLGYEYVTAIRNLREGTCPEAPTDECKPVK	81%
+5	SCHTGLGRSAGWNIPIGLLYCDLPEPRKPLEK	74%
+5	LGEYGFQNALIVRYTRKVPQVSTPTLVEVSRSLGK	78%
+5	LCMGSGLNLCEPNNKEGYYGYTGAFRCLVEKGDVAFVK	78%
+5	AVVQDPALKPLALVYGEATSRRMVNNGHSFNVEYDDSQDK	78%
+6	VGTRCCTKPESERMPCTEDYLSLILNRLCVLHEK	87%
+6	DYELLCLDGTRKPVEEYANCHLARAPNHAVVTRK*	74%
+6	AVVQDPALKPLALVYGEATSRRMVNNGHSFNVEYDDSQDK	84%

***** Peptides with the same composition but with a lysine residue at the N-terminus rather than the C-terminus were generated by Lys N digestion and also examined with ECD (see also Table 4.9). ^ = Product ions that cannot be distinguished based on their mass.

Table 4.9. ECD fragmentation summary for all $[M + 5H]^{5+}$ and all $[M + 6H]^{6+}$ precursor ions from Lys N digestion

Charge	Peptide Sequence	Seq. Cov. %
+5	KPVEEYANCHLARAPNHAVVTR	79%
+5	KECHLAQVPSHAVVARSVDGKEDLIW	79%
+5	KDAFLGSFLYEYSRRHPEYAVSVLLRLA*	96%
+5	KNLRETAEEVKARYTRVVWCAVGPEEQK	92%
+5	KPLALVYGEATSRRMVNNGHSFNVEYDDSQD	100%
+5	KDYELLCLDGTRKPVEEYANCHLARAPNHAVVTR	81%
+6	KKSCHTGLGRSAGWNIPIGLLYCDLPEPRKPLE	82%
+6	KDGPLTGTYRLVQFHFHWGSSDDQGSEHTVDR	67%
+6	KDYELLCLDGTRKPVEEYANCHLARAPNHAVVTR*	77%
+6	KNLNEKDYELLCLDGTRKPVEEYANCHLARAPNHAVVTR	75%

* Peptides with the same amino acid composition but with a lysine residue at the C-terminus rather than the N-terminus were generated by Lys C digestion and also examined with ECD (see also Table 4.8). ^ = Product ions that cannot be distinguished based on their mass.

Table 4.10. ECD fragmentation summary for all $[M + 5H]^{5+}$ and all $[M + 6H]^{6+}$ precursor ions from Glu C digestion

Charge	Peptide Sequence	Seq. Cov. %
+5	YANCHLARAPNHAVVTRKDKE	95%
+5	RALKAWSVARLSQKFPKAEFVE	85%
+5	TKDLLFRDDTVCLAKLHDRNTYE	82%
+5	FAKTCVADESHAGCEKSLHTLFGDE	75%
+5	KLFTFHADICTLPDTEKQIKKQTALVE	96%
+5	YKDCHLAQVPSHTVVARSMGGKEDLIWE	92%
+5	CFLSHKDDSPDLPKLKPDPNTLCDEFKADE	96%
+5	IAHRFKDLGEEHFKGLVLIAFSQYLQQCPFDE	80%
+5	MKASEDLKKHGTVVLTALGGILKKKGHHEAE	93%
+5	NRKSSKHSSLDCVLRPTEGYLAVAVVKKANE	86%
+5	GCAPGSKKDSSLCKLCMGSGLNLCEPNNKE	81%
+5	CHLAQVPSHAVVARSVDGKEDLIWKLLSKAQE	73%
+5	CCHGDLLECADDRADLAKYICDNQDTISSKLKE	78%
+5	FQLFSSPHGKDLLFKDSAHGFLKVPPRMDAKMYLGYE	70%
+6	YANCHLARAPNHAVVTRKDKE	58%
+6	WFKCRRWQWRMKKLGAPSITCVRRAFALE	81%
+6	CCHGDLLECADDRADLAKYICDNQDTISSKLKE	75%
+6	KGDVAFVKHQTVPQNTGGKNPDPWAKNLNEKDYE	90%
+6	FQLFSSPHGKDLLFKDSAHGFLKVPPRMDAKMYLGYE	91%
+6	ATKCQSFRDHMKSVIPSDGPSVACVKKASYLDCIRAIAANE	71%
+6	LLCLDNTRKPVDEYKDCHLAQVPSHTVVARSMGGKEDLIWE	66%

Figure 4.3 displays the ECD spectrum of $[M + 5H]^{5+}$ precursor ions of a Lys N digest peptide from BSA with a molecular weight of 3300 Da. ECD resulted in formation of 43 out of 52 possible *c*- and *z*-type product ions and 25 out of 26 backbone

interresidue bonds were cleaved, resulting in nearly complete peptide sequence coverage. Eighteen out of 26 possible complementary fragment pairs were detected. A second example is shown in Figure 4.4. for $[M + 6H]^{6+}$ precursor ions of a Lys C digest peptide from carbonic anhydrase having a molecular weight of 4433 Da.. Following ECD, 31 out of 37 possible N-Cα backbone bonds were cleaved, resulting in 84% sequence coverage. Similar to the ECD spectrum of the Lys N digest peptide (Fig. 4.3), several complementary fragment pairs are observed.

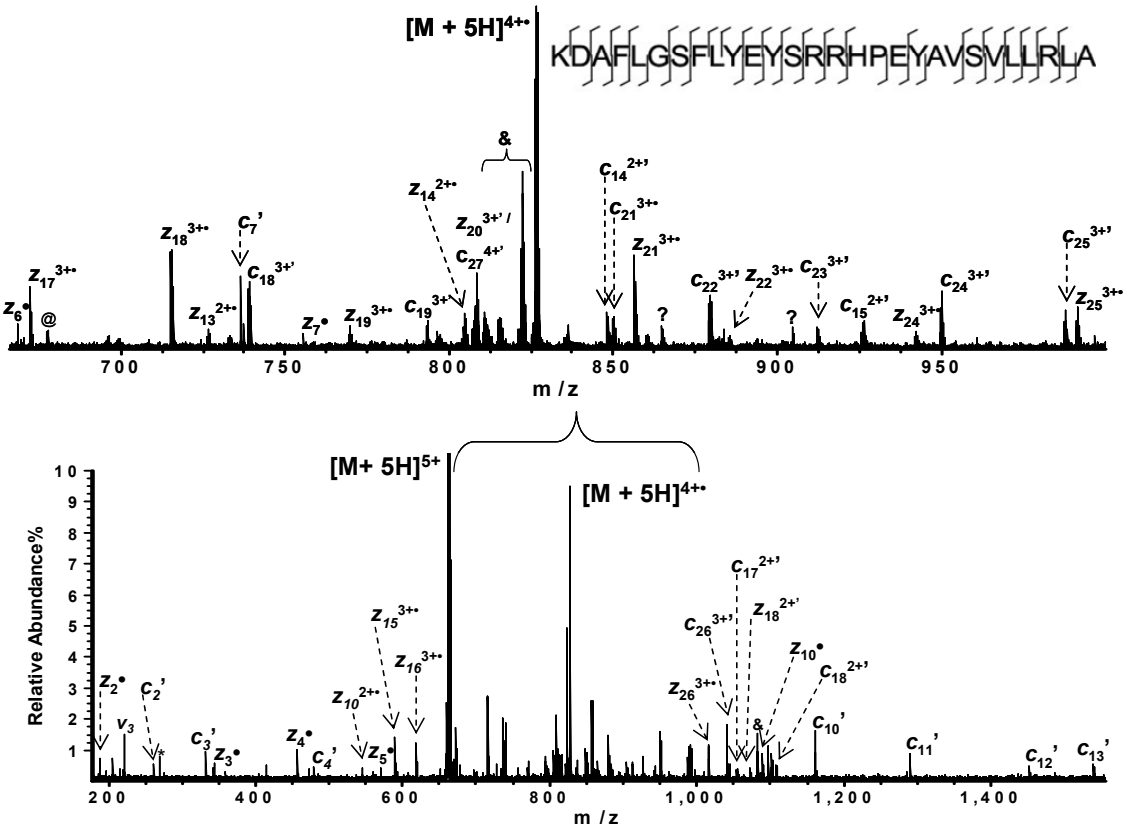

Figure 4.3. ECD of $[M + 5H]^{5+}$ precursor ions from a BSA Lys N digest peptide. Cleavages at 25 out of 26 possible N-Cα backbone bonds are observed, resulting in extensive peptide sequence coverage. v_3 = 3rd harmonic, & = neutral losses, ? = unidentified product ions, @ = *y*-type product ion.

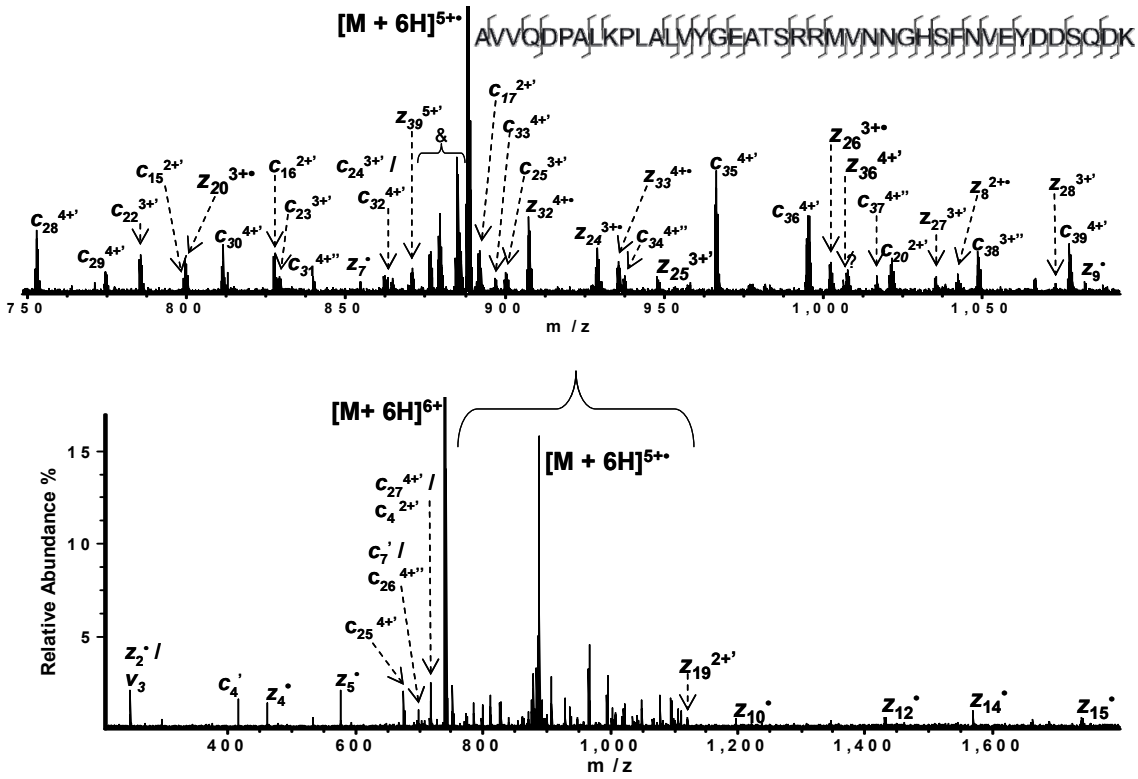

Figure 4.4. ECD of $[M + 6H]^{6+}$ precursor ions from a peptide derived from Lys C digestion of carbonic anhydrase. For this 40 amino acid residue peptide, ECD resulted in cleavages at 31 out of 37 possible N-Cα backbone bonds, resulting in 84% peptide sequence coverage. v_3 = 3rd harmonic, & = neutral losses, ? = unidentified product ions.

In contrast to the behavior observed for triply protonated peptides, ECD sequence coverage for these higher charge states (+4, +5, and +6) is less affected by the precursor m/z value (Figures 4.5 A-C). However, it should be noted that these peptides, carrying 4, 5 and 6 charges, were detected at m/z values less than 950 whereas triply protonated species showing a significant decrease in peptide sequence coverage were detected at m/z>960. Some $[M + 4H]^{4+}$, $[M + 5H]^{5+}$, and $[M + 6H]^{6+}$ species were detected at higher m/z values (>950) but were of low abundance (<10% relative abundance). There are two reasons we elected not to examine low abundance species: first, the low fragmentation

efficiency of ECD[73-75] requires relatively abundant precursor ions for generation of detectable product ions, and, second, in common data dependent MS/MS approaches, only the most abundant species are selected for fragmentation. We believe that precursor ions carrying more or equal to four charges at high m/z values would also show a decrease in peptide sequence coverage, similar to triply protonated species. However, such behavior does not appear to pose a problem for ECD experiments because precursor ions carrying four to six protons were mainly detected at low m/z values that are optimal for ECD.

As illustrated in Figures 4.5 A-C, the majority of highly charged peptides, 89 out of 101 examined, resulted in ECD sequence coverage above 70%, independent of the precursor ion m/z value. It is worth mentioning that 31 out of 101 peptides showed complete or near complete ECD sequence coverage, 90-100%. Only few peptides, 12 out of 101 examined, showed moderate ECD sequence coverage (50-70%). However, the lower peptide sequence coverage observed for the latter species is not directly correlated with their m/z values because some of these species were detected at low m/z values. Differences in fragmentation behavior may be attributed to differences in gas-phase structures of the individual peptides. Gas-phase conformations and structures of precursor ions have been shown to influence the fragmentation outcome in ECD.[76-78] The average peptide sequence coverage, the total number of *c*- and *z*-type product ions, and the number of complementary fragment pairs for each charge state (+4, +5, and +6), and for each proteolytic enzyme are displayed in Tables 4.11 A-C. Overall, for these higher charge states, the extent of fragmentation, i.e., number of ECD products, is very similar

regardless of precursor ion charge state and enzyme used for digestion. Some variations from this general trend are observed and discussed in detail below.

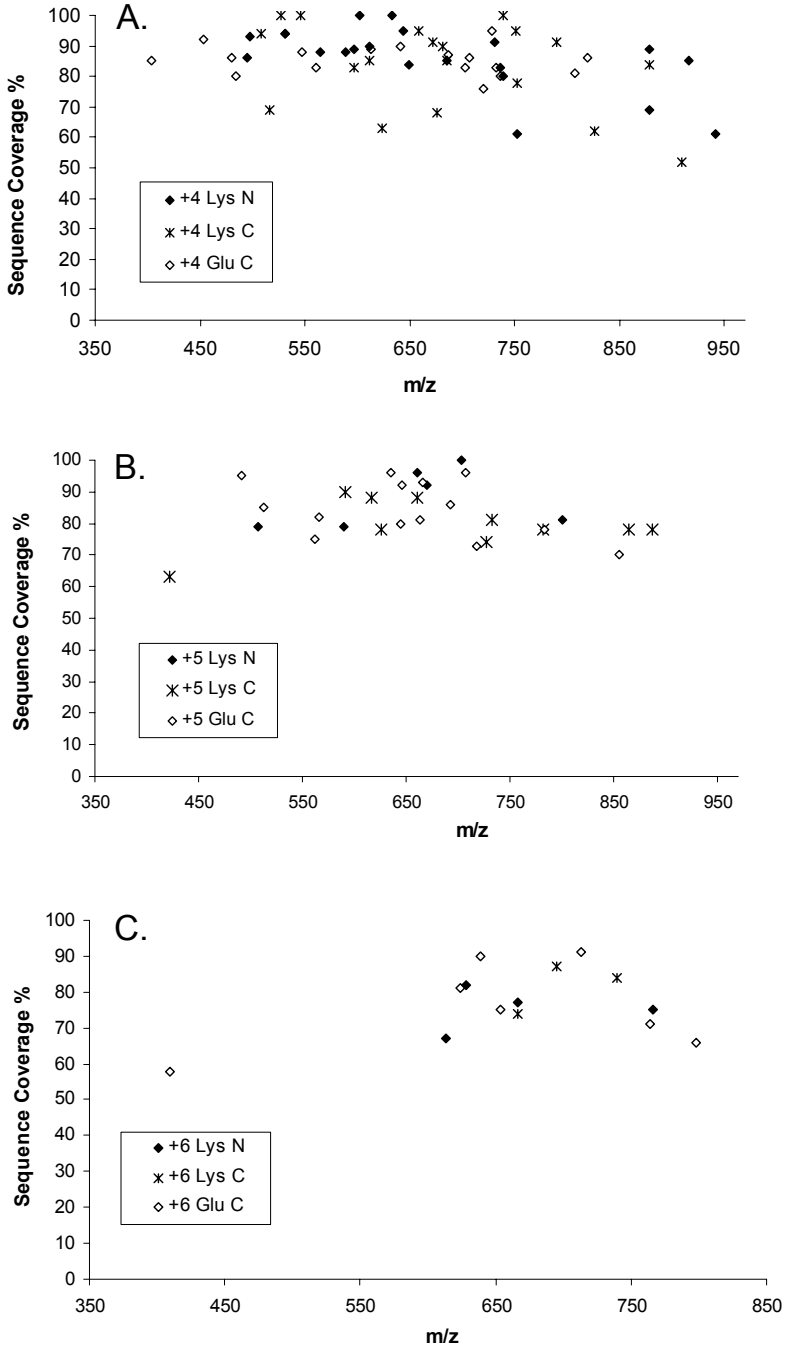

Figure 4.5. ECD sequence coverage as function of precursor ion m/z ratio for A) $[M + 4H]^{4+}$, B) $[M + 5H]^{5+}$, and C) $[M + 6H]^{6+}$ species from Lys C, Lys N and Glu C digestion. These highly charged proteolytic peptides were detected at relatively low m/z values and their ECD sequence coverage is not strongly affected by the precursor m/z ratio.

For quadruply protonated species (Table 4.11A), both the ECD sequence coverage and the total number of *c*- and *z*-type product ions are very similar for Lys C, Lys N, and Glu C digest peptides. Similar to triply protonated species, ECD of quadruply protonated Lys C digest peptides resulted in a higher number of complementary fragment pairs for the reasons discussed above. The sequence coverage, and the total number of *c*- and *z*-type product ions were higher for quadruply protonated species compared to triply protonated species, particularly for Glu C digest peptides. The higher extent of fragmentation observed for quadruply protonated species can be attributed to increased Coulomb repulsion, due to the presence of one additional charge compared to triply protonated species, which results in more unfolded gas-phase structures and also enhances separation of complementary fragment pairs. Because triply and quadruply protonated species from Glu C digestion have very similar average peptide length, a greater increase in peptide sequence coverage was observed for quadruply protonated species compared to Lys C and Lys N derived peptides.

$[M + 5H]^{5+}$ precursor ions showed very similar peptide ECD sequence coverage as quadruply protonated species (Tables 4.11A and 4.11B). Also, the total number of product ions and the number of complementary fragment pairs are similar for +4 and +5 precursor ions. The similar extent of fragmentation observed for the +4 and +5 precursor ions was not expected but is not surprising considering that the examined +4 and +5 multiply protonated peptides have different amino acid compositions (see discussion below). Furthermore, $[M + 5H]^{5+}$ precursor ions have a higher average peptide length compared to the quadruply protonated species. Another factor to be considered is once

again the gas-phase structures of precursor ions. Williams and co-workers suggested that ion shape can have a greater effect on ECD efficiency than ion charge state.[78]

$[M + 5H]^{5+}$ precursor ions from Lys C derived peptides showed lower ECD sequence coverage but very similar, or equal, numbers of total product ions and complementary fragment pairs compared to Lys N and Glu C digest peptides. This outcome may be attributed to the fact that $[M + 5H]^{5+}$ Lys C digest peptides were longer compared to the +5 Lys N and Glu C digest peptides. However, this explanation is in disagreement with the data obtained for $[M + 6H]^{6+}$ precursor ions (Table 4.11C). For +6 precursor ions, Lys C digest peptides showed the highest ECD sequence coverage although these peptides were, on average, larger in size compared to the other +6 precursor ions. Once again, differences in ion gas-phase structures may explain these differences. Another factor is the amino acid context of the individual peptides. It has been suggested that ECD cleavage frequencies are determined by the local sequence[79] and sequence preferences in ECD have been previously reported by Savitski et. al.[80] Similar to the +5 precursor ions, the total number of *c*- and *z*-type product ions, and the number of complementary fragment pairs were very similar, or identical, for +6 precursor ions from Lys C, Lys N and Glu C digest peptides. Interestingly, for $[M + 6H]^{6+}$ precursor ions, peptides from Lys N and Glu C digestion exhibited lower fragmentation compared to the +4 and +5 charge states, whereas Lys C digest peptides showed very similar fragmentation for all three charge states. $[M + 6H]^{6+}$ precursor ions have the highest average peptide length and, therefore, are expected to exhibit increased intramolecular non-covalent interactions, resulting in more folded structures. Increasing peptide charge state is expected to cause, to some extent, unfolding of the peptide gas-

phase structure due to Coulomb repulsion. However, depending on peptide size, more than six charges may be required to effectively unfold these structures. Therefore, the decrease in fragmentation observed for peptides in the +6 charge state can be due to the presence of intramolecular non-covalent interactions.

Table 4.11. ECD summary for A) all $[M + 4H]^{4+}$, B) all $[M + 5H]^{5+}$, and C) all $[M + 6H]^{6+}$ species examined [a]

A. $[M + 4H]^{4+}$	Lys N digest peptides	Lys C digest peptides	Glu C digest peptides
# of total backbone N-C_α cleavages	349/414 84%	325/395 82%	305/355 86%
# of total product ions	520/828 (191 z• / z' 329 c• / c') 63%	541/790 (247 z• / z' 294 c• / c') 68%	464/710 (184 z• / z' 280 c• / c') 65%
# of complementary fragment pairs	170/414 41%	214/395 54%	159/355 45%
Average Peptide Length	23.4	23.3	21.8

B. $[M + 5H]^{5+}$	Lys N digest peptides	Lys C digest peptides	Glu C digest peptides
# of total backbone N-C_α cleavages	137/155 88%	214/268 80%	312/372 84%
# of total product ions	215/310 (88 z• / z' 127 c• / c') 69%	344/536 (166 z• / z' 178 c• / c') 65%	480/744 (189 z• / z' 291 c• / c') 64%
# of complementary fragment pairs	74/155 47%	127/268 47%	168/372 45%
Average Peptide Length	28.2	29.8	28.7

C. $[M + 6H]^{6+}$	Lys N digest peptides	Lys C digest peptides	Glu C digest peptides
# of total backbone N-C_α cleavages	94/125 75%	81/99 82%	166/217 76%
# of total product ions	153/250 (68 z• / z' 85 c• / c') 61%	123/198 (56 z• / z' 67 c• / c') 62%	259/434 (111 z• / z' 148 c• / c') 60%
# of complementary fragment pairs	54/125 43%	42/99 42%	93/217 43%
Average Peptide Length	34.5	36.0	33.7

[a] Similar numbers of ECD product ions were obtained for these higher charge state peptides, independent of the enzyme used for digestion. $[M + 6H]^{6+}$ precursor ions from Lys N and Glu C digestion exhibited lower ECD sequence coverage compared to peptides carrying four and five positive charges, whereas $[M + 4H]^{4+}$, $[M + 5H]^{5+}$, and $[M + 6H]^{6+}$ species from Lys C digestion resulted in similar ECD sequence coverage.

4.3.3. Effect of Charge State, Charge Location, and Peptide mass on ECD

In order to directly examine the effect of charge state on ECD fragmentation behavior, we selected a subset of peptides (having the same amino acid sequence) that were detected in more than one charge state. The ECD sequence coverage of these peptides was examined as a function of peptide mass (Figures 4.6, 4.7 and 4.8) . Figure 4.6 displays peptides from Lys C digestion. Seven out of 12 peptides yielded increased sequence coverage when higher charge states were fragmented with ECD. A particularly significant increase in sequence coverage was observed for two peptides with molecular weights of 2952 and 2999 Da when the quadruply rather than triply protonated species were fragmented. For the former peptide, the triply protonated species resulted in 33% sequence coverage whereas the quadruply protonated species showed 95% sequence coverage. For the latter peptide, cleavages at all possible backbone amine bonds were observed when the quadruply protonated species was fragmented. By contrast, ECD of the triply protonated form showed 50% sequence coverage. Four out of 12 peptides showed similar ECD sequence coverage for higher and lower charge states and only one peptide showed decreased ECD sequence coverage (63%) when its +5 charge state was used for fragmentation. This peptide with a molecular weight of 2107 Da (18 amino acid residues) showed cleavages at all possible backbone amine bonds when its +4 charge state was fragmented.

For Glu C and Lys N derived peptides (Figures 4.7 and 4.8), similar trends were observed as for the Lys C derived peptides discussed above. For Glu C derived peptides (Figure 4.7), half of the peptides examined exhibited increased sequence coverage when fragmenting a higher charge state. Two peptides with molecular weights of 2879 and 2911 Da showed two-fold increase in their sequence coverage when their quadruply

rather than triply protonated species were fragmented. For five out of the 10 peptides examined, very similar ECD sequence coverage was observed for both these charge states. Only one peptide exhibited lower ECD sequence coverage when the +6 precursor ions were fragmented in ECD. This +6 precursor ion showed 58% sequence coverage compared to 89% for its quadruply protonated counterpart and 95% for its +5 protonated form. This peptide was the smallest +6 precursor ion we examined here, having a molecular weight of 2449 Da (21 amino acid residues).

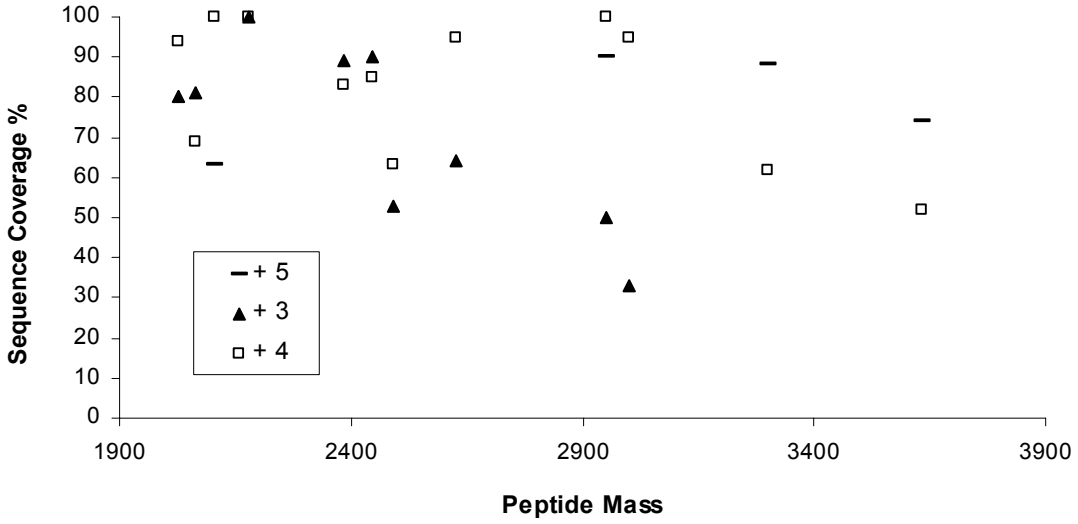

Figure 4.6. ECD sequence coverage as function of peptide mass for Lys C derived peptides detected in more than one charge state. Most of the peptides exhibit greater sequence coverage when a higher charge state was fragmented. However, some peptides showed very similar sequence coverage, independent of charge state, and one peptide resulted in lower ECD sequence coverage when a higher charge state was fragmented.

For Lys N derived peptides (Figure 4.8), six out of 10 peptides showed increased sequence coverage when higher charge states were fragmented in ECD. Three out of 10 peptides showed very similar ECD sequence coverage for higher and lower precursor ion charge states. One peptide exhibited lower ECD sequence coverage when the +5 charge

state was fragmented compared to the +4 charge state. The latter, rather small (22 amino acid residues) peptide showed cleavages at all possible backbone amine bonds in ECD of its quadruply protonated form. For small size peptides (derived from digestion with either proteolytic enzyme) for which ECD of a higher charge state resulted in decreased peptide sequence coverage, we noted that the abundance of the charge reduced species (i.e., the species resulting from electron capture but without dissociation) was higher compared to precursor ions that fragmented efficiently in ECD. Breuker et al have reported that hydrogen ejection from the charge-reduced species without further fragmentation can effectively compete with *c*- and *z*-type product ion generation for some charge states of ubiquitin.[81] In our experiments, charge reduced species are mixtures of radical and even electron hydrogen-ejected species, however, such mixtures were also seen for peptides that fragmented well in ECD. Further experiments are therefore needed to elucidate the basis for this behavior.

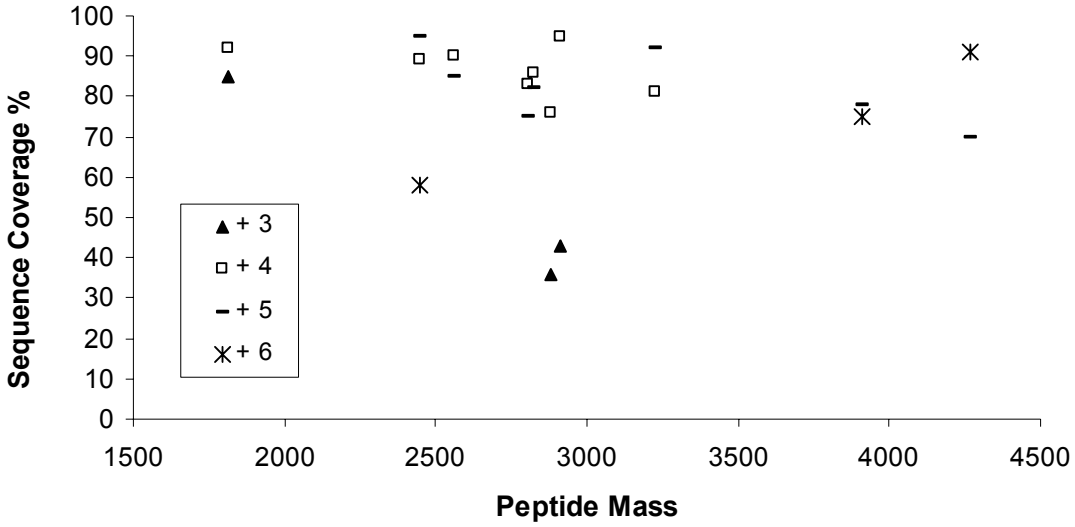

Figure 4.7. ECD sequence coverage as function of peptide mass for Glu C derived peptides detected in more than one charge state.

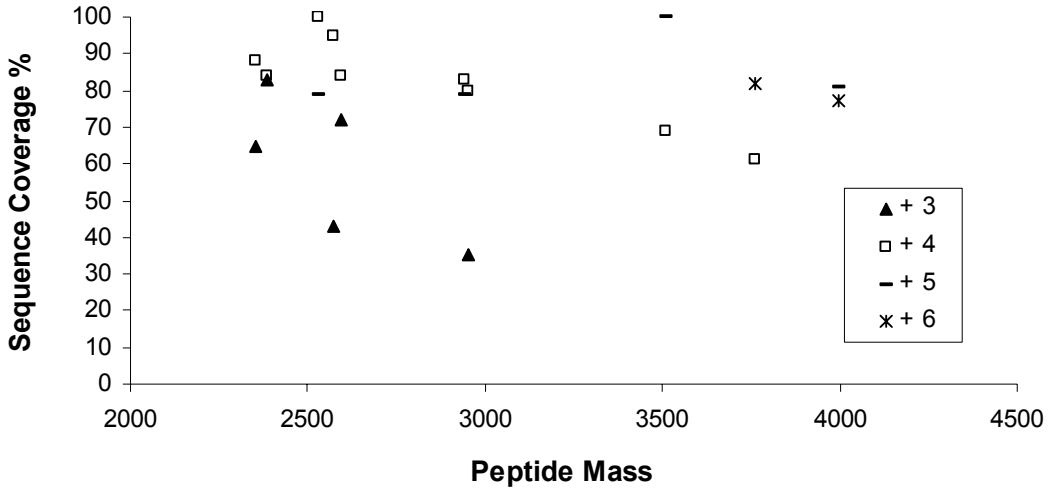

Figure 4.8. ECD sequence coverage as function of peptide mass for Lys N derived peptides detected in more than one charge state.

The data presented in Figures 4.6, 4.7 and 4.8 suggest that, for peptides with the same amino acid composition, a higher charge state will, generally, result in increased peptide sequence coverage. This behavior is in agreement with the existence of more unfolded gas-phase structures with increasing charge state (due to increased Coulomb repulsion). However, our data also suggest that, depending on the peptide size, there is a maximum number of charges for which the highest sequence coverage is obtained, and that increasing the charge state above this optimum value does not increase the sequence coverage.

The effect of charge location in ECD was investigated by comparing peptides from Lys C and Lys N digestion, resulting in peptides with the same amino acid composition but differing in the location of a lysine residue: peptides from Lys N digestion have a Lys residue at the N-terminus whereas peptides from Lys C digestion have a Lys residue at the C-terminus. Selected examples are displayed in Tables 4.12 A and 4.12 B (all other

examples are displayed in Tables 4.1, 4.2, 4.5, 4.6, 4.8, and 4.9, marked with an asterisk). ECD of peptides 1a and 1b (Table 4.12A) resulted in the same sequence coverage (100%) whereas peptides 6a and 6b showed almost identical ECD sequence coverage (77% and 74%, corresponding to cleavage of 24 and 23 backbone interresidue bonds, respectively). ECD of peptides 2a, 4a, and 5a from Lys N digestion resulted in higher sequence coverage compared to ECD of peptides 2b, 4b, and 5b from Lys C digestion. By constrast, peptide 3b from Lys C digestion showed higher ECD sequence coverage compared to peptide 3a derived from Lys N digestion. The same trends were observed for doubly protonated species (Table 4.12B). These results suggest that charge location does influence the ECD fragmentation behavior but not in a consistent manner, indicative of other influencing factors such as the peptide gas-phase structure.

Recently, Heck and co-workers performed ETcaD of doubly protonated peptides from Lys N and Lys C digestion.[64] These authors reported that dissociation of doubly protonated species from Lys N derived peptides containing a single lysine residue resulted in formation of solely N-terminal *c*-type product ions whereas Lys C derived peptides yielded both *c*- and *z*-type product ions. This behavior is in agreement with our ECD data for peptides 2a, 2b, 3a, 3b, 5a, and 5b (Table 4.12B). The same authors also reported that, when more than one basic residue was present in Lys N derived peptides, both *c*-and *z*-type product ions were detected, similar to our ECD data for peptides 1a and 4a (Table 4.12B).

Table 4.12. ECD fragmentation summary of A) selected peptides at +3, +4, +5, and +6 charge states, and B) all doubly protonated peptides from Lys N and Lys C digestion.[a]

A.

Charge	Lys N digest peptides	Seq. Cov. %	Lys C digest peptides	Seq. Cov. %
+3	KVPQVSTPTLVEVSRSLG 1a	100%	VPQVSTPTLVEVSRSLGK 1b	100%
+3	KECCHGDLLECADDRADLA 2a	94%	ECCHGDLLECADDRADLAK 2b	89%
+4	KYLYEIARRHPVFYAPELLYYAN 3a	80%	YLYEIARRHPYFYAPELLYYANK 3b	100%
+4	KSHCIAEVEKDAIPENLPPLTADFAEDKDVC 4a	89%	SHCIAEVEKDAIPENLPPLTADFAEDKDVCK 4b	84%
+5	KDAFLGSFLYEYSRRHPEYAVSVLLRLA 5a	96%	DAFLGSFLYEYSRRHPEYAVSVLLRLAK 5b	88%
+6	KDYELLCLDGTRKPVEEYANCHLARAPNHAVVTR 6a	77%	DYELLCLDGTRKPVEEYANCHLARAPNHAVVTRK 6b	74%

B.

Charge	Lys N digest peptides	Seq. Cov %	Lys C digest peptides	Seq. Cov %
+2	KSLHTLFGDELC 1a	91%	SLHTLFGDELCK 1b	100%
+2	KTVMENFVAFVD 2a	64%	TVMENFVAFVDK 2b	91%
+2	KYNGVFQECCQAED 3a	46%	YNGVFQECCQAEDK 3b	38%
+2	KLFTFHADICTLPDTE 4a	79%	LFTFHADICTLPDTEK 4b	71%
+2	KDAIPENLPPLTADFAED 5a	57%	DAIPENLPPLTADFAEDK 5b	29%

[a] The peptides presented here have the same amino acid composition but differ in the location of the lysine residue. In some cases, Lys N derived peptides resulted in higher ECD sequence coverage compared to Lys C derived peptides, and, in other cases, peptides from Lys C digestion resulted in better peptide sequence coverage

Figure 4.9 displays ECD sequence coverage as a function of peptide mass for all peptides examined. It is apparent from this Figure that ECD sequence coverage is not strongly affected by the peptide mass. Low sequence coverage is observed for triply protonated species with a molecular weight around 3000 Da. These peptides were detected at high m/z values (>960), as discussed. Peptides at the +4 and +5 charge states with similar molecular weights (around 3000 Da) fragment efficiently in ECD. These +4 and +5 species were detected at lower m/z values compared to triply protonated species with similar molecular weights. Good ECD sequence coverage was also obtained for

longer peptides having molecular weights up to 4779 Da and carrying five or six positive charges. Due to the presence of five or six charges, these larger peptides were detected at low m/z values and, therefore, fragment fairly well in ECD.

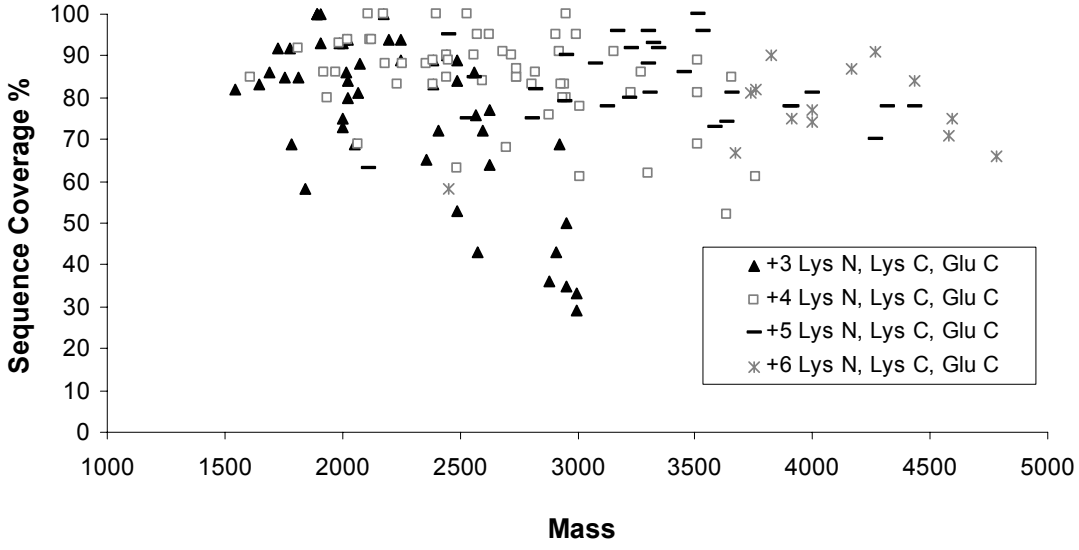

Figure 4.9. ECD sequence coverage as function of precursor ion mass for all peptides examined. ECD sequence coverage does not correlate strongly with peptide mass. Only triply protonated species with high molecular weight (detected at high m/z ratios) showed low peptide sequence coverage.

4.3.4. Summary of the ECD Behavior of Lys C, Lys N, and Glu C Digest Peptides

Table 4.13 summarizes the average peptide sequence coverage, the number of *c*- and *z*-type product ions, and the number of complementary fragment pairs for all peptides examined, independent of precursor ion charge state. The average ECD sequence coverage is almost identical for Lys C, Lys N, and Glu C digest peptides. Furthermore, the total number of ECD product ions is similar, regardless of which proteolytic enzyme was used for digestion. Lys N and Glu C derived peptides produced more *c*-type product ions, for reasons discussed above, whereas, for Lys C digest peptides, the number of *c*- and *z*-type fragments is comparable. Lys C digest peptides showed a slightly higher

number of complementary fragment pairs compared to Lys N and Glu C digest peptides, as previously discussed. It is apparent from the data presented in Table 4.13 that protease selection does not affect the ECD outcome, and that ECD provides high peptide sequence coverage independent of the proteolytic enzyme used for digestion. It is also worth mentioning that the majority of peptides examined here, 125 out of 152 (82%), exhibited good to high peptide sequence coverage, ranging from 70 to 100% (Figure 4.10). Thirteen percent of all peptides examined (20 out of 151) showed a moderate sequence coverage, ranging from 50 to 70% and only 5% of all peptides showed low peptide sequence coverage below 50%. All of the latter peptides were triply protonated and detected at high m/z values.

Table 4.13 ECD summary of all peptides examined, independent of precursor ion charge state [a]

$[M + 3H]^{3+}$, $[M + 4H]^{4+}$, $[M + 5H]^{5+}$, $[M + 6H]^{6+}$	Lys N digest peptides	Lys C digest peptides	Glu C digest peptides
# of total backbone N-C_α cleavages	854/1051 81%	857/1065 80%	928/1150 81%
# of total product ions	1282/2102 (485 z• / z' 797 c'/ c•) 61%	1374/2130 (649 z• / z' 725 c' / c•) 64%	1392/2300 (559 z• / z' 833 c' / c•) 60%
# of complementary fragment pairs	418/1051 40%	508/1065 48%	463/1150 40%
Average Peptide Length	23	24	25
Average Charge State	3.8	4.0	4.4

[a] The total number of observed N-Cα bond cleavages, the total number of *c*- and z-type productt ions, and the total number of complementary fragment pairs are displayed. Almost identical ECD sequence coverage was obtained for Lys C, Lys N, and Glu C derived peptides. The number of ECD products is also very similar for all three peptide types whereas a slightly higher number of complementary fragment pairs was detected for proteolytic peptides derived from Lys C digestion.

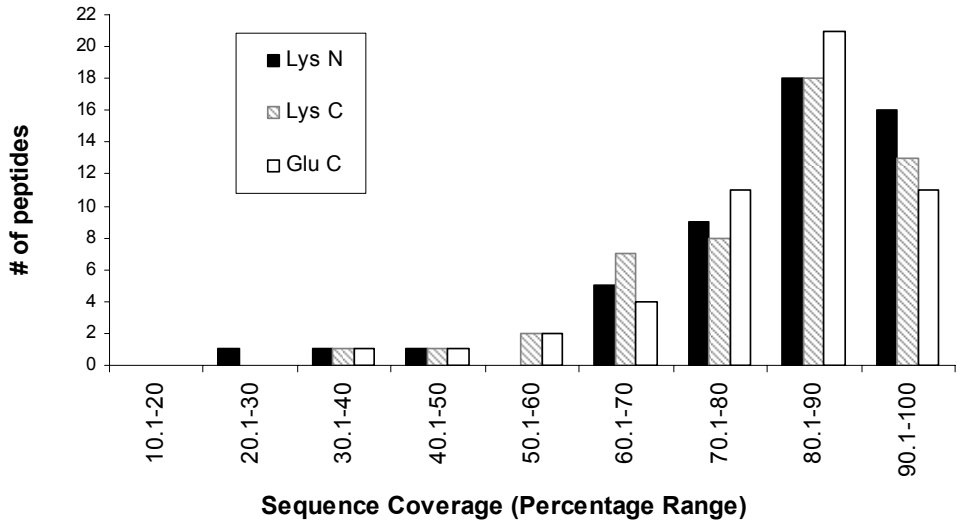

Figure 4.10. Percent ECD sequence coverage obtained for all proteolytic peptides. The majority of peptides exhibited good or high ECD sequence coverage.

4.4. Conclusions

We have compared and evaluated the utility of ECD in conjunction with Lys C, Lys N, and Glu C digestion for the analysis of medium size proteolytic peptides carrying multiple charges. Our results demonstrate that, independent of the enzyme used for digestion, ECD provides considerable sequence information for proteolytic peptides containing 14 to 41 amino acid residues at high charge states (+3 to +6). The average ECD sequence coverage was 81% whereas the average % fragmentation (total number of observed *c*- and *z*-type product ions divided by the theoretical number of *c*- and *z*-type product ions) was 62%. Generation and detection of all possible *c*- and *z*-type product ions is more challenging compared to observation of cleavage at each backbone interresidue bond (the latter requires detection of only one of the two complementary product ions) and, therefore, the % fragmentation is lower than the % sequence coverage.

We have also investigated the effects of precursor ion charge, precursor ion m/z value, precursor ion mass, and charge location on ECD. We observed that precursor ion m/z value is a major factor affecting the extent of fragmentation in ECD. Triply protonated peptides detected at m/z values higher than 960 did not fragment efficiently in ECD whereas triply protonated species detected at lower m/z values provided rich sequence information. Precursor ions carrying +4, +5, and +6 charges were mainly detected at m/z values less than 950 and resulted in informative ECD spectra. In addition, gas-phase conformations and structures of precursor ions appear to influence ECD fragmentation behavior. ECD sequence coverage was less affected by precursor ion mass and charge location.

Furthermore, from the data presented here, it appears that, for a given peptide length, there is an optimum number of charges for which high ECD sequence coverage can be obtained. Nevertheless, good to high peptide sequence coverage (70% -100%) was obtained for the majority of peptides, demonstrating that ECD is a powerful tool for structural characterization of medium size proteolytic peptides carrying multiple charges.

4.5. References

1. Biemann, K., Mass-Spectrometry of Peptides and Proteins. *Annu. Rev. Biochem.* **1992,** 61, 977-1010.
2. Branca, R. M. M.; Bodo, G.; Bagyinka, C.; Prokai, L., De novo sequencing of a 21-kDa cytochrome c(4) from Thiocapsa roseopersicina by nanoelectrospray ionization ion-trap and Fourier-transform icon-cyclotron resonance mass spectrometry. *J. Mass. Spectrom.* **2007,** 42, 1569-1582.
3. Deon, C., Combined mass spectrometric methods for the characterization of human hemoglobin variants localized within alpha T9 peptide: Identification of Hb Villeurbanne alpha 89 (FG1) His->Tyr. *J. Mass Spectrom.* **1997,** 32, 880-887.
4. Dodds, E. D.; German, J. B.; Lebrilla, C. B., Enabling MALDI-FTICR-MS/MS for high-performance proteomics through combination of infrared and collisional activation. *Anal. Chem.* **2007,** 79, 9547-9556.
5. Gatlin, C. L.; Eng, J. K.; Cross, S. T.; Detter, J. C.; Yates, J. R., Automated identification of amino acid sequence variations in proteins by HPLC/microspray tandem mass spectrometry. *Anal. Chem.* **2000,** 72, 757-763.
6. Henderson, L. E., Gag Proteins of the Highly Replicative Mn Strain of Human-Immunodeficiency-Virus Type-1 - Posttranslational Modifications, Proteolytic Processings, and Complete Amino-Acid-Sequences. *J. Virol.* **1992,** 66, 1856-1865.
7. Henderson, R. A., Hla-A2.1-Associated Peptides from a Mutant-Cell Line - a 2nd Pathway of Antigen Presentation. *Science* **1992,** 255, 1264-1266.
8. Hopper, S., Glutaredoxin from Rabbit Bone-Marrow - Purification, Characterization, and Amino-Acid Sequence Determined by Tandem Mass-Spectrometry. *J. Biol. Chem.* **1989,** 264, 20438-20447.
9. Hunt, D. F.; Yates, J. R.; Shabanowitz, J.; Winston, S.; Hauer, C. R., Protein Sequencing by Tandem Mass-Spectrometry. *Proc. Natl. Acad. Sci. U.S.A* **1986,** 83, 6233-6237.
10. Johnson, R. S.; Biemann, K., The Primary Structure of Thioredoxin from Chromatium Vinosum Determined by High-Performance Tandem Mass-Spectrometry. *Biochemistry* **1987,** 26, 1209-1214.
11. Johnson, R. S.; Mathews, W. R.; Biemann, K.; Hopper, S., Amino-Acid Sequence of Thioredoxin Isolated from Rabbit Bone-Marrow Determined by Tandem Mass-Spectrometry. *J. Biol. Chem.* **1988,** 263, 9589-9597.
12. Martin, S. E., Subfemtomole MS and MS/MS peptide sequence analysis using nano-HPLC micro-ESI Fourier transform ion cyclotron resonance mass spectrometry. *Anal. Chem.* **2000,** 72, 4266-4274.
13. Medzihradszky, K. F., Peptide sequence analysis. *Biol. Mass Spectrom.* **2005,** 402, 209-244.
14. Standing, K. G., Peptide and protein de novo sequencing by mass spectrometry. *Curr. Opin. Struct. Biol.* **2003,** 13, 595-601.
15. Aebersold, R., Mass spectrometry of proteins and peptides in biotechnology. *Curr. Opin. Biotechnol.* **1993,** 4, 412-419.
16. Bruni, R.; Gianfranceschi, G.; Koch, G., On peptide de novo sequencing: a new approach. *J. Pept. Sci.* **2005,** 11, 225-234.

17. Fenselau, C., Beyond Gene Sequencing - Analysis of Protein-Structure with Mass-Spectrometry. *Annu. Rev. Biophys. Biophys. Chem.* **1991,** 20, 205-220.
18. Metzger, J. W., Ladder Sequencing of Peptides and Proteins - a Combination of Edman Degradation and Mass-Spectrometry. *Angew. Chem. Int. Ed.* **1994,** 33, 723-725.
19. Nokihara, K., Procedures leading to primary structure determination of proteins in complex mixtures by gel electrophoresis and modern micro-scale analyses. *Anal. Chim. Acta* **1998,** 372, 21-32.
20. Hayes, R. N.; Gross, M. L., Collision-Induced Dissociation. *Methods Enzymol.* **1990,** 193, 237-263.
21. McLuckey, S. A., Principles of Collisional Activation in Analytical Mass-Spectrometry. *J. Am. Soc. Mass Spectrom.* **1992,** 3, 599-614.
22. Hauser, N. J.; Han, H. L.; McLuckey, S. A.; Basile, F., Electron transfer dissociation of peptides generated by microwave D-cleavage digestion of proteins. *J. Proteome Res.* **2008,** 7, 1867-1872.
23. Kjeldsen, F.; Giessing, A. M. B.; Ingrell, C. R.; Jensen, O. N., Peptide sequencing and characterization of post-translational modifications by enhanced ion-charging and liquid chromatography electron-transfer dissociation tandem mass spectrometry. *Anal. Chem.* **2007,** 79, 9243-9252.
24. Simpson, R. J.; Connolly, L. M.; Eddes, J. S.; Pereira, J. J.; Moritz, R. L.; Reid, G. E., Proteomic analysis of the human colon carcinoma cell line (LIM 1215): Development of a membrane protein database. *Electrophoresis* **2000,** 21, 1707-1732.
25. Zubarev, R., Protein primary structure using orthogonal fragmentation techniques in Fourier transform mass spectrometry. *Expert Rev. Proteomics* **2006,** 3, 251-261.
26. Zubarev, R. A., Electron-capture dissociation tandem mass spectrometry. *Curr. Opin. Biotechnol.* **2004,** 15, 12-16.
27. Zubarev, R. A.; Kelleher, N. L.; McLafferty, F. W., Electron capture dissociation of multiply charged protein cations. A nonergodic process. *J. Am. Chem. Soc.* **1998,** 120, 3265-3266.
28. Mikesh, L. M.; Ueberheide, B.; Chi, A.; Coon, J. J.; Syka, J. E. P.; Shabanowitz, J.; Hunt, D. F., The utility of ETD mass spectrometry in proteomic analysis. *Biochim. Biophys. Acta* **2006,** 1764, 1811-1822.
29. Syka, J. E. P.; Coon, J. J.; Schroeder, M. J.; Shabanowitz, J.; Hunt, D. F., Peptide and protein sequence analysis by electron transfer dissociation mass spectrometry. *Proc. Natl. Acad. Sci. U.S.A* **2004,** 101, 9528-9533.
30. Kalli, A.; Hakansson, K., Comparison of the electron capture dissociation fragmentation behavior of doubly and triply protonated peptides from trypsin, Glu-C, and chymotrypsin digestion. *J. Proteome Res.* **2008,** 7, 2834-2844.
31. O'Connor, P. B.; Lin, C.; Cournoyer, J. J.; Pittman, J. L.; Belyayev, M.; Budnik, B. A., Long-lived electron capture dissociation product ions experience radical migration via hydrogen abstraction. *J. Am. Soc. Mass Spectrom.* **2006,** 17, 576-585.

32. Savitski, M. M.; Kjeldsen, F.; Nielsen, M. L.; Zubarev, R. A., Hydrogen rearrangement to and from radical z fragments in electron capture dissociation of peptides. *J. Am. Soc. Mass Spectrom.* **2007,** 18, 113-120.
33. Zubarev, R. A.; Horn, D. M.; Fridriksson, E. K.; Kelleher, N. L.; Kruger, N. A.; Lewis, M. A.; Carpenter, B. K.; McLafferty, F. W., Electron capture dissociation for structural characterization of multiply charged protein cations. *Anal. Chem.* **2000,** 72, 563-573.
34. Kjeldsen, F.; Haselmann, K. F.; Budnik, B. A.; Jensen, F.; Zubarev, R. A., Dissociative capture of hot (3-13 eV) electrons by polypeptide polycations: an efficient process accompanied by secondary fragmentation. *Chem. Phys. Lett.* **2002,** 356, 201-206.
35. Cooper, H. J.; Hakansson, K.; Marshall, A. G., The role of electron capture dissociation in biomolecular analysis. *Mass Spectrom. Rev.* **2005,** 24, 201-222.
36. Chalmers, M. J.; Kolch, W.; Emmett, M. R.; Marshall, A. G.; Mischak, H., Identification and analysis of phosphopeptides. *J. Chromatogr. B* **2004,** 803, 111-120.
37. Kweon, H. K.; Hakansson, K., Metal oxide-based enrichment combined with gas-phase ion-electron reactions for improved mass spectrometric characterization of protein phosphorylation. *J. Proteome. Res.* **2008,** 7, 749-755.
38. Molina, H.; Horn, D. M.; Tang, N.; Mathivanan, S.; Pandey, A., Global proteomic profiling of phosphopeptides using electron transfer dissociation tandem mass spectrometry. *Proc. Natl. Acad. Sci. USA* **2007,** 104, 2199-2204.
39. Shi, S. D. H.; Hemling, M. E.; Carr, S. A.; Horn, D. M.; Lindh, I.; McLafferty, F. W., Phosphopeptide/phosphoprotein mapping by electron capture dissociation mass spectrometry. *Anal. Chem.* **2001,** 73, 19-22.
40. Stensballe, A.; Jensen, O. N.; Olsen, J. V.; Haselmann, K. F.; Zubarev, R. A., Electron capture dissociation of singly and multiply phosphorylated peptides. *Rapid Commun. Mass Spectrom.* **2000,** 14, 1793-1800.
41. Kjeldsen, F.; Haselmann, K. F.; Budnik, B. A.; Sorensen, E. S.; Zubarev, R. A., Complete characterization of posttranslational modification sites in the bovine milk protein PP3 by tandem mass spectrometry with electron capture dissociation as the last stage. *Anal. Chem.* **2003,** 75, 2355-2361.
42. Adamson, J. T.; Hakansson, K., Infrared multiphoton dissociation and electron capture dissociation of high-mannose type glycopeptides. *J. Proteome Res.* **2006,** 5, 493-501.
43. Hakansson, K.; Chalmers, M. J.; Quinn, J. P.; McFarland, M. A.; Hendrickson, C. L.; Marshall, A. G., Combined electron capture and infrared multiphoton dissociation for multistage MS/MS in a Fourier transform ion cyclotron resonance mass spectrometer. *Anal. Chem.* **2003,** 75, 3256-3262.
44. Hakansson, K.; Cooper, H. J.; Emmett, M. R.; Costello, C. E.; Marshall, A. G.; Nilsson, C. L., Electron capture dissociation and infrared multiphoton dissociation MS/MS of an N-glycosylated tryptic peptide to yield complementary sequence information. *Anal. Chem.* **2001,** 73, 4530-4536.
45. Haselmann, K. F.; Budnik, B. A.; Olsen, J. V.; Nielsen, M. L.; Reis, C. A.; Clausen, H.; Johnsen, A. H.; Zubarev, R. A., Advantages of external

accumulation for electron capture dissociation in Fourier transform mass spectrometry. *Anal. Chem.* **2001,** 73, 2998-3005.

46. Hogan, J. M.; Pitteri, S. J.; Chrisman, P. A.; McLuckey, S. A., Complementary structural information from a tryptic N-linked glycopeptide via electron transfer ion/ion reactions and collision-induced dissociation. *J. Proteome Res.* **2005,** 4, 628-632.
47. Mirgorodskaya, E.; Roepstorff, P.; Zubarev, R. A., Localization of O-glycosylation sites in peptides by electron capture dissociation in a fourier transform mass spectrometer. *Anal. Chem.* **1999,** 71, 4431-4436.
48. Kelleher, R. L.; Zubarev, R. A.; Bush, K.; Furie, B.; Furie, B. C.; McLafferty, F. W.; Walsh, C. T., Localization of labile posttranslational modifications by electron capture dissociation: The case of gamma-carboxyglutamic acid. *Anal. Chem.* **1999,** 71, 4250-4253.
49. Liu, H.; Hakansson, K., Electron capture dissociation of tyrosine O-sulfated peptides complexed with divalent metal cations. *Anal. Chem.* **2006,** 78, 7570-7576.
50. Axelsson, J.; Palmblad, M.; Hakansson, K.; Hakansson, P., Electron capture dissociation of substance P using a commercially available Fourier transform ion cyclotron resonance mass spectrometer. *Rapid Commun. Mass Spectrom.* **1999,** 13, 474-477.
51. Kruger, N. A.; Zubarev, R. A.; Carpenter, B. K.; Kelleher, N. L.; Horn, D. M.; McLafferty, F. W., Electron capture versus energetic dissociation of protein ions. *Int. J. Mass Spectrom.* **1999,** 183, 1-5.
52. Kruger, N. A.; Zubarev, R. A.; Horn, D. M.; McLafferty, F. W., Electron capture dissociation of multiply charged peptide cations. *Int. J. Mass Spectrom.* **1999,** 187, 787-793.
53. Xia, Y.; Han, H.; McLuckey, S. A., Activation of intact electron-transfer products of polypeptides and proteins in cation transmission mode ion/ion reactions. *Anal. Chem.* **2008,** 80, 1111-1117.
54. Pitteri, S. J.; Chrisman, P. A.; Hogan, J. M.; McLuckey, S. A., Electron transfer ion/ion reactions in a three-dimensional quadrupole ion trap: Reactions of doubly and triply protonated peptides with SO2 center dot. *Anal. Chem.* **2005,** 77, 1831-1839.
55. Pitteri, S. J.; Chrisman, P. A.; McLuckey, S. A., Electron-transfer ion/ion reactions of doubly protonated peptides: Effect of elevated bath gas temperature. *Anal. Chem.* **2005,** 77, 5662-5669.
56. Swaney, D. L.; McAlister, G. C.; Wirtala, M.; Schwartz, J. C.; Syka, J. E. P.; Coon, J. J., Supplemental activation method for high-efficiency electron-transfer dissociation of doubly protonated peptide precursors. *Anal. Chem.* **2007,** 79, 477-485.
57. Iavarone, A. T.; Jurchen, J. C.; Williams, E. R., Supercharged protein and peptide lone formed by electrospray ionization. *Anal. Chem.* **2001,** 73, 1455-1460.
58. Iavarone, A. T.; Williams, E. R., Supercharging in electrospray ionization: effects on signal and charge. *Int. J. Mass Spectrom.* **2002,** 219, 63-72.
59. Iavarone, A. T.; Williams, E. R., Mechanism of charging and supercharging molecules in electrospray ionization. *J. Am. Chem. Soc.* **2003,** 125, 2319-2327.

60. Perkins, D. N.; Pappin, D. J. C.; Creasy, D. M.; Cottrell, J. S., Probability-based protein identification by searching sequence databases using mass spectrometry data. *Electrophoresis* **1999,** 20, 3551-3567.
61. Good, D. M.; Wirtala, M.; McAlister, G. C.; Coon, J. J., Performance characteristics of electron transfer dissociation mass spectrometry. *Mol. Cell. Proteomics* **2007,** 6, 1942-1951.
62. Wu, S. L.; Huehmer, A. F. R.; Hao, Z. Q.; Karger, B. L., On-line LC-MS approach combining collision-induced dissociation (CID), electron-transfer dissociation (ETD), and CID of an isolated charge-reduced species for the trace-level characterization of proteins with post-translational modifications. *J. Proteome. Res.* **2007,** 6, 4230-4244.
63. Nonaka, T.; Ishikawa, H.; Tsumuraya, Y.; Hashimoto, Y.; Dohmae, N.; Takio, K., Characterization of a Thermostable Lysine-Specific Metalloendopeptidase from the Fruiting Bodies of a Basidiomycete, Grifola-Frondosa. *J. Biochem.* **1995,** 118, 1014-1020.
64. Taouatas, N.; Drugan, M. M.; Heck, A. J. R.; Mohammed, S., Straightforward ladder sequencing of peptides using a Lys-N metalloendopeptidase. *Nat. Methods* **2008,** 5, 405-407.
65. Yang, J.; Mo, J. J.; Adamson, J. T.; Hakansson, K., Characterization of oligodeoxynucleotides by electron detachment dissociation Fourier transform ion cyclotron resonance mass spectrometry. *Anal. Chem.* **2005,** 77, 1876-1882.
66. de Koning, L. J.; Nibbering, N. M. M.; van Orden, S. L.; Laukien, F. H., Mass selection of ions in a Fourier transform ion cyclotron resonance trap using correlated harmonic excitation fields (CHEF). *Int. J. Mass Spectrom.* **1997,** 165, 209-219.
67. Senko, M. W.; Canterbury, J. D.; Guan, S. H.; Marshall, A. G., A high-performance modular data system for Fourier transform ion cyclotron resonance mass spectrometry. *Rapid Commun. Mass Spectrom.* **1996,** 10, 1839-1844.
68. Ledford, E. B.; Rempel, D. L.; Gross, M. L., Space-Charge Effects in Fourier-Transform Mass-Spectrometry - Mass Calibration. *Anal. Chem.* **1984,** 56, 2744-2748.
69. Chalmers, M. J.; Hakansson, K.; Johnson, R.; Smith, R.; Shen, J. W.; Emmett, M. R.; Marshall, A. G., Protein kinase A phosphorylation characterized by tandem Fourier transform ion cyclotron resonance mass spectrometry. *Proteomics* **2004,** 4, 970-981.
70. Horn, D. M.; Ge, Y.; McLafferty, F. W., Activated ion electron capture dissociation for mass spectral sequencing of larger (42 kDa) proteins. *Anal. Chem.* **2000,** 72, 4778-4784.
71. Breuker, K.; Oh, H. B.; Horn, D. M.; Cerda, B. A.; McLafferty, F. W., Detailed unfolding and folding of gaseous ubiquitin ions characterized by electron capture dissociation. *J. Am. Chem. Soc.* **2002,** 124, 6407-6420.
72. Horn, D. M.; Breuker, K.; Frank, A. J.; McLafferty, F. W., Kinetic intermediates in the folding of gaseous protein ions characterized by electron capture dissociation mass spectrometry. *J. Am. Chem. Soc.* **2001,** 123, 9792-9799.

73. Gorshkov, M. V.; Masselon, C. D.; Nikolaev, E. N.; Udseth, H. R.; Pasa-Tolic, L.; Smith, R. D., Considerations for electron capture dissociation efficiency in FTICR mass spectrometry. *Int. J. Mass Spectrom.* **2004,** 234, 131-136.
74. McFarland, M. A.; Chalmers, M. J.; Quinn, J. P.; Hendrickson, C. L.; Marshall, A. G., Evaluation and optimization of electron capture dissociation efficiency in Fourier transform ion cyclotron resonance mass spectrometry. *J. Am. Soc. Mass Spectrom.* **2005,** 16, 1060-1066.
75. Mormann, M.; Peter-Katalinic, J., Improvement of electron capture efficiency by resonant excitation. *Rapid Commun. Mass Spectrom.* **2003,** 17, 2208-2214.
76. Chen, X. H.; Turecek, F., The arginine anomaly: Arginine radicals are poor hydrogen atom donors in electron transfer induced dissociations. *J. Am. Chem. Soc.* **2006,** 128, 12520-12530.
77. Mihalca, R.; Kleinnijenhuis, A. J.; McDonnell, L. A.; Heck, A. J. R.; Heeren, R. M. A., Electron capture dissociation at low temperatures reveals selective dissociations. *J. Am. Soc. Mass Spectrom.* **2004,** 15, 1869-1873.
78. Robinson, E. W.; Leib, R. D.; Williams, E. R., The role of conformation on electron capture dissociation of ubiquitin. *J. Am. Soc. Mass Spectrom.* **2006,** 17, 1469-1479.
79. Budnik, B. A.; Nielsen, M. L.; Olsen, J. V.; Haselmann, K. F.; Horth, P.; Haehnel, W.; Zubarev, R. A., Can relative cleavage frequencies in peptides provide additional sequence information? *Int. J. Mass Spectrom.* **2002,** 219, 283-294.
80. Savitski, M. M.; Kjeldsen, F.; Nielsen, M. L.; Zubarev, R. A., Complementary sequence preferences of electron-capture dissociation and vibrational excitation in fragmentation of polypeptide polycations. *Angew. Chem. Int. Ed.* **2006,** 45, 5301-5303.
81. Breuker, K.; Oh, H. B.; Cerda, B. A.; Horn, D. M.; McLafferty, F. W., Hydrogen atom loss in electron-capture dissociation: a Fourier transform-ion cyclotron resonance study with single isotopomeric ubiquitin ions. *Eur. J. Mass Spectrom.* **2002,** 8, 177-180.

Chapter 5

Electron Induced Dissociation of Singly Deprotonated Peptides

5.1. Introduction

The dissociation of peptides in tandem mass spectrometry (MS/MS) is a widely used technique for obtaining sequence information, with the vast majority of tandem mass spectrometric techniques utilizing positive ion mode and frequently relying on fragmentation of doubly protonated species generated by electrospray ionization (ESI).[1] Biomolecules can also be introduced into the gas phase by matrix-assisted laser desorption/ionization (MALDI),[2, 3] which is more tolerant to salts and impurities, and shows less ion suppression compared to ESI. However, because MALDI produces predominantly singly charged ions, generation of informative tandem mass spectra is more challenging compared to the dissociation of multiply charged precursor ions.[4-9] Specifically, low-energy collision induced dissociation (CID) MS/MS of singly protonated peptides containing lysine and arginine often results in highly selective bond cleavages and poor sequence coverage,[10-13] due to the absence of a mobile proton that can promote backbone bond cleavages.[10-12, 14]

To overcome this limitation, Lebrilla and co-workers employed a combination of infrared and collisional activation (CIRCA) to access higher energy fragmentation pathways.[11, 12] These authors demonstrated that, for singly protonated model and tryptic peptides, CIRCA provided greater sequence coverage and higher quality spectra compared to CID or infrared multiphoton dissociation (IRMPD) alone. In a different approach, Reilly and co-workers have shown that 157 nm photodissociation of singly protonated peptides produces informative spectra from which structural information can be obtained.[15-17] The fragmentation pathways observed in 157 nm photodissociation are different compared to those observed in vibrational excitation of precursor ions: *x*-, *v*-, and *w*- type product ions were observed when the charge was localized at the C-terminus whereas *a*- and *d*- type product ions were detected when the charge was localized at the N-terminus.[15] Photodissociation at 193 nm has also been exploited for fragmentation of singly protonated peptides.[18-22] Similar to 157 nm dissociation, formation of *a*- and *d*- type product ions was observed when arginine residues were in close proximity to the N-terminus and *y*-, *x*-, *v*- and *w*- type fragments were detected when Arg residues were located near the C-terminus.[20, 21] 193 nm photodissociation has been reported for singly protonated ubiquitin (m/z 8561), however, product ion yields are small above m/z 4000.[20] Detailed investigations of 193 nm photodissociation revealed that the fragmentation behavior is significantly affected by the presence and location of arginine residues,[19] and that product ion types and abundances vary depending on precursor ion charge location.[23] Photodissociation at 157 and 193 nm have been directly compared for several peptides in tandem time-of-flight (TOF/TOF) and linear ion trap mass spectrometers and it was shown that product ion distributions can be influenced by both the activating wavelength

and the type of mass analyzer: in a TOF/TOF instrument, different photodissociation spectra were obtained at 157 and 193 nm whereas, in an ion trap, similar spectra were observed at the two wavelengths.[24]

All the aforementioned work focuses on fragmentation of singly protonated peptides, i.e., positive ion mode MS/MS. However, utilization of negative ion mode is often desired, given that ~50% of naturally occurring proteins are acidic. Peptides containing numerous acidic residues (e.g., glutamic and aspartic acid) may be challenging to detect in positive ion mode.[25-27] On the other hand, it has been shown that highly basic peptides can easily form singly deprotonated ions with sufficient intensities.[28] Furthermore, negative ion mode provides enhanced sensitivity for peptides containing acidic post-translational modifications such as sulfation[29] and phosphorylation.[30]

Cassady and co-workers have examined the dissociation of singly charged basic and acidic peptides in positive and negative ion mode post source decay (PSD) and showed that negative ion PSD results in structurally informative spectra, complementary to those obtained in positive ion mode.[25, 28, 31] The main product ion types in negative ion mode PSD correspond to *y*-, *b*-, and *c*-type ions. Bowie and co-workers have extensively examined the dissociation of singly deprotonated peptides in negative ion mode CID and demonstrated that sequence information can be derived.[32-36] For example, comparison of positive and negative ion mode CID of singly charged bioactive peptides containing 4 to 5 amino acids showed that negative ion spectra were as informative, or at least complementary to the positive ion spectra.[35] Harrison has shown that low-energy CID of singly deprotonated peptides resulted in sufficient fragmentation to establish the amino acid sequence of di- to pentapeptides containing H or alkyl side chains and he concluded

that negative ion mode CID provided as much information as positive ion mode CID of protonated peptides.[37] However, one drawback of negative ion mode peptide PSD and CID is extensive neutral and side chain loss, and the formation of internal product ions. Neutral losses do not provide sequence information and the diverse fragmentation processes yield complex spectra, thereby reducing MS/MS sensitivity and rendering spectral interpretation more difficult.

Electron capture dissociation (ECD)[38] and electron transfer dissociation (ETD),[39] have been shown to be complementary and result in more extensive fragmentation compared to slow heating techniques such as CID.[40-42] However, ECD and ETD are only applicable to positively charged precursor ions carrying at least two charges. Electron detachment dissociation (EDD)[43, 44] involves dissociation of multiply charged anions and results in the formation of *a*- and *x*- type product ions. A major advantage of EDD compared to slow heating techniques is the retention of phosphorylation[45] and sulfation.[43] Similar fragmentation pathways, i.e., formation of *a*- and *x*- type product ions, was observed in negative electron transfer dissociation (NETD), although phosphate loss was prevalent in that approach.[46] EDD and NETD spectra are less complex compared to those obtained from PSD and CID because neutral and side chain losses are significantly less prevalent. However, both EDD and NETD require at least doubly negatively charged precursor ions, limiting their applicability for singly charged peptides.

Ion-electron reactions of singly charged cations were first examined for small organic molecules.[47-49] For such cationic species, interaction with electrons in the energy range 2-70 eV, produced by a continuous electron beam, resulted in excitation followed by fragmentation similar to that obtained in CID. This technique was originally termed

electron impact excitation of ions from organics (EIEIO)[48, 49] and later termed electron induced dissociation (EID),[47] which is the term we will use here. McLafferty and co-workers performed 70 eV EID of sodium cationized, $[M + Na]^+$, precursor ions from the cyclic peptide gramicidin S.[50] Similar to the case of small organic molecules, the fragmentation observed in EID was similar to that in CID.

More recently, O'Hair and co-workers explored EID of singly protonated aromatic amino acids, cystine, and small peptides. These authors showed that EID yielded different and complementary fragmentation compared to CID and suggested that ion activation in EID proceeds via both electronic and vibrational excitation.[51] The same group also examined the fragmentation of singly protonated and sodiated betaine dimers in EID and reported that betaine loss was the dominant fragmentation pathway for both the protonated and sodiated species.[52] Zubarev and co-workers performed EID of protonated and sodiated oligosaccharides and showed that full sequence coverage could be obtained, similar to CID of the same species and to ECD of the corresponding doubly protonated species.[53] EID of singly charged anions has, to our knowledge, not been explored until quite recently. Yoo and Hakansson applied negative ion mode EID to phosphate-containing metabolites and showed that EID results in complementary fragmentation compared to CID and IRMPD.[54] In addition, EID was recently applied to singly charged anions from sulfated glycosaminoglycans.[55] It was shown that EID resulted in fragmentation similar to that observed in EDD, but different from that observed in CID and IRMPD of the same molecule. Both odd and even electron product ions were observed in EID.[55]

Here, we examine the applicability of EID for the dissociation and characterization of singly deprotonated peptides and compare the fragmentation patterns to those observed in negative ion mode CID. These experiments aimed to examine the fragmentation pathways in EID of model peptides and also to address whether EID provides complementary information compared to CID.

5.2. Experimental Procedures

5.2.1. Sample Preparation

The peptides H-RPKPQQFFGLM-NH_2, H-RPKPQQFFGLM-OH, CH_3CO-RRA(pS)VA-OH (phosphorylated at serine), H-WHWLQL-OH, pEHWSYGLRPG-NH_2, pEHWSYGLRPG-OH, H-PPGFSPFR-OH, pEQWFWWM-NH_2, pEVNFSPGWGT-NH2, and H-GNLWATGHFM-NH_2 were purchased from Sigma (St. Louis, MO) and the peptides H-DY*MGWMDF-NH_2 (sulfated at tyrosine) and H-DYMGWMDF-NH_2 were obtained from Advanced Chemtech (Louisville, KY) and used without further purification. Peptide H-WHWLQL-OH was diluted to a final concentration of 1 μM, peptide CH_3CO-RRA(pS)VA-OH was diluted to a final concentration of 1.7 μM, and peptide H-PPGFSPFR-OH was diluted to a final concentration of 3 μM. The other peptides were diluted to a final concentration of 5 μM. All peptides, except H-WHWLQL-OH, were electrosprayed from a spraying solvent containing 1:1 isopropanol:water (Fischer Scientific, Fair Lawn, NJ) and 10 mM ammonium acetate (Fischer Scientific). For the peptide H-WHWLQL-OH, 0.4% piperidine (Acros Organics, Morris Plains, NJ) was used instead of 10 mM ammonium acetate.

5.2.2. Mass Spectrometry

All experiments were performed with an actively shielded 7 T quadrupole Fourier transform ion cyclotron resonance (Q-FT-ICR) mass spectrometer (Apex-Q, Bruker Daltonics, Billerica, MA) which has been previously described.[56] The peptides were electrosprayed in negative ion mode at a flow rate of 70 μl/hr. Ions were accumulated in the first hexapole for 0.1 s, transferred through the mass selective quadrupole (10 m/z isolation window), mass selectively accumulated in the second hexapole for 0.1 to 3 s to optimize ion abundances for MS/MS experiments, transferred through high-voltage ion optics, and captured in the ICR cell[57] by dynamic trapping. This accumulation sequence was looped twice. EID was performed with an indirectly heated hollow dispenser cathode at a bias voltage of 10-12 V and an irradiation time of 5, 8, or 10 s. A lens electrode located in front of the hollow cathode was kept 0.3-1.0 V lower than the cathode bias voltage. CID was performed in the hexapole collision cell with argon as collision gas.

All spectra were acquired with XMASS (version 6.1, Bruker Daltonics) using 256 or 512 K data points and summed over 32 (for CID experiments) or 64 (for EID experiments) scans. Data processing was performed with the MIDAS[58] analysis software. Internal frequency-to-mass calibration was performed by Microsoft Excel with a two term calibration equation.[59] The calculated masses of the precursor ions and abundant product ions were used for calibration. Product ions used for calibration are indicated in Tables 5.1 to 5.24. Product ion spectra were interpreted using the MS Product function (http://prospector.ucsf.edu/prospector/4.0.8/html/msprod.htm) in Protein Prospector. Only peak assignments with a mass accuracy better than 15 ppm were accepted.

5.3. Results and Discussion

5.3.1. EID and CID of Singly Deprotonated Amidated and Free Acid Forms of Substance P

EID of singly deprotonated substance P, H-RPKPQQFFGLM-NH_2, is shown in Figure 5.1A. CID of the same species was performed for comparison (Figure 5.1B). All assigned product ions are summarized in Tables 5.1 and 5.2. EID of the substance P anion resulted in the formation of several *b*- and *y*- type product ions, which dominate in slow heating techniques such as CID and IRMPD. However, for this peptide several odd electron species, $z_7^{\bullet}$, $z_9^{\bullet}$, $a_9^{\bullet}$, and $a_{10}^{\bullet}$, were also detected. The a_8 product ion was a mixture of odd and even electron species (see inset, Figure 1A). These radical ions were unique to EID (absent following CID). In EID, the *y*-type product ions corresponding to cleavages on the N-terminal side of proline were observed as y_8 and [y_8 - 2H] and y_{10} and [y_{10} - 2H]. These hydrogen deficient species were not observed in CID. Side chain losses from phenylalanine ($PhCH_2$, 91.055 Da) and methionine (CH_2CH_2SMe, 75.027 Da) were only detected following EID. Such side chain losses have been previously reported in CID of singly deprotonated dipeptides formed by fast atom bombardment (FAB),[60, 61] however they were absent in our low energy CID of substance P-NH_2 (Fig. 1B). CID of C-terminally amidated substance P resulted in the formation of mainly *b*- and *y*-type product ions although some *c*-type products, c_7, c_8, and c_9, were also detected. In EID, only the c_9 product ion was observed. Formation of *c*-type product ions is generally observed in negative ion mode CID.[27, 37, 62] Some *y*- and *b*- type ions, y_4, b_4, and b_7, observed in CID were absent in EID. Interestingly, several CID product ions could not be identified based on known fragmentation pathways (*a*-, *b*-, *c*-, *x*-, *y*-, and *z*-type product ions, NH_3 and H_2O losses from precursor and product ions, and amino acid

side chain losses from precursor and product ions). In contrast, EID resulted in less complex spectra in which all product ions were identified.

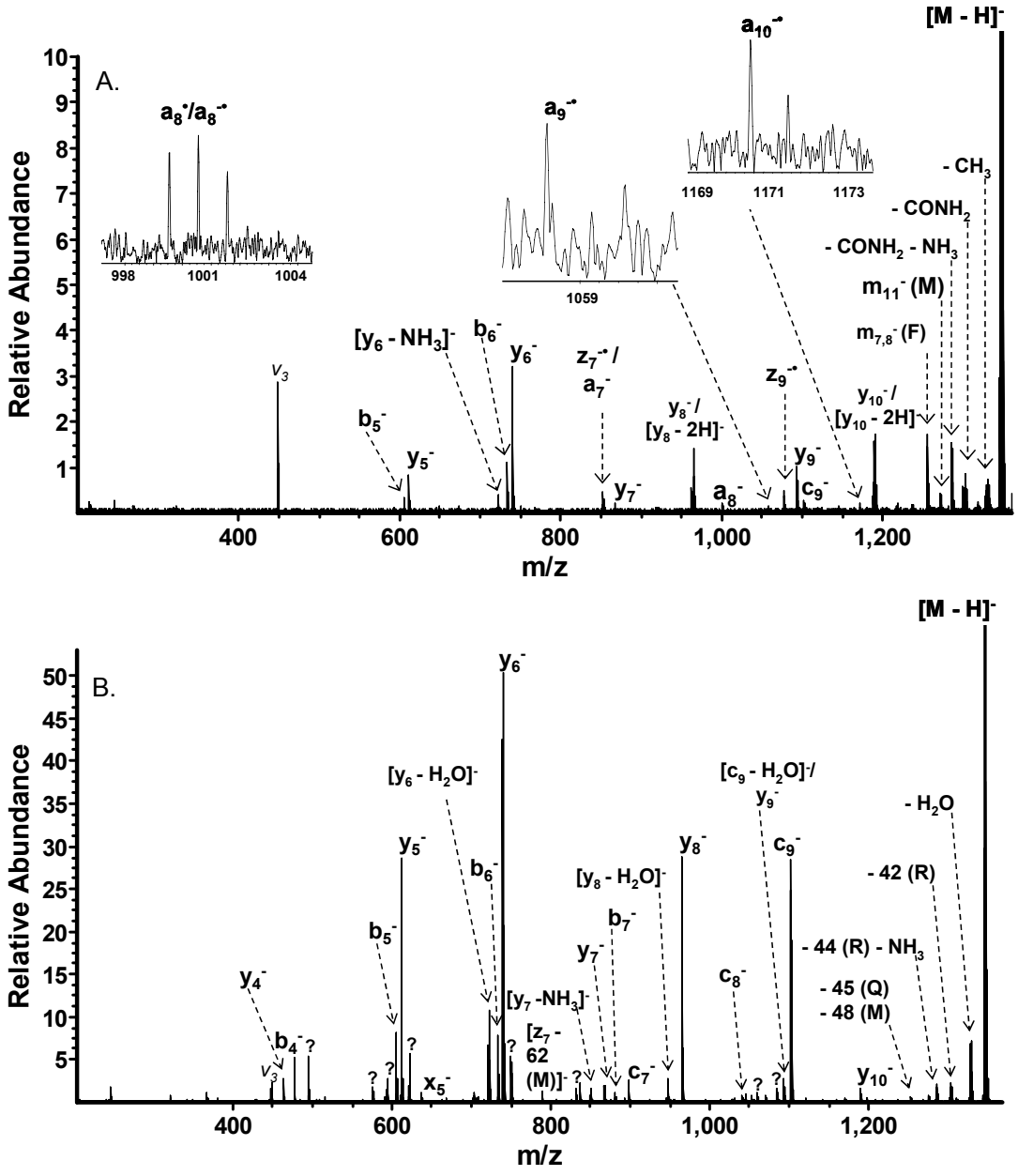

Figure 5.1. EID (A) and CID (B) spectra of the singly deprotonated amidated form of substance P (H-RPKPQQFFGLM-NH_2). Following both electron irradiation and collisional activation, *b*- and *y*- type product ions are observed. However, in EID, several radical species are detected. By contrast, no odd electron species are formed in CID. Characteristic side chain losses from phenylalanine and methionine are detected in EID. Several product ions in the CID spectrum could not be assigned based on known fragmentation pathways. $^{?}$ = unidentified product ions, v_3 = 3rd harmonic.

Table 5.1. Product ions observed following EID of singly deprotonated substance P-NH_2

Observed m/z	Theoretical m/z	Assignment	Error (ppm)
	1345.7208	$[M - H]^-$	Calibrant
1270.7014	1270.6940	m_{11}^- (M)	-5.8
1254.666	1254.666	$m_{7,8}^-$ (F)	0.3
1189.618	1189.620	y_{10}^-	1.2
1187.605	1187.604	$[y_{10} - 2H]^-$	-1.0
1170.666	1170.667	$a_{10}^{-\bullet}$	0.4
1101.595	1101.596	c_9^-	1.3
1092.566	1092.567	y_9^-	0.9
1076.549	1076.548	$z_9^{-\bullet}$	-0.5
1057.579	1057.582	$a_9^{-\bullet}$	3.5
1000.552	1000.561	$a_8^{-\bullet}$	8.8
999.5560	999.5538	a_8^-	-2.2
964.4713	964.4720	y_8^-	0.7
962.4563	962.4564	$[y_8 - 2H]^-$	0.1
867.4200	867.4192	y_7^-	-0.9
852.4844	852.4854	a_7^-	1.2
851.3997	851.4005	$z_7^{-\bullet}$	1.0
739.3601	739.3606	y_6^-	0.7
733.4117	733.4114	b_6^-	-0.4
722.3333	722.3341	$[y_6 - NH_3]^-$	1.1
	611.3021	y_5^-	Calibrant
605.3524	605.3529	b_5^-	0.9

Table 5.2. Product ions observed following CID of singly deprotonated substance P-NH_2

Observed m/z	Theoretical m/z	Assignment	Error (ppm)
	1345.721	$[M - H]^-$	Calibrant
1327.695	1327.710	$[M - H_2O]^-$	11
1303.705	1303.699	$[M - 42 (R)]^-$	-4.6
1284.665	1284.657	$[M - 44 (R) - NH_3]^-$	-6.0
1252.691	1252.696	$[M - 45 (Q) - 48 (M)]^-$	3.9
1189.627	1189.620	y_{10}^-	-6.6
1101.600	1101.596	c_9^-	-3.7
1092.568	1092.567	y_9^-	-1.5
1083.590	1083.586	$[c_9 - H_2O]^-$	-3.6
1044.584	1044.575	c_8^-	-8.7
1030.563	1030.548	$[y_9 - 62 (M)]^-$	-15
	964.4720	y_8^-	Calibrant
946.4604	946.4614	$[y_8 - H_2O]^-$	1.0
897.5088	897.5064	c_7^-	-2.6
880.4849	880.4798	b_7^-	-5.8
867.4225	867.4192	y_7^-	-3.8
850.3952	850.3927	$[y_7 - NH_3]^-$	-2.9
789.3767	789.3815	$[z_7 - 62 (M)]^-$	6.0
739.3610	739.3606	y_6^-	-0.5
733.4119	733.4114	b_6^-	-0.7
722.3354	722.3341	$[y_6 - NH_3]^-$	-0.1
637.2830	637.2813	x_5^-	-2.6
611.3017	611.3021	y_5^-	0.7
605.3524	605.3529	b_5^-	0.9
477.2923	477.2943	b_4^-	4.3
464.2317	464.2338	y_4^-	4.6

EID and CID of the singly deprotonated free acid form of substance P, H-RPKPQQFFGLM-OH, are displayed in Figures 5.2A and 5.2B (complete lists of all assigned product ions are shown in Tables 5.3 and 5.4). Similar to EID and CID of the singly deprotonated amidated form, extensive *b*- and *y*- type product ions are formed. For this peptide, only one radical species, $z_9^{\bullet}$, was detected in EID. Some *a*-type product ions, a_8, a_9, a_{10}, are also observed, however they are even electron species whereas, in

EID of amidated substance P, the *a*-type products were detected as odd electron species. The product ions $z_9^{\bullet}$, a_8, a_9, and a_{10} were absent in the CID spectrum. Also, the product ions x_4, x_5, and y_3 were present only in the EID spectrum. Side chain losses from methionine (MeSMe, 62.019 Da), phenylalanine (91.055 Da), arginine ($CH_2CH_2CH_2NHC(NH)NH_2$, (100. 087 Da), leucine ($CH_2CH(CH_3)CH_3$, 57.070 Da), and glutamine ($CH_2CH_2CNH_2$, 72.045 Da) were observed in EID, but were absent in CID. As observed for the amidated form of substance P, *y*-type product ions, y_8 and y_{10}, corresponding to cleavage at the N-terminal side of proline were detected as both y_n and [y_n - 2H]-type species. These hydrogen deficient species were not observed following CID. The c_5, c_6, c_8, and b_8 product ions were only detected following CID. For both the amidated and free acid form of substance P, several product ions were unique in the EID or CID spectra, respectively, suggesting that EID and CID can provide complementary structural information.

The differences observed between the EID spectra of the amidated and free acid singly deprotonated forms of substance P, and also between the CID spectra of these two singly deprotonated forms, suggest that charge location can affect fragmentation patterns in both EID and CID. For example, side chains losses from arginine (100. 087 Da), leucine (57.070 Da), glutamine, and methionine (62.019 Da), and *x*-type product ions were only detected in EID of the free acid form. Also, the y_3 and y_4 product ions were only present in EID of the free acid form whereas the b_6, a_7, and c_9 product ions were only detected for the amidated form. Several product ions in the EID spectrum of the free acid form could not be assigned based on know fragmentation pathways (as defined above) whereas, in EID of the amidated form, all product ions were assigned.

Differences in fragmentation patterns between the amidated and free acid form of substance P were also reported by Tsybin et al. in ECD spectra of doubly protonated species: ECD of the free acid form resulted in formation of several *a*-type product ions, not detected following ECD of the amidated form.[63] These authors suggested that charge location affects the ECD outcome.[63] Differences observed in negative ion mode CID (Figs. 1B and 2B) of the two forms of substance P include the product ions b_4, b_7, c_7, z_7, x_5, and c_9, only detected for the amidated form whereas the product ions c_5, c_6, c_8, and b_8 were present only in CID of the free acid form. Furthermore, the free acid form produced a less complex spectrum compared to that of the amidated form. For the free acid form, the C-terminal carboxylic acid is likely the deprotonation site whereas, for the amidated form, the charge location is less predictable because no acidic groups are present. It has been suggested that backbone amide hydrogens are the next most acidic hydrogens after the hydrogen atoms of carboxylate groups.[44] Therefore, for the amidated form of substance P, possible deprotonation sites include any of the backbone amide hydrogens. Regardless of the exact position of the deprotonation site, it appears that charge location influences the fragmentation outcome in both EID and CID of singly deprotonated species.

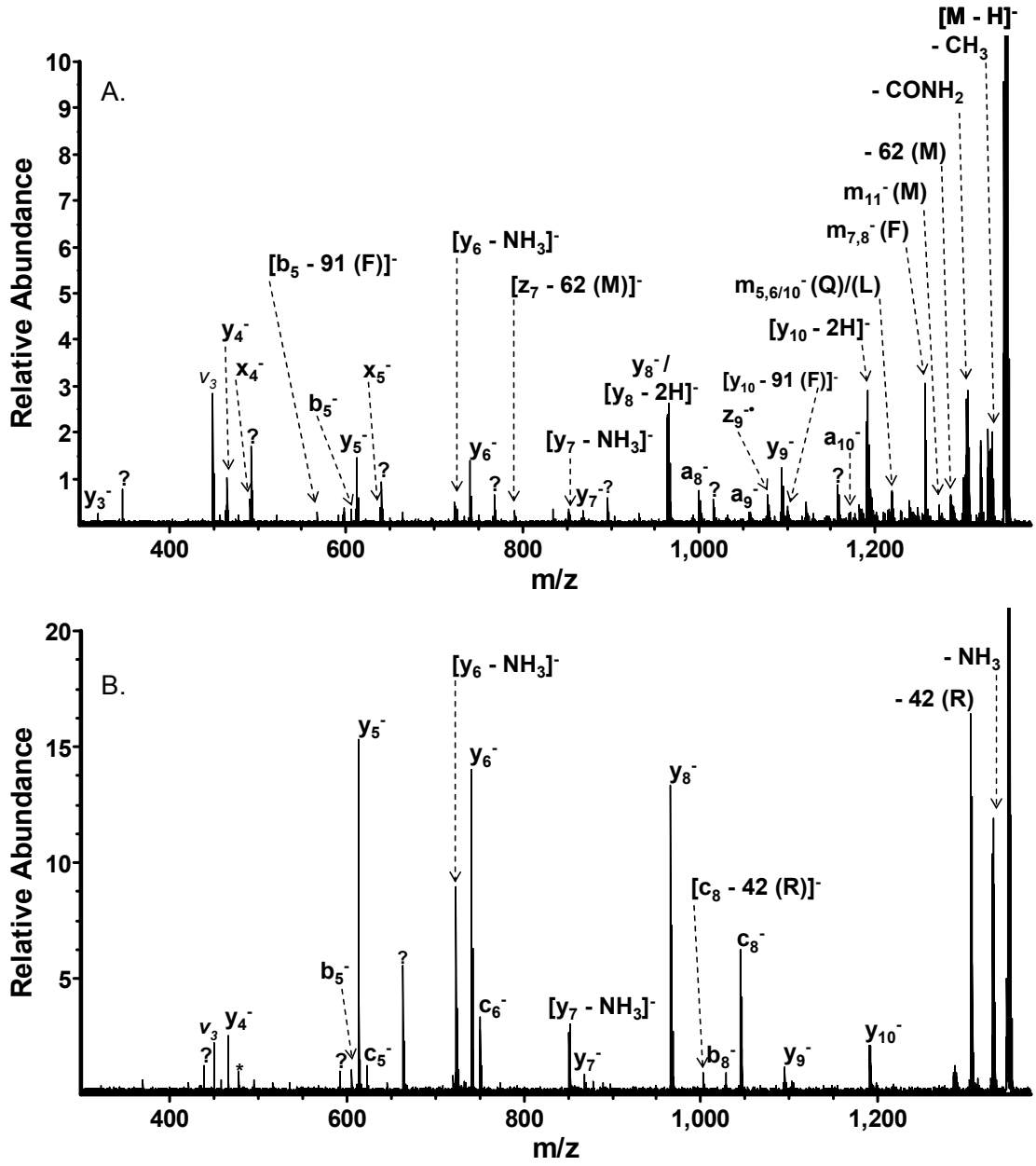

Figure 5.2. EID (A) and CID (B) spectra of the singly deprotonated free acid form of substance P (H-RPKPQQFFGLM-OH). EID resulted in more extensive fragmentation compared to CID. *a*- and *x*-type product ions were solely formed in EID. Characteristic side chain losses from the precursor and product ions are dominant in EID. Some product ions formed in EID could not be assigned based on known fragmentation pathways. Only the major peaks are labeled in the Figure, complete lists of all observed product ions are given in Tables 5.3 and 5.4. $^{?}$ = unidentified product ions, * = noise peak.

Table 5.3. Product ions observed following EID of singly deprotonated Substance P-OH

Observed m/z	Theoretical m/z	Assignment	Error (ppm)
	1346.706	$[M - H]^-$	Calibrant
1331.680	1331.682	$[M - CH_3]^-$	1.3
1318.707	1318.710	$[M - 28 (CO)]^-$	2.1
1302.670	1302.691	$[M - 44 (CONH_2)]^-$	-6.4
1284.680	1284.686	$[M - 62 (M)]^-$	4.4
1271.677	1271.678	m_{11}^- (M)	1.3
1255.648	1255.650	$m_{7,8}^-$(F)	2.0
1246.625	1246.617	m_1^- (R)	-6.3
1237.640	1237.639	$[m_{7,8} - H_2O]^-$	-0.2
1227.630	1227.615	$[m_{10}$ (L) - 62 (M)$]^-$	-12
1217.590	1217.589	$m_{5,6/10}^-$ (Q)/(L)	-0.6
1190.602	1190.604	y_{10}^-	1.0
1188.588	1188.588	$[y_{10} - 2H]^-$	0.5
1181.635	1181.631	$m_{7,8/11}^-$ (F)/(M)	-3.7
1169.669	1169.659	a_{10}^-	-8.5
1099.545	1099.548	$[y_{10} - 91 (F)]^-$	3.8
1093.554	1093.551	y_9^-	-3.0
1077.532	1077.532	$z_9^{-\bullet}$	-0.1
1056.585	1056.575	a_9^-	-9.7
999.5511	999.5533	a_8^-	2.3
	965.4560	y_8^-	Calibrant
963.4445	963.4404	$[y_8 - 2H]^-$	-4.2
868.4052	868.4032	y_7^-	-2.3
851.3821	851.3767	$[y_7 - NH_3]^-$	-6.3
791.3736	791.3734	$[z_7 - 62 (M)]^-$	-0.2
740.3481	740.3547	y_6^-	8.9
723.3209	723.3181	$[y_6 - NH_3]^-$	-3.9
638.2664	638.2653	x_5^-	-1.7
612.2903	612.2861	y_5^-	-6.9
605.3532	605.3529	b_5^-	-0.5
595.2650	595.2596	$[y_5 - 2NH_3]^-$	-9.0
521.2334	521.2308	$[y_5 - 91 (F)]^-$	-5.0
491.1997	491.1969	x_4^-	-5.8
465.2212	465.2177	y_4^-	-7.5
318.1533	318.1493	y_3^-	-13

Table 5.4. Product ions observed following CID of singly deprotonated Substance P-OH

Observed m/z	Theoretical m/z	Assignment	Error (ppm)
	1346.705	$[M - H]^-$	Calibrant
1329.677	1329.678	$[M - NH_3]^-$	1.1
1304.685	1304.683	$[M - 42 (R)]^-$	-1.8
1190.605	1190.604	y_{10}^-	-0.9
1093.555	1093.551	y_9^-	-3.8
1044.578	1044.575	c_8^-	-3.3
1027.562	1027.548	b_8^-	-13
1002.540	1002.553	$[c_8 - 42 (R)]^-$	13
965.4573	965.4560	y_8^-	-1.4
868.4055	868.4032	y_7^-	-2.7
851.3795	851.3767	$[y_7 - NH_3]^-$	-3.3
750.4392	750.4416	c_6^-	3.2
740.3457	740.3448	y_6^-	-1.3
723.3193	723.3181	$[y_6 - NH_3]^-$	-1.7
622.3817	622.3794	c_5^-	-3.7
612.2861	612.2861	y_5^-	Calibrant
605.3512	605.3529	b_5^-	2.9
465.2166	465.2177	y_4^-	2.4

5.3.2. EID and CID of Singly Deprotonated Amidated and Free Acid Forms of LHRH

EID and CID of the singly deprotonated amidated form of luteinizing hormone releasing hormone (LHRH, pEHWSYGLRPG-NH_2) showed relatively similar fragmentation, including formation of mainly *b*- and *y*-type product ions (Tables 5.3 and 5.4). Products corresponding to loss of HCHO (30.011 Da) from the serine residue were present in both spectra, although this loss was more dominant in the CID spectrum. Characteristic side chain loss from serine- (formaldehyde, HCHO) and threonine- (acetaldehyde, CH_3CHO) containing peptides have previously been reported in negative ion mode CID.[32, 33, 64-66] Recently, Pu and Cassady extensively examined the dissociation

of singly deprotonated hexapeptides containing hydroxyl side chains in sustained off-resonance irradiation (SORI) CID and PSD[62] and, in agreement with previous reports, loss of formaldehyde was observed from serine side chains and loss of acetaldehyde was observed from threonine side chains. These authors suggested that these characteristic side chain losses are due to deprotonation of hydroxyl side chains in negative ion mode.[62]

Table 5.5. Product ions observed following EID of singly deprotonated LHRH-NH_2

Observed m/z	Theoretical m/z	Assignment	Error (ppm)
	1180.566	$[M - H]^-$	Calibrant
1162.559	1162.555	$[M - H_2O]^-$	-3.4
1150.545	1150.555	m_4^- (S)	8.6
1136.549	1136.552	$[M - 44\ (CONH_2)]^-$	2.9
1079.522	1079.531	$a_9^{-\bullet}$	8.1
1052.509	1052.507	$[y_9 - NH_3]^-$	-1.4
1050.494	1050.500	m_3^- (W)	5.6
1022.493	1022.505	$[m_3\ (W) - 28\ (CO)]^-$	12
982.4749	982.478	$a_8^{-\bullet}$	3.0
	932.4748	y_8^-	Calibrant
902.4591	902.4642	$[y_8 - 30\ (S)]^-$	5.6
711.3555	711.3583	$[y_7 - H_2O - NH_3]^-$	4.0

In CID of singly deprotonated LHRH-NH_2, product ions corresponding to multiple neutral losses are formed. For example, combined loss of the side chains of tryptophan (see discussion below) and serine from the precursor ions is observed (the corresponding product ion is indicated as $m_{3/4}$ (W)/(S)). Another example is the combined loss of HCHO from serine and NH=C=NH (42.022 Da) from arginine, a fragment absent in EID. The loss of NH=C=NH from arginine has been previously reported for dipeptides in CID of singly deprotonated peptides formed by FAB.[67] Neutral loss from tryptophan side chains was observed in both CID and EID. In CID, loss of 129 Da (C_9H_7N, 129.058 Da) was seen whereas, in EID, loss of 130 Da (C_9H_8N, 130.066 Da) was observed. In

agreement with our results, loss of 129 Da from Trp residues has been previously observed in CID of singly deprotonated peptides formed by FAB.[61] This loss was also reported in the recent EID experiments involving singly protonated amino acids.[51] In ECD, loss of 131 Da (C_9H_9N, 131.074 Da) from Trp residues has been reported[68] and we have documented loss of 129 Da from the Trp side chain in EDD.[69]

A major difference between CID and EID of singly deprotonated LHRH-NH_2 is the detection of two radical species, a_8• and a_9•, in EID, similar to EID of substance P-NH_2. These radical species are absent in CID. The [y_9 - NH_3] product ion was only detected in EID whereas the c_3 and b_8 product ions were only observed in CID. The b_8 product ion was detected as b_8 - 30 (HCHO) - 42 (NH=C=NH).

Table 5.6. Product ions observed following CID of singly deprotonated LHRH-NH_2

Observed m/z	Theoretical m/z	Assignment	Error (ppm)
	1180.566	$[M - H]^-$	Calibrant
1162.561	1162.555	$[M - H_2O]^-$	-4.9
1150.548	1150.555	m_4^- (S)	6.1
1108.534	1108.533	$[m_4$ (S) - 42 (R)$]^-$	-0.6
1021.485	1021.497	$m_{3/4}^-$ (W)/(S)	12
1004.489	1004.477	$[m_{3/4}$ (W)/(S) - $NH_3]^-$	-11
937.4301	937.4325	$[b_8$ - 42 (R) - 30 (S)$]^-$	2.6
	932.4748	y_8^-	Calibrant
914.4664	914.4642	$[y_8 - NH_3]^-$	-2.5
902.4604	902.4642	$[y_8$ - 30 (S)$]^-$	4.2
746.3936	746.3955	y_7^-	2.5
728.3806	728.3849	$[y_7 - H_2O]^-$	5.9
716.3858	716.3849	$[y_7$ - 30 (S)$]^-$	-1.2
711.3550	711.3584	$[y_7 - H_2O - NH_3]^-$	4.8
681.3486	681.3478	$[y_7 - H_2O - NH_3$ - 30 (S)$]^-$	-1.2
450.1859	450.1894	c_3^-	7.8

The free acid form of LHRH was also investigated (Tables 5.7 and 5.8). For this peptide, no odd electron products were detected in EID of the singly deprotonated

species. Some *a*-type ions, a_7 and a_8, were formed but they were detected as even electron species, similar to EID of the free acid form of substance P. These product ions were absent in CID. Also, the c_5 product ion was present only in the EID spectrum. Some *b*- and *y*-type product ions, y_8, y_5, and b_7, were only formed in CID. Similar to CID of LHRH-NH_2, the b_8 product ion was detected as b_8 - 30 (HCHO) - 42 (NH=C=NH). Loss of the entire tryptophan side chain was observed in both CID and EID, similar to the amidated form. Characteristic side chain loss from serine was also detected. For the free acid form of LHRH, loss of NH=C=NH from the side chain of arginine was observed. This loss was particularly prevalent in CID. For the amidated form of LHRH, the NH=C=NH loss was significantly less pronounced in CID and it was absent in EID. In EID of the free acid form, a loss of 59.038 Da was detected from the y_7 product ion. This loss can be attributed to the arginine side chain ($C_1H_5N_3$, 59.048 Da) and it has been previously reported in ECD.[70] Furthermore, the aforementioned side chain losses, and H_2O and NH_3 losses from both the precursor and product ions were significantly more pronounced in CID compared to EID. The observed differences between CID and EID spectra of substance P and LHRH suggest that these two fragmentation techniques proceed via different activation pathways.

Similar to EID of the amidated and free acid forms of substance P, differences are observed between the EID spectra of the amidated and free acid form of LHRH. For example, formation of odd electron species was not observed for the free acid form. Furthermore, the y_6, c_5, and a_7 product ions were only detected for the free acid form whereas the y_8 product ion was only observed for the amidated form. Similar trends were observed in CID spectra, in which some product ions were only observed for the

amidated or free acid form, respectively. Neutral losses from the precursor and product ions were more abundant in CID of the free acid form. Therefore, as discussed above, the charge location appears to influence the fragmentation outcome in both EID and CID. Differences in fragmentation behavior were also reported in ECD of the amidated and free acid forms of LHRH.[63] For example, for the free acid form, several *y*- type product ions were detected, which were not observed in ECD of the amidated form.

Table 5.7. Product ions observed following EID of singly deprotonated LHRH-OH

Observed m/z	Theoretical m/z	Assignment	Error (ppm)
	1181.550	$[M - H]^-$	Calibrant
1163.541	1163.539	$[M - H_2O]^-$	-1.4
1151.540	1151.539	m_4^- (S)	-0.9
1139.527	1139.528	$[M - 42 (R)]^-$	1.0
1051.480	1051.484	m_3^- (W)	3.8
981.4695	981.4700	a_8^-	0.5
967.4436	967.4431	$[b_8 - 42 (R)]^-$	-0.5
825.3686	825.3689	a_7^-	0.4
	747.3795	y_7^-	Calibrant
729.3699	729.3689	$[y_7 - H_2O]^-$	-1.4
712.3431	712.3424	$[y_7 - H_2O - NH_3]^-$	-0.9
700.2851	700.2848	c_5^-	-0.4
694.3326	694.3318	$[y_7 - 2H_2O - NH_3]^-$	-1.1
688.3418	688.3315	$[y_7 - 59 (R)]^-$	-15
660.3476	660.3474	y_6^-	-0.4

Table 5.8. Product ions observed following CID of singly deprotonated LHRH-OH

Observed m/z	Theoretical m/z	Assignment	Error (ppm)
	1181.550	$[M - H]^-$	Calibarnt
1164.527	1164.523	$[M - NH_3]^-$	-3.7
1151.534	1151.539	m_4^- (S)	4.5
1146.5117	1146.513	$[M - NH_3 - H_2O]-$	0.8
1139.5300	1139.528	$[M - 42 (R)]^-$	-1.8
1134.511	1134.513	$[m_4 (S) - NH_3]^-$	1.7
1109.517	1109.530	$[m_4 (S) - 42 (R)]^-$	12
967.4476	967.4431	$[b_8 - 42 (R)]^-$	-4.7
937.4308	937.4325	$[b_8 - 42 (R) - 30 (S)]^-$	1.9
933.4617	933.4588	y_8-	-3.1
915.4477	915.4482	$[y_8 - H_2O]^-$	0.6
903.4489	903.4482	$[y_8 - 30 (S)]^-$	-0.7
886.4260	886.4217	$[y_8 - 30 (S) - NH_3]^-$	-4.8
861.4242	861.4264	$[y_8 - 30 (S) - 42(R)]^-$	2.6
853.3622	853.3638	b_7^-	1.9
	747.3795	y_7^-	Calibrant
729.3687	729.3689	$[y_7 - H_2O]^-$	0.3
717.3693	717.3689	$[y_7 - 30 (S)]^-$	-0.6
712.3427	712.3424	$[y_7 - H_2O - NH_3]^-$	-0.4
694.3332	694.3318	$[y_7 - 2H_2O - NH_3]^-$	-2.1
682.3340	682.3318	$[y_7 - H_2O - NH_3 - 30 (S)]^-$	-3.2
670.3183	670.3206	$[y_7 - H_2O - NH_3 - 42 (R)]^-$	3.4
660.3484	660.3474	y_6^-	-1.5
497.2824	497.2841	y_5^-	3.5

5.3.3. EID and CID of Other C-terminally Amidated Peptides without Acidic Sites

Because C-terminally amidated substance P and LHRH (neither of which contains acidic sites) yielded more radical (unique) product ions in EID compared to their free acid forms, we proceeded to characterize EID of other C-terminally amidated peptides without acidic sites. Product ions observed in EID and CID of singly deprotonated neuromedin B, H-GNLWATGHFM-NH_2, are listed in Tables 5.9 and 5.10.

Table 5.9. Product ions observed following EID of singly deprotonated neuromedin B [a]

Observed m/z	Theoretical m/z	Assignment	Error (ppm)
	1130.521	$[M - H]^-$	Calibrant
1112.498	1112.510	$[M - H_2O]^-$	11
1086.483	1086.495	m_6^- (T)	10
1056.462	1056.473	$[y_9 - NH_3]^-$	10
1038.448	1038.461	$[y_9 - NH_3 - H_2O]^-$	13
1012.441	1012.447	$[z_9 - 45\ (T)]^-$	5.6
1012.441	1012.447	$[y_9 - NH_3 - 44\ (T)]^-$	5.5
1000.448	1000.455	m_4^- (W)	7.1
959.4596	959.4564	y_8^-	-3.4
955.4720	955.4670	$a_9^{-\bullet}$	-5.2
942.4300	942.4302	$[y_8 - NH_3]^-$	0.2
915.4279	915.4305	$[y_8 - 44\ (T)]^-$	2.8
898.4065	898.4039	$[z_8 - 45\ (T)]^-$	2.8
898.4065	898.4040	$[y_8 - NH_3 - 44\ (T)]^-$	-2.9
829.3461	829.3461	$[y_7 - NH_3]^-$	Calibrant
785.3240	785.3199	$[z_7 - 45\ (T)]^-$	-5.2
785.3240	785.3199	$[y_7 - NH_3 - 44\ (T)]^-$	-5.2
644.2783	644.2746	$z_6^{-\bullet}$	-5.7

[a]. Based on their masses, product ions at m/z = 1012.441, 898.4065, and 785.3240 can be assigned as either *y*-type product ions exhibiting NH_3 loss, and a 44 Da loss from threonine ($C_2H_4O_1$, 44.026 Da), or as z-type product ions exhibiting 45 Da loss from Thr ($C_2H_5O_1$, 45.034 Da).

The precursor ions and the majority of product ions exhibited abundant neutral loss of CH_3CHO (44.026 Da) from the threonine residue. As discussed above, this characteristic side chain cleavage has been previously reported in CID and PSD.[32, 62, 64-66] *y*-type product ions were detected in both CID and EID. In EID, product ions at m/z = 1012.441, 898.4065, and 785.3240 can be assigned as either *y*-type fragments exhibiting NH_3 loss, and a 44 Da loss from threonine ($C_2H_4O_1$, 44.026 Da), or as z-type fragments exhibiting a 45 Da loss from threonine ($C_2H_5O_1$, 45.034 Da). In CID, only the product ion at m/z = 1012.441 was detected. The y_7 product ion was observed only in EID

whereas the c_8 product ion was only present in CID. Furthermore, for this peptide, side chain loss from tryptophan was only detected in EID. By contrast, in the case of LHRH, side chain loss from tryptophan was present in both CID and EID. Two radical species, $z_6^{\bullet}$ and $a_9^{\bullet}$, were only formed in EID, although the $a_9^{\bullet}$ product ion was detected with low abundance. Similar to CID of substance P-NH_2, several product ions detected in CID of neuromedin B could not be assigned based on known fragmentation pathways.

Table 5.10. Product ions observed following CID of singly deprotonated neuromedin B [a]

Observed m/z	Theoretical m/z	Assignment	Error (ppm)
	1130.521	$[M - H]^-$	Calibrant
1112.507	1112.510	$[M - H_2O]^-$	2.7
1086.495	1086.495	m_6^- (T)	-0.7
1068.484	1068.484	$[m_6$ (T) $- H_2O]^-$	-0.2
1056.476	1056.473	$[y_9 - NH_3]^-$	-2.8
1039.448	1039.446	$[y_9 - 2NH_3]^-$	-1.3
1012.445	1012.447	$[z_9 - 45$ (T) $]^-$	2.2
1012.445	1012.447	$[y_9 - NH_3 - 44$ (T)$]^-$	2.1
959.4567	959.4567	y_8^-	Calibrant
808.3832	808.3860	$[c_8 - 44$(T)$]^-$	3.5
915.4284	915.4305	$[y_8 - 44$ (T)$]^-$	2.3

a. Based on its mass, the product ion at m/z = 1012.441 can be assigned as either a *y*-type fragment exhibiting NH_3 loss, and a 44 Da loss from threonine ($C_2H_4O_1$, 44.026 Da), or as a z-type fragment exhibiting 45 Da loss from Thr ($C_2H_5O_1$, 45.034 Da).

EID (Table 5.11) of the singly deprotonated peptide pEVNFSPGWGT-NH_2 resulted in several product ions not detected in CID (Table 5.12), including c_7, $[b_7 - H]^{\bullet}$, $[b_6 - 30]$ (serine side chain loss), a_5 and c_4. Also, the $a_9^{\bullet}$ radical species was only detected in EID. In CID, only two product ions corresponding to backbone bond cleavages were observed, y_7 and y_8. Loss of the phenylalanine side chain (91.055 Da) was observed from the y_8 product ion in both EID and CID. This loss is characteristic for

Phe-containing peptides, as previously reported for collisional activation of singly deprotonated dipeptides formed by FAB.[61]

Table 5.11. Product ions observed following EID of singly deprotonated pEVNFSPGWGT-NH_2 [a]

Observed m/z	Theoretical m/z	Assignment	Error (ppm)
	1072.486	$[M - H]^-$	Calibrant
1042.475	1042.475	m_5^- (S)	0.1
1028.463	1028.459	m_{10}^- (T)	3.8
1028.463	1028.472	$[M - 44 (CONH_2)]^-$	8.5
1024.462	1024.464	$[m_5 (S) - H_2O]^-$	1.9
1010.455	1010.449	$[m_{10} (T) - H_2O]^-$	5.7
1010.455	1010.461	$[M - 44 (CONH_2) - H_2O]^-$	6.7
998.4481	998.449	$m_{5/10}^-$ (S)/(T)	0.8
998.4481	998.460	$[m_5 (S) - 44 (CONH_2)]^-$	12
980.4379	980.4383	$[m_{5/10} (S)/(T) - H_2O]^-$	0.4
980.4379	980.4509	$[m_5 (S) - 44 (CONH_2) - H_2O]^-$	13
927.4261	927.4244	$a_9^{-\bullet}$	-1.9
815.3510	815.3481	$[y_8 - 30 (S) - NH_3]^-$	-3.6
771.3224	771.3305	$[y_8 - 91 (F)]^-$	10
753.3116	753.3199	$[y_8 - 91 (F) - H_2O]^-$	11
	728.3372	c_7^-	Calibrant
710.3055	710.3034	$[b_7 - H]^-$	-2.9
674.3060	674.3056	$[y_7 - 30 (S) - 44 (T)]^-$	-0.5
624.2787	624.2791	$[b_6 - 30 (S)]^-$	0.6
529.2423	529.2450	a_5^-	5.0
487.2318	487.2310	c_4^-	-1.6

[a] The 44 Da loss can be assigned to loss of the threonine side chain (CH_3CHO, 44.026 Da), or to loss of the amidated C-terminus ($CONH_2$, 44.014 Da).

Similar to the previously examined peptides containing Ser or Thr residues, characteristic HCHO (30.0106 Da) and CH_3CHO (44.026 Da) losses were highly abundant in CID and EID spectra of pEVNFSPGWGT-NH_2. For this peptide, the 44 Da loss could also be assigned as the loss of $CONH_2$ (44.014 Da) from the amidated C-terminus. However, the mass error was higher for this assignment and, also, because CH_3CHO loss from the Thr residue is known to be prevalent in negative ion mode

MS/MS of Thr containing peptides (as discussed above), this assignment seems more likely. Furthermore, in CID the assignment [m_5 – 44] (44.014 Da, $CONH_2$) has an error higher than 15 ppm and it was therefore excluded. The EID spectrum of pEVNFSPGWGT-NH_2 was more informative compared to CID because it contained more backbone product ions.

Table 5.12. Product ions observed following CID of singly deprotonated pEVNFSPGWGT-NH2 [a]

Observed m/z	Theoretical m/z	Assignment	Error (ppm)
	1072.486	$[M - H]^-$	Calibrant
1042.473	1042.475	m_5^- (S)	2.4
1028.461	1028.459	m_{10}^- (T)	1.6
1028.461	1028.472	$[M - 44\ (CONH_2)]^-$	11
1024.467	1024.464	$[m_5\ (S) - H_2O]^-$	-2.1
1010.448	1010.449	$[m_{10} - H_2O]^-$	0.7
1010.448	1010.461	$[M - 44\ (CONH_2) - H_2O]^-$	13
998.4464	998.4600	$[m_5\ (S) - 44\ (CONH_2)]^-$	14
980.4399	980.4509	$[m_5\ (S) - 44\ (CONH_2) - H_2O]^-$	11
	815.3482	$[y_8 - 30\ (S) - NH_3]^-$	Calibrant
771.3211	771.3305	$[y_8 - 91\ (F)]^-$	12
718.3319	718.3318	$[y_7 - 30(S)]^-$	-0.1
674.3047	674.3056	$[y_7 - 30(S) - 44\ (T)]^-$	1.4

[a] The 44 Da loss can be assigned to loss of the threonine side chain (CH_3CHO, 44.026 Da) or loss of the amidated C-terminus ($CONH_2$, 44.014 Da).

The peptide pEQWFWWM-NH_2 was the only peptide examined here for which EID (Table 5.13) resulted in less extensive fragmentation compared to CID (Table 5.14). Four product ions, y_3, [z_4 – 75], [x_5 – 62], and [z_6 – 130], detected in CID, were absent in the EID spectrum. The neutral losses of 75.027 Da and 62.013 Da correspond to losses of CH_2CH_2SMe (75.027 Da) and MeSMe (62.019 Da), respectively, from the methionine side chain. Such cleavages have been previously reported in negative ion mode FAB-CID.[60] One additional neutral loss of 45.013 Da was observed from the precursor ions in

CID. This loss, corresponding to loss of $HCONH_2$ (45.021 Da) from a glutamine residue, has previously been observed in ECD,[70] but it has not been reported in negative ion mode CID. Similar to other tryptophan-containing peptides, Trp side chain loss is present. In EID a loss of 130 Da from the precursor ions is observed, similar to the peptides LHRH and neuromedin B, whereas loss of 129 Da was observed from the c_5 product ion. The loss of 129 Da is particularly abundant from both precursor and product ions in CID. One product ion, z_6, in CID exhibited a loss of 130 Da.

Table 5.13. Product ions observed following EID of singly deprotonated pEQWFWWM-NH_2

Observed m/z	Theoretical m/z	Assignment	Error (ppm)
	1091.457	$[M - H]^-$	Calibrant
1073.448	1073.446	$[M - H_2O]^-$	-1.5
1047.436	1047.443	$[M - 44\ (CONH_2)]^-$	6.4
963.3990	963.3981	$[y_6 - NH_3]^-$	-1.0
961.3932	961.3909	$m_{3,5,6}^-$ (W)	-2.4
852.3673	852.3660	y_5^-	-1.6
835.3405	835.3395	$[y_5 - NH_3]^-$	-1.2
774.3384	774.3368	c_5^-	-2.1
692.2698	692.2660	x_4^-	-5.5
	649.2602	$[y_4 - NH_3]^-$	Calibrant
645.2791	645.2789	$[c_5 - 129\ (W)]^-$	-0.4
588.2585	588.2575	c_4^-	-1.6
441.1901	441.1891	c_3^-	-2.2

We have previously examined EDD of the doubly deprotonated peptide pEQWFWWM-NH_2.[69] EID of the $[M - H]^-$ precursor ions from this peptide (Table 5.13) showed similar fragmentation as EDD of the $[M - 2H]^{2-}$ precursor ions, however, some differences between these spectra were also observed. For example, formation of *c*- and *x*-type product ions was observed in both techniques whereas formation of *y*-type product ions was detected only in EID. Neutral loss of the tryptophan side chain and neutral loss

of the amidated C-terminus were present in both spectra, however, these losses were more predominant in EDD spectra.

Table 5.14. Product ions observed following CID of singly deprotonated pEQWFWWM-NH_2

Observed m/z	Theoretical m/z	Assignment	Error (ppm)
	1091.457	$[M - H]^-$	Calibrant
1073.454	1073.446	$[M - H_2O]^-$	-7.5
1046.443	1046.435	$[M - 45 (Q)]^-$	-8.0
962.4033	962.4041	$m_{3,5,6}^-$ (W)	1.0
944.3922	944.3881	$[M - 129 (W) - H_2O]^-$	-4.1
917.3780	917.3772	$[M - 129 (W) - 45 (Q)]^-$	-0.6
901.3876	901.3791	$[y_6 - 62 (M) - NH_3]^-$	-9.1
852.3663	852.3661	y_5^-	0.2
834.3472	834.3402	$[z_6 - 130 (W)]^-$	-7.9
816.3325	816.3263	$[x_5 - 62 (M)]^-$	-7.1
774.3377	774.3368	c_5^-	-0.7
756.3260	756.3262	$[c_5 - H_2O]^-$	0.8
723.3093	723.3082	$[y_5 - 129 (W)]^-$	-1.0
692.2654	692.2660	x_4^-	1.5
	666.2867	y_4^-	Calibrant
649.2597	649.2602	$[y_4 - NH_3]^-$	0.7
645.2789	645.2789	$[c_5 - 129 (W)]^-$	0.8
630.2507	630.2559	$[c_5 - 129 (W) - 15 (CH_3)]^-$	8.9
594.2482	594.2418	$[y_4 - 72 (Q)]^-$	-10
588.2573	588.2575	c_4^-	1.2
575.2412	575.2414	$[z_4 - 75 (M)]^-$	1.1
519.2161	519.2183	y_3^-	5.1
441.1869	441.1891	c_3^-	6.0

In our previous work,[69] we also performed EDD of the peptides pEVNFSPGWGT-NH_2 and H-GNLWATGHFM-NH_2 For these two peptides only one backbone product ion was observed and instead neutral loss corresponding to cleavage of the tryptophan side chain was dominant suggesting that the presence of Trp can direct the fragmentation in EDD. By contrast, EID and CID of the corresponding singly deprotonated species (Table 5.9 for H-GNLWATGHFM-NH_2 and Table 5.11 for the peptide

pEVNFSPGWGT-NH_2) produced more informative spectra, allowing structural information to be derived although Trp side chain loss was also present for the peptide H-GNLWATGHFM-NH_2.

5.3.4. EID and CID of Peptides with a C-terminal Carboxylic Site but No Acidic Residues

Because most natural peptides are not C-terminally amidated, we proceeded to characterize the EID behavior of peptides with a carboxylate C-terminus but no other acidic sites. EID and CID spectra of singly deprotonated bradykinin, H-PPGFSPFR-OH, are shown in Figures 5.3A and 5.3B, respectively. Complete lists of observed product ions are included in Tables 5.15 and 5.16. The observed fragmentation behavior for singly deprotonated bradykinin was similar to that of the peptide pEVNFSPGWGT-NH_2 (see previous section), for which EID resulted in more extensive fragmentation compared to CID. Several product ions from backbone bond cleavage, including y_2, x_2, y_3, y_4, b_4, [z_4 – 30], $z_6^{\bullet}$, [c_6 – 30], [y_6 – 30], [y_7 – H]$^{\bullet}$, [c_7 – 30], and a_7, were detected in EID but absent in CID. Therefore, for bradykinin, EID was more informative than CID. CID resulted in the formation of only two backbone product ions, b_7 and [y_6 – 30], which were also formed in EID. The y_3 product ion, corresponding to cleavage on the N-terminal side of proline was detected as both y_3 and [y_3 - 2H]. The same trend was observed in EID of substance P, for which *y*- type product ions corresponding to cleavages on the N-terminal side of proline showed a mixture of y_n and [y_n - 2H] species. In EID, side chain losses from phenylalanine (91.055 Da) and arginine (100.087 Da) were observed. These side chain losses were absent in CID although Phe side chain loss was observed in CID of the peptide pEVNFSPGWGT-NH_2 discussed above and, as mentioned above, such losses have been previously reported in FAB-CID of singly deprotonated dipeptides.[61] Similar

to the peptides pEVNFSPGWGT-NH_2, LHRH-NH_2, and LHRH-OH, neutral loss of HCHO was observed in EID and CID of bradykinin. Neutral loss of NH=C=NH (42 Da) from arginine is also present in both spectra, although this loss is more dominant in CID.

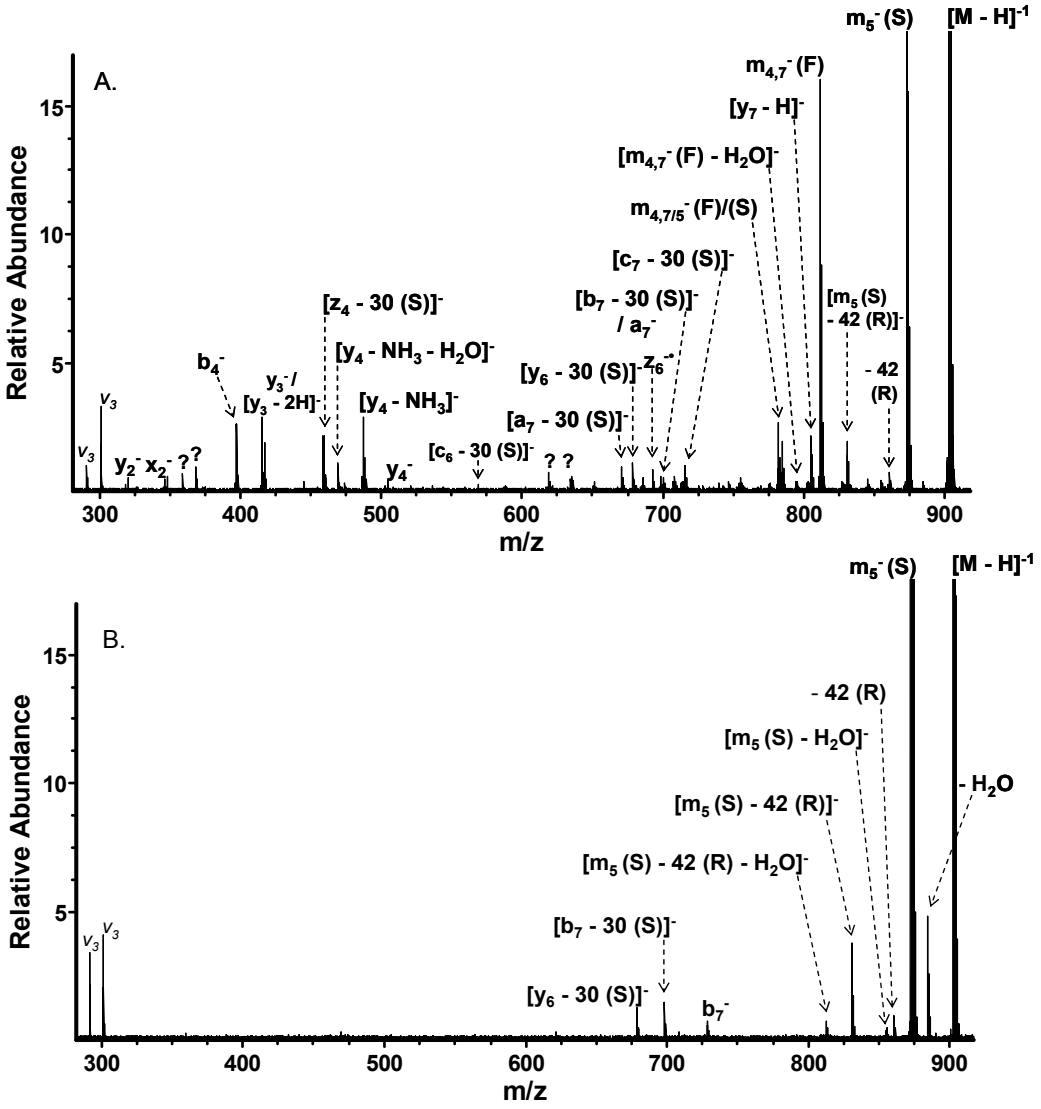

Figure 5.3. EID (A) and CID (B) spectra of singly deprotonated bradykinin (H-PPGFSPFR-OH). EID resulted in a highly informative spectrum: a series of *b*- and *y*-type product ions is observed, and *a*-, *x*-, and *z*- type product ions are also detected, resulting in highly extensive fragmentation. Product ions corresponding to loss of serine and phenylalanine side chains are also present. In CID, few sequence specific product ions were formed. Instead, side chain and small molecule neutral losses are mainly observed. Only the major peaks are labeled in the Figure, complete lists of all observed product ions are given in Tables 5.15 and 5.16. $^?$ = unidentified product ions, v_3 = 3rd harmonic.

Table 5.15. Product ions observed following EID of singly deprotonated bradykinin

Observed m/z	Theoretical m/z	Assignment	Error (ppm)
	902.4530	$[M - H]^-$	Calibrant
884.4466	884.4424	$[M - H_2O]^-$	-4.8
872.4424	872.4424	m_5^- (S)	0.0
860.4309	860.4312	[M - 42 (R)]$^-$	0.3
854.4410	854.4318	$[m_5^-$ (S) - $H_2O]$-	-11
844.4505	844.4475	$[m_5$ (S)- 28 (CO)]$^-$	-3.6
830.4212	830.4206	$[m_5$ - 42 (R)]$^-$	-0.7
826.4379	826.4369	$[m_5$ - 28 (CO) - $H_2O]^-$	-1.2
811.3993	811.3982	$m_{4,7}^-$ (F)	-1.4
804.3933	804.3907	$[y_7 - H]^-$	-3.3
802.3595	802.3655	m_8^- (R)	7.5
794.3751	794.3717	$[m_{4,7}$ (F) - $H_2O]^-$	-4.3
781.3899	781.3876	$m_{4,7/5}^-$ (F)/(S)	-3.0
774.3792	774.3824	$[y_7$- 30 (S) - H]$^-$	4.1
746.3510	746.3519	$[y_7$ - 42 - $NH_3]^-$	1.1
728.3439	728.3413	b_7^-	-3.6
715.3543	715.3572	$[c_7$ - 30 (s)]$^-$	4.0
698.3317	698.3307	$[b_7$ - 30 (S)]$^-$	-1.5
700.3468	700.3464	a_7^-	-0.5
692.3296	692.3287	z_6^-	-1.3
678.3390	678.3368	$[y_6$ - 30 (S)]$^-$	-3.2
670.3364	670.3358	$[a_7$ - 30 (S)]$^-$	-0.9
587.2801	587.2860	$[z_5$ - NH_3 - $H_2O]^-$	10
568.2939	568.2888	$[c_6$ - 30 (S)]$^-$	-9.0
504.2522	504.2576	y_4^-	11
487.2309	487.2310	$[y_4$ - $NH_3]^-$	0.1
469.2203	469.2205	$[y_4$ - NH_3 - $H_2O]^-$	0.5
458.2282	458.2282	$[z_4$ - 30 (S)]$^-$	-0.1
	417.2255	y_3^-	Calibrant
415.2095	415.2099	$[y_3$ - 2H]$^-$	1.0
397.1840	397.1881	b_4^-	10
346.1503	346.1520	x_2^-	4.8
320.1726	320.1728	y_2^-	0.6

Table 5.16. Product ions observed following CID of singly deprotonated bradykinin

Observed m/z	Theoretical m/z	Assignment	Error (ppm)
	902.4530	$[M - H]^-$	Calibrant
884.4421	884.4424	$[M - H_2O]^-$	0.4
872.4410	872.4424	m_5^- (S)	1.6
860.4309	860.4312	[M - 42 (R)]$^-$	0.3
854.4361	854.4318	$[m_5 - H_2O]^-$	-5.0
830.4216	830.4206	$[m_5$ - 42 (R)]$^-$	-1.2
812.4078	812.4100	$[m_5$ - 42(R) - $H_2O]$	2.7
728.3358	728.3413	b_7^-	7.5
698.3310	698.3307	$[b_7$ - 30 (S)]$^-$	-0.4
	678.3368	[y6 - 30 (S)]$^-$	Calibrant

EID (Figure 5.4A and Table 5.17) of the peptide H-WHWLQL-OH showed similar fragmentation to that observed in CID (Figure 5.4B and Table 5.18), including formation of *c*-, *y*- and *b*-type product ions. However, some product ions detected in EID were not observed in CID. These include mainly even electron species; y_2, b_2, [b_3 – 129], [z_5 – 129], and a_5. Two odd electron species, $z_3^{\bullet}$ and $z_5^{\bullet}$, are also unique to EID. On the other hand, the product ions a_3, a_4, and y_5, are unique to CID. Therefore, EID and CID provide complementary structural information. Similar to other tryptophan-containing peptides, loss of the Trp side chain was observed in both EID and CID. In EID a loss of 129 Da was detected from the product ions z_5 and b_3, similar to the peptide pEQWFWWM-NH_2. The same loss (129 Da) was observed from product ions in CID. Product ions formed in EID exhibited less neutral losses compared to CID, resulting in a less complex spectrum. For example, in CID, the product ions c_3 and c_4 exhibited multiple neutral losses whereas these product ions did not show any neutral losses in EID. We have also previously examined EDD of the peptide H-WHWLQL-OH.[69] We observed that, similar to the peptides pEVNFSPGWGT-NH_2 and H-GNLWATGHFM-NH_2, loss of the tryptophan

side chain dominated the EDD spectrum. In contrast EID (Figure 5.4A, and Table 5.17) and CID (Figure 5.4B, and Table 5.18) of this peptide provided more extensive fragmentation as was observed for the peptides H-GNLWATGHFM-NH_2 (Tables 5.9 and 5.10) and pEVNFSPGWGT-NH_2 (Tables 5.13 and 5.14).

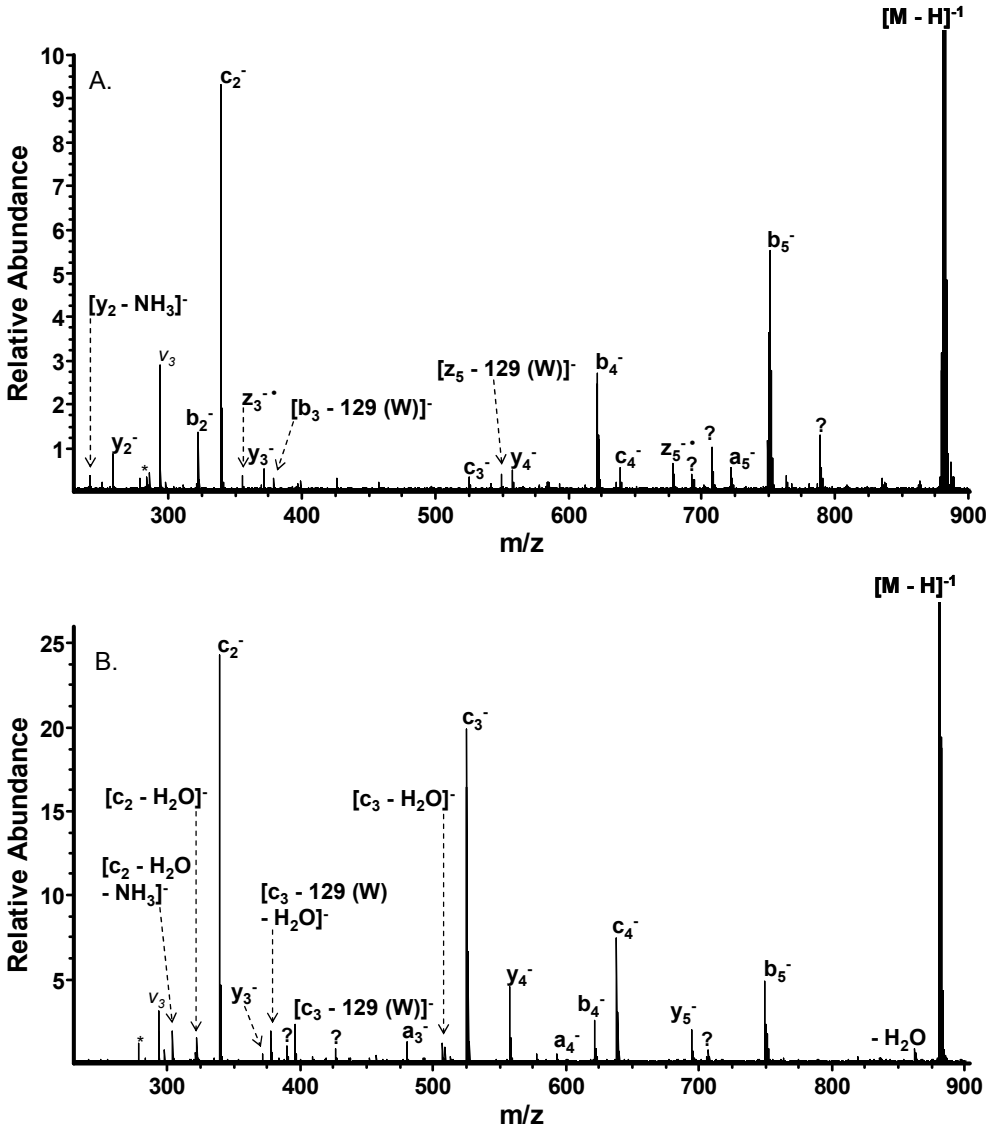

Figure 5.4. EID (A) and CID (B) spectra of the singly deprotonated peptide H-WHWLQL-OH. EID and CID show similar fragmentation patterns, however, EID resulted in the formation of more backbone product ions. Several product ions are unique to EID or CID, respectively. Products ions corresponding to tryptophan side chain loss are detected in both spectra. $^{?}$ = unidentified product ions, ^{v3} = 3rd harmonic, * = noise peak.

Table 5.17. Product ions observed following EID of singly deprotonated H-WHWLQL-OH

Observed m/z	Theoretical m/z	Assignment	Error (ppm)
	880.4475	$[M - H]^-$	Calibrant
862.4313	862.4369	$[M - H_2O]^-$	6.5
834.4424	834.4420	$[M - H_2O - 28 (CO)]^-$	-0.5
749.3603	749.3529	b_5^-	-9.9
721.3533	721.3579	a_5^-	6.4
678.3505	678.3494	$z_5^{-\bullet}$	-1.6
638.3191	638.3208	c_4^-	2.6
621.2876	621.2943	b_4^-	11
557.3094	557.3093	y_4^-	-0.3
549.2877	549.2915	$[z_5 - 129 (W)]^-$	6.9
525.2377	525.2368	c_3	-1.6
379.1519	379.1523	$[b_3 - 129 (W)]^-$	1.0
	371.2299	y_3^-	Calibrant
355.2105	355.2112	$z_3^{-\bullet}$	1.9
339.1568	339.1575	c_2^-	2.2
322.1301	322.1309	b_2^-	2.5
258.1453	258.1459	y_2^-	2.5
241.1189	241.1193	$[y_2 - NH_3]^-$	1.7

Table 5.18. Product ions observed following CID of singly deprotonated H-WHWLQL-OH

Observed m/z	Theoretical m/z	Assignment	Error (ppm)
	880.4475	$[M - H]^-$	Calibrant
862.4363	862.4369	$[M - H_2O]^-$	0.7
749.3545	749.3529	b_5^-	-2.2
694.3692	694.3682	y_5^-	-1.4
638.3218	638.3208	c_4^-	-1.5
621.2948	621.2943	b_4^-	-0.8
593.3038	593.2994	a_4-	-7.5
557.3096	557.3090	y_4^-	-1.1
525.2368	525.2368	c_3^-	0.0
507.2250	507.2262	$[c_3 - H_2O]^-$	2.3
509.2624	509.2629	$[c_4 - 129 (W)]^-$	0.9
480.2157	480.2153	a_3^-	-0.8
396.1781	396.1789	$[c_3 - 129 (W)]^-$	2.0
378.1676	378.1683	$[c_3 - H_2O - 129 (W)]^-$	1.9
	371.2299	y_3^-	Calibrant
339.1567	339.1575	c_2^-	2.3
321.1465	321.1469	$[c_2 - H_2O]^-$	1.3
304.1196	304.1204	$[c_2 - H_2O - NH_3]^-$	2.7

5.3.5. EID and CID of Cholecystokinin

Cholecystokinin, H-DYMGWMDF-NH_2, which is C-terminally amidated but has two acidic residues, was also examined in our previous EDD experiments.[69] EDD of this doubly deprotonated peptide resulted solely in the formation of the charge reduced species and CO_2 loss from this species. No backbone product ions were detected in EDD. By contrast, EID (Table 5.19) and CID (Table 5.20) of the singly deprotonated species produced more informative spectra, allowing structural information to be derived. For this peptide Trp side chain loss was absent in EID and CID spectra, similar to the results obtained with EDD.[69]

Table 5.19. Product ions observed following EID of singly deprotonated cholecystokinin [a]

Observed m/z	Theoretical m/z	Assignment	Error (ppm)
	1061.387	$[M - H]^-$	Calibrant
1043.381	1043.376	$[M - H_2O]^-$	-5.1
1026.354	1026.349	$[M - H_2O - NH_3]^-$	-4.6
1008.346	1008.339	$[M- 2H_2O - NH_3]^-$	-6.8
999.3701	999.3676	$[M - 62 (M) - H_2O]^-$	-2.5
986.3706	986.3598	$m_{3,6}^-$ (M)	-11
946.3633	946.3596	y_7^-	-3.9
870.3092	870.3097	$[z_7 - 62 (M)]^-$	0.6
782.2836	782.2885	$[y_6 - H]^-$	6.3
764.2586	764.2541	$[b_6 - H_2O]^-$	-5.8
764.2586	764.2541	$[c_6 - H_2O - NH_3]^-$	-5.8
764.2586	764.2626	$[a_7 - 107 (Y)]^-$	5.3
754.2722	754.2698	a_6-	-3.2
	652.2558	y_5^-	Calibrant
623.2281	623.2293	a_5-	1.9

[a] The product ion at m/z = 764.2586 can be assigned as either $[b_6 - H_2O]^-$, $[c_6 - H_2O - NH_3]^-$ or as $[a_7 - 107 (Y)]^-$.

EID of singly deprotonated cholecystokinin resulted in the formation of several backbone product ions, a_5, y_5, a_6, and z_7, which were not observed following CID of the same species. Furthermore, side chain loss from methionine (62.019 Da) was only observed in EID. A product ion at m/z = 764.2586 could correspond to loss of the tyrosine side chain (107.050 Da) from the a_7 product ion, or it could correspond to water loss from the b_6 product ion. This product ion was detected in both EID and CID. All backbone product ions formed in CID were also present in the EID spectrum, therefore CID did not produce any additional structural information for this peptide.

Table 5.20. Product ions observed following CID of singly deprotonated cholecystokinin [a]

Observed m/z	Theoretical m/z	Assignment	Error (ppm)
	1061.387	$[M - H]^-$	Calibrant
1043.378	1043.376	$[M - H_2O]^-$	-2.0
1026.350	1026.349	$[M - H_2O - NH_3]^-$	-0.6
1008.340	1008.339	$[M - 2H_2O - NH_3]^-$	-1.5
	946.3596	y_7^-	Calibrant
781.2826	781.2807	$[y_6 - 2H]^-$	-2.5
764.2561	764.2626	$[a_7 - 107\ (Y)]^-$	8.5
764.2561	764.2541	$[c_6 - H_2O - NH_3]^-$	-2.7
764.2561	764.2541	$[b_6 - H_2O]^-$	-2.7

[a] The product ion at m/z = 764.2561 can be assigned as either $[b_6 - H_2O]^-$, $[c_6 - H_2O - NH_3]^-$, or as $[a_7 - 107\ (Y)]^-$.

5.3.6. EID and CID of Modified Peptides

Lastly, two modified peptides were examined with EID: the first peptide, CH_3CO-RRA(pS)VA-OH, contains a phosphorylated serine residue and the second peptide, H-DY*MGWMDF-NH_2, contains a sulfated tyrosine residue. Both these modifications are acidic and therefore may benefit from negative ion mode analysis. In EID of the singly

deprotonated Ser4-phosphorylated peptide, a major product ion corresponding to neutral phosphate (H_3PO_4) loss from the precursor ions is observed in both EID (Figure 5.5A) and CID (Figure 5.5B). All assigned product ions are displayed in Tables 5.21 and 5.22. However, in EID, the majority of backbone product ions, y_4, a_4, z_5, and a_5, retained the labile phosphate group, allowing localization of the phosphorylation site. Retention of phoshorylation has been previously reported for multiply charged protonated precursor ions in ECD,[45, 71-73] and ETD,[39] and it was demonstrated that these electron based reactions can successfully be applied for localization of phosphorylation sites. In sharp contrast, following CID, only one product ion, b_5, retained the phosphorylation.

Similar results were observed for the Tyr2-sulfated peptide (complete lists of all assigned product ions are provided in Tables 22 and 24). Facile SO_3 loss is observed from the precursor ions following EID (Figure 5.6A) and CID (Figure 5.6B). However in EID, almost all backbone product ions containing the sulfated tyrosine residue retained the labile sulfate group, analogous to the behavior of the phosphorylated peptide discussed above. Only one backbone product ion, y_7, displayed loss of the phosphate moiety, and the c_6 product ion was detected as both a sulfated and non-sulfated species. These results are similar to those observed in EDD of a Tyr-sulfated peptide, in which a mixture of sulfated and non-sulfated products was observed.[43] Following CID, SO_3 loss from both the precursor and product ions dominated the spectrum. All, but one, product ions containing the sulfated tyrosine residue lost the modification. Furthermore, for this peptide EID resulted in more extensive fragmentation compared to CID. A series of *a*-type product ions, a_2, a_3, a_5, a_6 and a_7, was observed for this peptide. These *a*-type product ions were absent in CID. The c_3 and x_7 product ions were also only present

following EID. Neutral losses of 59.013 Da, 75.027 Da, and 130.066 Da were observed from the precursor ion upon electron irradiation. These losses can be attributed to the loss of CH_2COOH (59.013 Da) from the aspartic acid, loss of CH_2CH_2SMe (75.027 Da) from Met residue and loss of C_9H_8N (130.066 Da) from Trp residue. These losses were absent following CID.

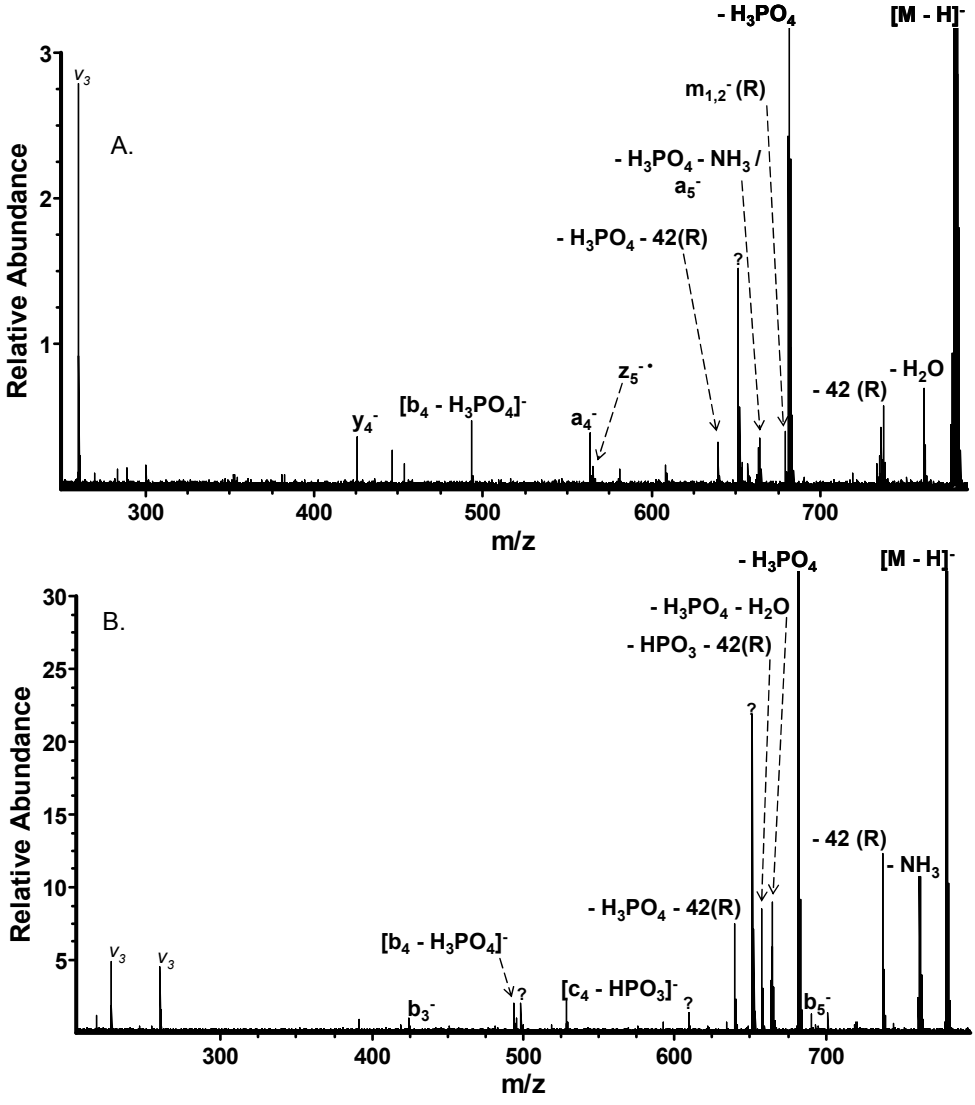

Figure 5.5. EID (A) and CID (B) spectra of the singly deprotonated serine-phosphorylated peptide CH_3CO-RRA(pS)VA-OH. The majority of product ions from EID retained the labile phosphate group, allowing its localization. By contrast, in CID, all product ions exhibited loss of the phosphate group. $^{?}$ = unidentified product ions, v_3 = 3rd harmonic.

Table 5.21. Product ions observed following EID of singly deprotonated CH_3CO-RRA(pS)VA-OH

Observed m/z	Theoretical m/z	Assignment	Error (ppm)
	779.3570	$[M - H]^-$	Calibrant
761.3467	761.3464	$[M - H_2O]^-$	-0.4
737.3364	737.3352	$[M - 42 (R)]^-$	-1.6
	681.3801	$[M - H_3PO_4]^-$	Calibrant
679.2653	679.2695	$m_{1,2}^-$ (R)	6.1
662.3138	662.3144	a_5^-	1.0
664.3545	664.3536	$[M - H_3PO_4 - NH_3]^-$	-1.4
639.3561	639.3583	$[M - H_3PO_4 - 42 (R)]^-$	3.5
565.2288	565.2266	$z_5^{-\bullet}$	-3.8
563.2453	563.2460	a_4^-	1.3
493.2632	493.2640	$[b_4 - H_3PO_4]^-$	1.6
425.1419	425.1442	y_4^-	5.5

Table 5.22. Product ions observed following CID of singly deprotonated CH_3CO-RRA(pS)VA-OH

Observed m/z	Theoretical m/z	Assignment	Error (ppm)
	779.3570	$[M - H]^-$	Calibrant
761.3490	761.3464	$[M - H_2O]^-$	-3.5
762.3324	762.3305	$[M - NH_3]^-$	-2.5
737.3367	737.3352	$[M - 42 (R)]^-$	-2.0
719.3320	719.3248	$[M - 42 - H_2O]^-$	-10
690.3118	690.3093	b_5^-	-3.6
681.3804	681.3801	$[M - H_3PO_4]$	-0.4
663.3692	663.3691	$[M - H_3PO_4 - H_2O]^-$	-0.2
657.3699	657.3689	[M - HPO3 - 42 (R)]$^-$	-1.5
639.3593	639.3583	$[M - H_3PO_4 - 42 (R)]$-	-1.4
528.3025	528.3012	$[c_4 - HPO_3]^-$	-2.6
	493.2642	$[b_4 - H_3PO_4]^-$	Calibrant
424.2435	424.2426	b_3-	-2.0

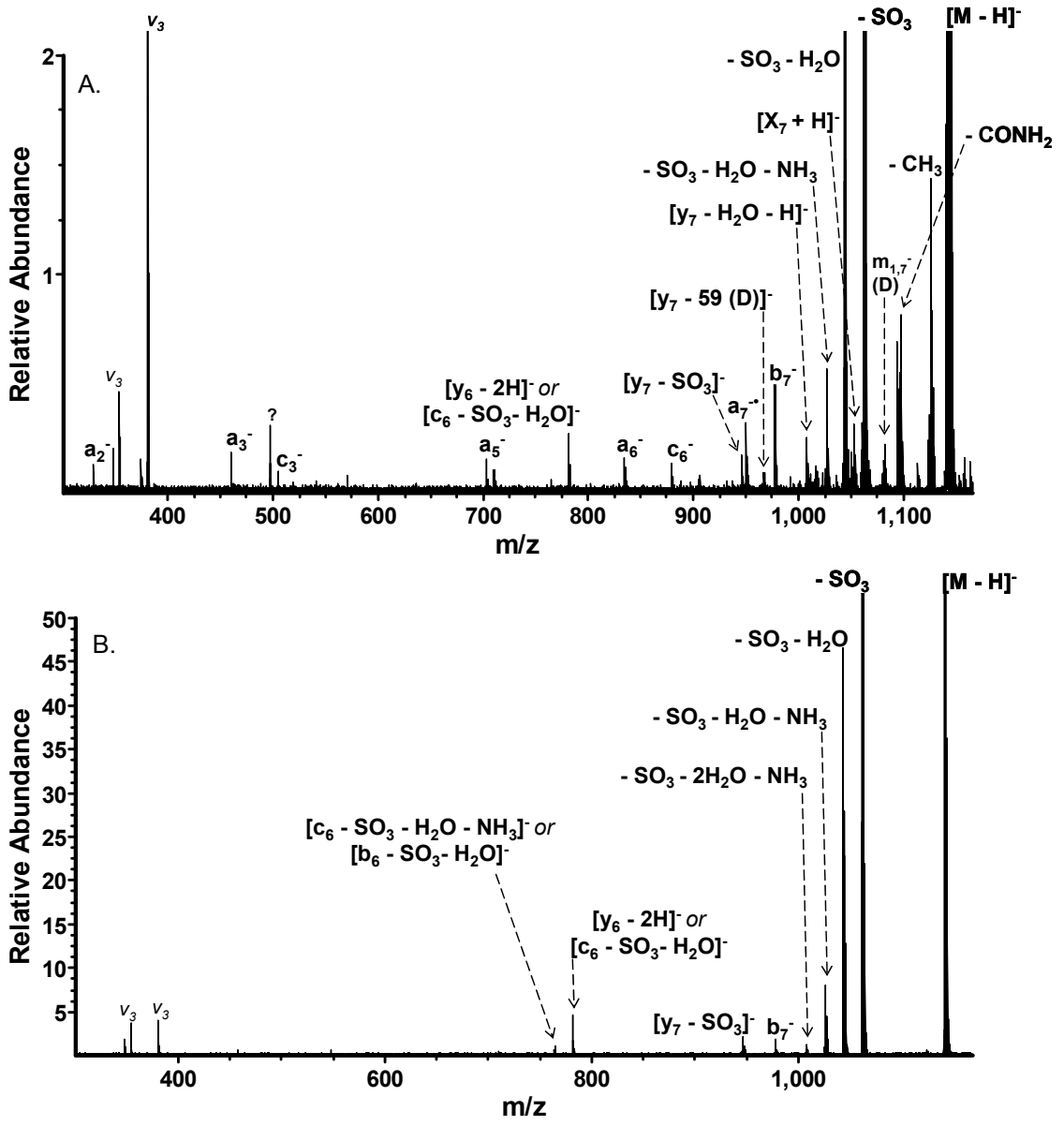

Figure 5.6. EID (A) and CID (B) spectra of the singly deprotonated tyrosine-sulfated peptide cholecystokinin, H-DY*MGWMDF-NH_2. EID produced *b*, *y*, *c*, and mainly *a*-type product ions that retained the sulfate group, allowing its localization. By contrast, CID resulted in sulfate loss from all, but one, product ions. For complete lists of all generated product ions see Tables 5.23 and 5.24 $^?$ = unidentified product ions, v_3 = 3rd harmonic

Table 5.23. Product ions observed following EID of singly deprotonated tyrosine 2-sulfated cholecystokinin [a]

Observed m/z	Theoretical m/z	Assignment	Error (ppm)
	1141.343	$[M - H]^-$	Calibrant
1126.325	1126.320	$[M - CH_3]^-$	-4.3
1123.340	1123.333	$[M - H_2O]^-$	-6.3
1097.338	1097.354	$[M - CO_2]^-$	14
1097.338	1097.330	$[M - CONH_2]^-$	-7.4
1082.331	1082.331	$m_{1,7}^-$ (D)	-0.5
1066.320	1066.317	$m_{3,6}^-$ (M)	-3.6
1061.393	1061.387	$[M - SO3]^-$	-6.0
1053.299	1053.304	$[x_7 + H]^-$	4.2
1043.377	1043.376	$[M - SO_3 - H_2O]^-$	-1.5
1026.360	1026.350	$[M - SO_3 - H_2O - NH_3]^-$	-11
1011.274	1011.278	m_5^- (W)	3.6
1007.312	1007.298	$[y_7 - H_2O - H]^-$	-14
	977.2485	b_7^-	Calibrant
967.2931	967.3032	$[y_7 - 59 (D)]^-$	10
950.2614	950.2613	$a_7^{-\bullet}$	-0.5
946.3619	946.3597	$[y_7 - SO_3]^-$	-2.8
905.2597	905.2637	$[a_7 - CO_2]^-$	4.0
879.2493	879.2480	c_6^-	-2.0
834.2244	834.2267	a_6^-	2.1
781.2811	781.2806	$[c_6 - SO_3 - H_2O]^-$	-0.7
781.2811	781.2807	$[y_6 - 2H]^-$	-0.6
764.2509	764.2542	$[c_6 - SO_3 - H_2O - NH_3]^-$	4.2
764.2509	764.2542	$[b_6 - SO_3 - H_2O]^-$	4.2
703.1823	703.1861	a_5^-	4.5
505.1022	505.1068	c_3^-	7.8
460.0797	460.0854	a_3^-	11.0
329.0402	329.0449	a_2^-	12.8

[a] The product ion at m/z = 781.2811 can be assigned as either $[y_2 - 2H]^-$, or $[c_6 - SO_3 - H_2O]^-$ and the product ion at m/z = 764.2509 can be assigned as $[b_6 - SO_3 - H_2O]^-$, or as $[c_6 - SO_3 - H_2O - NH_3]^-$.

Table 5.24. Product ions observed following CID of singly deprotonated tyrosine 2-sulfated cholecystokinin [a]

Observed m/z	Theoretical m/z	Assignment	Error (ppm)
	1141.3434	$[M - H]^-$	Calibrant
1124.3301	1124.3169	$[M - NH_3]^-$	-11.7
1061.3844	1061.3867	$[M - SO_3]^-$	2.2
1043.3773	1043.3745	$[M - SO_3 - H_2O]$	-2.7
1026.3489	1026.3563	$[M - SO_3 - H_2O - NH_3]^-$	7.2
1008.3273	1008.3388	$[M - SO_3 - 2H_2O - NH_3]^-$	11.4
	946.3597	$[y_7 - SO_3]^-$	Calibrant
977.2476	977.2484	b_7^-	0.8
781.2820	781.2806	$[c_6 - SO_3 - H_2O]^-$	-1.8
781.2820	781.2807	$[y_6 - 2H]^-$	-1.7
764.2511	764.2541	$[c_6 - SO_3 - H_2O - NH_3]^-$	4.0
764.2511	764.2541	$[b_6 - SO_3 - H_2O]^-$	4.0

[a] The product ion at m/z = 781.2820 can be assigned as either $[y_2 - 2H]^-$, or as $[c_6 - SO_3 - H_2O]^-$ and the product ion at m/z = 764.2511 can be assigned as $[b_6 - SO_3 - H_2O]^-$, or as $[c_6 - SO_3 - H_2O - NH_3]^-$.

5.4. Conclusions

EID of singly charged peptide anions has been examined and compared with CID of the same species. Formation of *b*-, y-, *a*-, *c*- and some *x*- and *z*- type product ions was detected in both EID and CID and some product ions were common to both fragmentation techniques. However, unique product ions, observed solely in EID or CID spectra, respectively, were also detected and, in some cases, significant differences were observed between EID and CID spectra of the same species. The different fragmentation pathways observed between EID and CID suggest differences in the manner of ion activation in the two techniques. Freiser and co-workers suggested that ion activation during electron-ion collisions proceed through excitation of electronic modes, whereas CID proceeds via excitation of vibrational modes.[47] O'Hair and co-workers suggested

that EID proceeds via both electronic and vibrational excitation, however, as these authors mention, the exact mechanism of EID is likely to be complex.[51, 52]

Regardless of the fragmentation mechanism, we show that electron irradiation of singly charged deprotonated peptides results in formation of several unique backbone product ions, not detected following CID of the same species and, thus, providing more extensive structural information. Interestingly, for some peptides CID provided poor fragmentation whereas EID resulted in very informative spectra. Furthermore, characteristic amino acid side chains losses from the precursor ions corresponding to side chain loss from Phe, Met, Arg, and Trp residues were present in the majority of EID spectra of peptides containing these amino acid residues. These characteristic amino acid side chain losses were less consistent in CID spectra. Formation of several radical species was also unique to EID. In EID of a phosphorylated and a sulfated peptide, abundant neutral loss of H_3PO_4 and SO_3 was observed from the precursor ions, similar to CID. However, in EID, the majority of product ions retained the phosphorylation and sulfation, respectively. Therefore, EID can reveal the presence of phosphorylation, or sulfation, and also identify its location.

One drawback of negative ion CID and EID is the lack of selective fragmentation to produce specific types of product ions. Both CID and EID result in the formation of various product ion types and uninformative small neutral losses from precursor and product ions are also observed, although these losses are less pronounced in EID spectra, rendering them less complex compared to CID. Nevertheless, the results presented here demonstrate that EID may be a useful fragmentation technique for the analysis of singly

deprotonated peptides, and suggest that EID can provide complementary structural information to that observed in negative ion mode CID.

5.5. References

1. Fenn, J. B.; Mann, M.; Meng, C. K.; Wong, S. F.; Whitehouse, C. M., Electrospray Ionization for Mass-Spectrometry of Large Biomolecules. *Science* **1989,** 246, 64-71.
2. Hillenkamp, F.; Karas, M.; Beavis, R. C.; Chait, B. T., Matrix-Assisted Laser Desorption Ionization Mass-Spectrometry of Biopolymers. *Anal. Chem.* **1991,** 63, A1193-A1202.
3. Tanaka, K.; Waki, H.; Ido, Y.; Akita, S.; Yoshida, Y.; Yoshida, T.; Matsuo, T., Protein and polymer analyses up to m/z 100 000 by laser ionization time-of-flight mass spectrometry. *Rapid Commun. Mass Spectrom.* **1988,** 2, 151-153.
4. Dongre, A. R.; Jones, J. L.; Somogyi, A.; Wysocki, V. H., Influence of peptide composition, gas-phase basicity, and chemical modification on fragmentation efficiency: Evidence for the mobile proton model. *J. Am. Chem. Soc.* **1996,** 118, 8365-8374.
5. Fukui, K.; Naito, Y.; Akiyama, Y.; Takahashi, K., Charge-state selective fragmentation analysis for protonated peptides in infrared multiphoton dissociation. *Int. J. Mass Spectrom.* **2004,** 235, 25-32.
6. Paizs, P.; Suhai, S., Fragmentation pathways of protonated peptides. *Mass Spectrom. Rev.* **2005,** 24, 508-548.
7. Tabb, D. L.; Smith, L. L.; Breci, L. A.; Wysocki, V. H.; Lin, D.; Yates, J. R., Statistical characterization of ion trap tandem mass spectra from doubly charged tryptic peptides. *Anal. Chem.* **2003,** 75, 1155-1163.
8. Wattenberg, A.; Organ, A. J.; Schneider, K.; Tyldesley, R.; Bordoli, R.; Bateman, R. H., Sequence dependent fragmentation of peptides generated by MALDI quadrupole time-of-flight (MALDI Q-TOF) mass spectrometry and its implications for protein identification. *J. Am. Soc. Mass Spectrom.* **2002,** 13, 772-783.
9. Cramer, R.; Corless, S., The nature of collision-induced dissociation processes of doubly protonated peptides: comparative study for the future use of matrix-assisted laser desorption/ionization on a hybrid quadrupole time-of-flight mass spectrometer in proteomics. *Rapid Commun. Mass Spectrom.* **2001,** 15, 2058-2066.
10. Cox, K. A.; Gaskell, S. J.; Morris, M.; Whiting, A., Role of the site of protonation in the low-energy decompositions of gas-phase peptide ions. *J. Am. Soc. Mass Spectrom.* **1996,** 7, 522-531.
11. Dodds, E. D.; German, J. B.; Lebrilla, C. B., Enabling MALDI-FTICR-MS/MS for high-performance proteomics through combination of infrared and collisional activation. *Anal. Chem.* **2007,** 79, 9547-9556.
12. Dodds, E. D.; Hagerman, P. J.; Lebrilla, C. B., Fragmentation of singly protonated peptides via a combination of infrared and collisional activation. *Anal. Chem.* **2006,** 78, 8506-8511.
13. Qin, J.; Chait, B. T., Collision-induced dissociation of singly charged peptide ions in a matrix-assisted laser desorption ionization ion trap mass spectrometer. *Int. J. Mass Spectrom.* **1999,** 191, 313-320.

14. Wysocki, V. H.; Tsaprailis, G.; Smith, L. L.; Breci, L. A., Special feature: Commentary - Mobile and localized protons: a framework for understanding peptide dissociation. *J. Mass Spectrom.* **2000,** 35, 1399-1406.
15. Cui, W. D.; Thompson, M. S.; Reilly, J. P., Pathways of peptide ion fragmentation induced by vacuum ultraviolet light. *J. Am. Soc. Mass Spectrom.* **2005,** 16, 1384-1398.
16. Thompson, M. S.; Cui, W. D.; Reilly, J. P., Fragmentation of singly charged peptide ions by photodissociation at lambda=157 nm. *Angew. Chem. Int. Ed.* **2004,** 43, 4791-4794.
17. Zhang, L. Y.; Cui, W. D.; Thompson, M. S.; Reilly, J. P., Structures of alpha-type ions fonned in the 157 nm photodissociation of singly-charged peptide ions. *J. Am. Soc. Mass Spectrom.* **2006,** 17, 1315-1321.
18. Barbacci, D. C.; Russell, D. H., Sequence and side-chain specific photofragment (193 nm) ions from protonated substance P by matrix-assisted laser desorption ionization time-of-flight mass spectrometry. *J. Am. Soc. Mass Spectrom.* **1999,** 10, 1038-1040.
19. Choi, K. M.; Yoon, S. H.; Sun, M. L.; Oh, J. Y.; Moon, J. H.; Kim, M. S., Characteristics of photodissociation at 193 nm of singly protonated peptides generated by matrix-assisted laser desorption ionization (MALDI). *J. Am. Soc. Mass Spectrom.* **2006,** 17, 1643-1653.
20. Moon, J. H.; Shin, Y. S.; Cha, H. J.; Kim, M. S., Photo dissociation at 193 nm of some singly protonated peptides and proteins with m/z 2,000-9000 using a tandem time-of-flight mass spectrometer equipped with a second source for delayed extraction/post-acceleration of product ions. *Rapid Commun. Mass Spectrom.* **2007,** 21, 359-368.
21. Moon, J. H.; Yoon, S. H.; Kim, M. S., Photodissociation of singly protonated peptides at 193 nm investigated with tandem time-of-flight mass spectrometry. *Rapid Commun. Mass Spectrom.* **2005,** 19, 3248-3252.
22. Morgan, J. W.; Hettick, J. M.; Russell, D. H., Peptide sequencing by MALDI 193-nm photodissociation TOF MS. *Biol. Mass Spectrom.* **2005,** 402, 186-209.
23. Morgan, J. W.; Russell, D. H., Comparative studies of 193-nm photodissociation and TOF-TOFMS analysis of bradykinin analogues: The effects of charge site(s) and fragmentation timescales. *J. Am. Soc. Mass Spectrom.* **2006,** 17, 721-729.
24. Thompson, M. S.; Cui, W. D.; Reilly, J. P., Factors that impact the nacuum ultraviolet photofragmentation of peptide ions. *J. Am. Soc. Mass Spectrom.* **2007,** 18, 1439-1452.
25. Jai-nhuknan, J.; Cassady, C. J., Negative ion postsource decay time-of-flight mass spectrometry of peptides containing acidic amino acid residues. *Anal. Chem.* **1998,** 70, 5122-5128.
26. Vinh, J.; Loyaux, D.; Redeker, V.; Bossier, J., Sequencing branched peptides with CID/PSD MALDI-TOF in the low picomole range: Application to the structural study of the posttranslational polyglycylation of tubulin. *Anal. Chem.* **1997,** 69, 3979-3985.
27. Ewing, N. P.; Cassady, C. J., Dissociation of multiply charged negative ions for hirudin (54-65), fibrinopeptide B, and insulin A (oxidized). *J. Am. Soc. Mass Spectrom.* **2001,** 12, 105-116.

28. Clipston, N. L.; Jai-nhuknan, J.; Cassady, C. J., A comparison of negative and positive ion time-of-flight post-source decay mass spectrometry for peptides containing basic residues. *Int. J. Mass Spectrom.* **2003,** 222, 363-381.
29. Yagami, T.; Kitagawa, K.; Futaki, S., Liquid Secondary-Ion Mass-Spectrometry of Peptides Containing Multiple Tyrosine-O-Sulfates. *Rapid Commun. Mass Spectrom.* **1995,** 9, 1335-1341.
30. Janek, K.; Wenschuh, H.; Bienert, M.; Krause, E., Phosphopeptide analysis by positive and negative ion matrix-assisted laser desorption/ionization mass spectrometry. *Rapid Commun. Mass Spectrom.* **2001,** 15, 1593-1599.
31. Jai-nhuknan, J.; Cassady, C. J., Anion and cation post-source decay time-of-flight mass spectrometry of small peptides: Substance P, angiotensin II, and renin substrate. *Rapid Commun. Mass Spectrom.* **1996,** 10, 1678-1682.
32. Boontheung, P.; Alewood, P. F.; Brinkworth, C. S.; Bowie, J. H.; Wabnitz, P. A.; Tyler, M. J., Negative ion electrospray mass spectra of caerulein peptides: an aid to structural determination. *Rapid Commun. Mass Spectrom.* **2002,** 16, 281-286.
33. Bowie, J. H.; Brinkworth, C. S.; Dua, S., Collision-induced fragmentations of the (M-H)(-) parent anions of underivatized peptides: An aid to structure determination and some unusual negative ion cleavages. *Mass Spectrom. Rev.* **2002,** 21, 87-107.
34. O'Hair, R. A. J.; Blanksby, S.; Styles, M.; Bowie, J. H., Characterization of [M-H] cations, radicals and anions of glycine in the gas phase: a combined experimental and ab initio study. *Int. J. Mass Spectrom.* **1999,** 183, 203-211.
35. Steinborner, S. T.; Bowie, J. H., A comparison of the positive- and negative-ion mass spectra of bio-active peptides from the dorsal secretion of the Australian red tree frog, Litoria rubella. *Rapid Commun. Mass Spectrom.* **1996,** 10, 1243-1247.
36. Brinkworth, C. S.; Dua, S.; Bowie, J. H., Backbone cleavages of M-H (-) anions of peptides. Cyclisation of citropin 1 peptides involving reactions between the C-terminal CONH (-) residue and backbone amide carbonyl groups. A new type of beta cleavage: a joint experimental and theoretical study. *Rapid Commun. Mass Spectrom.* **2002,** 16, 713-721.
37. Harrison, A. G., Sequence-specific fragmentation of deprotonated peptides containing H or alkyl side chains. *J. Am. Soc. Mass Spectrom.* **2001,** 12, 1-13.
38. Zubarev, R. A.; Kelleher, N. L.; McLafferty, F. W., Electron capture dissociation of multiply charged protein cations. A nonergodic process. *J. Am. Chem. Soc.* **1998,** 120, 3265-3266.
39. Syka, J. E. P.; Coon, J. J.; Schroeder, M. J.; Shabanowitz, J.; Hunt, D. F., Peptide and protein sequence analysis by electron transfer dissociation mass spectrometry. *Proc. Natl. Acad. Sci. U.S.A* **2004,** 101, 9528-9533.
40. Cooper, H. J.; Hakansson, K.; Marshall, A. G., The role of electron capture dissociation in biomolecular analysis. *Mass Spectrom. Rev.* **2005,** 24, 201-222.
41. Mikesh, L. M.; Ueberheide, B.; Chi, A.; Coon, J. J.; Syka, J. E. P.; Shabanowitz, J.; Hunt, D. F., The utility of ETD mass spectrometry in proteomic analysis. *Biochim. Biophys. Acta* **2006,** 1764, 1811-1822.
42. Zubarev, R., Protein primary structure using orthogonal fragmentation techniques in Fourier transform mass spectrometry. *Expert Rev. Proteomics* **2006,** 3, 251-261.

43. Budnik, B. A.; Haselmann, K. F.; Zubarev, R. A., Electron detachment dissociation of peptide di-anions: an electron-hole recombination phenomenon. *Chem. Phys. Lett.* **2001,** 342, 299-302.
44. Kjeldsen, F.; Silivra, O. A.; Ivonin, I. A.; Haselmann, K. F.; Gorshkov, M.; Zubarev, R. A., C-alpha-C backbone fragmentation dominates in electron detachment dissociation of gas-phase polypeptide polyanions. *Chem. Eur. J.* **2005,** 11, 1803-1812.
45. Kweon, H. K.; Hakansson, K., Metal oxide-based enrichment combined with gas-phase ion-electron reactions for improved mass spectrometric characterization of protein phosphorylation. *J. Proteome. Res.* **2008,** 7, 749-755.
46. Coon, J. J.; Shabanowitz, J.; Hunt, D. F.; Syka, J. E. P., Electron transfer dissociation of peptide anions. *J. Am. Soc. Mass Spectrom.* **2005,** 16, 880-882.
47. Gord, J. R.; Horning, S. R.; Wood, J. M.; Cooks, R. G.; Freiser, B. S., Energy Deposition During Electron-Induced Dissociation. *J. Am. Soc. Mass Spectrom.* **1993,** 4, 145-151.
48. Cody, R. B.; Freiser, B. S., Electron-Impact Excitation of Ions in Fourier-Transform Mass-Spectrometry. *Anal. Chem.* **1987,** 59, 1054-1056.
49. Cody, R. B.; Freiser, B. S., Electron-Impact Excitation of Ions from Organics - Alternative to Collision-Induced Dissociation. *Anal. Chem.* **1979,** 51, 547-551.
50. Wang, B. H.; McLafferty, F. W., Electron-Impact Excitation of Ions from Larger Organic-Molecules. *Org. Mass Spectrom.* **1990,** 25, 554-556.
51. Lioe, H.; O'Hair, R. A. J., Comparison of collision-induced dissociation and electron-induced dissociation of singly protonated aromatic amino acids, cystine and related simple peptides using a hybrid linear ion trap-FT-ICR mass spectrometer. *Anal. Bioanal. Chem.* **2007,** 389, 1429-1437.
52. Feketeova, L.; Khairallah, G. N.; Hair, R. A. J., Letter: Intercluster chemistry of protonated and sodiated betaine dimers upon collision induced dissociation dissociation. *Eur. J. Mass Spectrom.* **2008,** 14, 107-110.
53. Budnik, B. A.; Haselmann, K. F.; Elkin, Y. N.; Gorbach, V. I.; Zubarev, R. A., Applications of electron-ion dissociation reactions for analysis of polycationic chitooligosaccharides in Fourier transform mass spectrometry. *Anal. Chem.* **2003,** 75, 5994-6001.
54. Yoo, H. J.; Liu, H. C.; Hakansson, K., Infrared multiphoton dissociation and electron-induced dissociation as alternative MS/MS strategies for metabolite identification. *Anal. Chem.* **2007,** 79, 7858-7866.
55. Wolff, J. J.; Laremore, T. N.; Aslam, H.; Linhardt, R. J.; Amster, I. J., Electron-Induced Dissociation of Glycosaminoglycan Tetrasaccharides. *J. Am. Soc. Mass Spectrom.* **2008,** 19, 1449-1458.
56. Yang, J.; Mo, J. J.; Adamson, J. T.; Hakansson, K., Characterization of oligodeoxynucleotides by electron detachment dissociation Fourier transform ion cyclotron resonance mass spectrometry. *Anal. Chem.* **2005,** 77, 1876-1882.
57. Caravatti, P.; Allemann, M., The Infinity Cell - a New Trapped-Ion Cell with Radiofrequency Covered Trapping Electrodes for Fourier-Transform Ion-Cyclotron Resonance Mass-Spectrometry. *Org. Mass Spectrom.* **1991,** 26, 514-518.

58. Senko, M. W.; Canterbury, J. D.; Guan, S. H.; Marshall, A. G., A high-performance modular data system for Fourier transform ion cyclotron resonance mass spectrometry. *Rapid Commun. Mass Spectrom.* **1996,** 10, 1839-1844.
59. Ledford, E. B.; Rempel, D. L.; Gross, M. L., Space-Charge Effects in Fourier-Transform Mass-Spectrometry - Mass Calibration. *Anal. Chem.* **1984,** 56, 2744-2748.
60. Waugh, R. J.; Bowie, J. H.; Gross, M. L., Collision-Induced Dissociations of Deprotonated Peptides - Dipeptides Containing Methionine or Cysteine. *Rapid Commun. Mass Spectrom.* **1993,** 7, 623-625.
61. Waugh, R. J.; Bowie, J. H.; Hayes, R. N., Collision-Induced Dissociations of Deprotonated Peptides - Dipeptides Containing Phenylalanine, Tyrosine, Histidine and Tryptophan. *Int. J. Mass Spectrom. Ion Processes* **1991,** 107, 333-347.
62. Pu, D.; Cassady, C. J., Negative ion dissociation of peptides containing hydroxyl side chains. *Rapid Commun. Mass Spectrom.* **2008,** 22, 91-100.
63. Tsybin, Y. O.; Haselmann, K. F.; Emmett, M. R.; Hendrickson, C. L.; Marshall, A. G., Charge location directs electron capture dissociation of peptide dications. *J. Am. Soc. Mass Spectrom.* **2006,** 17, 1704-1711.
64. Bradford, A. M.; Waugh, R. J.; Bowie, J. H., Characterization of Underivatized Tetrapeptides by Negative-Ion Fast-Atom-Bombardment Mass-Spectrometry. *Rapid Commun. Mass Spectrom.* **1995,** 9, 677-685.
65. Reiter, A.; Teesch, L. M.; Zhao, H.; Adams, J., Gas-Phase Fragmentations of Anionic Complexes of Serine-Containing and Threonine-Containing Peptides. *Int. J. Mass Spectrom. Ion Processes* **1993,** 127, 17-26.
66. Waugh, R. J.; Eckersley, M.; Bowie, J. H.; Hayes, R. N., Collision-Induced Dissociations of Deprotonated Peptides - Dipeptides Containing Serine or Threonine. *Int. J. Mass Spectrom. Ion Processes* **1990,** 98, 135-145.
67. Waugh, R. J.; Bowie, J. H.; Gross, M. L., Collision-Induced Dissociations of Deprotonated Peptides - Dipeptides Containing Asn, Arg and Lys. *Aust. J. Chem.* **1993,** 46, 693-702.
68. Haselmann, K. F.; Budnik, B. A.; Kjeldsen, F.; Polfer, N. C.; Zubarev, R. A., Can the (M center dot-X) region in electron capture dissociation provide reliable information on amino acid composition of polypeptides? *Eur. J. Mass Spectrom.* **2002,** 8, 461-469.
69. Kalli, A.; Hakansson, K., Preferential cleavage of S-S and C-S bonds in electron detachment dissociation and infrared multiphoton dissociation of disulfide-linked peptide anions. *Int. J. Mass Spectrom.* **2007,** 263, 71-81.
70. Cooper, H. J.; Hudgins, R. R.; Hakansson, K.; Marshall, A. G., Characterization of amino acid side chain losses in electron capture dissociation. *J. Am. Soc. Mass Spectrom.* **2002,** 13, 241-249.
71. Chalmers, M. J.; Hakansson, K.; Johnson, R.; Smith, R.; Shen, J. W.; Emmett, M. R.; Marshall, A. G., Protein kinase A phosphorylation characterized by tandem Fourier transform ion cyclotron resonance mass spectrometry. *Proteomics* **2004,** 4, 970-981.

72. Shi, S. D. H.; Hemling, M. E.; Carr, S. A.; Horn, D. M.; Lindh, I.; McLafferty, F. W., Phosphopeptide/phosphoprotein mapping by electron capture dissociation mass spectrometry. *Anal. Chem.* **2001,** 73, 19-22.
73. Stensballe, A.; Jensen, O. N.; Olsen, J. V.; Haselmann, K. F.; Zubarev, R. A., Electron capture dissociation of singly and multiply phosphorylated peptides. *Rapid Commun. Mass Spectrom.* **2000,** 14, 1793-1800.

Chapter 6

Collision Induced Dissociation and Infrared Multiphoton Dissociation of Native Lantibiotics Anions and Oxidized Lantibiotics Ions of both Polarities

6.1. Introduction

Lantibiotics are a unique class of antimicrobial peptides produced by Gram-positive bacteria.[1-3] They are produced on the ribosome and they undergo a series of post-translational modifications to produce their biologically active forms.[4-6] These post-translational modifications include thioether cross-linked amino acids, lanthionine and 3-methyllanthionine, and the unusual amino acids 2,3-didehydroalanine (Dha), (*Z*)-2-3,-didehydrobutyrine (Dhb), and β-hydroxy-aspartate. Lanthionine and 3-methyllanthionine bridges are formed by dehydration of a serine and a threonine to form dehydroalanine and dehydrobutyrine, respectively, followed by addition of the thiol group of a cysteine to the α,β unsaturated residue.[7] Disruption of lanthionine bridges results in complete loss of lantibiotic activity, thus lanthionine bridges serve to stabilize biologically active conformations and they also provide structural stability against proteases.[8, 9]

Lantibiotic research has recently drawn significant attention because these molecules hold great promise for the development of novel antimicrobial agents for biomedical and food applications.[2, 3, 5, 10] For example, nisin exhibits antimicrobial activity against a wide range of Gram positive bacteria and it has been used as a food preservative for almost 50 years without development of significant bacterial resistance.[11-14] Lacticin 481 also shows bactericidal activity against Gram positive bacteria.[15, 16] Furthermore, mersacidin has been shown to be very effective in the treatment of systematic staphylococcal infections[17] and gallidermin is highly active against *Propionibacterium acnes*.[18]

Structural elucidation of lantibiotics has been hampered by the presence of the unusual amino acids and thioether bridges, as these modifications block routine Edman sequencing. Chemical derivatization procedures which convert the dehydro amino acids and thioether bridges to sequencing friendly amino acids suitable for Edman degradation facilitates the structural determination of lantibiotics. Nisin was the first lantibiotic for which the primary structure was determined. This feat was achieved by a combination of chemical derivatization, enzymatic and chemical cleavage followed by Edman sequencing.[19, 20] Furthermore, direct sequence analysis of gallidermin and Pep5 was achieved by chemical modification employing an alkaline ethanethiol-containing mixture to open the lanthionine bridges and convert the unsaturated 2,3-didehydroamino acids into saturated S-ethylcysteinyl derivatives, followed by Edman degradation.[21] Another approach involves nickel boride for desulfurization of the thioether bridges and reduction of the dehydro amino acids, followed by Edman degradation and mass spectrometry to identify the locations of dehydro side chains and lanthionine bridges.[22] Nuclear magnetic

resonance (NMR) spectroscopy is an alternative method for obtaining structural information when significant quantities of pure samples are available.[23-30] In many cases, a combination of peptide chemistry, mass spectrometry and NMR is required to determine lantibiotic structures.[22, 31-34]

Reports of the use of tandem mass spectrometry (MS/MS) for structural elucidation of lantibiotics have been rare because the presence of thioether bridges is expected to complicate fragmentation patterns and to limit the extent of fragmentation. However, Lavanant et al. obtained some amino acid sequence information for nisin and some from its variant using sustained off-resonance irradiation collision induced dissociation (SORI-CID)[35] in positive ion mode.[36] These authors showed that, in SORI-CID, fragmentation occurred mainly at the N- or C-terminus of the molecule. Fragmentation of the two thioether bridges located towards the N-terminus was also observed. This work also reported that the obtainable structural information is somewhat limited by the small number of product ions detected, and by the fact that fragmentation occurred only at the termini of the peptide. Nevertheless, the authors successfully assigned the hydration site in [nisin + 18 Da], and the sites of mutation in nisin variants from the product ion spectra.[36, 37] Furthermore, positive ion mode CID has been applied to the characterization of mutacin 1140. In contrast to CID of nisin and its variants, cleavages at the thioether bridges, and an almost complete series of *b*- and *y*-type product ions were observed for mutacin 1140.[32]

Electron capture dissociation (ECD), which involves cation fragmentation, has also been shown to provide structural information for lantibiotics.[38] Kleinnijenhuis et al. examined nisin A and Z, mersacidin, and lacticin 481 with ECD. These authors observed

cleavages of both the backbone amine bonds, and the thioether bridges and they reported that cleavages occur mainly near the location of the lanthionine bridges. However, ECD of lacticin 481 resulted in very limited fragmentation,[38, 39] probably due to its less linear structure compared to nisin.

Negative ion mode, although not nearly as extensively used as positive ion mode for peptide and protein analysis, is particularly informative for acidic molecules and it can provide complementary information compared to positive ion mode.[40-45] For example, it has been demonstrated that a number of tryptic peptides that were not observed in positive ion mode were detected in negative ion mode.[40] In addition, it has been shown that positive and negative ion post source decay (PSD) provides complementary information on peptide primary structure.[41] Furthermore, disulfide bonds, which are not cleaved in low energy positive ion mode CID, can easily be cleaved in negative ion mode CID and IRMPD.[46, 47] Negative ion mode is also very useful for the characterization of acidic post-translational modifications such as phosphorylation[48] and sulfation.[49]

Here, we examine the fragmentation behavior of three lantibiotics, nisin, (produced by *Lactococcus lacti)*[19] gallidermin, (produced by *Staphylococcus gallinarium* Tü3928),[50] and duramycin, (produced by *Streptoverticillium hachijoense* DSM 40114)[51] in negative ion mode CID and IRMPD. We also investigate the fragmentation behavior of oxidized gallidermin in negative ion mode, and we characterize the fragmentation patterns of oxidized gallidermin and nisin in positive ion mode. These experiments aimed to address whether negative ion mode MS/MS provides additional information for structural elucidation of lantibiotics, and also to reveal similarities, or differences, between the

fragmentation behavior of lantibiotics and oxidized lantibiotics in both negative and positive ion mode CID and IRMPD. It has been shown that CID of peptides containing oxidized carbamidomethyl cysteine residues results in characteristic neutral loss of RSOH (where R represents the carbamidomethyl group, $-CH_2CONH_2$) from the precursor and product ions.[52, 53] Furthermore, diagnostic neutral loss of methane sulfenic acid (CH_3SOH) is observed from both precursor and product ions in CID of methionine sulfoxide containing peptides.[54-57] The loss of CH_3SOH (64 Da) is specific to methionine sulfoxide containing peptides and it can be useful for identifying oxidized methionine residues, thereby possibly increasing the confidence of protein identifications.[54-57]

An improved understanding of the fragmentation behavior of lantibiotics and oxidized lantibiotics may allow further application of MS/MS to the structural elucidation of this important class of biomolecules.

6.2 Experimental Procedures

6.2.1. Sample preparation

Duramycin and nisin were obtained from Sigma (St. Louis, MO). 4.7 mg of nisin (2.5% purity) were dissolved in 340 μl water. The sample was centrifuged to precipitate denatured milk solids. The supernatant was taken and 4.1 nanomoles of nisin were desalted with C_{18} Ziptips (Millipore, Billerica, MA) and diluted into 380 μl spraying solvent containing 1:1 isopropanol:water and 20 mM ammonium acetate (Fisher Scientific, Fair Lawn, NJ) for negative ion mode electrospray ionization. Duramycin was used without further purification, diluted to a final concentration of 1.7 μM into a spraying solvent containing 1:1 isopropanol:water and 10 mM ammonium acetate (Fisher). Gallidermin, oxidized gallidermin, and oxidized nisin were provided by the

laboratory of Professor Leif Smith (Department of Biological Sciences and Department of Basic Sciences at the College of Veterinary Medicine, Mississippi State University, Mississippi State, Mississippi). Gallidermin and oxidized gallidermin were electrosprayed in negative ion mode at a final concentration of 0.3 μM from a spraying solvent containing 1:1 isopropanol:water and 10 mM ammonium acetate.

For positive ion mode electrospray ionization, oxidized gallidermin and nisin were diluted to a final concentration of 0.3 μM and 0.9 μM, respectively, into a spraying solvent containing 1:1 acetonitile:water and 0.1% formic acid (Acros Organics, Morris Plains, NJ).

6.2.2. Mass spectrometry

All experiments were performed with an actively shielded 7T quadrupole (Q)-FT-ICR mass spectrometer (Apex-Q, Bruker Daltonics, Billerica MA), which has been previously described.[58] Lantibiotics and oxidized lantibiotics were electrosprayed in negative or positive ion mode at a flow rate of 70 μL/h. Ions were accumulated in the first hexapole for 0.1 s, transferred through the mass selective quadrupole (10 m/z isolation window) and mass selectively accumulated in the second hexapole for 1 to 5 s. IRMPD experiments were performed with a vertically mounted 25 W, 10.6 μm, CO_2 laser (Synrad, Mukilteo, WA). Photon irradiation was performed for 0.04 to 0.2 s at 40 % laser power. CID was performed in the collision cell with argon.

All spectra were acquired with XMASS (version 6.1, Bruker Daltonics) using 256k or 512k data points and summed over 16 to 32 scans. Data processing was performed with the MIDAS analysis software.[59] CID and IRMPD spectra for nisin and gallidermin were internally calibrated using the calculated masses of the precursor ions and the

protonated species [M - (n - 1)H](n-1)-, where n is the charge of the precursor ions. In cases where protonated precursor ions were absent, abundant product ions were used for calibration. In the case of duramycin, external calibration was performed using product ions from neurotensin as external calibrants. All frequency-to-mass calibrations were performed by Microsoft Excel using a two term calibration equation.[60] Only peak assignments with a mass accuracy better than 15 ppm were accepted.

6.3. Results and Discussion

The structures of nisin,[19] duramycin,[29, 51, 61] and gallidermin[50] are shown in Scheme 6.1. Nisin contains 5 thioether bridges, gallidermin contains 4 thioether bridges and duramycin contains 3 thioether bridges and one lysinoalanine bridge. All product ions are labeled according to Scheme 6.2. The chemical structures of lanthionine, 3-methyllanthionine, and the lysinoalanine bridge are shown in Schemes 6.3 and 6.4 respectively

6.3.1. Negative Ion Mode CID and IRMPD of Nisin

IRMPD (Figure 6.1) and CID (Figure 6.2) spectra of the $[M - 3H]^{3-}$ precursor ions of nisin showed very similar fragmentation patterns, involving abundant SH_2 neutral losses from both the precursor and product ions. Mainly C-terminal *y*-type product ions are detected, consistent with the most acidic site being the free C-terminus. However, some N-terminal *c*-type product ions are also observed. Although *c*-type product ions are generally not observed in positive ion mode, their formation in negative ion mode CID has been previously discussed. For example, Cassady and co-workers examined the negative ion mode fragmentation behavior of hirudin (54-65), fibrinopeptide B, and insulin chain A and reported that *c*- and *y*- type product ions were predominant in CID

spectra. In addition, these authors reported the observation of internal product ions and neutral losses.[42] Our observations are in agreement with their results.

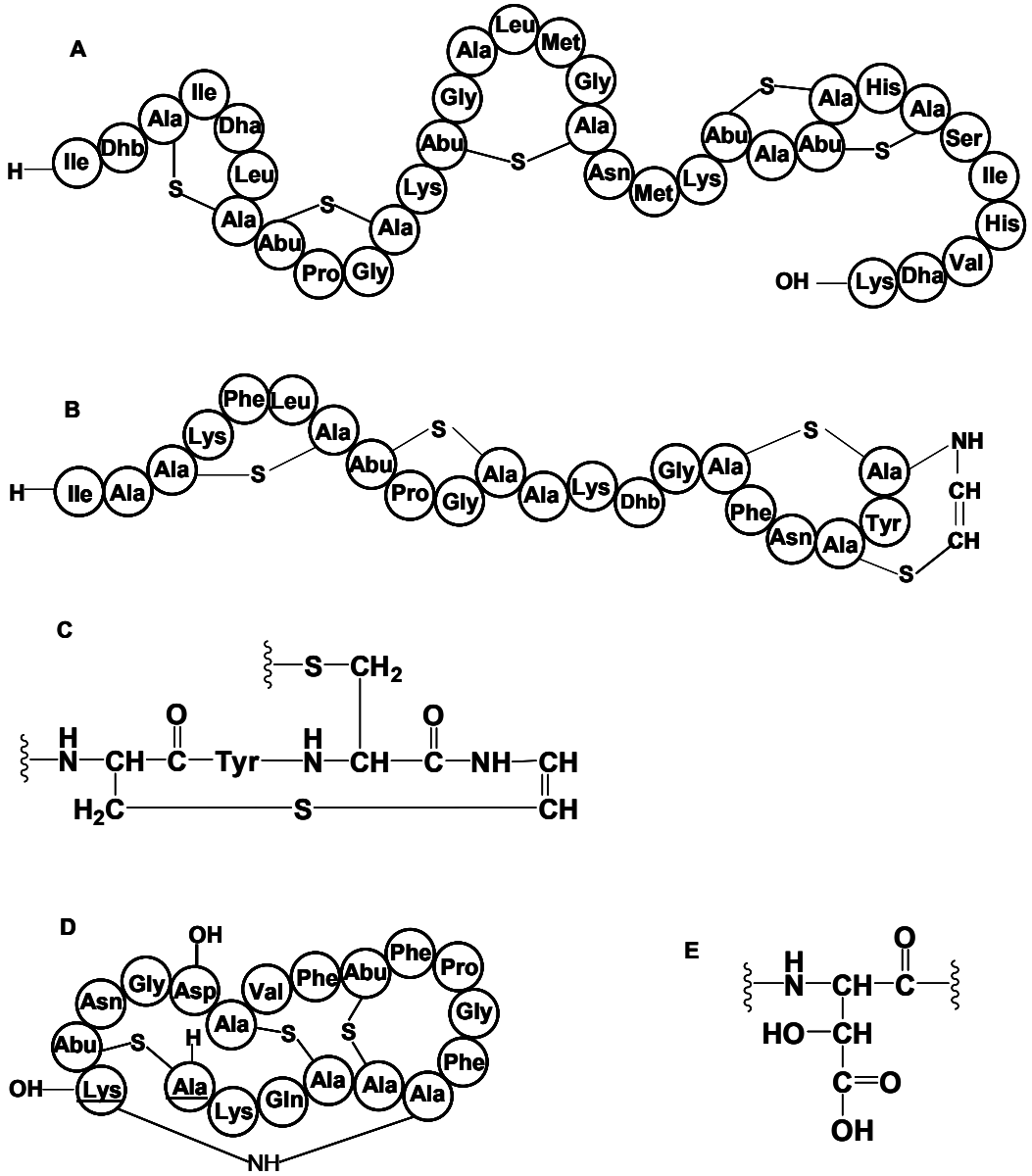

Scheme 6.1. Structures of lantibiotics examined, A) nisin,[19] B) gallidermin,[50] C) detailed structure of gallidermin C-terminus,[50, 62, 63] D) duramycin,[29, 51, 61] (the N-terminal Ala and C-terminal Lys are underlined) and E) structure of hydroxyaspartic acid. Dha represents dehydrated serine and Dhb represents dehydrated threonine. Ala-S-Ala represents lanthionine and Abu-S-Ala represents 3-methyllanthionine.

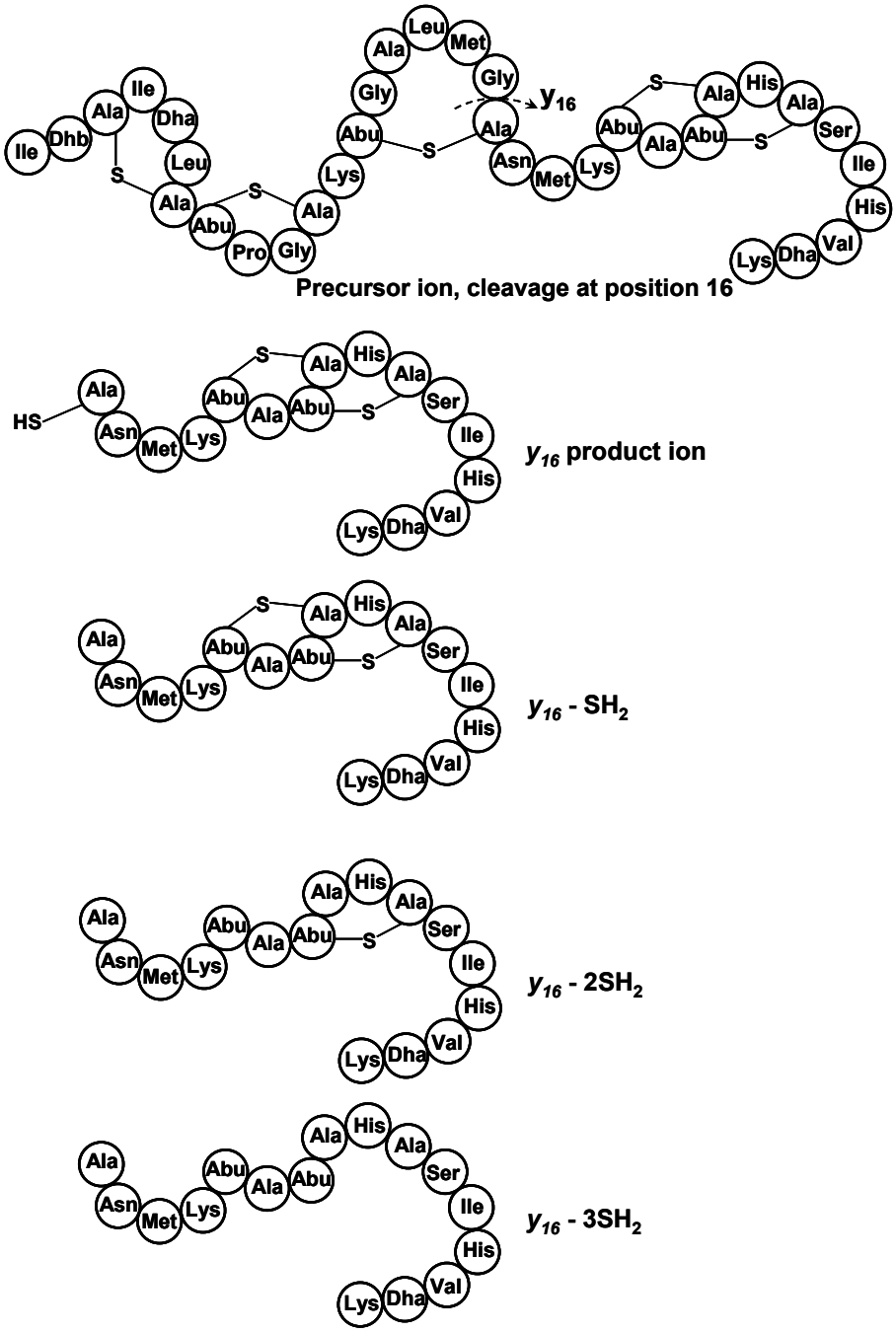

Scheme 6.2. Nomenclature used for the observed product ions in negative ion mode CID and IRMPD. A y_{16} product ion from nisin is used as an example (the exact position of SH_2 elimination cannot be determined based on the product ions masses). For example, for the y_{16} product ion, SH_2 can either be lost from the terminus or from internal thioether bridges and therefore there are three possibilities for elimination of SH_2 groups. For clarity, only one possibility is shown in each case). The same behavior was observed for nisin, gallidermin, and duramycin. For oxidized lantibiotics, the same nomenclature was used but the thioether group is replaced with an oxidized (+ O) thioether group.

Differences in product ion abundances are observed between the IRMPD and CID spectra. For example, the c_4 and $[c_4 - SH_2]$ product ions are the most abundant fragments in the IRMPD spectrum whereas, in the CID spectrum, both these product ions were detected at very low abundance (c_4 is not labeled in the CID spectrum due to its low abundance). Furthermore, the y_{12} product ion was only detected following IRMPD whereas the $[y_{15} - SH_2]$ and $[y_{15} - 2SH_2]$ products ions were only observed following CID.

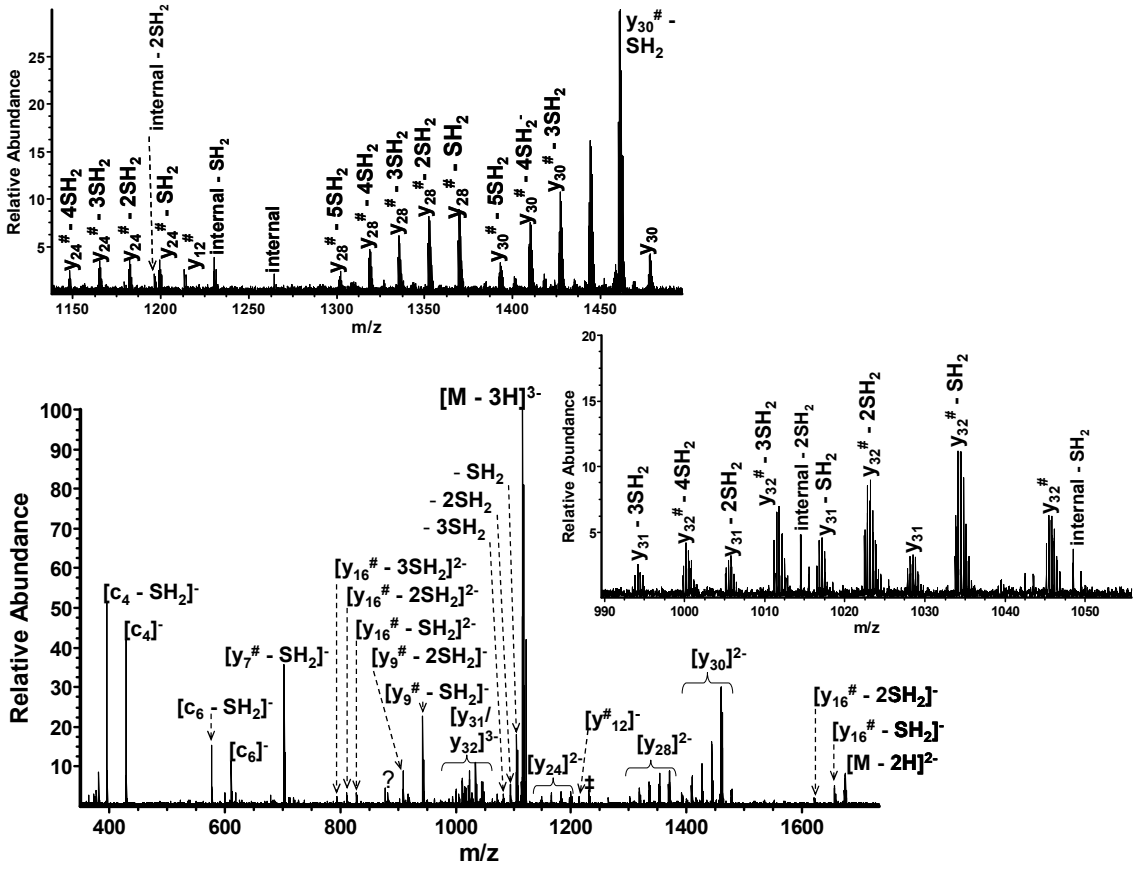

Figure 6.1. Negative ion mode IRMPD spectrum of the triply deprotonated precursor ions of nisin. Sequential SH_2 neutral losses from both the precursor and product ions are observed. These SH_2 neutral losses are due to cleavage of the thioether bridges. The y_{24}, y_{28}, y_{30}, y_{31}, and y_{32} product ions and their secondary fragments are shown in detail in the insets. # = NH_3 loss, □ = internal product ions, ? = unidentified product ions.

A closer inspection of the IRMPD and CID spectra (see insets in Figures 6.1 and 6.2) reveals sequential SH_2 neutral losses, originating from the thioether bridges, from both the precursor ions and backbone product ions. These SH_2 neutral losses suggest that thioether bridges are labile in negative ion mode. SH_2 neutral loss has been previously reported by Bowie and co-workers for singly deprotonated peptides containing free cysteine residues.[64-66] Possible structures of product ions formed after cleavage of the thioether bridges and elimination of SH_2 are shown in Scheme 6.3.

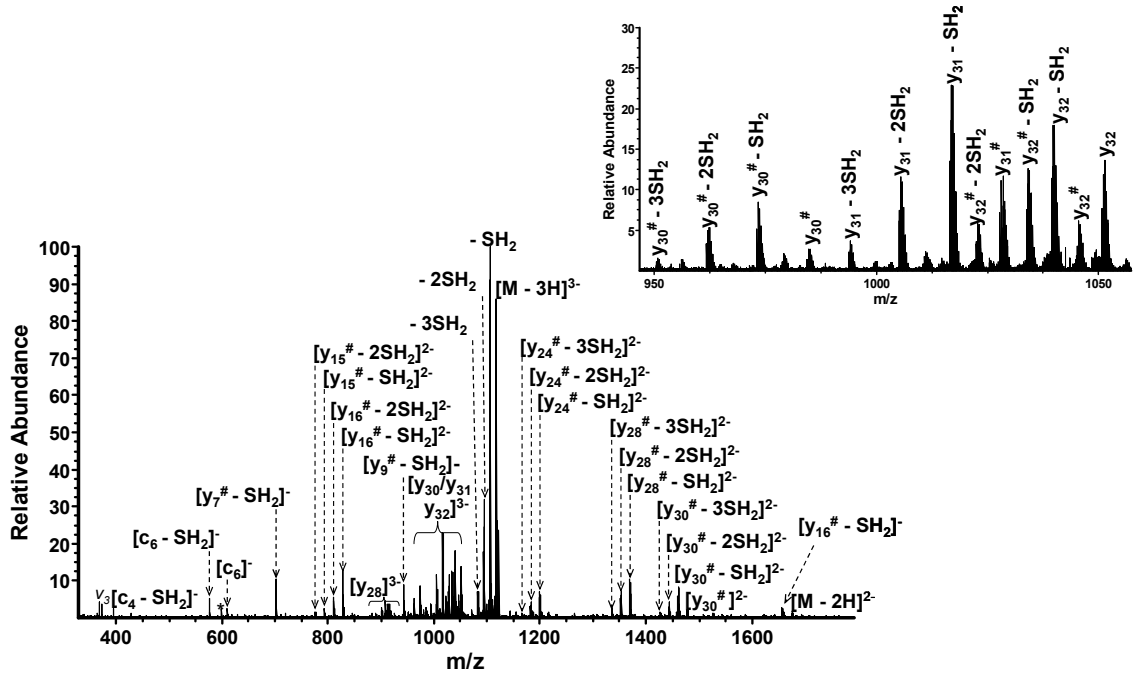

Figure 6.2. CID of the $[M - 3H]^{3-}$ precursor ions of nisin. Similar to IRMPD (Fig. 1), the CID spectrum shows abundant SH_2 losses from the precursor and product ions. Sequential SH_2 losses are shown in the inset. # = NH_3 loss, * = noise peak, v_3 = 3rd harmonic.

It is worth noting that, in IRMPD, the majority of product ions (y_7, y_9, y_{16}, y_{24}, y_{28}, y_{30}, c_4, and c_6) exhibited sequential SH_2 losses equal to the number of constituent thioether bridges. For example, the y_{16} product ion contains 3 thioether bridges and exhibited three SH_2 losses. Another example is the y_{30} product ion, containing 5 thioether bridges and

showing up to 5 SH_2 losses. Although assignment of the exact position of thioether bridges is not straightforward from these data, the SH_2 neutral losses observed in IRMPD can be used for assigning the number of thioether bridges present in lantibiotics. In CID spectra, these SH_2 losses do not correspond to the number of constituent thioether bridges. In CID, a maximum of 3 SH_2 losses were observed from product ions regardless of the number of thioether bridges present. For example, the product ion y_{28}, containing 5 thioether bridges, exhibited 3 SH_2 losses in CID whereas it exhibited 5 SH_2 losses in IRMPD. The absence of these additional sequential SH_2 losses in CID is not unexpected because they derive from secondary fragmentation. Secondary product ions (resulting from multiple bond cleavages) are more easily observed in IRMPD because primary product ions can further absorb IR photons and thereby become further activated to yield secondary product ions. Even though secondary fragmentation is in many cases undesirable (because it can complicate spectral interpretation), it appears useful for lantibiotic characterization because it provides information about the number of thioether bridges present in the molecule.

It is also worth noting that negative ion mode CID of nisin resulted in additional structural information compared to positive ion mode SORI-CID of the same molecule.[36] In positive ion mode SORI-CID, only two out of five thioether bridges were cleaved and fragmentation was mainly observed close to the N- or C-terminus. In negative ion mode, we observed cleavages at all five thioether bridges and several *y*- and *c*-type product ions were detected. Therefore, negative ion mode can be used in combination with positive ion mode to provide complementary information.

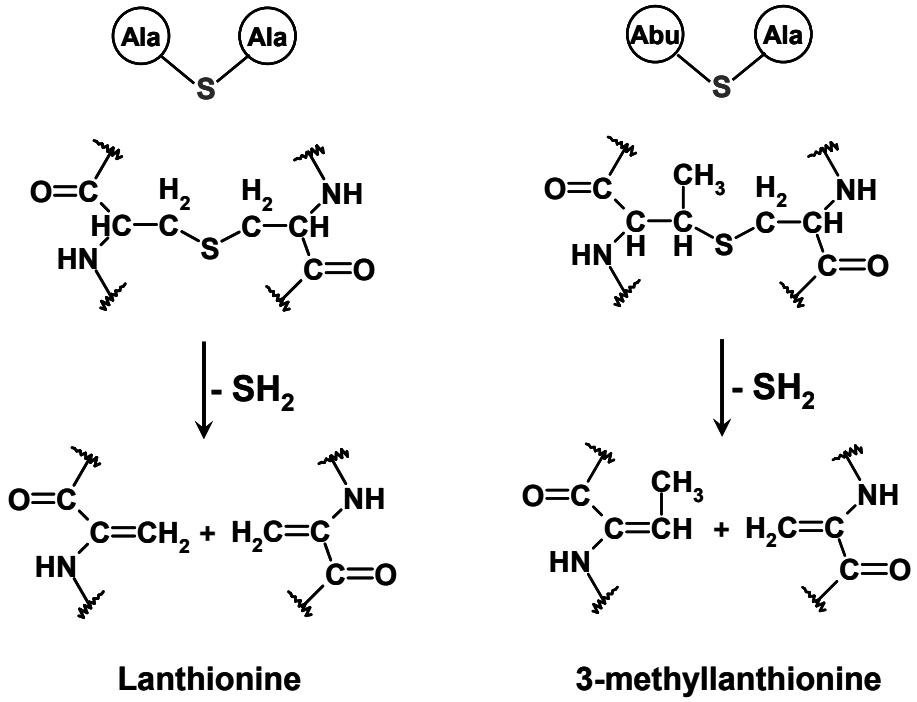

Scheme 6.3. Possible structures of product ions following cleavage of a thioether bridge and SH_2 elimination.

6.3.2. Negative Ion Mode CID and IRMPD of Gallidermin

For gallidermin, $[M - 2H]^{2-}$ precursor ions were selected for fragmentation because this charge state was the most abundant. CID (Figure 6.3A) and IRMPD (Figure 6.3B) fragmentation patterns of gallidermin were very similar to those of nisin. Formation of mainly *y*- and *c*-type product ions was observed, and sequential SH_2 losses from both the precursor and product ions dominated the spectra. Similar to IRMPD of nisin, several product ions (y_{18}, y_{19}, and c_6) from gallidermin exhibited sequential SH_2 losses equal to the number of constituent thioether bridges. By contrast, CID products showed a maximum of 3 SH_2 losses, as observed in CID of nisin.

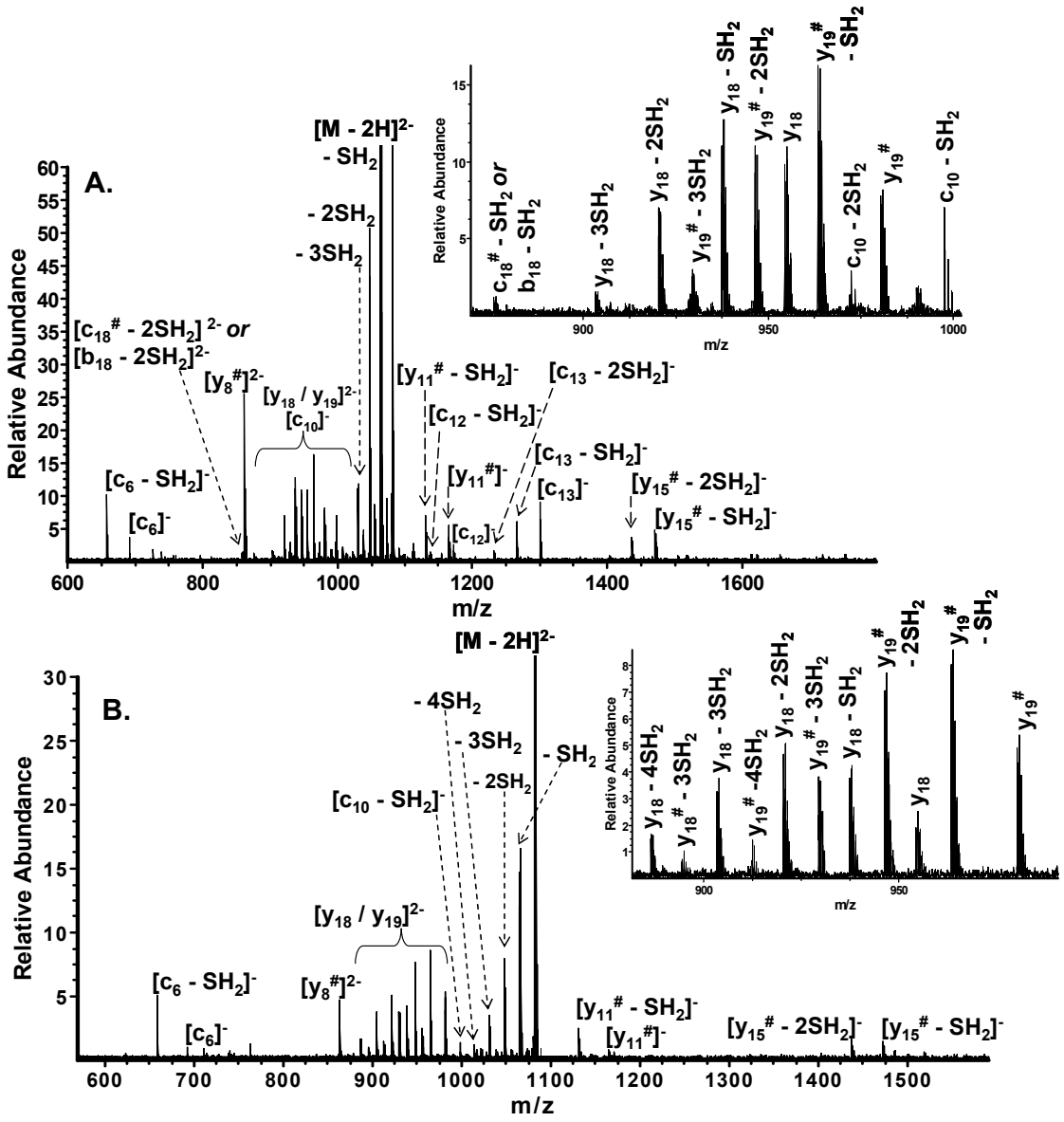

Figure 6.3. CID (A) and IRMPD (B) spectra from the doubly deprotonated precursor ions of gallidermin. Characteristic SH_2 losses due to cleavage of thioether bridges are abundant in both CID and IRMPD. CID resulted in more backbone bond cleavages compared to IRMPD. $^{\#} = NH_3$ loss

For gallidermin, the CID spectrum contains several unique product ions not observed in IRMPD. These product ions correspond mainly to *c*-type fragments, c_{13}, [c_{13} - SH_2], [c_{13} - $2SH_2$], c_{12}, [c_{12} - SH_2], and [c_{10} - $2SH_2$]. The product ions at m/z 875.914

[c_{18} - NH_3 - SH_2 or b_{18} - SH_2] and 858.921 [c_{18} - NH_3 - $2SH_2$ or b_{18} - $2SH_2$] were also observed only in the CID spectrum. These product ions cannot be distinguished based on their masses, however, because we did not detect *b*- type product ions for nisin and, also, because formation of *c*-type product ions is common in negative ion mode,[42] we believe that these ions are most likely *c*-type fragments. Although CID and IRMPD are both "slow heating" activation methods and therefore have many common characteristics, differences between these two dissociation techniques have been previously reported.[67-73] For example, it has been shown that photodissociation of protonated ethanol resulted exclusively in the lowest energy product ion, whereas low energy CID produced a mixture of higher- and lower-energy product ions.[73] These authors suggested that IRMPD is much more energy selective and more discriminative against higher energy fragmentation pathways compared to (SORI)-CID, and that the average energy deposition is smaller in IRMPD. Furthermore, Keller and Brodbelt reported differences between CID and IRMPD spectra of protonated and deprotonated oligonucleotides[70] and Volmer and co-workers reported variation between CID and IRMPD spectra of protonated saxitoxin and neosaxitoxin.[69] Differences between CID and IRMPD spectra were also reported for alkali metal-coordinated oligosaccharides,[71] and it was suggested that, for CID, the larger variations in energy transferred during collisions provide dissociation pathways that are not accessible in IRMPD. In addition, CID and IRMPD of doubly protonated petrobactin showed some differences in fragmentation patterns[67] and it was suggested that these differences may be related to the different activation processes involved in CAD versus IRMPD. Finally, one more factor to be considered is that efficient fragmentation in IRMPD requires good overlap between the laser beam and the

ion cloud. Accomplishing such overlap can be particularly challenging for ions having a large magnetron radius. By contrast, CID is insensitive to ion position.[74]

6.3.3. Negative Ion Mode CID and IRMPD of Duramycin

For duramycin, $[M - 2H]^{2-}$ precursor ions were selected for fragmentation (Figure 6.4.A). In addition to the three thioether bridges, this lantibiotic contains one lysinoalanine bridge (Scheme 6.1.D and Scheme 6.4.A). In CID (Figure 6.4.A) and IRMPD (Figure 6.4.B) of duramycin, the precursor ions exhibited a neutral loss of 36.003 Da instead of 33.988 Da (corresponding to SH_2 loss), suggesting elimination of two hydrogen atoms in addition to the SH_2 loss. We believe that the additional H_2 loss (which was only observed for duramycin) is due to cleavage of the lysinoalanine bridge, as shown in Scheme 6.4. This explanation is in agreement with the observation that two product ions (z_{14} and y_{18} - NH_3 - $3SH_2$) containing the lysinoalanine bridge also exhibited loss of two hydrogen atoms.

For duramycin, less extensive fragmentation was observed in both CID and IRMPD, compared to nisin and gallidermin. Also, *x*-type product ions, which were not observed for nisin and gallidermin, were detected. An additional product ion, detected in both singly and doubly deprotonated form at m/z 1529.586 and 764.296, respectively, and its secondary product ions following one and two SH_2 losses, can be assigned as y_{14} - H_2O or $[z_{14} - 2H]$ based on their masses. Even though we did not detect any *z*-type product ions for the other two lantibiotics examined, this assignment cannot be eliminated because duramycin showed different fragmentation behavior. The x_{17} and y_{18} product ions were only observed in the CID spectrum. Most of the product ions resulting from CID were observed as both singly and doubly deprotonated species whereas, in

IRMPD, only doubly deprotonated product ions were detected. In CID, the most abundant product ion corresponds to a neutral loss of 73.992 Da from the $[M - H]^-$ protonated species. This loss is most likely due to cleavage of the hydroxyaspartic acid side chain (74.000 Da, see Scheme 6.1.E for structure). This product ion was absent in the IRMPD spectrum.

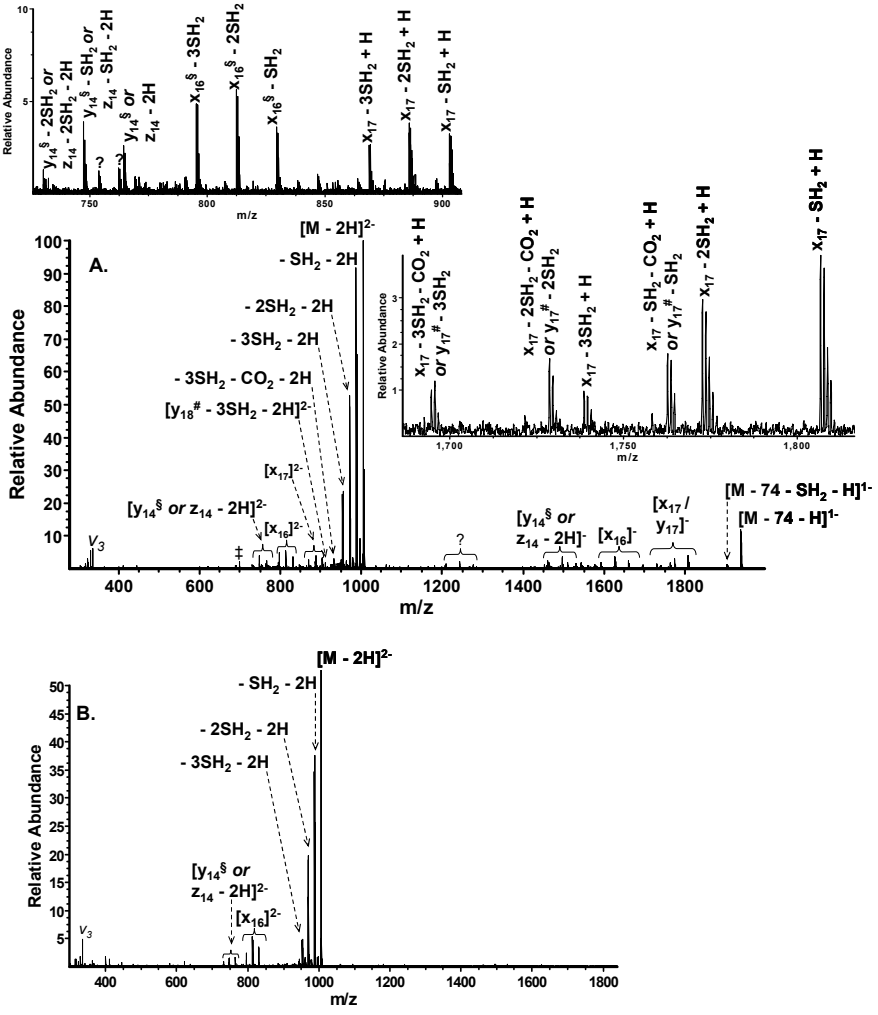

Figure 6.4. CID (A) and IRMPD (B) of the $[M - 2H]^{2-}$ precursor ions from duramycin. The major fragmentation pathway corresponds to cleavage of the thioether bridges, resulting in abundant SH_2 losses. Product ions are shown in detail in the insets. In IRMPD, zoomed-in regions for the y_{14}, z_{14} and x_{16} product ions and their secondary fragments are very similar to CID, as shown in A. # = NH_3 loss, § = water loss, □ = internal product ions, v_3 = 3rd harmonic, ? = unidentified product ions.

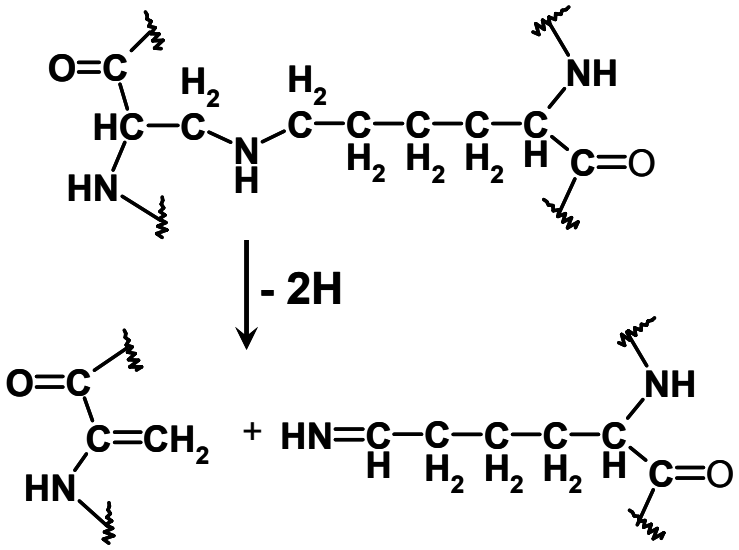

Scheme 6.4. Cleavage of the lysinoalanine bridge and loss of two hydrogen atoms was observed in negative ion mode CID and IRMPD of duramycin.

The results obtained for duramycin are similar to those obtained for ECD of lacticin 481 in that limited fragmentation was observed.[38, 39] Both lacticin 481 and duramycin are less linear molecules compared to, e.g., nisin, for which more extensive fragmentation was observed. Duramycin exhibits a cyclic structure (Scheme 6.1.D) due to the arrangement of the thioether bridges, and the presence of the lysinoalanine bridge, which may hamper its fragmentation. In fact, all product ions observed for duramycin were formed from cleavages close to the N-terminus, which is more accessible.

Although, the fragmentation pattern for duramycin is different compared to those of nisin and gallidermin, sequential SH_2 losses are still present. Assignment of the number of thioether bridges is feasible because the precursor and product ions exhibited up to 3 SH_2 sequential losses, which is equal to the number of constituent thioether bridges.

6.3.4. Negative Ion Mode CID of Oxidized Gallidermin

The CID fragmentation of $[M - 2H]^{2-}$ precursor ions from oxidized gallidermin is shown in Figure 6.5.A Oxidized nisin was not detected in negative ion mode and therefore was not examined. Oxidized duramycin was not available for these experiments.

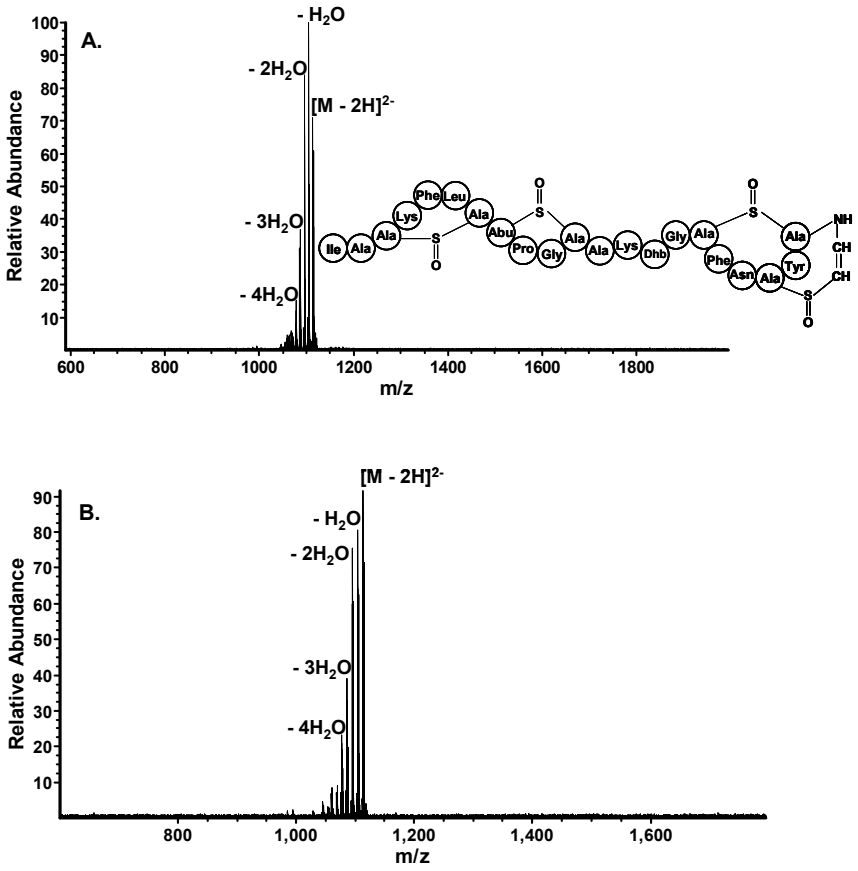

Figure. 6.5. Negative ion mode CID (A) and IRMPD (B) of the $[M - 2H]^{2-}$ precursor ions of oxidized gallidermin. Very limited fragmentation is observed. Water losses are observed from the oxidized thioether bridges. The structure of oxidized gallidermin is also shown in A.

Following CID of the oxidized molecule of gallidermin only limited fragmentation is observed with no backbone bond cleavages. This behavior is in stark contrast to non-oxidized gallidermin (see above). These results indeed show that oxidation of the

thioether bridges significantly affects the fragmentation behavior. The main fragmentation pathway for oxidized gallidermin anions corresponds to abundant neutral H_2O losses. We propose two different pathways for this water elimination: First, an oxidized thioether bridge may be cleaved but retain the sulfur atom on either one of the two carbons linked by the bridge (Scheme 6.5.A), or ejection of water may occur without cleavage of the oxidized thioether bridge (Scheme 6.5.B). Water loss is commonly observed from Asp, Glu, Thr, and Ser residues, however, gallidermin does not contain any of these residues. Furthermore, we observed four water losses, which are equal to the number of oxidized thioether bridges, strongly suggesting that these water losses originate from the oxidized thioether bridges. The same fragmentation pattern was observed in IRMPD (Figure 6.5.B). Structural information for oxidized gallidermin could not be obtained from negative ion mode CID or IRMPD due to the limited fragmentation observed, however, the stark differences in fragmentation patterns between non-oxidized and oxidized lantibiotics may be useful for easily distinguishing between these two forms.

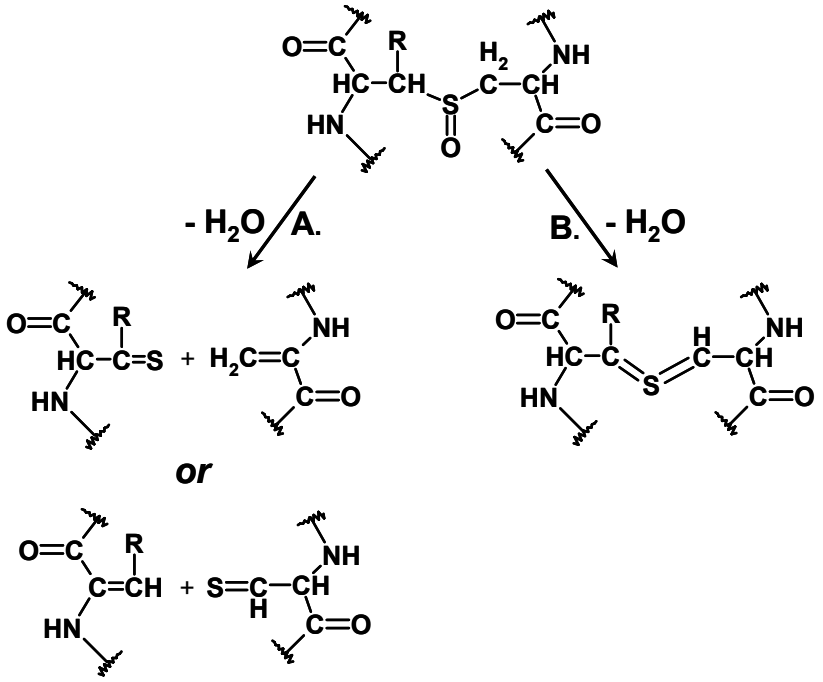

Scheme 6.5. Ejection of water from an oxidized thioether bridge may proceed A) by cleavage of the thioether bridge or B) without cleavage of the thioether bridge. In both cases double bonds are formed between the thioether sulfur atom and a neighboring carbon. R = CH_3 or H.

6.3.5. Positive Ion Mode CID and IRMPD of Oxidized Gallidermin

Because negative ion mode CID and IRMPD of gallidermin resulted in limited fragmentation, we decided to examine whether positive ion mode provides more structural information for oxidized lantibiotics. Such experiments have, to our knowledge, not been previously reported. The CID spectrum of the $[M + 3H]^{3+}$ precursor ions from oxidized gallidermin is displayed in Figure 6.6. A complete list of detected product ions is shown in Table 6.1. Similar to negative ion mode CID, positive ion mode CID resulted in sequential water losses from the precursor ions. However, in addition to these abundant water losses, positive ion mode resulted in several backbone bond cleavages that provide sequence information for this molecule. A series of *b*-type (b_4, b_6, b_8, b_{10}, b_{11}, b_{13}, b_{14}, b_{15}, b_{16}, b_{18}) and also several *y*-type (y_6, y_7, y_8, y_{11}, y_{13} (not shown in

Figure 6.6, see Table 6.1*)*, and y_{19}*)* product ions are observed. The b_{13} and b_{14} product ions were detected as b_{13} / [b_{13} - 2H], and b_{14} / [b_{14} - 2H], whereas the y_6 product ion was solely detected as [y_6 - 2H]. The majority of product ions were detected with accompanying single and multiple water losses. Neutral losses of –OH and –SOH were also accompanying some product ions. We propose that these neutral losses both originate from the oxidized thioether bridges. Hydroxyl loss may occur via elimination of the oxygen atom of the thioether bridge and a neighboring hydrogen atom whereas –SOH loss may involve elimination of the oxidized thioether SO group and a neighboring hydrogen atom. Possible structures of the corresponding products are shown in Scheme 6.6. These mechanisms are supported by the fact that these neutral losses were observed from product ions originating from cleavage between two thioether bridges.

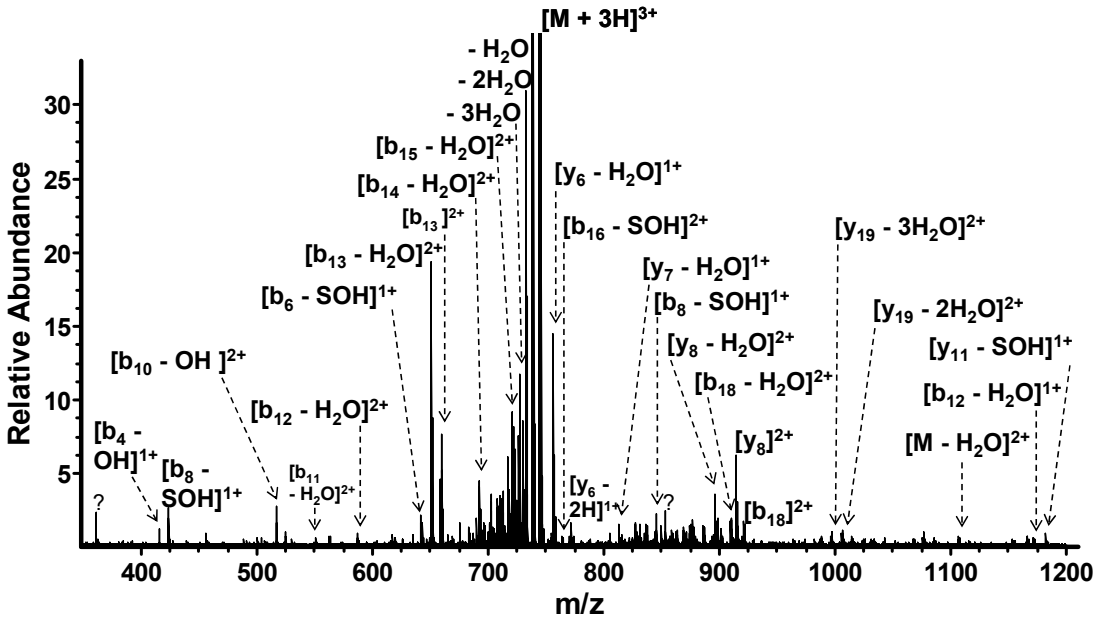

Figure.6.6. Positive ion mode CID of triply protonated oxidized gallidermin. Oxidized thioether bridges exhibit characteristic -SOH and -OH losses from the product ions. Water losses from oxidized thioether bridges are also prevalent. Not all product ions are labeled in Figure. For a complete list of all generated product ions refer to Table 6.1. $^{?}$ = unidentified product ions.

IRMPD (Table 6.2) of oxidized gallidermin resulted in less extensive fragmentation compared to CID. Several product ions (y_6, y_7, y_{11}, y_{13}, y_{19}, b_4, b_6, b_{10}, b_{11}, b_{12}, b_{14}, b_{16}) observed in CID were not detected in the IRMPD spectrum. Interestingly, the same trend, i.e., more extensive backbone bond cleavage in CID compared to IRMPD, was also observed in negative ion mode fragmentation of gallidermin. The characteristic loss of SOH from the oxidized thioether bridges was present following IRMPD, however, the OH loss was absent. These results are consistent with previous data suggesting that CID and IRMPD may provide complementary structural information even though they are both slow heating activation techniques.[68, 70, 75]

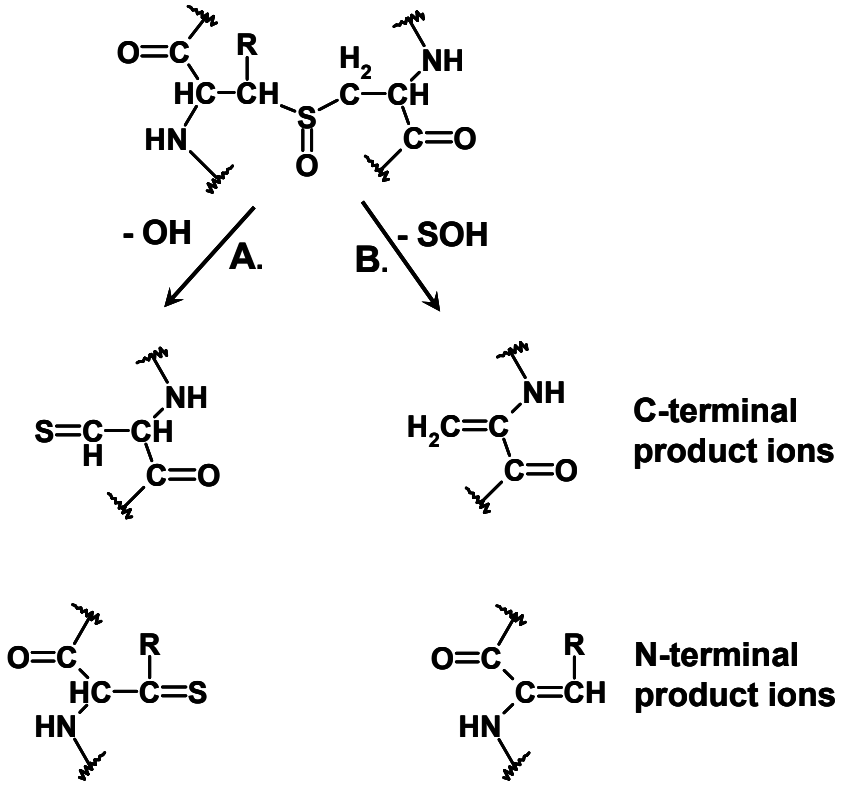

Scheme 6.6. Possible structures of product ions formed after cleavage of an oxidized thioether bridge and A) elimination of -OH, or B) elimination of -SOH.

Table 6.1. Product ions observed in CID of triply protonated precursor ions of oxidized gallidermin

Observed m/z	Theoretical m/z	Assignment	Error (ppm)
1181.4537	1181.4503	y_{11} - SOH	-2.9
1170.5464	1170.5441	b_{12} - H_2O	-2.0
1105.9731	1105.9676	M - H_2O	-4.9
1013.9010	1013.9070	y_{19} - H_2O	5.9
1004.8983	1004.9017	y_{19} - $2H_2O$	3.4
995.8954	995.8964	y_{19} - $3H_2O$	1.0
908.9029	908.9024	b_{18} - H_2O	-0.5
	913.2967	y_8	Calibrant
917.9090	917.9077	b_{18}	-1.5
986.8851	986.8911	y_{19} - $4H_2O$	6.1
895.2861	895.2861	y_8 - H_2O	0.0
876.4127	876.4113	b_8 - OH	-1.6
858.4066	858.4010	b_8 - OH - H_2O	-6.6
844.4391	844.4391	b_8 - SOH	0.0
830.2624	830.2596	y_7	-3.4
826.4292	826.4285	b_8 - SOH - H_2O	-0.9
812.2485	812.2490	y_7 - H_2O	0.6
771.2245	771.2219	y_6 - 2H	-3.4
763.3678	763.3685	b_{16} - SOH	0.9
	743.6510	$[M + 3H]^{3+}$	Calibrant
755.2284	755.2275	y_6 - H_2O	-1.2
737.6477	737.6475	M - H_2O	-0.3
731.6443	731.6440	M - $2H_2O$	-0.4
725.6411	725.6404	M - $3H_2O$	-0.9
728.8577	728.8578	b_{15}	0.2
719.6361	719.6369	M - $4H_2O$	1.2
719.8528	719.8525	b_{15} - H_2O	-0.4
700.3474	700.3471	b_{14}	-0.4
699.3406	699.3393	b_{14} - 2H	-1.9
691.3426	691.3417	b_{14}- H_2O	-1.3
682.3361	682.3364	b_{14} - $2H_2O$	0.5
674.3693	674.3701	b_6 - OH	1.2
668.2655	668.2659	y_{13} - SOH	0.6
658.8281	658.8285	b_{13}	0.6
657.8210	657.8207	b_{13} - 2H	-0.4
649.8233	649.8229	b_{13} - H_2O	-0.6
642.3976	642.3974	b_6 - SOH	-0.3
640.8181	640.8176	b_{13} - $2H_2O$	-0.8
585.7764	585.7757	b_{12} - H_2O	-1.3
550.2581	550.2571	b_{11} - H_2O	-1.8
523.7440	523.7439	b_{10} - H	-0.3
515.7465	515.7464	b_{10} - OH	-0.2
499.7618	499.7604	b_{10} - SOH	-2.8
422.7236	422.7232	b_8 - SOH	-1.0
414.2176	414.2176	b_4 - OH	0.1

Table 6.2. Product ions observed in IRMPD of triply protonated precursor ions of oxidized gallidermin

Observed m/z	Theoretical m/z	Assignment	Error (ppm)
	1114.9729	$[M + 4H]^{4+}$	Calibrant
1105.9628	1105.9676	$M - H_2O$	4.3
913.2923	913.2816	y_8	-11.8
895.2855	895.2861	$y_8 - H_2O$	0.7
884.9132	884.9186	$b_{18} - SO - H_2O$	6.1
755.2294	755.2275	$y_6 - H_2O$	-2.5
	743.6510	$[M + 3H]^{3+}$	Calibrant
737.6481	737.6475	$M - H_2O$	-0.8
731.6445	731.6440	$M - 2H_2O$	-0.6
728.8568	728.8578	b_{15}	1.4
725.6410	725.6404	$M - 3H_2O$	-0.9
719.6372	719.6369	$M - 4H_2O$	-0.4
719.8527	719.8525	$b_{15} - H_2O$	-0.3
710.8481	710.8469	$b_{15} - 2H_2O$	-1.7
691.3424	691.3417	$b_{14} - H_2O$	-1.0
682.3357	682.3364	$b_{14} - 2H_2O$	1.1
657.8229	657.8207	$b_{13} - 2H$	-3.3
649.8248	649.8229	$b_{13} - H_2O$	-2.9
640.8202	640.8176	$b_{13} - 2H_2O$	-4.0
633.8374	633.8369	$b_{13} - SOH - H$	-0.8
624.8320	624.8316	$b_{13} - SOH - H - H_2O$	-0.6
619.2007	619.1969	$y_5 - SOH - H_2O - NH_3$	-6.1
585.7775	585.7757	$b_{12} - H_2O$	-3.1
422.7273	422.7232	$b_8 - SOH$	-9.8

6.3.6. Positive Ion Mode CID and IRMPD of Oxidized Nisin

CID and IRMPD of oxidized nisin showed very similar fragmentation patterns. Complete lists of product ions detected in CID and IRMPD of the $[M + 5H]^{5+}$ precursor ions are displayed in Tables 6.3 and 6.4 respectively. Figure 6.7 shows the IRMPD spectrum of the $[M + 5H]^{5+}$ species. Similar to gallidermin, neutral water losses from both the precursor and product ions dominate both CID and IRMPD spectra of nisin. Some backbone product ions (y_{21}, y_{30}, y_{31}, y_{32}, y_{33}, b_3, b_4, b_{13}, and b_{32}) are also observed, providing sequence information. The product ions $[b_{32} - H_2O]^{4+}$ and $[y_{32} - 3H_2O]^{4+}$, detected at m/z = 804.350, cannot be distinguished based on their masses. One additional *b*-type product ion, b_2, was detected in IRMPD but was absent in the CID spectrum.

Furthermore, the characteristic -SO and -OH losses from the thioether bridges (Scheme 6.6), observed for oxidized gallidermin, are also present in nisin MS/MS spectra.

Table 6.3. Product ions observed in CID of the $[M + 5H]^{5+}$ precursor ions of oxidized nisin

Observed m/z	Theoretical m/z	Assignment	Error (ppm)
866.8848	866.8848	$[M + 4H]^{4+}$	Calibrant
862.3822	862.3821	$M - H_2O$	-0.1
838.6124	838.6138	y_{33}	1.7
834.1113	834.1112	$y_{33} - H_2O$	-0.1
857.8821	857.8795	$M - 2H_2O$	-3.0
853.3739	853.3768	$M - 3H_2O$	3.4
829.8559	829.8545	$y_{33} - H_2O - NH_3$	-1.7
825.3537	825.3519	$y_{33} - 2H_2O - NH_3$	-2.2
820.8508	820.8492	$y_{33} - 3H_2O - NH_3$	-2.0
816.3503	816.3466	$y_{33} - 4H_2O - H_2O$	-4.6
813.3546	813.3519	$y_{32} - H_2O$	-3.3
808.8513	808.8492	$y_{32} - 2H_2O$	-2.5
808.6065	808.6005	$b_{32} - H_2O$	-7.5
804.3491	804.3465	$y_{32} - 3H_2O$	-3.3
804.3491	804.3439	$b_{32} - H_2O - NH_3$	-6.5
799.8482	799.8439	$y_{32} - 4H_2O$	-5.4
796.0959	796.0965	$y_{31} - OH$	0.8
791.5912	791.5938	$y_{31} - OH - H_2O$	3.2
787.0911	787.0912	$y_{31} - OH - 2H_2O$	0.2
767.8252	767.8255	$y_{30} - OH$	0.4
763.3235	763.3228	$y_{30} - OH - H_2O$	-0.9
758.8204	758.8202	$y_{30} - OH - 2H_2O$	-0.3
754.3165	754.3175	$y_{30} - OH - 3H_2O$	1.3
733.9761	733.9791	y_{21}	4.1
727.9761	727.9756	$y_{21} - H_2O$	-0.7
721.9704	721.9721	$y_{21} - 2H_2O$	2.3
	693.7093	M + 5H	
690.1065	690.1072	$M - H_2O$	1.0
686.5051	686.5051	$M - 2H_2O$	-0.1
682.9026	682.9029	$M - 3H_2O$	0.4
679.2998	679.3008	$M - 4H_2O$	1.5
675.6954	675.6987	$M - 5H_2O$	4.9
664.0853	664.0851	$y_{33} - NH_3 - H_2O$	-0.2
660.4828	660.4830	$y_{33} - NH_3 - 2H_2O$	0.3
615.2946	615.2943	$b_{13} - SOH - H_2O$	-0.5
379.2335	379.2346	$b_4 - SOH$	2.9
266.1491	266.1505	b_3 -SOH	5.4

Table 6.4. Product ions observed in IRMPD of the $[M + 5H]^{5+}$ precursor ions of oxidized nisin

Observed m/z	Theoretical m/z	Assignment	Error (ppm)
	866.8848	M + 4H	Calibrant
862.3812	862.3821	M - H_2O	1.0
834.1107	834.1112	y33 - H_2O	0.6
857.8783	857.8795	M - $2H_2O$	1.4
853.3785	853.3768	M - $3H_2O$	-1.9
848.8727	848.8742	M - $4H_2O$	1.8
834.3593	834.3572	y_{33} - NH_3	-2.5
829.8547	829.8545	y_{33} - H_2O - NH_3	-0.2
825.3528	825.3519	y_{33} - $2H_2O$ - NH_3	-1.1
820.8481	820.8492	y_{33} - $3H_2O$ - NH_3	1.3
816.3475	816.3466	y_{33} - 4H2O - NH_3	-1.1
813.3516	813.3519	y_{32} - H_2O	0.3
811.8463	811.8439	y_{33} - $5H_2O$ - NH_3	-3.0
808.8499	808.8492	y_{32} - $2H_2O$	-0.9
808.5943	808.6005	b_{32} - H_2O	7.7
804.3504	804.3465	y_{32} - $3H_2O$	-4.9
804.3504	804.3439	b_{32} - H_2O - NH_3	-8.1
799.8441	799.8439	y_{32} - $4H_2O$	-0.3
791.5936	791.5938	y_{31} - OH - H_2O	0.2
787.0934	787.0912	y_{31} - OH - $2H_2O$	-2.9
782.5870	782.5885	y_{31} - OH - $3H_2O$	1.9
767.8258	767.8255	y_{30} - OH	-0.3
763.3227	763.3228	y_{30} - OH - H_2O	0.1
758.8184	758.8202	y_{30} - OH - $2H_2O$	2.3
754.3171	754.3175	y_{30} - OH - $3H_2O$	0.5
749.8147	749.8149	y_{30} - OH - $4H_2O$	0.3
745.5588	745.5582	y_{30} - OH - $4H_2O$ - NH3	-0.8
733.9806	733.9791	y_{21} - OH	-2.1
727.9725	727.9756	y_{21} - OH - H_2O	4.2
721.9716	721.9721	y_{21} - OH - $2H_2O$	0.7
	693.7093	M + 5H	Calibrant
690.1070	690.1072	M - H_2O	0.3
686.5052	686.5051	M - $2H_2O$	-0.1
682.9032	682.9029	M - $3H_2O$	-0.5
679.3009	679.3008	M - $4H_2O$	-0.2
675.6970	675.6987	M - $5H_2O$	2.6
664.0852	664.0851	y_{33} - NH_3 - H_2O	-0.2
660.4818	660.4830	y_{33} - NH_3 - $2H_2O$	1.8
656.8814	656.8809	y_{33} - NH_3 - $3H_2O$	-0.8
653.2775	653.2787	y_{33} - NH_3 - $4H_2O$	1.9
615.2952	615.2943	b_{13} - SOH - H_2O	-1.4
266.1506	266.1505	b_3 - SOH	-0.2
379.2347	379.2346	b_4 - SOH	-0.4
197.1288	197.1285	b_2	-1.6

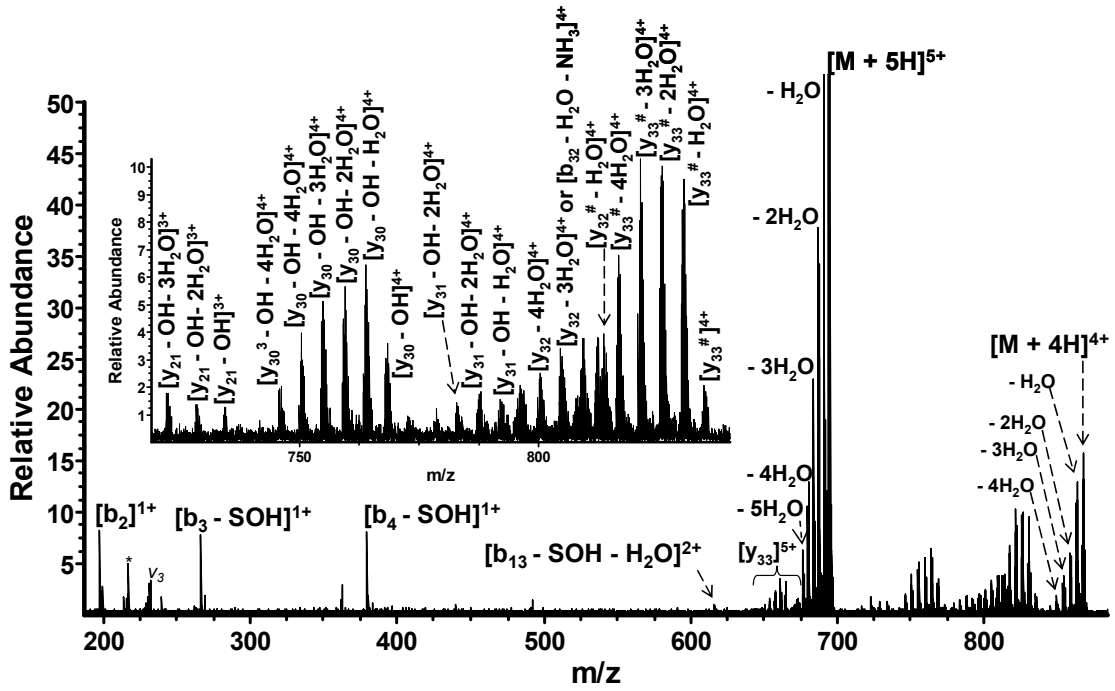

Figure 6.7. IRMPD of the $[M + 5H]^{5+}$ precursor ions of oxidized nisin. Product ions corresponding to cleavage of the oxidized thioether bridges are detected. Not all product ions are labeled in the Figure, see Table 6.4 for a complete list of all generated product ions. * = noise peak, $v_3 = 3^{rd}$ harmonic. # = NH_3 loss.

The $[M +6H]^{6+}$ precursor ions of nisin were also subjected to fragmentation with IRMPD and the results are summarized in Table 6.5. Only minor differences were observed between the IRMPD spectrum of this charge state as compared to CID and IRMPD of the $[M +5H]^{5+}$ precursor ions. More specifically, the product ions [b_{13} - SO - H - H_2O], [y_{31} - OH - H_2O], [y_{31} - OH - $2H_2O$], and [y_{31} - OH - $3H_2O$], were not detected in IRMPD of the $[M + 6H]^{6+}$ precursor ions.

Table. 6.5. Product ions observed in IRMPD of the $[M + 6H]^{6+}$ precursor ions of oxidized nisin

Observed m/z	Theoretical m/z	Assignment	Error (ppm)
829.8544	829.8545	$y_{33} - H_2O - NH_3$	0.2
825.3529	825.3519	$y_{33} - 2H_2O - NH_3$	-1.2
820.8516	820.8492	$y_{33} - 3H_2O - NH_3$	-2.9
816.3492	816.3466	$y_{33} - 4H_2O - NH_3$	-3.2
813.3527	813.3519	$y_{32} - H_2O$	-1.0
804.3550	804.3465	$y_{32} - 3H_2O$	-10.6
804.3550	804.3439	$b_{32} - H_2O - NH_3$	-13.8
866.8848		$[M + 4H]^{4+}$	Calibrant
862.3835	862.3821	M - H2O	-1.6
857.8785	857.8795	$M - 2H_2O$	1.1
767.8248	767.8255	$y_{30} - OH$	1.0
763.3247	763.3228	$y_{30} - OH - H_2O$	-2.5
758.8177	758.8202	$y_{30} - OH - 2H_2O$	3.3
754.3207	754.3175	y_{30} -OH - $3H_2O$	-4.3
749.8170	749.8149	y_{30}- OH - $4H_2O$	-2.8
733.9822	733.9791	$y_{21} - OH$	-4.3
727.9768	727.9756	$y_{21} - OH - H_2O$	-1.6
721.9712	721.9721	$y_{21} - OH - 2H_2O$	1.2
578.2590		$[M + 6H]^{6+}$	Calibrant
575.2575	575.2572	$M - H_2O$	-0.5
572.2558	572.2554	$M - 2H_2O$	-0.7
569.2542	569.2537	$M - 3H_2O$	-0.8
566.2532	566.2519	$M - 4H_2O$	-2.2
553.5727	553.5721	$y_{33} - H_2O - NH_3$	-1.1
664.0848	664.0851	$y_{33} - H_2O - NH_3$	0.5
660.4831	660.4830	$y_{33} - 2H_2O - NH_3$	-0.2
656.8812	656.8809	$y_{33} - 3H_2O - NH_3$	-0.5
653.2786	653.2787	$y_{33} - 4H_2O - NH_3$	0.1
649.6753	649.6766	$y_{33} - 5H_2O - NH_3$	2.0
693.7094	693.7093	$[M + 5H]^{5+}$	-0.1
690.1071	690.1072	$M - H_2O$	0.1
686.5057	686.5051	$M - 2H_2O$	-0.8
682.9036	682.9029	$M - 3H_2O$	-1.0
679.2987	679.3008	$M - 4H_2O$	3.1
675.6998	675.6987	$M - 5H_2O$	-1.6
614.4632	614.4618	$y_{30} - OH$	-2.3
610.8608	610.8597	$y_{30} - OH - H_2O$	-1.9
607.2584	607.2576	y_{30} -OH - $2H_2O$	-1.4
379.2343	379.2346	b_4 - SOH	0.8
266.1500	266.1505	b_3 - SOH	1.8
197.1284	197.1285	b_2	0.4

6.4. Conclusions

We have investigated the fragmentation patterns of native and oxidized lantibiotics in CID and IRMPD. These experiments revealed that lantibiotics exhibit characteristic sequential SH_2 losses, originating from the thioether bridges, in negative ion mode CID and IRMPD. In IRMPD, the majority of product ions exhibited sequential SH_2 losses equal to the number of constituent thioether bridges. Therefore, this tandem mass spectrometric technique can be applied to newly discovered lantibiotics for determination of thioether bridges.

Following oxidation of thioether bridges, we observed limited fragmentation in negative ion mode CID and IRMPD. However, oxidized lantibiotics showed extensive fragmentation in positive ion mode. Neutral losses corresponding to –OH and –SOH elimination were characteristic of the oxidized thioether bridges. The differences in fragmentation patterns observed between native and oxidized lantibiotics may be used to easily distinguish between these two forms. In some cases, CID resulted in more backbone bond cleavages, resulting in more structural information, compared to IRMPD. However, IRMPD of non-oxidized lantibiotics provided information about the exact number of thioether bridges. Therefore, use of both CID and IRMPD for the characterization of lantibiotics would yield the maximum amount of information.

The experiments presented here provide insights into the fragmentation behavior of native and oxidized lantibiotics and allow us to be able to predict their fragmentation pathways, assisting the use of tandem mass spectrometric techniques for the characterization of these unique peptides.

6.5. References

1. Willey, J. M.; van der Donk, W. A., Lantibiotics: Peptides of diverse structure and function. *Annu. Rev. Microbiol.* **2007,** 61, 477-501.
2. Nagao, J. I.; Asaduzzaman, S. M.; Aso, Y.; Okuda, K.; Nakayama, J.; Sonomoto, K., Lantibiotics: Insight and foresight for new paradigm. *J. Biosci. Bioeng.* **2006,** 102, 139-149.
3. Patton, G. C.; van der Donk, W. A., New developments in lantibiotic biosynthesis and mode of action. *Curr. Opin. Microbiol.* **2005,** 8, 543-551.
4. Xie, L. L.; van der Donk, W. A., Post-translational modifications during lantibiotic biosynthesis. *Curr. Opin. Chem. Biol.* **2004,** 8, 498-507.
5. Sahl, H.-G.; Bierbaum, G., Lantibiotics: Biosynthesis and biological activities of uniquely modified peptides from gram-positive bacteria. *Annu. Rev. Microbiol.* **1998**, 41-79.
6. Jack, R. W.; Sahl, H. G., Unique Peptide Modifications Involved in the Biosynthesis of Lantibiotics. *Trends Biotechnol.* **1995,** 13, 269-278.
7. Ingram, L., Ribosomal Mechanism for Synthesis of Peptides Related to Nisin. *Biochim. Biophys. Acta* **1970,** 224, 263-265.
8. van Kraaij, C.; Breukink, E.; Rollema, H. S.; Bongers, R. S.; Kosters, H. A.; de Kruijff, B.; Kuipers, O. P., Engineering a disulfide bond and free thiols in the lantibiotic nisin Z. *Eur. J. Biochem.* **2000,** 267, 901-909.
9. Bierbaum, G.; Szekat, C.; Josten, M.; Heidrich, C.; Kempter, C.; Jung, G.; Sahl, H. G., Engineering of a novel thioether bridge and role of modified residues in the lantibiotic pep5. *Appl. Environ. Microbiol.* **1996,** 62, 385-392.
10. van Kraaij, C.; de Vos, W. M.; Siezen, R. J.; Kuipers, O. P., Lantibiotics: biosynthesis, mode of action and applications. *Nat. Prod. Rep.* **1999,** 16, 575-587.
11. DelvesBroughton, J., Nisin and Its Uses as a Food Preservative. *Food Technol.* **1990,** 44, 100-117.
12. DelvesBroughton, J.; Blackburn, P.; Evans, R. J.; Hugenholtz, J., Applications of the bacteriocin, nisin. *Anton van Leeuwwenhoek Int. J. Gen. Microbiol.* **1996,** 69, 193-202.
13. Hansen, J. N., Nisin as a Model Food Preservative. *Crit. Rev. Food Sci. Nutr.* **1994,** 34, 69-93.
14. Rayman, M. K.; Aris, B.; Hurst, A., Nisin - a Possible Alternative or Adjunct to Nitrite in the Preservation of Meats. *Appl. Environ. Microbiol.* **1981,** 41, 375-380.
15. Thuault, D.; Beliard, E.; Leguern, J.; Bourgeois, C. M., Inhibition of Clostridium-Tyrobutyricum by Bacteriocin-Like Substances Produced by Lactic-Acid Bacteria. *J. Dairy Sci.* **1991,** 74, 1145-1150.
16. Piard, J. C.; Delorme, F.; Giraffa, G.; Commissaire, J.; Desmazeaud, M., Evidence for a Bacteriocin Produced by Lactococcus-Lactis Cnrz-481. *Neth. Milk Dairy J.* **1990,** 44, 143-158.
17. Chatterjee, S.; Chatterjee, D. K.; Jani, R. H.; Blumbach, J.; Ganguli, B. N.; Klesel, N.; Limbert, M.; Seibert, G., Mersacidin, a New Antibiotic from Bacillus Invitro and Invivo Antibacterial Activity. *J. Antibiot.* **1992,** 45, 839-845.

18. Jung, G., Lantibiotics - Ribosomally Synthesized Biologically-Active Polypeptides Containing Sulfide Bridges and Alpha-Beta-Didehydroamino Acids. *Angew. Chem. Int. Ed. Engl.* **1991,** 30, 1051-1068.
19. Gross, E.; Morell, J. L., Structure of Nisin. *J. Am. Chem. Soc.* **1971,** 93, 4634-4635.
20. Gross, E.; Morell, J. L., Nisin - Assignment of Sulfide Bridges of Beta-Methyllanthionine to a Novel Bicyclic Structure of Identica6 Ring Size. *J. Am. Chem. Soc.* **1970,** 92, 2919-2920.
21. Meyer, H. E.; Heber, M.; Eisermann, B.; Korte, H.; Metzger, J. W.; Jung, G., Sequence-Analysis of Lantibiotics - Chemical Derivatization Procedures Allow a Fast Access to Complete Edman Degradation. *Anal. Biochem.* **1994,** 223, 185-190.
22. Martin, N. I.; Sprules, T.; Carpenter, M. R.; Cotter, P. D.; Hill, C.; Ross, R. P.; Vederas, J. C., Structural characterization of lacticin 3147, a two-peptide lantibiotic with synergistic activity. *Biochemistry* **2004,** 43, 3049-3056.
23. Chatterjee, C.; Paul, M.; Xie, L. L.; van der Donk, W. A., Biosynthesis and mode of action of lantibiotics. *Chem. Rev.* **2005,** 105, 633-683.
24. Freund, S.; Jung, G.; Gutbrod, O.; Folkers, G.; Gibbons, W. A.; Allgaier, H.; Werner, R., The Solution Structure of the Lantibiotic Gallidermin. *Biopolymers* **1991,** 31, 803-811.
25. Lian, L. Y.; Chan, W. C.; Morley, S. D.; Roberts, G. C. K.; Bycroft, B. W.; Jackson, D., Solution Structures of Nisin-a and Its 2 Major Degradation Products Determined by Nmr. *Biochem. J.* **1992,** 283, 413-420.
26. Slijper, M.; Hilbers, C. W.; Konings, R. N. H.; Vandeven, F. J. M., Nmr-Studies of Lantibiotics Assignment of the H-1-Nmr Spectrum of Nisin and Identification of Interresidual Contacts. *FEBS Lett.* **1989,** 252, 22-28.
27. vandenHooven, H. W.; Doeland, C. C. M.; vandeKamp, M.; Konings, R. N. H.; Hilbers, C. W.; vandeVen, F. J. M., Three-dimensional structure of the lantibiotic nisin in the presence of membrane-mimetic micelles of dodecylphosphocholine and of sodium dodecylsulphate. *Eur. J. Biochem.* **1996,** 235, 382-393.
28. Vandeven, F. J. M.; Vandenhooven, H. W.; Konings, R. N. H.; Hilbers, C. W., Nmr-Studies of Lantibiotics - the Structure of Nisin in Aqueous-Solution. *Eur. J. Biochem.* **1991,** 202, 1181-1188.
29. Zimmermann, N.; Freund, S.; Fredenhagen, A.; Jung, G., Solution Structures of the Lantibiotics Duramycin-B and Duramycin-C. *Eur. J. Biochem.* **1993,** 216, 419-428.
30. Kettenring, J. K.; Malabarba, A.; Vekey, K.; Cavalleri, B., Sequence Determination of Actagardine, a Novel Lantibiotic, by Homonuclear 2d Nmr-Spectroscopy. *J. Antibiot.* **1990,** 43, 1082-1088.
31. Jack, R. W.; Carne, A.; Metzger, J.; Stefanovic, S.; Sahl, H. G.; Jung, G.; Tagg, J., Elucidation of the Structure of Sa-Ff22, a Lanthionine-Containing Antibacterial Peptide Produced by Streptococcus-Pyogenes Strain Ff22. *Eur. J. Biochem.* **1994,** 220, 455-462.
32. Smith, L.; Novak, J.; Rocca, J.; McClung, S.; Hillman, J. D.; Edison, A. S., Covalent structure of mutacin 1140 and a novel method for the rapid identification of lantibiotics. *Eur. J. Biochem.* **2000,** 267, 6810-6816.

33. Smith, L.; Zachariah, C.; Thirumoorthy, R.; Rocca, J.; Novak, J.; Hillman, J. D.; Edison, A. S., Structure and dynamics of the lantibiotic mutacin 1140. *Biochemistry* **2003,** 42, 10372-10384.
34. vandenHooven, H. W.; Lagerwerf, F. M.; Heerma, W.; Haverkamp, J.; Piard, J. C.; Hilbers, C. W.; Siezen, R. J.; Kuipers, O. P.; Rollema, H. S., The structure of the lantibiotic lacticin 481 produced by Lactococcus lactis: Location of the thioether bridges. *FEBS Lett.* **1996,** 391, 317-322.
35. Gauthier, J. W.; Trautman, T. R.; Jacobson, D. B., Sustained Off-Resonance Irradiation for Collision-Activated Dissociation Involving Fourier-Transform Mass-Spectrometry - Collision-Activated Dissociation Technique That Emulates Infrared Multiphoton Dissociation. *Anal. Chim. Acta* **1991,** 246, 211-225.
36. Lavanant, H.; Derrick, P. J.; Heck, A. J. R.; Mellon, F. A., Analysis of nisin A and some of its variants using Fourier transform ion cyclotron resonance mass spectrometry. *Anal. Biochem.* **1998,** 255, 74-89.
37. Lavanant, H.; Heck, A.; Derrick, P. J.; Mellon, F. A.; Parr, A.; Dodd, H. M.; Giffard, C. J.; Horn, N.; Gasson, M. J., Characterisation of genetically modified nisin molecules by Fourier transform ion cyclotron resonance mass spectrometry. *Eur. Mass Spectrom.* **1998,** 4, 405-416.
38. Kleinnijenhuis, A. J.; Duursma, M. C.; Breukink, E.; Heeren, R. M. A.; Heck, A. J. R., Localization of intramolecular monosulfide bridges in lantibiotics determined with electron capture induced dissociation. *Anal. Chem.* **2003,** 75, 3219-3225.
39. Kleinnijenhuis, A. J.; Heck, A. J. R.; Duursma, M. C.; Heeren, R. M. A., Does double electron capture lead to the formation of biradicals? An ECD-SORI-CID study on lacticin 481. *J. Am. Soc. Mass Spectrom.* **2005,** 16, 1595-1601.
40. Bigwarfe, P. M.; Wood, T. D., Effect of ionization mode in the analysis of proteolytic protein digests. *Int. J. Mass Spectrom.* **2004,** 234, 185-202.
41. Jai-nhuknan, J.; Cassady, C. J., Negative ion postsource decay time-of-flight mass spectrometry of peptides containing acidic amino acid residues. *Anal. Chem.* **1998,** 70, 5122-5128.
42. Ewing, N. P.; Cassady, C. J., Dissociation of multiply charged negative ions for hirudin (54-65), fibrinopeptide B, and insulin A (oxidized). *J. Am. Soc. Mass Spectrom.* **2001,** 12, 105-116.
43. Deguchi, K.; Ito, H.; Takegawa, Y.; Shinji, N.; Nakagawa, H.; Nishimura, S. I., Complementary structural information of positive- and negative-ion MSn spectra of glycopeptides with neutral and sialylated N-glycans. *Rapid Commun. Mass Spectrom.* **2006,** 20, 741-746.
44. Hua, Y. S.; Wainhaus, S. B.; Yang, Y. N.; Shen, L. X.; Xiong, Y. S.; Xu, X. Y.; Zhang, F. G.; Bolton, J. L.; van Breemen, R. B., Comparison of negative and positive ion electrospray tandem mass spectrometry for the liquid chromatography tandem mass spectrometry analysis of oxidized deoxynucleosides. *J. Am. Soc. Mass Spectrom.* **2001,** 12, 80-87.
45. Steinborner, S. T.; Bowie, J. H., A comparison of the positive- and negative-ion mass spectra of bio-active peptides from the dorsal secretion of the Australian red tree frog, Litoria rubella. *Rapid Commun. Mass Spectrom.* **1996,** 10, 1243-1247.

46. Chrisman, P. A.; McLuckey, S. A., Dissociations of disulfide-linked gaseous polypeptide/protein anions: Ion chemistry with implications for protein identification and characterization. *J. Proteome Res.* **2002,** 1, 549-557.
47. Kalli, A.; Hakansson, K., Preferential cleavage of S-S and C-S bonds in electron detachment dissociation and infrared multiphoton dissociation of disulfide-linked peptide anions. *Int. J. Mass Spectrom.* **2007,** 263, 71-81.
48. Janek, K.; Wenschuh, H.; Bienert, M.; Krause, E., Phosphopeptide analysis by positive and negative ion matrix-assisted laser desorption/ionization mass spectrometry. *Rapid Commun. Mass Spectrom.* **2001,** 15, 1593-1599.
49. Yagami, T.; Kitagawa, K.; Futaki, S., Liquid Secondary-Ion Mass-Spectrometry of Peptides Containing Multiple Tyrosine-O-Sulfates. *Rapid Commun. Mass Spectrom.* **1995,** 9, 1335-1341.
50. Kellner, R.; Jung, G.; Horner, T.; Zahner, H.; Schnell, N.; Entian, K. D.; Gotz, F., Gallidermin - a New Lanthionine-Containing Polypeptide Antibiotic. *Eur. J. Biochem.* **1988,** 177, 53-59.
51. Hayashi, F.; Nagashima, K.; Terui, Y.; Kawamura, Y.; Matsumoto, K.; Itazaki, H., The Structure of Pa48009 - the Revised Structure of Duramycin. *J. Antibiot.* **1990,** 43, 1421-1430.
52. Chowdhury, S. M.; Munske, G. R.; Ronald, R. C.; Bruce, J. E., Evaluation of low energy CID and ECD fragmentation behavior of mono-oxidized thio-ether bonds in peptides. *J. Am. Soc. Mass Spectrom.* **2007,** 18, 493-501.
53. Steen, H.; Mann, M., Similarity behween condensed phase and gas phase chemistry: Fragmentation of peptides containing oxidized cysteine residues and its implications for proteomics. *J. Am. Soc. Mass Spectrom.* **2001,** 12, 228-232.
54. Betancourt, L.; Takao, T.; Gonzalez, J.; Reyes, O.; Besada, V.; Padron, G.; Shimonishi, Y., The metastable decomposition of a peptide containing oxidized methionine(s) in matrix-assisted laser desorption ionization time-of-flight mass spectrometry. *Rapid Commun. Mass Spectrom.* **1999,** 13, 1075-1076.
55. Jiang, X. Y.; Smith, J. B.; Abraham, E. C., Identification of a MS-MS fragment diagnostic for methionine sulfoxide. *J. Mass Spectrom.* **1996,** 31, 1309-1310.
56. Lagerwerf, F. M.; vandeWeert, M.; Heerma, W.; Haverkamp, J., Identification of oxidized methionine in peptides. *Rapid Commun. Mass Spectrom.* **1996,** 10, 1905-1910.
57. Reid, G. E.; Roberts, K. D.; Kapp, E. A.; Simpson, R. J., Statistical and mechanistic approaches to understanding the gas-phase fragmentation behavior of methionine sulfoxide containing peptides. *J. Proteome Res.* **2004,** 3, 751-759.
58. Yang, J.; Mo, J. J.; Adamson, J. T.; Hakansson, K., Characterization of oligodeoxynucleotides by electron detachment dissociation Fourier transform ion cyclotron resonance mass spectrometry. *Anal. Chem.* **2005,** 77, 1876-1882.
59. Senko, M. W.; Canterbury, J. D.; Guan, S. H.; Marshall, A. G., A high-performance modular data system for Fourier transform ion cyclotron resonance mass spectrometry. *Rapid Commun. Mass Spectrom.* **1996,** 10, 1839-1844.
60. Ledford, E. B.; Rempel, D. L.; Gross, M. L., Space-Charge Effects in Fourier-Transform Mass-Spectrometry - Mass Calibration. *Anal. Chem.* **1984,** 56, 2744-2748.

61. Fredenhagen, A.; Fendrich, G.; Marki, F.; Marki, W.; Gruner, J.; Raschdorf, F.; Peter, H. H., Duramycin-B and Duramycin-C, 2 New Lanthionine Containing Antibiotics as Inhibitors of Phospholipase-A2 - Structural Revision of Duramycin and Cinnamycin. *J. Antibiot.* **1990,** 43, 1403-1412.
62. Allgaier, H.; Jung, G.; Werner, R. G.; Schneider, U.; Zahner, H., Elucidation of the Structure of Epidermin, a Ribosomally Synthesized, Tetracyclic Heterodetic Polypeptide Antibiotic. *Angew. Chem. Int. Ed.* **1985,** 24, 1051-1053.
63. Allgaier, H.; Jung, G.; Werner, R. G.; Schneider, U.; Zahner, H., Epidermin - Sequencing of a Heterodet Tetracyclic 21-Peptide Amide Antibiotic. *Eur. J. Biochem.* **1986,** 160, 9-22.
64. Bilusich, D.; Brinkworth, C. S.; Bowie, J. H., Negative ion mass spectra of Cys-containing peptides. The characteristic Cys gamma backbone cleavage: a joint experimental and theoretical study. *Rapid Commun. Mass Spectrom.* **2004,** 18, 544-552.
65. Bilusich, D.; Brinkworth, C. S.; McAnoy, A. M.; Bowie, J. H., The fragmentations of [M-H](-) anions derived from underivatised peptides. The side-chain loss of H2S from Cys. A joint experimental and theoretical study. *Rapid Commun. Mass Spectrom.* **2003,** 17, 2488-2494.
66. Waugh, R. J.; Bowie, J. H.; Gross, M. L., Collision-Induced Dissociations of Deprotonated Peptides - Dipeptides Containing Methionine or Cysteine. *Rapid Commun. Mass Spectrom.* **1993,** 7, 623-625.
67. Liu, H. C.; Hakansson, K.; Lee, J. Y.; Sherman, D. H., Collision-activated dissociation, infrared multiphoton dissociation, and electron capture dissociation of the Bacillus anthracis siderophore petrobactin and its metal ion complexes. *J. Am. Soc. Mass Spectrom.* **2007,** 18, 842-849.
68. Crowe, M. C.; Brodbelt, J. S., Infrared multiphoton dissociation (IRMPD) and collisionally activated dissociation of peptides in a quadrupole ion trap with selective IRMPD of phosphopeptides. *J. Am. Soc. Mass Spectrom.* **2004,** 15, 1581-1592.
69. Sleno, L.; Volmer, D. A.; Kovacevic, B.; Maksic, Z. B., Gas-phase dissociation reactions of protonated saxitoxin and neosaxitoxin. *J. Am. Soc. Mass Spectrom.* **2004,** 15, 462-477.
70. Keller, K. M.; Brodbelt, J. S., Collisionally activated dissociation and infrared multiphoton dissociation of oligonucleotides in a quadrupole ion trap. *Anal. Biochem.* **2004,** 326, 200-210.
71. Xie, Y. M.; Lebrilla, C. B., Infrared multiphoton dissociation of alkali metal-coordinated oligosaccharides. *Anal. Chem.* **2003,** 75, 1590-1598.
72. Goolsby, B. J.; Brodbelt, J. S., Tandem infrared multiphoton dissociation and collisionally activated dissociation techniques in a quadrupole ion trap. *Anal. Chem.* **2001,** 73, 1270-1276.
73. Tonner, D. S.; McMahon, T. B., Consecutive infrared multiphoton dissociations in a Fourier transform ion cyclotron resonance mass spectrometer. *Anal. Chem.* **1997,** 69, 4735-4740.
74. Laskin, J.; Futrell, J. H., Activation of large ions in FT-ICR mass spectrometry. *Mass Spectrom. Rev.* **2005,** 24, 135-167.

75. Zhang, J. H.; Schubothe, K.; Li, B. S.; Russell, S.; Lebrilla, C. B., Infrared multiphoton dissociation of O-linked mucin-type oligosaccharides. *Anal. Chem.* **2005,** 77, 208-214.

Chapter 7

Conclusions and Prospects for Future Work

7.1 Purpose of Dissertation

Mass spectrometry has become the method of choice for protein identification and characterization in proteomics research due to its sensitivity, high mass accuracy, and its ability to analyze complex protein samples from cells, tissues, and organisms.[1-5] Most proteomics approaches utilize the bottom-up approach for protein identification.[6-11] In this approach, proteins are digested with a sequence-specific protease, such as trypsin, Lys C, Glu C, or chymotrypsin. The resulting proteolytic peptides are analyzed by tandem mass spectrometry to provide sequence information for protein identification via database searches.

Successful and confident protein identification by database searching relies heavily on the extent and quality of the obtained sequence information generated by MS/MS.[12-14] The greater the number of product ions generated and detected in tandem mass spectra, the greater the peptide sequence coverage and, thus, the greater the probability of a

correct identification. Furthermore, the higher the peptide sequence coverage, the higher the probability of detecting the presence of PTMs.

For complete protein characterization it is particularly important to determine the presence and location of PTMs.[15] Disulfide bond formation, although not as widely examined in tandem mass spectrometry as phosphorylation and glycosylation, is a post-translational modification present in many extracellular proteins. However, disulfide bonds show only limited fragmentation in positive ion mode CID.

De novo sequencing of peptides is a promising tool for identification and characterization of proteins not present in databases, for proteins with incomplete genomic sequence, or for error-containing databases. Furthermore, *de novo* sequencing is essential for revealing information about splice variants, mutations, and modifications that are not apparent from databases. However, as mentioned in Chapter 1, *de novo* sequencing by mass spectrometry remains a challenge because it requires cleavage between each pair of amino acids and detection of all generated products. The development of electron based fragmentation techniques, ECD and EDD, has shown great promise for PTM analysis and improved peptide sequence coverage.

Lantibiotics are ribosomally synthesized and post-translationally modified peptide antimiocrobial agents that are produced by Gram-positive bacteria.[16, 17] The amount of amino acid modifications present in lantibiotics is extraordinarily high and these modifications are generally unique. These modifications include formation of thioether bridges, lanthionine and 3-methyllanthionine, formation of lysinoalanine bridges, 2,3-didehydroalanine (Dha), (*Z*)-2-3,-didehydrobutyrine (Dhb), and β-hydroxy-aspartate. Lantibiotics research is rapidly expanding because these molecules display antimicrobial

activity against Gram-positive bacteria, such as *streptococci*, *bacilli*, *listariea*, *clostridia*, and *staphylococci*, and they are usually several orders of magnitude more potent than traditional antibiotics, such as penicillin.[18, 19] Therefore, they have the potential of becoming the new generation of antibiotics. However, the presence of thioether bridges and unusual amino acids complicates their structural elucidation. More often a combination of peptide chemistry, mass spectrometry and NMR spectrscopy is required to reveal their structure.

The main purpose of this dissertation was to examine the utility of gas phase ion-electron reactions for peptide sequencing and disulfide bond determination by FT-ICR mass spectrometry. Moreover, we examined factors, such as precursor ion charge state, m/z ratio, peptide mass, and protease selection, that influence the dissociation outcome in electron capture dissociation aiming to improve peptide sequence coverage. Advantages of improved peptide sequence coverage are improved protein identification via database searches, increased probability of detecting PTMs, and facilitation of *de novo* sequencing. Finally, dissociation via vibrational excitation was investigated for structural elucidation of native and oxidized lantibiotics.

7.2. Summary of Results

The formation of disulfide linkages in proteins is an important PTM process leading to stabilization of protein structure. The fragmentation behavior of disulfide bonded peptides was examined in EDD and negative ion mode IRMPD. EDD resulted in preferential and facile cleavage of S-S and C-S bonds in most cases examined. However, when multiple disulfide linkages are present, as is the case for insulin, EDD did not provide any detectable disulfide bond cleavage. Fragmentation in IRMPD was more

consistent showing strongly favored cleavage of both S-S and C-S bonds in all peptides examined. In EDD, the resulting product ions were mainly radical species whereas, in IRMPD, only even electron species were formed, as expected. These observations suggest that the mechanism of disulfide bond cleavage is different in these two fragmentation processes. We also showed that the presence of tryptophan residues can compete with disulfide bond cleavage in EDD and result in abundant loss of the tryptophan side chain. This behavior correlates with the vertical ionization energies of a disulfide bond and of tryptophan. Tryptophan has the lowest ionization energy of all amino acids (7.07-11.61 eV, depending on its conformation)[20] whereas the ionization energy of disulfide bonds is 8.46-9.1 eV.[21] We proposed that direct electron detachment from the disulfide bonds, or from tryptophan, can occur and initiate dissociation. In IRMPD, the presence of tryptophan had no effect on disulfide bond cleavage, once again supporting that different fragmentation mechanisms are involved in EDD and IRMPD. Nevertheless, both dissociation techniques can be useful for probing disulfide bonding in peptide anions.

Most bottom-up proteomics approaches rely on tryptic doubly protonated peptides for generating sequence information. However, the effectiveness, in terms of peptide sequence coverage, of tryptic doubly protonated peptides in ECD remained to be characterized. We performed for the first time a systematic comparison of ECD of doubly versus triply protonated peptides generated from trypsin, chymotrypsin, and Glu-C digestion. We showed that tryptic peptides resulted in higher degree of peptide sequence coverage compared to chymotryptic and Glu-C digest peptides, particularly in the case of doubly protonated species. Furthermore, our findings demonstrate that ECD

of triply protonated precursor ions significantly increases the number of *c*- and *z*-type product ions, thereby providing greater peptide sequence coverage and greater number of complementary fragment pairs as compared to doubly protonated species. More specifically, ECD of triply protonated precursor ions increased peptide sequence coverage by 26% and the number of complementary fragment pairs increased by 44% compared to ECD of doubly protonated species. The higher number of complementary fragment pairs and the higher degree of sequence coverage obtained from triply protonated species can improve protein identification via data base searches and facilitate *de novo* sequencing.

When comparing ECD of doubly and triply protonated species we also observed that, for doubly protonated species, the ECD peptide sequence coverage decreased with increasing precursor ion m/z ratio. For triply protonated species at the m/z ratios we examined we did not observe a strong correlation between precursor ion m/z value and ECD peptide sequence coverage. Furthermore, as mentioned above, higher ECD peptide sequence coverage was obtained for triply protonated species. Based on these observations, the next step was to examine whether triply protonated species at higher m/z values show decreased ECD peptide sequence coverage, and also to examine the fragmentation behavior of medium size (i.e., 1600-4800 Da) proteolytic peptides, generated by Lys C, Lys N and Glu C digestion, detected at higher charge states (+4, +5, and +6). With these experiments, we aimed to examine how precursor ion charge state, m/z ratio, and protease selection affects the ECD outcome.

Our results revealed that the major factor determining a successful ECD outcome is the precursor ion m/z ratio. Triply protonated species detected at m/z ratios>960 showed

decreased ECD sequence coverage whereas triply protonated precursor ions at m/z<960 fragment efficiently in ECD. The majority of precursor ions carrying four, five, and six charges were detected at low m/z ratios and exhibited good to high ECD sequence coverage.

In summary, 82% of the peptides we examined showed high ECD peptide sequence coverage ranging from 70-100% whereas 13% of the examined peptides showed a moderate sequence coverage ranging from 50-60%. Only 5% of the peptides examined showed an average peptide sequence coverage below 50% and these were all triply protonated species detected at high m/z values. Furthermore, the average peptide sequence coverage we obtained for Lys N and Glu C generated peptides was 81% and, for Lys C derived peptides, we obtained an average sequence coverage of 80%. The extent of fragmentation, measured by the total number of *c*- and *z*-type productt ions, was also very similar for Lys N, Lys C and Glu C digest peptides. These experiments allowed us to gain a better understanding of the ECD fragmentation behavior of proteolytic peptides generated by different proteases, and to explore the strengths and limitations of this technique to most effectively use it for obtaining the highest possible peptide sequence coverage.

MALDI generally produces singly charged ions in contrast to ESI which generates multiply charged ions. ECD and EDD require multiply charged precursor ions because one charge is neutralized upon electron capture or detachment, respectively. Therefore, these two electron based fragmentation techniques are not compatible with MALDI. Furthermore, dissociation of singly charged species is more challenging compared to that of multiply charged precursor ions, and it is often difficult to obtain informative tandem

mass spectra from this type of ions because singly charged precursor ions do not fragment as efficiently as multiply charged precursor ions.

We investigated the possibility of applying medium energy (~10 eV) electron irradiation, EID, for the dissociation of singly deprotonated model peptides and compared the resulting product ion spectra with those obtained in CID of the same species. We observed that fragmentation induced upon electron irradiation is not specific and results in the formation of *b*-, *y*-, *a*-, *c*- and some *x*- and *z*-type product ions, similar to the results obtained upon collision activation. However, significant differences are also observed between EID and CID product ion spectra. Formation of several radical product ions was only detected in EID spectra. Characteristic amino acid side chains losses from the precursor ions, corresponding to side chain loss from Phe, Met, Arg, and Trp residues were always present following EID of peptides containing these amino acid residues whereas these characteristic amino acid side chain losses were not always detected in CID. Furthermore, EID resulted in formation of several new backbone product ions, not detected in CID, thereby providing more extensive fragmentation. Following EID of modified peptides, the majority of product ions retained phosphorylation and sulfation. By contrast, in CID, the majority of product ions did not retain the modification. Therefore, EID not only reveals the presence of phosphorylation, or sulfation, but also identifies its location. The observed differences between EID and CID suggest differences in the manner of activation involved in these two techniques.

One drawback of both negative ion mode CID and EID is the lack of selective fragmentation to produce specific types of product ions. Nevertheless, we demonstrated that EID is a useful fragmentation technique for the dissociation of singly deprotonated

species, and that it provides additional sequence information for such species compared to CID.

We also explored the utility of negative ion mode CID and IRMPD for structural elucidation of native and oxidized lantibiotics. Oxidized lantibiotics were also examined in positive ion mode CID and IRMPD. We demonstrated that thioether bridges are easily cleaved in negative ion mode CID and IRMPD and that characteristic sequential SH_2 neutral losses, originating from lanthionine bridges, were abundant in both spectra. In IRMPD, the majority of product ions exhibited sequential SH_2 losses equal to the number of constituent thioether bridges and, thus, this tandem mass spectrometric technique can be applied to newly discovered lantibiotics for determining the number of thioether bridges present. Following oxidation of the thioether bridges, very limited fragmentation was observed in negative ion CID and IRMPD. In sharp contrast, CID and IRMPD of protonated oxidized precursor ions resulted in extensive fragmentation. The differences in fragmentation patterns observed between native and oxidized lantibiotics can be used to easily distinguish between these two forms. These experiments provided information about the fragmentation behavior of native and oxidized lantibiotics and generated clues for the prediction of their fragmentation pathways, thereby assisting the use of tandem mass spectrometric techniques for structural elucidation of lantibiotics.

7.3. Prospects for Future Work

In Chapter 2, we demonstrated that EDD and IRMPD result in selective and preferential S-S and C-S bond cleavages, thereby allowing determination of disulfide linkages. These experiments were performed on disulfide bonded peptides generated from proteolytic digestion of model proteins. The next step would be to investigate the

utility of EDD and IRMPD for probing disulfide bonds in peptides from biological samples, i.e., peptides generated from proteins extracted from cells or tissues.

Chapters 3 and 4 investigated how precursor ion charge state, precursor ion m/z value, and protease selection affect the ECD outcome. However, ECD is only applicable to positively charged precursor ions. Given that 50% of naturally occurring proteins are acidic, and that peptides containing numerous acidic residues such as Glu or Asp may not be easily detected in positive ion mode, use of negative ion mode would be essential for characterizing acidic peptides and proteins. As mentioned in Chapter 1, EDD is suitable for negatively charged anions and has shown promise for localizing PTMs. However, how precursor ion charge state, precursor ion m/z, and protease selection affect the dissociation outcome is not well established. It would be essential to perform a systematic comparison of the EDD fragmentation behavior of proteolytically derived peptides to examine whether this dissociation technique can be widely applied to proteomics research for obtaining sequence information from acidic proteins.

As illustrated in Chapter 5, EID of singly deprotonated species from model peptides resulted in extensive fragmentation and provided additional information compared to CID of the same species. However, the fragmentation observed upon electron irradiation is not specific and results in formation of mainly *a*-, *b*- ,*y*- and *c*- and also several *z*- and *x*-type product ions. Although the formation of many types of product ions provides a spectrum rich in sequence information, it also complicates spectral interpretation, particularly for unknown species because it is not apparent from which terminus the product ions are generated. A method to distinguish between N-terminal and C-terminal product ions would significantly facilitate spectral interpretation. For example, by

isotope labeling of the N- or C- terminus, C-terminal and N-terminal product ions could be easily distinguished. Silberring and co-workers have used a mixture of acetic anhydride and deuterated acetic anhydride to incorporate a stable isotope label to the N-terminus.[22] This strategy allows labeling of all N-terminal product ions, resulting in simplification and faster interpretation of spectra. A different approach utilizes C-terminal labeling by incorporation of ^{18}O into the C-terminal carboxylic groups formed during enzymatic digestion of proteins.[23, 24] This labeling is achieved by digestion of the protein mixture in $H_2{}^{18}O$ whereas, in the control experiment, the sample is digested in normal H_2O. Several other procedures exist for N- or C- terminal labeling[25] that can be used in combination with EID to distinguish C- from N-terminal product ions in order to simplify spectral interpretation. Furthermore, the utility of EID for dissociation and structural analysis of proteolytically derived peptides should be tested.

Labeling procedures could also be used in combination with ECD to distinguish between *c*- and *z*- type product ions, particularly in cases where *de novo* sequencing is required. So far, no labeling approach has been combined with ECD for distinguishing between N- and C-terminal product ions. In fact, most of the isotope labeling methods have been developed and used for peptide quantitation in combination with CID. However, it has been shown that isotopic labeling could also be used for distinguishing between N- and C-terminal product ions.[26] Recently, a method was introduced in which N- and C-terminal product ions were distinguished based on changes in the relative abundance of *c*- and *z*• product ions produced in consecutive ECD and activated ion ECD. It was demonstrated that, in AI-ECD, the ratio of *c*•/*c* decreases whereas the ratio of *z*•/*z* increases compared to that observed in ECD.[27] A potential alternative method that

could distinguish between *c*- and *z*-type product ions is, as mentioned above, isotope labeling of the N- or C-terminus of proteolytic peptides prior to ECD.

In Chapter 6, we showed that IRMPD of deprotonated lantibiotics can reveal the number of thioether bridges in such molecules. However, a remaining challenge is to determine the precise lanthionine bridge connectivity. For this task, a combination of peptide chemistry and MS/MS is more suitable. It has been demonstrated that treatment with nickel boride, which is a reducing and desulfurizing agent, in the presence of deuterium gas resulted in lanthionine desulfurization with concomitant incorporation of a single deuterium atom at each residue participating in a thioether bridge. Following Edman degradation and mass spectrometry, the locations of the residues participating in lanthionine bridges could be identified based on the deuterium incorporation.[28] While this method is valuable for determining the location of the residues participating in a thioether bridge, it does not reveal the precise lanthionine bridging. We propose digestion of the lantibiotic of interest with a sequence specific protease, or several proteases independently or in combination, to ensure only one lanthionine bridge per proteolytic peptide, followed by reduction with nickel boride in the presence of deuterium gas. The resulting products can then be analyzed by MS/MS, such as ECD or CID, and mass analysis of the product ions can reveal the exact lanthionine bridging. The presence of solely one lanthionine bridge per proteolytic peptide after digestion can be tested in negative ion mode IRMPD as described in Chapter 6.

7.4. References

1. Aebersold, R.; Mann, M., Mass spectrometry-based proteomics. *Nature* **2003,** 422, 198-207.
2. Guerrera, I. C.; Kleiner, O., Application of mass spectrometry in proteomics. *Biosci. Rep.* **2005,** 25, 71-93.
3. Liu, T.; Belov, M. E.; Jaitly, N.; Qian, W. J.; Smith, R. D., Accurate mass measurements in proteomics. *Chem. Rev.* **2007,** 107, 3621-3653.
4. Zubarev, R.; Mann, M., On the proper use of mass accuracy in proteomics. *Mol. Cell. Proteomics* **2007,** 6, 377-381.
5. Link, A. J.; Eng, J.; Schieltz, D. M.; Carmack, E.; Mize, G. J.; Morris, D. R.; Garvik, B. M.; Yates, J. R., Direct analysis of protein complexes using mass spectrometry. *Nat. Biotechnol.* **1999,** 17, 676-682.
6. Aebersold, R.; Goodlett, D. R., Mass spectrometry in proteomics. *Chem. Rev.* **2001,** 101, 269-295.
7. Biemann, K.; Papayannopoulos, I. A., Amino-Acid Sequencing of Proteins. *Acc. Chem. Res.* **1994,** 27, 370-378.
8. Henzel, W. J.; Billeci, T. M.; Stults, J. T.; Wong, S. C.; Grimley, C.; Watanabe, C., Identifying Proteins from 2-Dimensional Gels by Molecular Mass Searching of Peptide-Fragments in Protein-Sequence Databases. *Proc. Natl. Acad. Sci. USA* **1993,** 90, 5011-5015.
9. Mann, M.; Wilm, M., Error Tolerant Identification of Peptides in Sequence Databases by Peptide Sequence Tags. *Anal. Chem.* **1994,** 66, 4390-4399.
10. Qin, J.; Fenyo, D.; Zhao, Y. M.; Hall, W. W.; Chao, D. M.; Wilson, C. J.; Young, R. A.; Chait, B. T., A strategy for rapid, high confidence protein identification. *Anal. Chem.* **1997,** 69, 3995-4001.
11. Yates, J. R., Mass spectrometry and the age of the proteome. *J. Mass Spectrom.* **1998,** 33, 1-19.
12. Baldwin, M. A., Protein identification by mass spectrometry - Issues to be considered. *Mol. Cell. Proteomics* **2004,** 3, 1-9.
13. Kjeldsen, F.; Giessing, A. M. B.; Ingrell, C. R.; Jensen, O. N., Peptide sequencing and characterization of post-translational modifications by enhanced ion-charging and liquid chromatography electron-transfer dissociation tandem mass spectrometry. *Anal. Chem.* **2007,** 79, 9243-9252.
14. Zubarev, R., Protein primary structure using orthogonal fragmentation techniques in Fourier transform mass spectrometry. *Expert Rev. Proteomics* **2006,** 3, 251-261.
15. Mann, M.; Jensen, O. N., Proteomic analysis of post-translational modifications. *Nat. Biotechnol.* **2003,** 21, 255-261.
16. Chatterjee, C.; Paul, M.; Xie, L. L.; van der Donk, W. A., Biosynthesis and mode of action of lantibiotics. *Chem. Rev.* **2005,** 105, 633-683.
17. Sahl, H.-G.; Bierbaum, G., Lantibiotics: Biosynthesis and biological activities of uniquely modified peptides from gram-positive bacteria. *Annu. Rev. Microbiol.* **1998**, 41-79.
18. Jack, R. W.; Sahl, H. G., Unique Peptide Modifications Involved in the Biosynthesis of Lantibiotics. *Trends Biotechnol.* **1995,** 13, 269-278.

19. van Kraaij, C.; de Vos, W. M.; Siezen, R. J.; Kuipers, O. P., Lantibiotics: biosynthesis, mode of action and applications. *Nat. Prod. Rep.* **1999,** 16, 575-587.
20. Dehareng, D.; Dive, G., Vertical ionization energies of alpha-L-amino acids as a function of their conformation: an ab initio study. *Int. J. Mol. Sci.* **2004,** 5, 301-332.
21. Butler, J. J.; Baer, T.; Evans, S. A., Energetics and Structures of Organosulfur Ions - Ch3ssch3+, Ch3ss+, C2h5s+, and Ch2sh+. *J. Am. Chem. Soc.* **1983,** 105, 3451-3455.
22. Noga, M. J.; Lewandowski, J. J.; Suder, P.; Silberring, J., An enhanced method for peptides sequencing by N-terminal derivatization and MS. *Proteomics* **2005,** 5, 4367-4375.
23. Yao, X. D.; Freas, A.; Ramirez, J.; Demirev, P. A.; Fenselau, C., Proteolytic O-18 labeling for comparative proteomics: Model studies with two serotypes of adenovirus. *Anal. Chem.* **2001,** 73, 2836-2842.
24. Mirgorodskaya, O. A.; Kozmin, Y. P.; Titov, M. I.; Korner, R.; Sonksen, C. P.; Roepstorff, P., Quantitation of peptides and proteins by matrix-assisted laser desorption/ionization mass spectrometry using O-18-labeled internal standards. *Rapid Commun. Mass Spectrom.* **2000,** 14, 1226-1232.
25. Leitner, A.; Lindner, W., Current chemical tagging strategies for proteome analysis by mass spectrometry. *J. Chromatogr. B* **2004,** 813, 1-26.
26. Munchbach, M.; Quadroni, M.; Miotto, G.; James, P., Quantitation and facilitated de novo sequencing of proteins by isotopic N-terminal labeling of peptides with a fragmentation directing moiety. *Anal. Chem.* **2000,** 72, 4047-4057.
27. Tsybin, Y. O.; He, H.; Emmett, M. R.; Hendrickson, C. L.; Marshall, A. G., Ion activation in electron capture dissociation to distinguish between N-terminal and C-terminal productions. *Anal. Chem.* **2007,** 79, 7596-7602.
28. Martin, N. I.; Sprules, T.; Carpenter, M. R.; Cotter, P. D.; Hill, C.; Ross, R. P.; Vederas, J. C., Structural characterization of lacticin 3147, a two-peptide lantibiotic with synergistic activity. *Biochemistry* **2004,** 43, 3049-3056.

Appendix A

Measurement of the Intrinsic Deuterium Kinetic Isotope Effect in Glutamate Mutase by Ultra-High Resolution FT-ICR MS

A.1. Introduction

Glutamate mutase belongs to the group of adenosylcobalamin (AdoCbl, coenzyme B_{12})-dependent enzymes that catalyze unusual isomerization reactions involving 1,2 hydrogen atom migration and proceeding through a mechanism involving carbon-based free radical intermediates.[1-6] Radicals are generated by homolysis of the reactive cobalt-carbon bond of the coenzyme to form cob(II)alamin and the 5'-deoxyadenosyl radical. The 5'-deoxyadenosyl radical abstracts the migrating hydrogen from the substrate to form 5'-deoxyadenosine and the substrate radical. The substrate radical then undergoes rearrangement to yield the product radical which is then quenched by hydrogen transfer from 5'-deoxyadenosine to yield the product and regenerate the 5'-deoxyadenosyl radical. In the last step of the reaction, the 5'-deoxyadenosyl radical recombines with the cob(II)alamin to reform the coenzyme and the catalytic cycle is completed.

Kinetic isotope effects (KIE) are one of the most powerful tools for investigating enzyme mechanisms,[7] given that the intrinsic kinetic isotope effect, i.e., the isotope effect undiminished by other isotope-insensitive steps that may contribute to the overall reaction rate, of the chemical step of interest can be measured. Deuterium KIE are widely measured in enzymatic reactions as they provide a useful method to probe enzyme mechanisms.[7] Mass spectrometry can be used to measure deuterium KIEs, however the natural presence of ^{13}C in substrates and products complicate accurate analysis of deuterium context because peaks due to deuterated and ^{13}C containing molecules generally overlap. Because FT-ICR mass spectrometry provides high resolution, it can be used to overcome this limitation. As defined in Chapter 1, resolution refers to the ability to separate two species with closely spaced mass values.

There are two modes of detection in FT-ICR mass spectrometry.[8-10] Most common is the broadband mode, which allows detection over a wide m/z range. The second mode is called heterodyne detection, or narrowband mode, which facilitates the achievement of ultra-high resolution.[9, 10] High resolution is achieved by recording long lived transient (time domain) signals. The number of data points, N, that are required to record a transient of duration T depends on the rate, S, at which data are sampled and is given by the equation $T = N/S$.[9] To digitize a signal without introducing artifacts, the sampling rate, S, must be at least twice the highest frequency that is recorded. The sampling rate is determined by the lowest mass ion that is recorded because the mass to charge ratio is inversely proportional to cyclotron frequency. Narrowband mode detection serves to reduce the frequency of the ICR signal and therefore allowing sampling to occur at a lower rate.[9, 11] As a result, a longer transient can be acquired compared to broadband

mode detection, and, thus, higher resolution can be obtained. In narrowband detection, the image signal is multiplied by a reference frequency that is close to that of the analyte cyclotron frequency. This multiplication produces additional signals at the sum and difference frequencies of the reference and analyte frequencies. The high frequency component is removed with a low pass filter to leave only the difference frequency signal. As a result, the frequency of the original signal is reduced and, thus, it can be sampled at a lower rate. As the sampling rate of narrowband mode decreases, longer transients can be recorded but the detected mass range becomes narrower.

Marshall and co-workers demonstrated that with a 9.4T FT-ICR mass spectrometer operated in narrowband mode, the isotopic fine structure of proteins up to 15.8 kDa could be resolved.[12] For example, for bovine insulin, isotope combinations differing by only 2.5 mDa were successfully resolved. Furthermore, because isotopic fine structure reveals elemental composition directly, the authors were able to determine the number of sulfur atoms solely from the abundance ratio of the resolved ^{34}S peak to the monoisotopic peak.

Baseline resolution of two isobaric 904 Da peptides, RVMRGMR and RSHRGHR, differing by only 0.00045 Da was also achieved by a 9.4T FT-ICR mass spectrometer in narrowband mode.[13] Interestingly the mass difference of these two peptides is less than one electron mass (0.00055 Da).

Negative ion microelectrospray ionization FT-ICR mass spectrometry in broadband mode detection was used to baseline resolve endohedral fullerenes containing ~1% ^4He or ^3He from closely adjacent ^{13}C-containg nuclides of C_{60} itself.[14] More specifically, $^4He@C_{60}^-$ was baseline resolved from $^{13}C_4{}^{12}C_{56}^-$ (Δm =10.8 mDa) and $^3He@C_{60}^-$ was

baseline resolved from $^{13}C_3{}^{12}C_{57}^-$ (Δm =5.96 mDa). Resolution of these species enabled the direct determination of the extent of He incorporation into a fullerene by measuring the mass spectral peak heights.

In the experiments presented here, we measured the intrinsic deuterium KIE in glutamate mutase using methylaspartate, specifically monodeuterated in its methyl group [$^2H_1$]methylaspartate, as the substrate. The 5'-deoxyadenosyl radical, generated by homolysis of AdoCbl, can abstract either a protium or deuterium from the methyl group of the same substrate molecule, to form a mixture of non- and mono-deuterated 5'-deoxyadenosine (5'-dA) (Scheme A1). Hydrogen or deuterium abstraction generates methylasparate radical, which rapidly rearranges to the more stable glutamyl radical so that, at sufficiently short times (< 100 ms), the reaction is effectively irreversible and the intrinsic isotope effect is determined. The mixture of non- and mono-deuterated 5'-dA was detected and analyzed by ultrahigh-resolution FT-ICR MS.

In order to precisely detect the mixture of non- and mono-deuterated 5'-dA, a resolution of 70,000 is required. The mass of $^{12}C_9\ ^1H_{13}\ ^{13}C_1\ ^{14}N_5\ ^{16}O_3$ (second isotopic peak of the non-deuterated species) is 252.10436 Da and the mass of $^{12}C_{10}\ ^1H_{12}\ ^2D_1\ ^{14}N_5\ ^{16}O_3$ (first isotopic peak of the mono-deuterated species) is 252.10799 Da. The mass difference (Δm) between these two species is 3.6 mDa and, therefore, the resolution can be calculated by dividing the mass of the non-deuterated species with this mass difference: m/Δm = 252.10436/0.00363 = 69,450.

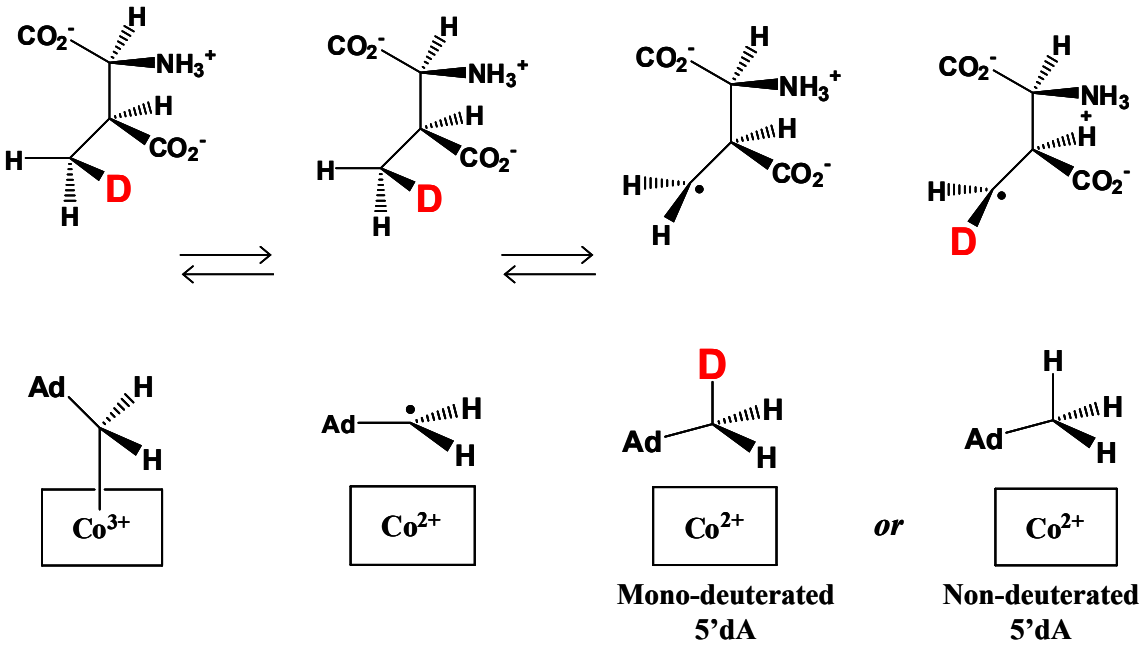

Scheme A1. Reaction between monodeuterated methylaspartate and glutamate mutase. The 5'-deoxyadenosyl radical, generated by homolysis of AdoCbl, can abstract either a protium or deuterium from the methyl group of the same substrate molecule, to form a mixture of non- and mono-deuterated 5'-deoxyadenosine, which can be detected by ultra-high resolution FT-ICR mass spectrometry.

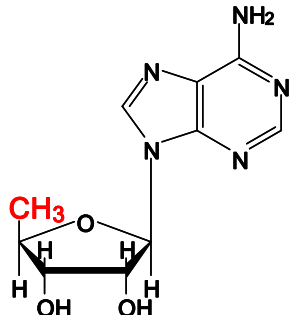

CH_3-Ad

Figure A1. Structure of 5'-deoxyadenosine (5'-dA).

A.2. Experimental Procedures

A.2.1 Sample preparation

Rapid quench experiments were performed at 10 °C with a Hi-Tech RQF-63 apparatus. 73.5 μL of 275 μM glutamate mutase in 50 mM potassium phosphate buffer (pH 7.0) was immediately mixed with 6.5 μL of 3.4 mM AdoCbl before the experiment to reconstitute the holoenzyme. The holoenzyme mixture was reacted with 80 μL of 2.2 mM [$^{2}H_{1}$]methylaspartate in 50 mM potassium phosphate buffer (pH 7.0). The reactions were quenched with 80 μL of 2.5% trifluoroacetic acid after aging for various times (28 - 76 ms). 5'-dA was purified by C_{18} reverse-phase HPLC, concentrated to dryness and stored at -20 °C prior to mass analysis. All the procedures were conducted in dim red light.

A.2.2 Mass Spectrometry

5'-dA was redissolved in an electrospray solvent containing 50% MeOH (Fisher Scientific, Fair Lawn, NJ) and 0.1% formic acid (Acros Organics, Morris Plains, NJ). Experiments were performed in positive ion mode at 50 μL/h with a 7T Q-FT-ICR mass spectrometer (Bruker Daltonics, Billerica, MA), which has been previously described.[15] Data were collected in narrowband mode. The masses of [$^{12}C_{9}$ $^{1}H_{13}$ $^{13}C_{1}$ $^{14}N_{5}$ $^{16}O_{3}$]5'-dA and [$^{12}C_{10}$ $^{1}H_{12}$ $^{2}D_{1}$ $^{14}N_{5}$ $^{16}O_{3}$ 5'-dA] are 252.10436Da and 252.10799Da, respectively: a mass difference of 3.6 mDa. The identities of the peaks due to unlabeled, ^{13}C-labeled, and ^{2}H-labeled 5'-dA were confirmed by examining a sample of commercially available 5'-dA (Sigma, St Louis, MO) under the same experimental conditions. Only the lower m/z peak was observed for nondeuterated 5'-dA, whereas two peaks, ($^{12}C_{9}$ $^{1}H_{13}$ $^{13}C_{1}$ $^{14}N_{5}$ $^{16}O_{3}$ and $^{12}C_{10}$ $^{1}H_{12}$ $^{2}D_{1}$ $^{14}N_{5}$ $^{16}O_{3}$), were seen following incubation in 1% D_2O. The experimental masses of the enzymatic samples compare accurately (<2ppm) with the

masses of the standards and the calculated theoretical masses. As internal control, the instrument was tuned to ensure that the detected relative abundance of ^{12}C-5'-dA to ^{13}C-5'-dA was as close as possible to the calculated ratio of 0.1324.

A.3. Results and Discussion

A.3.1. Broadband versus Narrowband Detection Mode

Broadband and narrowband detection modes were compared for commercially available 5'-dA, and for samples from enzymatic reactions. Examples are given in Figures A.1. and A.2. The resolving power (m/Δm, where m represents the ionic mass and Δm is the mass spectral peak width at half maximum peak height) for the peak of interest is also indicated in these figures. For broadband mode, data were collected using 512 K data points whereas 128K data points were used for narrowband mode. As can be seen from Figures A.1.A and A.1.B, higher mass resolving power is obtained in narrowband mode. Narrowband mode detection resulted in a mass resolving power of ~560,000, for the $^{12}C_9{}^{1}H_{13}{}^{13}C_1{}^{14}N_5{}^{16}O_3$ peak whereas the mass resolving power obtained in broadband mode was ~106,000.

Similar trends were observed for an enzymatic sample collected after 55.8 ms reaction time (Figures A.2.A and B). In this Figure, only peaks of interest, the non-deuterated peak ($^{12}C_9{}^{1}H_{13}{}^{13}C_1{}^{14}N_5{}^{16}O_3$, second isotopic peak) and the mono-deuterated peak ($^{12}C_{10}{}^{1}H_{12}{}^{2}D_1{}^{14}N_5{}^{16}O_3$), are displayed. Similar to the results obtained for commercially available 5'dA, higher resolving power was achieved in narrowband mode. For example, with broadband detection, a mass resolving power of ~93,000 and ~87,000 was obtained for the $^{12}C_9{}^{1}H_{13}{}^{13}C_1{}^{14}N_5{}^{16}O_3$ and $^{12}C_{10}{}^{1}H_{12}{}^{2}D_1{}^{14}N_5{}^{16}O_3$ peaks, respectively, whereas, in narrowband mode, a mass resolving power of ~321,000 and ~299,000 was

obtained for the non-deuterated and mono-deuterated peaks, respectively. Furthermore, the two peaks of interest are better baseline resolved in narrowband mode detection. Based on these observations, we performed the rest of the experiments presented here with narrowband mode detection.

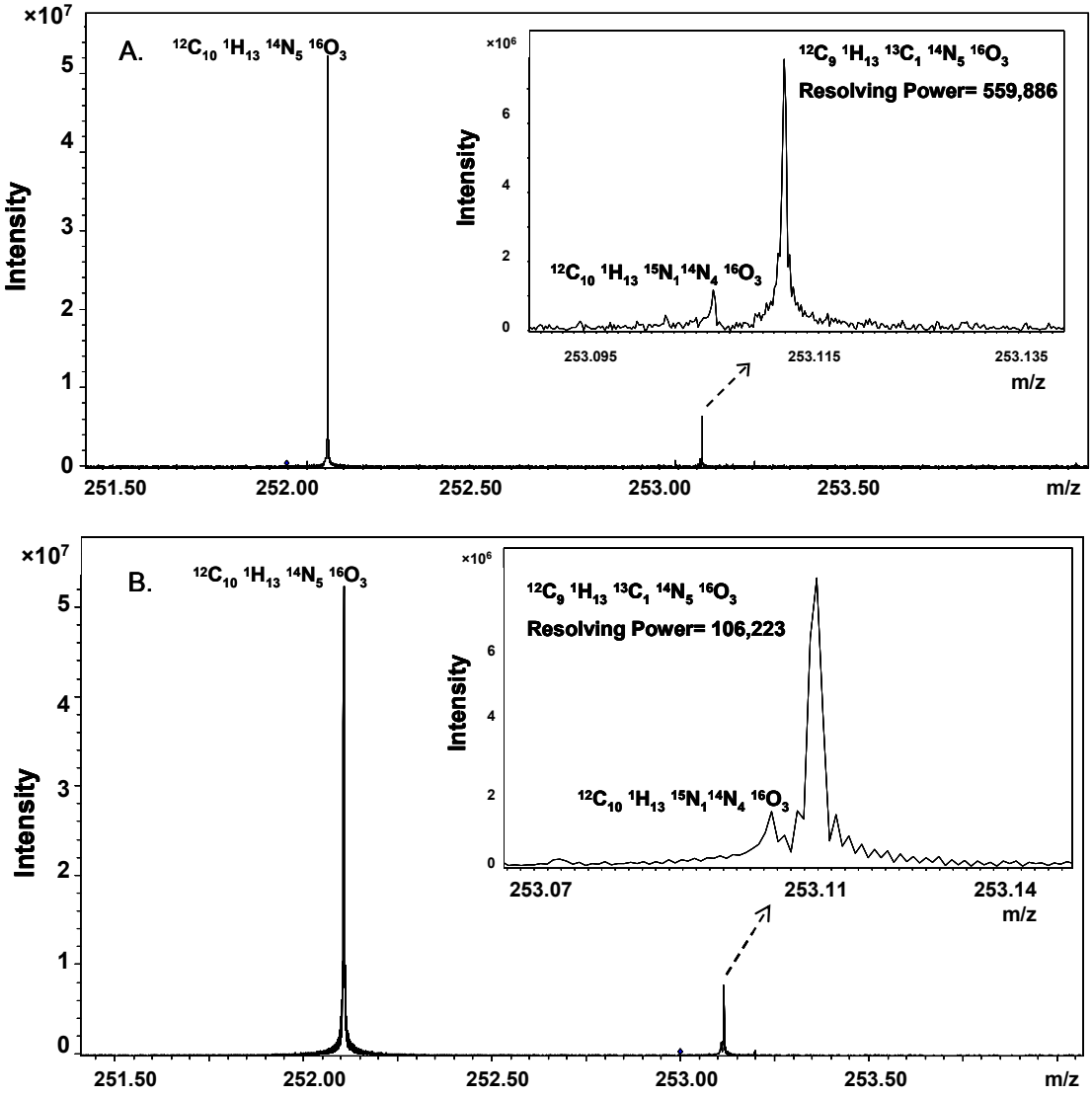

Figure A.2. Commercially available 5'dA tested in A) narrowband (data collected at 128K) mode and B) broadband (data collected at 512K) mode. Higher resolving power is more easily achieved in narrowband mode.

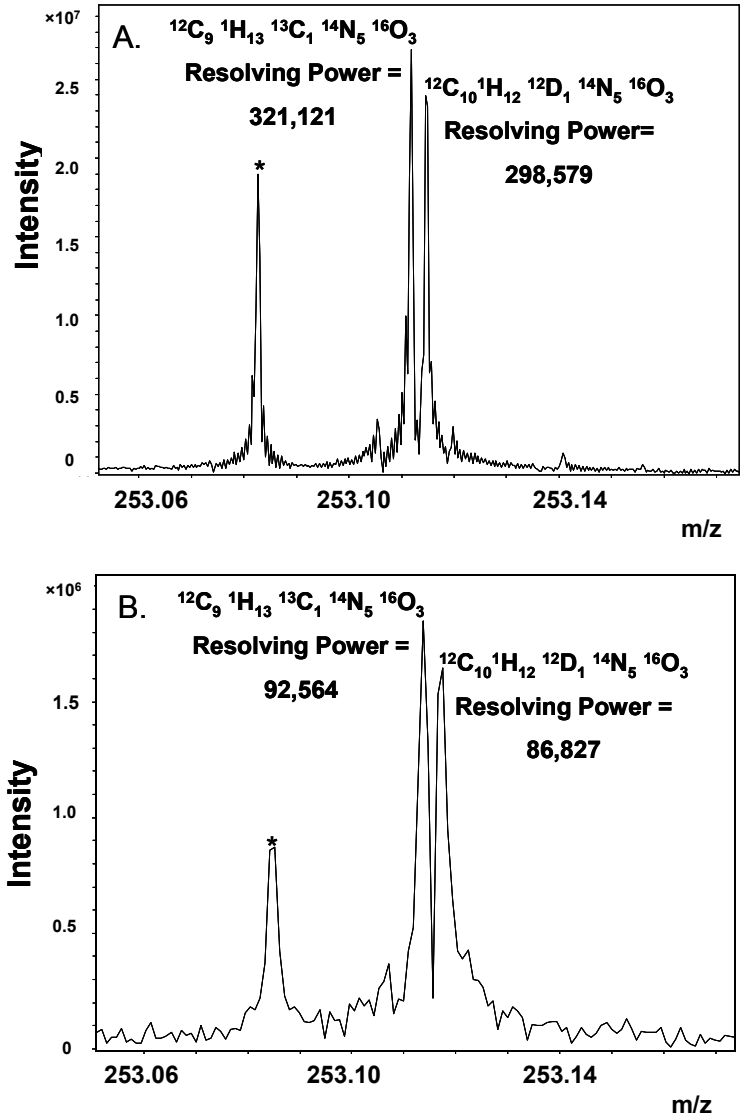

Figure A.3. Enzymatic sample collected after 55.8 ms reaction time tested at A) narrowband mode and B) broadband mode. Only the peaks of interest are displayed in the Figure. The second peak corresponds to the mono-deuterated species. Higher resolving power is observed in narrowband mode and the peaks of interest are better baseline resolved in this detection mode. * = peak from contaminant

A.3.2 Control Experiments

In order to examine whether we could measure the extent of deuterium incorporation into 5'-dA, we incubated commercially available 5'dA in 0.3% D_2O (Sigma, St Louis, MO), 0.5% D_2O, 0.8% D_2O, and 1% D_2O v/v. We then calculated the ratio of mono- to non-deuterated 5'-dA (Figure A.4. A-D). As can be seen from this

Figure, the ratio of the mono- to non-deuterated species increases as the concentration of D_2O increases,, allowing for quantification of the incorporation of deuterium into 5'-dA. For example, after incubation with 0.3% D_2O v/v the ratio of mono- to non-deuterated 5'-dA is 0.2950 whereas after incubation with 1% D_2O v/v the ratio of mono- to non-deuterated 5'-dA increases to 1.137. These observations suggest that the extent of deuterium incorporation into 5'-dA can be measured using FT-ICR mass spectrometry in narrowband detection mode.

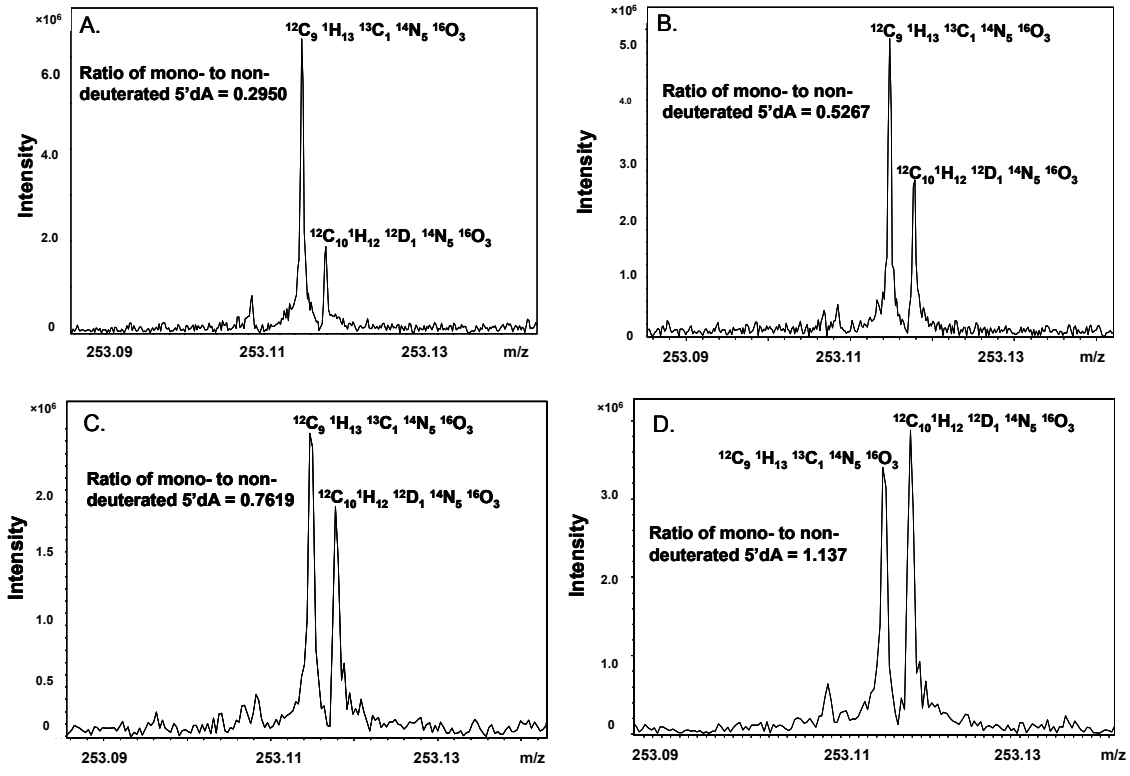

Figure A.4. Commercially available 5'-dA incubated in A) 0.3% D_2O, B) 0.5% D_2O, C) 0.8% D_2O, and D) 1% D_2O v/v. As the D_2O concentration increases, the ratio of mono- to non-deuterated 5'-dA also increases, allowing for quantification of the incorporation of deuterium into 5'-dA.

A.3.3. Determination of the Intrinsic Deuterium Kinetic Isotope Effect in Glutamate Mutase

Figure A.5. displays the mass spectrum of 5'-dA isolated from a reaction stopped after 36 ms. As illustrated above, the $^{12}C_9\,^{1}H_{13}\,^{13}C_1\,^{14}N_5\,^{16}O_3$ and $^{12}C_{10}\,^{1}H_{12}\,^{2}D_1\,^{14}N_5\,^{16}O_3$ peaks are baseline resolved. The intrinsic KIE can be calculated by measuring the peak heights for the two peaks and comparing their ratio. Because there are two protium atoms and only one deuterium atom in the methyl group of methylaspartate, the KIE must be corrected by a factor of 2. Alternatively, because the natural abundance of ^{13}C is known to great precision, the intrinsic KIE can also be calculated by comparing the ratio of $^{12}C_9\,^{1}H_{13}\,^{13}C_1\,^{14}N_5\,^{16}O_3$ to $^{12}C_{10}\,^{1}H_{12}\,^{2}D_1\,^{14}N_5\,^{16}O_3$ to and correcting the result for the natural abundance, *n*, by using the following equation:

$$KIE = \tfrac{1}{2}[(\,^{12}C_9\,^{1}H_{13}\,^{13}C_1\,^{14}N_5\,^{16}O_3)/\,^{12}C_{10}\,^{1}H_{12}\,^{2}D_1\,^{14}N_5\,^{16}O_3] \times [(1-n)/n]$$

The KIE for hydrogen transfer from methylaspartate to 5'-dA was calculated for reaction times ranging from 28 ms to 78 ms and the results are summarized in Table A.1. The KIEs calculated from either the ratio of $^{12}C_{10}\,^{1}H_{13}\,^{14}N_5\,^{16}O_3$ to $^{12}C_{10}\,^{1}H_{12}\,^{2}D_1\,^{14}N_5\,^{16}O_3$,or $^{12}C_9\,^{1}H_{13}\,^{13}C_1\,^{14}N_5\,^{16}O_3$ to $^{12}C_{10}\,^{1}H_{12}\,^{2}D_1\,^{14}N_5\,^{16}O_3$ are, as expected, the same within experimental error. Furthermore, these values do not change significantly over the timescale investigated, suggesting that multiple transits of deuterium between 5'-dA and methylaspartate do not occur on this timescale. The average value of the intrinsic deuterium KIE we obtained is 4.1 ± 0.2. This value is within the semiclassical limit for a deuterium isotope effect and is much smaller than the large KIEs, contributed to hydrogen tunneling, previously measured in other B_{12} enzymes. A control experiment in which the substrate was allowed to react with the enzyme for approximately 1 s gave, as

expected, a KIE close to 1, indicating that, at longer times, equilibration of deuterium between coenzyme and substrate occurs.

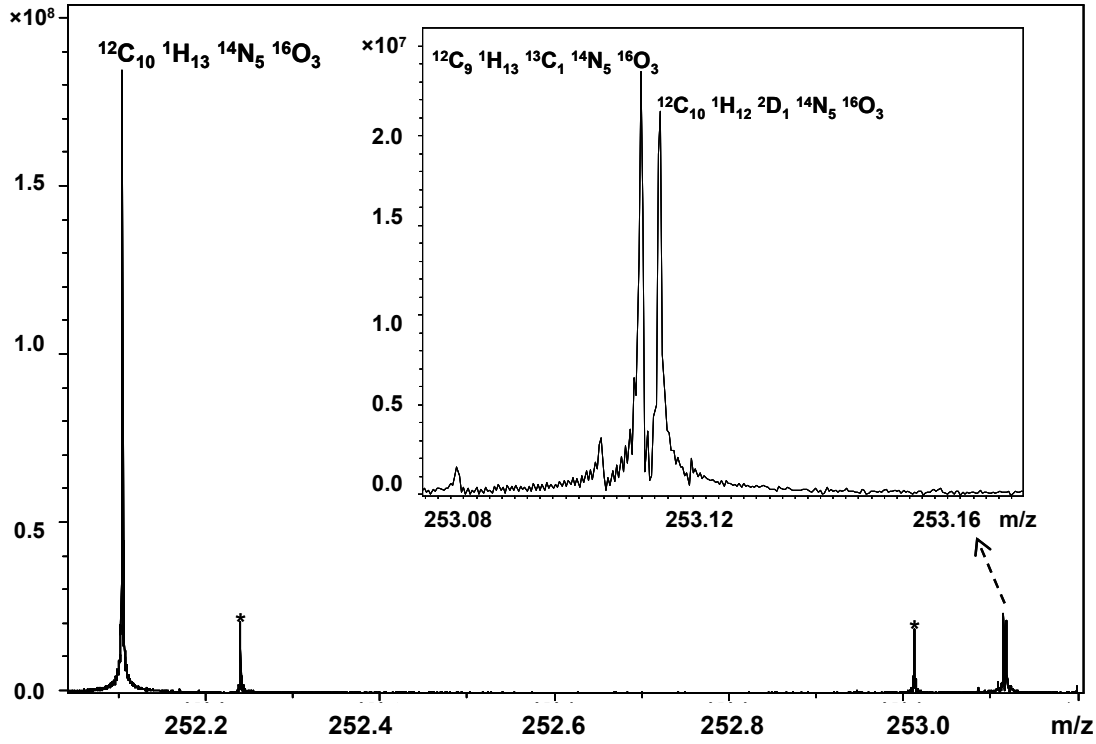

Figure A.5. Mass spectrum of 5'-dA isolated from glutamate mutase after reaction with [$^2H_1$]methylaspartate for 36 ms. The non- and mono-deuterated species are shown in the inset.

Table A.1. Intrinsic KIEs at 10 ^{0}C for hydrogen transfer, determined at various reaction times.

Reaction time (ms)	KIE [$^{12}C/^2H$] [(a)]	KIE [$^{13}C/^2H$] [(b)]	n[(c)]
28	**3.7±0.1**	**3.9±0.3**	**9**
37	**4.4±0.3**	**3.9±0.2**	**9**
56	**4.3±0.4**	**4.0±0.4**	**11**
76	**4.1±0.2**	**4.2±0.4**	**3**
≈1000	**0.95±0.04**	**0.96±0.06**	**4**

(a) KIE determined from the ratio of [$^{12}C_{10}$ $^1H_{13}$ $^{14}N_5$ $^{16}O_3$] to [$^{12}C_{10}$ $^1H_{12}$ $^2D_1$ $^{14}N_5$ $^{16}O_3$].
(b) KIE determined from the ratio of [$^{12}C_9$ $^1H_{13}$ $^{13}C_1$ $^{14}N_5$ $^{16}O_3$] to [$^{12}C_{10}$ $^1H_{12}$ $^2D_1$ $^{14}N_5$ $^{16}O_3$].
(c) Number of measurements.

A.4. Conclusions

Baseline resolution of $^{12}C_9\ ^{1}H_{13}\ ^{13}C_1\ ^{14}N_5\ ^{16}O_3$ (252.10436Da) and $^{12}C_{10}\ ^{1}H_{12}\ ^{2}D_1\ ^{14}N_5\ ^{16}O_3$ (252.10799Da) was achieved and, therefore, we were able to precisely follow the incorporation of deuterium into 5'-deoxyadenosine from the reaction between [$^{2}H_1$]methylaspartate and glutamate mutase/adenosylcobalamin. Assignments for the observed two peaks were confirmed by examining commercially available 5'-deoxyadenosine under the same experimental conditions. Only the lower m/z peak was observed for nondeuterated 5'-deoxyadenosine whereas two peaks ($^{12}C_9\ ^{1}H_{13}\ ^{13}C_1\ ^{14}N_5\ ^{16}O_3$ and $^{12}C_{10}\ ^{1}H_{12}\ ^{2}D_1\ ^{14}N_5\ ^{16}O_3$) were seen following incubation in 0.3-1% v/v D_2O. The experimental masses of the enzymatic samples compare accurately (<2 ppm) with the masses of the standard and the calculated theoretical masses. Data were collected in narrowband mode due to more facile generation of long (>4 s) transients compared to broadband mode. As a result, higher resolving power is obtained and the two peaks of interest are better baseline resolved in narrowband mode. For all experiments, the instrument was tuned to ensure that the detected relative abundance of $^{13}C_1$ versus the monoisotopic peak is as close as possible to the calculated ratio of 0.1324 before the ratio of mono- to nondeuterated 5'-deoxyadenosine was determined. The intrinsic deuterium KIE in glutamate mutase for hydrogen atom transfer from the substrate, [$^{2}H_1$] methylaspartate, to 5'dA was measured and determined to be 4.1.

A.5. References

1. Frey, P. A.; Hegeman, A. D.; Reed, G. H., Free radical mechanisms in enzymology. *Chem. Rev.* **2006,** 106, 3302-3316.
2. Banerjee, R., Radical carbon skeleton rearrangements: Catalysis by coenzyme B-12-dependent mutases. *Chem. Rev.* **2003,** 103, 2083-2094.
3. Frey, P. A., Radical mechanisms of enzymatic catalysis. *Annu. Rev. Biochem.* **2001,** 70, 121-148.
4. Marsh, E. N. G.; Drennan, C. L., Adenosylcobalamin-dependent isomerases: new insights into structure and mechanism. *Curr. Opin. Chem. Biol.* **2001,** 5, 499-505.
5. Marsh, E. N. G., Coenzyme-B-12-dependent glutamate mutase. *Bioorg. Chem.* **2000,** 28, 176-189.
6. Marsh, E. N. G.; Ballou, D. P., Coupling of cobalt-carbon bond homolysis and hydrogen atom abstraction in adenosylcobalamin-dependent glutamate mutase. *Biochemistry* **1998,** 37, 11864-11872.
7. Cleland, W. W., The use of isotope effects to determine enzyme mechanisms. *Arch. Biochem. Biophys.* **2005,** 433, 2-12.
8. Schmid, D. G.; Grosche, P.; Bandel, H.; Jung, G., FTICR-Mass spectrometry for high-resolution analysis in combinatorial chemistry. *Biotechnol. Bioeng.* **2000,** 71, 149-161.
9. Amster, I. J., Fourier transform mass spectrometry. *J. Mass Spectrom.* **1996,** 31, 1325-1337.
10. Marshall, A. G.; Hendrickson, C. L.; Jackson, G. S., Fourier transform ion cyclotron resonance mass spectrometry: A primer. *Mass Spectrom. Rev.* **1998,** 17, 1-35.
11. Drader, J. J.; Shi, S. D. H.; Blakney, G. T.; Hendrickson, C. L.; Laude, D. A.; Marshall, A. G., Digital quadrature heterodyne detection for high-resolution Fourier transform ion cyclotron resonance mass spectrometry. *Anal. Chem.* **1999,** 71, 4758-4763.
12. Shi, S. D. H.; Hendrickson, C. L.; Marshall, A. G., Counting individual sulfur atoms in a protein by ultrahigh-resolution Fourier transform ion cyclotron resonance mass spectrometry: Experimental resolution of isotopic fine structure in proteins. *Proc. Natl. Acad. Sci. USA* **1998,** 95, 11532-11537.
13. He, F.; Hendrickson, C. L.; Marshall, A. G., Baseline mass resolution of peptide isobars: A record for molecular mass resolution. *Anal. Chem.* **2001,** 73, 647-650.
14. Cooper, H. J.; Hendrickson, C. L.; Marshall, A. G., Direct detection and quantitation of He@C-60 by ultrahigh-resolution Fourier transform ion cyclotron resonance mass spectrometry. *J. Am. Soc. Mass Spectrom.* **2002,** 13, 1349-1355.
15. Yang, J.; Mo, J. J.; Adamson, J. T.; Hakansson, K., Characterization of oligodeoxynucleotides by electron detachment dissociation Fourier transform ion cyclotron resonance mass spectrometry. *Anal. Chem.* **2005,** 77, 1876-1882.

Appendix B

Electron Capture Dissociation of Fixed Charge Derivatized Tryptic Peptides

B.1. Introduction

De novo sequencing by mass spectrometry is a valuable method for obtaining peptide and protein sequence information, particularly in cases where the protein to be identified is not present in a database. However, in several cases, product ion mass spectra produced by vibrational excitation are difficult to interpret, either due to the formation of various types of product ions, or formation of internal product ions. In addition, product ions corresponding to small neutral losses can further complicate spectral interpretation. One approach for simplifying tandem mass spectra utilizes charge derivatizing reagents to incorporate a fixed charge group at one of the peptide termini to direct fragmentation so that solely N- or C-terminal product ions are formed.[1-5]

One of these fixed charge derivatizing reagents is tris(2,4,6-trimethoxyphenyl) phosphonium acetic acid N-hydroxysuccinimide ester (TMMP-Ac-OSu), which introduces a tris (2,4,6-trimethoxyphenyl)phosphonium-acetyl (TMPP-Ac) group at peptide N-termini, as shown in Scheme B1.[6-13] TMMP-Ac-OSu derivatization has been

used in combination with low and high energy collision induced dissociation (CID), and matrix assisted laser desorption/ionization post source decay (MALDI-PSD). Following dissociation of singly charged TMMP-Ac-peptides, formation of solely N-terminal product ions was observed, facilitating mass spectral analysis. Mainly *a*-type product ions were formed although some *b*-, *c*-and *d*-type product ions were also detected. A mechanism involving charge remote fragmentation has been proposed for the formation of *a*-type product ions from fixed charge derivatized peptides.[13, 14] An associated advantage with this approach is that for numerous of the peptides examined, higher peptide sequence coverage, reaching complete peptide sequence coverage for several peptides, is obtained for TMMP-Ac-peptides compared to the sequence coverage obtained for the corresponding underivatized peptides, thereby improving peptide *de novo* sequencing.

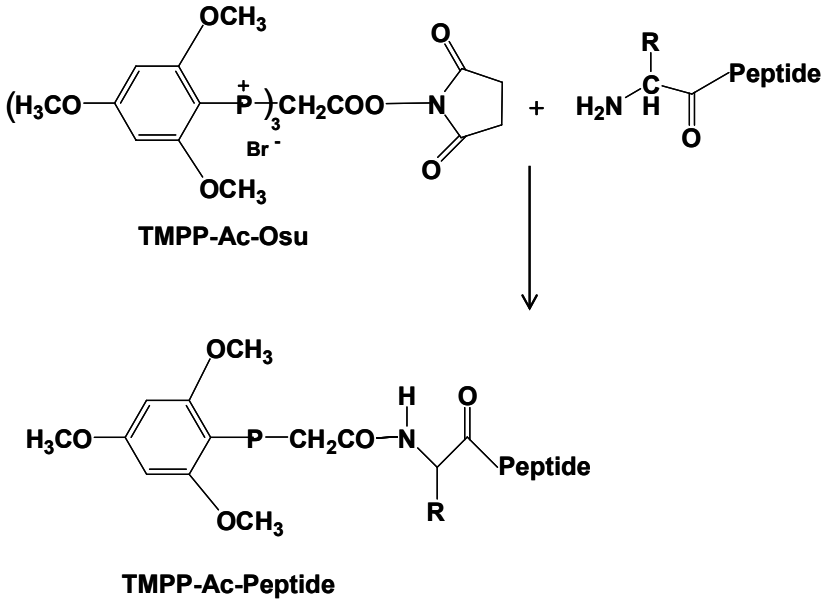

Scheme B.1. Reaction of tris(2,4,6-trimethoxyphenyl) phosphonium acetic acid N-hydroxysuccinimide ester, (TMMP-Ac-OSu), with the N-terminus of a peptide. Adapted from reference [7].

Recently, electron capture dissociation (ECD) of phosphorylated and glycosylated model peptides derivatized with the TMMP-Ac-OSu reagent has been examined.[15] It was demonstrated that, following ECD of doubly charged derivatized peptides, the sequence coverage was significantly increased compared to ECD of the corresponding underivatized species. Full sequence coverage was obtained for nearly all the glycopeptides and phosphopeptides examined, facilitating localization of these modifications. Furthermore, solely N-terminal *c*-type product ions were formed, resulting in simpler mass spectra.

Here, we examine the ECD fragmentation behavior of tryptic peptides derivatized with TMMP-Ac-OSu. We aimed to address whether simpler fragmentation and higher peptide sequence coverage can be obtained for proteolytically derived peptides, similar to the results obtained in ECD of modified model peptides, and in vibrational excitation of model and tryptic peptides. TMMP-Ac-peptides in +2, +3, and +5 charge states were examined in ECD and their fragmentation was compared with that of the corresponding underivatized species.

B.2. Experimental Procedure

B.2.1 Sample Preparation

Apomyoglobin from horse skeletal muscle (0.47 nmol, Sigma, St. Louis, MO) was digested with trypsin (Promega, Madison, WI) in 50 mM ammonium bicarbonate (Fisher Scientific, Fair Lawn, NJ) at 37 ^{0}C. The digestion was performed at an enzyme to protein ratio of 1:50 for 10 min. BSA (0.45 nmol, Sigma) was reduced with 10 mM dithiothreitol (DTT, Sigma, St. Louis, MO) in 50 mM ammonium bicarbonate for 45 min at 56 ^{0}C and then carboxyamidomethylated with 50 mM iodoacetamide (Sigma, St.

Louis, MO) in 50 mM ammonium bicarbonate in darkness for one hour. Following reduction and alkylation, BSA was digested with trypsin at an enzyme to protein ratio of 1:50 for four hours. Reactions were quenched with 0.2-0.5 % formic acid (Acros Organics, Morris Plains, NJ) and the proteolytic samples were evaporated to dryness. Tryptic peptide samples were then redissolved in 2 µl of 50 mM Tris-HCl (Promega, City, State) (pH = 8.2) in 80% acetonitrile and 10 µl of 10 mM (N-succinimidyloxycarbonylmethyl)tris-(2,4,6-trimethoxyphenyl)phosphonium bromide (Sigma) in anhydrous acetonitrile (Fisher) was added to the mixture. The mixture was vortexed for 30 s, placed in a water bath and allowed to react for 30 min at 27-28 ^{0}C. After derivatization, the mixture was evaporated to dryness, redissolved in 50 µl water and desalted with C_{18} Ziptips or with strong cation exchange (SCX) Ziptips (Millipore, Billerica, MA). Finally, it was diluted into 600-740 µL electrospray solvent containing 50% acetonitrile (Fisher) and 0.1% formic acid.

B.2.2 Mass Spectrometry

All experiments were performed with an actively shielded 7T quadrupole Fourier transform ion cyclotron resonance (Q-FT-ICR) mass spectrometer (Apex-Q, Bruker Daltonics, Billerica, MA), which has been previously described.[16] Proteolytic mixtures, derivatized or underivatized, were electrosprayed in positive ion mode at a flow rate of 70 µL/hour. Ions were accumulated in the first hexapole for 0.1 s, transferred through the mass selective quadrupole (1-6 m/z isolation window), mass selectively accumulated in the second hexapole for 0.1 to 4s, transferred through high-voltage ion optics, and captured in the ICR cell by dynamic trapping. This accumulation sequence was looped twice to maximize precursor ion signal. Further precursor ion isolation was achieved by correlated harmonic excitation fields[17] inside the ICR cell.

ECD was performed with an indirectly heated hollow dispenser cathode at a bias voltage of 0.01 to 0.40 V and an irradiation time of 30 to 60 ms. A lens electrode located in front of the hollow cathode was kept at 1.0 V. All spectra were acquired with XMASS (version 6.1, Bruker Daltonics) using 512 K data points and summed over 64 scans. Data processing was performed with the MIDAS analysis software.[18] Internal frequency-to-mass calibration was performed by Microsoft Excel using a two term calibration equation.[19] The calculated masses of the precursor ions and the charge-reduced species were used for calibration. Product ion spectra were interpreted with the assistance of the MS Product function (http://prospector.ucsf.edu/prospector/4.0.8/html/msprod.htm) in Protein Prospector. Only peak assignments with a mass accuracy better than 15 ppm were accepted.

B.3. Results and Discussion

Figure B.1. shows the ECD fragmentation of derivatized and underivatized tryptic doubly charged peptides. Following ECD of TMPP-Ac-peptides, solely N-terminal product ions are detected, similar to the results obtained in vibrational excitation of charge derivatized peptides. As expected, the N-terminal product ions formed following ECD are *c*-type product ions. The same trend, formation of solely N-terminal *c*-type product ions, was also observed in ECD of doubly charged fixed charge derivatized glyco- and phosphopeptides.[15]

ECD of underivatized peptides resulted in formation of *z*-type product ions due to the presence of basic residues at the tryptic peptide C-termini. However, for several peptides, peptides C, D, and E (Figure B.1.), both *c*- and *z*-type product ions were detected. For peptide B, *c*-type product ions were detected due to the presence of a lysine

residue close to the N-terminus. This peptide contains the C-terminus of the protein. Thus, ECD mass spectra obtained from charged derivatized doubly charged tryptic peptides are more easily interpretable compared to those obtained from underivatized species, due to formation of solely *c*-type product ions.

Figure B.1. ECD fragmentation summary of derivatized (TMPP-Ac-) and underivatized doubly charged tryptic peptides. The obtained peptide sequence coverage is indicated next to each peptide. Peptide B contains the C-terminus of the protein (apomyoglobin).

For some of the doubly charged TMPP-Ac-peptides, peptides A, B, and C (Figure B.1), the ECD sequence coverage was higher compared to that obtained for the corresponding underivatized species. The derivatized peptide D showed the same extent of fragmentation compared to its underivatized counterpart whereas the derivatized peptides E and F exhibited lower fragmentation compared to the corresponding underivatized species. The derivatized peptides E and F showed the lowest ECD sequence coverage compared to the other TMPP-Ac-peptides. We believe that this low sequence coverage is due to the fact that these two peptides were detected at high m/z ratio and, as discussed in Chapters 3 and 4, ECD sequence coverage decreases with increasing precursor ion m/z value, particularly when this value is above ~ 960. This trend was more pronounced for doubly protonated species. The derivatized peptide E was detected at m/z = 1026. 494 whereas its underivatized counterpart was detected at m/z = 740.401 and the TMPP-Ac-peptide F was detected at m/z= 1070. 466 whereas its underivatized species was detected at m/z = 784.375. The derivatized peptides are detected at higher m/z compared to their underivatized counterparts due to the addition of the fixed charge group (+ 573.188 Da) at the N-terminus of the peptide. These results suggest that charge derivatization of large size tryptic peptides followed by ECD is not the preferred method to obtain the highest possible sequence coverage because of the existing m/z limit in ECD. However, for small size tryptic peptides, the combination of fixed charge derivatization and ECD can be an effective way to simplify ECD mass spectra.

Our results are in some disagreement with those obtained in ECD of fixed charge derivatized modified model peptides.[15] For glycosylated and phosphorylated peptides,

ECD of the charge derivatized species resulted in significantly increased peptide sequence coverage compared to the corresponding underivatized species, regardless of precursor ion m/z ratio. In fact, complete peptide sequence coverage was obtained for nearly all the charge derivatized peptides examined, containing 9 to 17 amino acid residues. None of the underivatized species resulted in complete ECD sequence coverage. The differences observed in the two experiments can be attributed to possible differences in gas-phase structures/conformations of modified versus unmodified peptides. Structural dependence of the ECD fragmentation outcome has been previously reported in a number of experimental configurations.[20-25]

ECD fragmentation summary of some TMPP-Ac-peptides detected at higher charge states is shown in Figure B.2. For these more highly charged peptides, ECD of the TMPP-Ac-peptides resulted in formation of both N-terminal *c*-type product ions and C-terminal, *z*-type product ions, similar to ECD of the corresponding underivatized species. This behavior is in agreement with the results obtained in ECD of modified TMPP-Ac-peptides for which triply charged species resulted in formation of both *c*- and *z*-type product ions.[15]

For the peptides G and H, ECD of both derivatized and uderivatized species resulted in the same peptide sequence coverage. For peptide H, the $[M + 4H]^{5+}$ precursor ions (one charge is due to the fixed charge group) were selected for fragmentation of the derivatized species. For the underivatized peptide, the quadruply protonated ions were fragmented because the $[M + 5H]^{+5}$ precursor ions were detected with low abundance. Nevertheless, for both the derivatized and underivatized species, the same peptide sequence coverage was obtained regardless of precursor ion charge state. These

observations are in agreement with the results obtained in Chapter 4, in which it was shown that highly charged precursor ions (n>3) detected at low m/z values fragment efficiently in ECD regardless of their charge state.

For peptide I, slightly higher peptide sequence coverage was obtained for the underivatized species compared to that observed for the corresponding TMPP-Ac-peptide. The results obtained for highly charged derivatized tryptic peptides suggest that the incorporation of a fixed charge in peptides carrying multiple charges does not improve ECD sequence coverage, nor simplifies spectral interpretation.

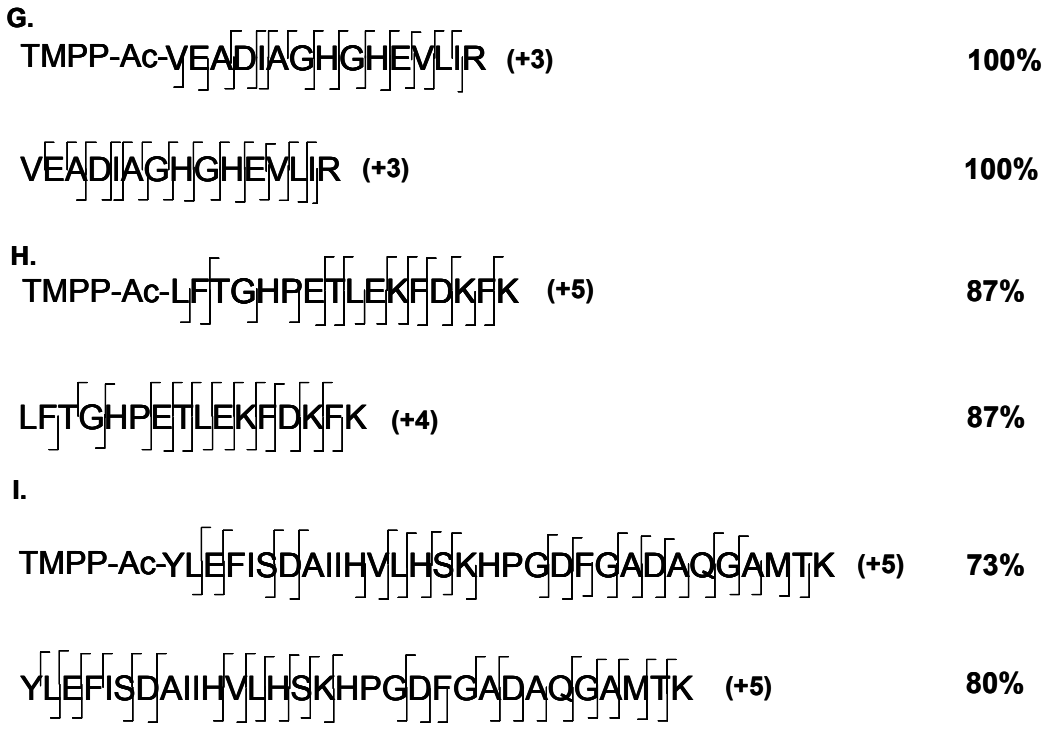

Figure B.2 ECD fragmentation summary of derivatized (TMPP-Ac-) and underivatized multiply charged tryptic peptides. The peptide sequence coverage is indicated next to each peptide and the precursor ion charge state is indicated in parenthesis

B.4. Conclusions.

We have investigated the ECD fragmentation behavior of tryptic peptides derivatized with tris(2,4,6-trimethoxyphenyl) phosphonium acetic acid N-hydroxysuccinimide ester (TMMP-Ac-OSu). Our results show that ECD of doubly charged derivatized tryptic peptides resulted in formation of solely *c*-type product ions, thereby simplifying spectral interpretation. For almost all small size peptides examined, complete peptide sequence coverage was observed. However, as the precursor ion m/z value of derivatized peptides increases, the ECD sequence coverage decreases, similar to the results reported in Chapters 3 and 4 for underivatized peptides. Therefore, for larger size peptides, ECD of the underivatized species provided higher peptide sequence coverage, mainly because the underivatized species were detected at lower m/z values. Differences in fragmentation behavior can also be attributed to differences in gas-phase structures and conformations, as mentioned earlier in the thesis.

ECD of highly charged TMPP-Ac-peptides was very similar to ECD of the corresponding underivatized species. Both *c*- and *z*-type product ions were detected and identical, or very similar, peptide sequence coverage was observed. Therefore, for highly charged precursor ions, fixed charge derivatization with TMMP-Ac groups did not provide any advantage for ECD sequencing compared to the underivatized species.

B.5. References

1. Roth, K. D. W.; Huang, Z. H.; Sadagopan, N.; Watson, J. T., Charge derivatization of peptides for analysis by mass spectrometry. *Mass Spectrom. Rev.* **1998,** 17, 255-274.
2. Sonsmann, G.; Romer, A.; Schomburg, D., Investigation of the influence of charge derivatization on the fragmentation of multiply protonated peptides. *J. Am. Soc. Mass Spectrom.* **2002,** 13, 47-58.
3. Zaia, J.; Biemann, K., Comparison of Charged Derivatives for High-Energy Collision-Induced Dissociation Tandem Mass-Spectrometry. *J. Am. Soc. Mass Spectrom.* **1995,** 6, 428-436.
4. Knapp, D. R., Chemical Derivatization for Mass-Spectrometry. *Method. Enzymol.* **1990,** 193, 314-329.
5. Wagner, D. S.; Salari, A.; Gage, D. A.; Leykam, J.; Fetter, J.; Hollingsworth, R.; Watson, J. T., Derivatization of Peptides to Enhance Ionization Efficiency and Control Fragmentation During Analysis by Fast-Atom-Bombardment Tandem Mass-Spectrometry. *Biol. Mass Spectrom.* **1991,** 20, 419-425.
6. Adamczyk, M.; Gebler, J. C.; Wu, J., Charge derivatization of peptides to simplify their sequencing with an ion trap mass spectrometer. *Rapid Commun. Mass Spectrom.* **1999,** 13, 1413-1422.
7. Chen, W. B.; Lee, P. J.; Shion, H.; Ellor, N.; Gebler, J. C., Improving de novo sequencing of peptides using a charged tag and C-terminal digestion. *Anal. Chem.* **2007,** 79, 1583-1590.
8. Huang, Z. H.; Shen, T. L.; Wu, J. A.; Gage, D. A.; Watson, J. T., Protein sequencing by matrix-assisted laser desorption ionization-postsource decay mass spectrometry analysis of the N-tris(2,4,6-trimethoxyphenyl)phosphine-acetylated tryptic digests. *Anal. Biochem.* **1999,** 268, 305-317.
9. Huang, Z. H.; Wu, J.; Roth, K. D. W.; Yang, Y.; Gage, D. A.; Watson, J. T., A picomole-scale method for charge derivatization of peptides for sequence analysis by mass spectrometry. *Anal. Chem.* **1997,** 69, 137-144.
10. Sadagopan, N.; Malone, M.; Watson, J. T. R., Effect of charge derivatization in the determination of phosphorylation sites in peptides by electrospray ionization collision-activated dissociation tandem mass spectrometry. *J. Mass Spectrom.* **1999,** 34, 1279-1282.
11. Sadagopan, N.; Watson, J. T., Investigation of the tris(trimethoxyphenyl)phosphonium acetyl charged derivatives of peptides by electrospray ionization mass spectrometry and tandem mass spectrometry. *J. Am. Soc. Mass Spectrom.* **2000,** 11, 107-119.
12. Shen, T. L.; Huang, Z. H.; Laivenieks, M.; Zeikus, J. G.; Gage, D. A.; Allison, J., Evaluation of charge derivatization of a proteolytic protein digest for improved mass spectrometric analysis: de Novo sequencing by matrix-assisted laser desorption/ionization post-source decay mass spectrometry. *J. Mass Spectrom.* **1999,** 34, 1154-1165.
13. Sadagopan, N.; Watson, J. T., Mass spectrometric evidence for mechanisms of fragmentation of charge-derivatized peptides. *J. Am. Soc. Mass Spectrom.* **2001,** 12, 399-409.

14. Liao, P. C.; Huang, Z. H.; Allison, J., Charge remote fragmentation of peptides following attachment of a fixed positive charge: A matrix-assisted laser desorption/ionization postsource decay study. *J. Am. Soc. Mass Spectrom.* **1997,** 8, 501-509.
15. Chamot-Rooke, J.; van der Rest, G.; Dalleu, A.; Bay, S.; Lemoine, J., The combination of electron capture dissociation and fixed charge derivatization increases sequence coverage for O-glycosylated and O-phosphorylated peptides. *J. Am. Soc. Mass Spectrom.* **2007,** 18, 1405-1413.
16. Yang, J.; Mo, J. J.; Adamson, J. T.; Hakansson, K., Characterization of oligodeoxynucleotides by electron detachment dissociation Fourier transform ion cyclotron resonance mass spectrometry. *Anal. Chem.* **2005,** 77, 1876-1882.
17. de Koning, L. J.; Nibbering, N. M. M.; van Orden, S. L.; Laukien, F. H., Mass selection of ions in a Fourier transform ion cyclotron resonance trap using correlated harmonic excitation fields (CHEF). *Int. J. Mass Spectrom.* **1997,** 165, 209-219.
18. Senko, M. W.; Canterbury, J. D.; Guan, S. H.; Marshall, A. G., A high-performance modular data system for Fourier transform ion cyclotron resonance mass spectrometry. *Rapid Commun. Mass Spectrom.* **1996,** 10, 1839-1844.
19. Ledford, E. B.; Rempel, D. L.; Gross, M. L., Space-Charge Effects in Fourier-Transform Mass-Spectrometry - Mass Calibration. *Anal. Chem.* **1984,** 56, 2744-2748.
20. Creese, A. J.; Cooper, H. J., The effect of phosphorylation on the electron capture dissociation of peptide ions. *J. Am. Soc. Mass Spectrom.* **2008,** 19, 1263-1274.
21. Adams, C. M.; Kjeldsen, F.; Zubarev, R. A.; Budnik, B. A.; Haselmann, K. F., Electron capture dissociation distinguishes a single D-amino acid in a protein and probes the tertiary structure. *J. Am. Soc. Mass Spectrom.* **2004,** 15, 1087-1098.
22. Breuker, K.; Oh, H. B.; Cerda, B. A.; Horn, D. M.; McLafferty, F. W., Hydrogen atom loss in electron-capture dissociation: a Fourier transform-ion cyclotron resonance study with single isotopomeric ubiquitin ions. *Eur. J. Mass Spectrom.* **2002,** 8, 177-180.
23. Breuker, K.; Oh, H. B.; Horn, D. M.; Cerda, B. A.; McLafferty, F. W., Detailed unfolding and folding of gaseous ubiquitin ions characterized by electron capture dissociation. *J. Am. Chem. Soc.* **2002,** 124, 6407-6420.
24. Chen, X. H.; Turecek, F., The arginine anomaly: Arginine radicals are poor hydrogen atom donors in electron transfer induced dissociations. *J. Am. Chem. Soc.* **2006,** 128, 12520-12530.
25. Mihalca, R.; Kleinnijenhuis, A. J.; McDonnell, L. A.; Heck, A. J. R.; Heeren, R. M. A., Electron capture dissociation at low temperatures reveals selective dissociations. *J. Am. Soc. Mass Spectrom.* **2004,** 15, 1869-1873.